1990

Central Metabolism Of Bacillus Thuringiensis During Growth And Sporulation

Gerald E. Rowe

CENTRAL METABOLISM OF *BACILLUS THURINGIENSIS* DURING GROWTH AND SPORULATION

by

Gerald E. Rowe

Department of Chemical and Biochemical Engineering

Submitted in partial fulfilment
of the requirements for the degree of
Doctor of Philosophy

Faculty of Graduate Studies
The University of Western Ontario
London, Ontario
June 1990

ISBN 0-315-59089-0

ABSTRACT

Several major features of central metabolism during the Bacillus thuringiensis fermentation for bioinsecticide production remain uncertain. Thus it was desired to identify and quantitate the central metabolic pathways of Bt growth and sporulation.

To achieve these objectives it was necessary to identify and measure all potentially significant cellular inputs and outputs. A set of pathways possibly comprising central metabolism was assumed, based on literature and experimental findings, including detection of several intermediates of the three branched - chain amino acid (viz. valine, leucine and isoleucine) pathways. Selected samples were incubated anaerobically to measure inhibition of catabolic flux through branched - chain 2-oxoacid dehydrogenase. Chloramphenicol was present to block enzyme induction and biosynthetic flows. Dehydrogenation rates of two branched - chain 2-oxoacids were calculated from the flux of the third one, by employing rates of branched - chain acyl-CoA use for fatty acid biosynthesis to determine relative pathway flow rates. This permitted model solution through molar balances around acetyl-CoA and pyruvate.

The following liquid - phase analytes were measured: glucose, ammonia and each of 16 amino acids after hydrolysis; volatile organic products: acetate, acetoin, isobutyrate, 2-methylbutyrate and isovalerate; and non - volatile organic

products: 2,3-butanediol, lactate, pyruvate, combined 2-keto-isovalerate and 2-hydroxy-isovalerate, 2-keto-3-methylvalerate, 2-keto-isocaproate and succinate. Biomass content of poly-β-hydroxybutyric acid (PHB), poly-β-hydroxyvaleric acid (PHV), and 15 fatty acids was also determined.

Anaerobic incubation generally led to accumulation of isoleucine pathway intermediates, which was used to calculate valine and leucine pathway fluxes. Increased 2-oxoisovalerate biosynthesis accompanied granulation as vegetative growth ended. Greater catabolic flux in valine and leucine pathways led to induction of the glyoxylate cycle and malic enzyme as sporulation began. After forespore membrane completion, relatively increased leucine pathway flux accompanied protein turnover. Subsequently leucine and valine catabolic pathways operated jointly, apparently to complete turnover of mother - cell into spore constituents and metabolic energy.

In conclusion, the three branched - chain amino acid pathways operate as complete amphibolic units, functionally integrated with the known pathways of central metabolism in B. thuringiensis (viz. glycolysis, tricarboxylic acid and glyoxylate cycles). These novel pathways complete potential cycles for interconversion and/or terminal oxidation of metabolic intermediates, especially during cellular differentiation.

ACKNOWLEDGEMENTS

I wish to sincerely thank my Thesis Supervisor, Dr. A. Margaritis, for his encouragement and support throughout the long process of bringing this thesis to fruition. Profound thanks to Todd Anderson for the fruit of our constant discussions at all stages of the present work. I would also like to thank the other members of my advisory committee, Dr. P.C. Fitz-James, Dr. M. Bergougnou, Dr. M.M. Ali and Dr. N. Kosaric, for their interest and support of this study. Thanks also to Dr. P. Fraser, Dr. A. Jutan, Dr. M. Kennard, Mr. P.S. Chahal, Mr. P. Herbert and to the many fellow students and staff who have helped along the way.

I would like to thank the Natural Sciences and Engineering Research Council and the International Development Research Centre (IDRC) for scholarships without which the present study would not have been possible. I would also like to take this opportunity to thank both IDRC and Inter Pares for their program of support for research on Bacillus thuringiensis bioinsecticides, from which the present work has benefitted. My personal thanks to Dr. M. Loevensohn and Mr. R. Tassé for their early and continued help.

TABLE OF CONTENTS

LIST OF FIGURES

LIST OF TABLES

LIST OF APPENDICES

1. Introduction

1.1 Rationale and Objectives

Because Bacillus thuringiensis (Bt) has become the most widely used biological insecticide, a large body of research and development literature has accumulated over more than 35 years. It is not my purpose to attempt even a limited review; and the interested reader is directed to existing works, such as: Kurstak (1982) and Burges (1981), regarding microbial and viral pesticides in general; Rowe and Margaritis (1987), for an overview of Bt technology; and Lereclus et al., (1989), regarding δ-endotoxin genetics.

Optimization and control of this fermentation to maximize productivity of biomass and toxicity, or "toxicity yield", are of primary biochemical engineering interest (Rowe and Margaritis, 1987). In order to control the fermentation in a desired state, it is necessary in some sense to "identify" that state in terms of observable variables (Graupe, 1972, p. 1). Since we observe the system through changes in concentration of substrates and products (including biomass), we need to know how the former are converted into the latter. A knowledge of how these pathways are controlled would also decrease the empirical component of a control strategy.

In spite of almost forty years of work on Bt (and B. cereus, Sect. 2.1.1), major aspects of its intermediary metabolism remain unknown:

> "The physiology of B. thuringiensis as it relates to the central metabolic pathways has received relatively little attention, except for the catabolism of glutamate via the gamma-aminobutyric pathway and certain aspects of amino acid metabolism and polypeptide synthesis." (Bulla et al., 1980).

Aspects of what is known in this area are problematic. For example, there appears to be no pathway or cycle active in terminal oxidation of the major fermentation intermediates. Since the organism must sporulate to yield the desired parasporal crystal product, we also need some understanding of this differentiation process (Sect. 1.2).

Thus the general research objectives were to identify the central metabolic pathways of Bt during growth and sporulation; to quantify their relative fluxes (ie. specific reaction rates); and to understand the evolution of metabolism which is bacterial sporulation.

As a work in biochemical engineering, as opposed to microbial biochemistry per se, it seemed expedient to adopt the classical approach of explicitly studying the organism's interactions with its environment. From this followed the strategy employed (cf. Holms, 1986), namely:

1) measure all possible carbon - containing substrates and products, except carbon dioxide;

2) assume a limited but sufficient set of possible metabolic pathways, based on literature and initial experimental findings;

3) solve the system of molar flux balances, justifying any assumptions.

This analytical procedure necessarily depends for its outcome on numerous measurements, calculations and assumptions; therefore the results obtained are subject to quite wide error bounds. Quantitative estimation of such bounds is performed in Appendix H. Since considerable biochemical terminology appears in the text, as well as symbols for quantities calculated during model solution, a glossary of nomenclature is included as Appendix I.

After analytical methods for volatile and non - volatile organic acids had been set up, evidence of several unexpected substances was found. Most of these turned out, after inspection by refined analytical procedures (Sect. 4.4), to be metabolites of the three branched - chain amino acids (BCAA's; ie. valine, leucine and isoleucine; Sect. 3). Eventually I discovered that branched fatty acids typically form about 80 per cent of fatty acids in all bacilli (Kaneda, 1977). Discovery of the substantial literature on various regulatory effects of BCAA's in mammalian tissues (cf. Odessey, 1986) has allowed speculation on mechanisms of metabolic control during sporulation. Although the work reported here may lead to more questions than answers, it is hoped that at least the questions will be better defined.

1.2 Sporulation as a Process of Metabolic Differentiation

Sonenshein (1989) described sporulation as follows:

> "...sporulation is a confluence of pathways that is chosen by a cell that has already perceived an environmental change and has called into play a multitude of regulatory responses..."

Mandelstam early identified the problem of pleiotropism inherent in spore research, which nevertheless influenced its direction:

> "...the conditions used for sporulation are conditions of metabolic stepdown and starvation, which lead to the induction of a variety of enzymes that are relevant to the change in nutritional environment of the cell but are not necessarily concerned with sporulation. The study of immediate changes in cells was long dominated by two observations. The first was the discovery that the TCA cycle has to be induced in order to allow sporulation, and the second was the observation of protein turnover at the beginning of sporulation." (Keynan and Sandler, 1989).

Literature on aspects of TCA cycle enzymes is reviewed in Sect. 2.4. Protein turnover is discussed in Sect. 2.1.2.

That research on sporulation based on derepression of TCA cycle enzymes has reached an impasse was eloquently stated recently by Sonenshein (1989):

> "In 1965, Schaeffer *et al.* published a seminal paper in which they concluded that sporulation of *Bacillus subtilis* is regulated by a form of catabolic repression that involves metabolites containing carbon or nitrogen or both...Ever since the publication of Schaeffer's work, the key metabolites and the regulatory proteins with which they are presumed to interact have been the Holy Grail for *Bacillus* sporulation physiologists. This search has led more often than not to blind alleys or, at best, to interesting red herrings."

Although sporulation is still believed to be dependent on breakdown and reuse (turnover) of intracellular protein, the details of its control remain a mystery (Sect. 2.1.2).

In the early 1960's Halvorson emphasized the importance of sporulation as a model system for study of cellular differentiation; this remains a useful tool.

> "One of the most important questions in modern biology deals with differentiation. How does a cell of one type give rise to one or more cells with completely different morphology, physiology, and function? In higher organisms, this problem has been discussed since the time of Atistotle, but only in the last few years has eucaryotic development been examined on the molecular level...As exciting and fundamental as these eucaryotic systems are for explorations into mechanisms of development, microorganisms, with their well-studied genetic systems and ease of manipulation, are ideal for this type of study...Sporulation in the genus Bacillus is the best-studied example of procaryotic differentiation..." (ibid.).

Any light which can be shed on the metabolic basis of sporulation in bacilli may help to answer fundamental questions about cellular differentiation in general.

2. Brief Review of Central Metabolism in *Bacillus thuringiensis* and Related Species

2.1 Principal Physiological Characteristics of *Bacillus thuringiensis*

2.1.1 General Aspects

Bacillus thuringiensis is believed to be very similar to, if not identical with, *B. cereus*. Thus the eigth edition of Bergey's Manual of Determinative Bacteriology (1974) lists this organism as a distinct entity in group I of the genus *Bacillus*; yet both a slightly earlier authority (Gordon *et al.*, 1973) and a more recent one (Laskin and Lechevalier, 1977) consider it to be a variety of *B. cereus*. Details of this controversy are summarized in Bulla *et al.* (1980). Zahner *et al.* (1989) studied 11 central enzymes in 32 strains of *B. cereus* and *B. thuringiensis*, concluding that all belong to the same species. Statistical analysis of fatty acid (FA) compostion of the two species on different media shows them to be indistinguishable (Sect. 3.3), as reported by Gordon *et al.* (1973).

The literature related to intermediary metabolism of *B. thuringiensis* was reviewed by Rowe and Margaritis (1987), and more recently by Anderson (1990). Freese and Fujita (1976) surveyed several enzymes of intermediary metabolism in *Bacillus*.

Vegetative growth is driven by the Embden - Meyerhoff - Parnas (EMP, glycolytic) pathway with aerobic formation of lactate, acetate, etc. (Sect. 2.2). All of the B. cereus group are capable of anaerobic growth on nutrient agar (Bergey's Manual, 1974; Laskin and Lechevalier, 1977); and the organism used in the present work was capable of essentially anaerobic growth and sporulation (unpublished observation). As research by Anderson (1990) showed, B. thuringiensis acts as a typical facultative anaerobe: "...vegetative phase biomass formation was approximately equal over a wide range of k_La [ie. oxygen mass - transfer rate]...". Energy generation by anaerobic glycolysis, even under good aeration, typifies the enterobacteria and other facultative anaerobes (Mandelstam and McQuillen, 1973, p.457). Thus,

> "Halvorson (1957) reported two peaks in oxygen demand [of B. cereus T]. One paralleled the increase in cell population, and the second occurred as the pH began to rise, when acetate began to disappear from the medium. The oxygen demand decreased before the pH rise was completed and remained at a low level until sporulation [ie. refractile spore formation] occurred." (Hanson et al., 1963).

The second oxygen demand peak, occurring after vegetative growth has ended, is by far the more intense (Halvorson, 1957). Likewise Anderson (1990) found the greatest effect of dissolved oxygen on biomass formation during transition phase. Using balanced C:N medium, biomass increased during transition phase by 36 per cent with k_La of 45 hr^{-1}; the increase was 82 per cent with k_La of 120 hr^{-1}. Subsequent oxygen requirement

decreases considerably: "Intact forespores [of B. cereus] released from sporulating cells at the end of stage III ($T_{3.5}$) had an endogenous oxygen uptake 20 % of that observed in whole sporulating cells and 12 % of that in exponential cells." (Andreoli et al., 1975).

The period of exponential growth by binary fission is quite short in B. cereus; and gives way to one of pH rise as intermediates are consumed (Hanson et al., 1963). The latter stage is associated with formation of intracellular granules, apparently composed mainly of poly-β-hydroxybutyric acid (PHB; Sect. 2.3). Use of acidic intermediates, especially acetate, is associated with induction of enzymes of the tricarboxylic acid (TCA) and glyoxylate cycles (Sect. 2.4 and 2.5 respectively). Pathways between the TCA cycle and pyruvate, with the exception of pyruvate dehydrogenase, are briefly reviewed in Sect. 2.6. The latter enzyme is discussed in Sect. 6.3.2.

2.1.2 Sporulation in Bacilli

For a general historical overview of spore research see Keynan and Sandler (1983). The most thorough modern review of metabolism of sporulation in Bacillus is by Freese and Heinze (1983; cf. Sonenshein, 1989).

Although the mechanisms involved are not known, sporulation can be initiated by partial inhibition of synthesis of guanine nucleotides (Freese and Heinze, 1983). However the

various methods of reducing GTP content induce no more than half the cells to sporulate, suggesting that other factors and/or signals are also involved (Sonenshein, 1985). Sporulation normally results from a slowing of growth in nutrient medium, or from the stringent response. In the latter, shortage of an amino acid causes production of highly phosphorylated guanine nucleotides, which serve as a potent signal for differentiation (Freese and Heinze, 1983). Three of the more important responses induced are decreased RNA and protein synthesis; elaboration of intracellular and extracellular proteases; and the start of intense hydrolysis (turnover) of intracellular protein (ibid.).

The beginning of sporulation - specific changes in bacteria, designated time "t_0" (Fig. 2.1), is indicated by a decrease in exponential growth rate (Freese and Heinze, 1983). It is a convention to denote time as "t_n", where n equals number of hours beyond t_0 (or until t_0, for $n < 0$). Another convention is division of the process of spore formation into seven stages based on cell morphology. These stages, as currently defined (ibid.; cf. Fitz-James and Young, 1969), are as follows:

1) stage 0: vegetative cell;

2) stage I: now considered same as Stage 0;

3) stage II: formation of pre - spore septum;

4) stage III: complete engulfment of forespore by mother cell ;

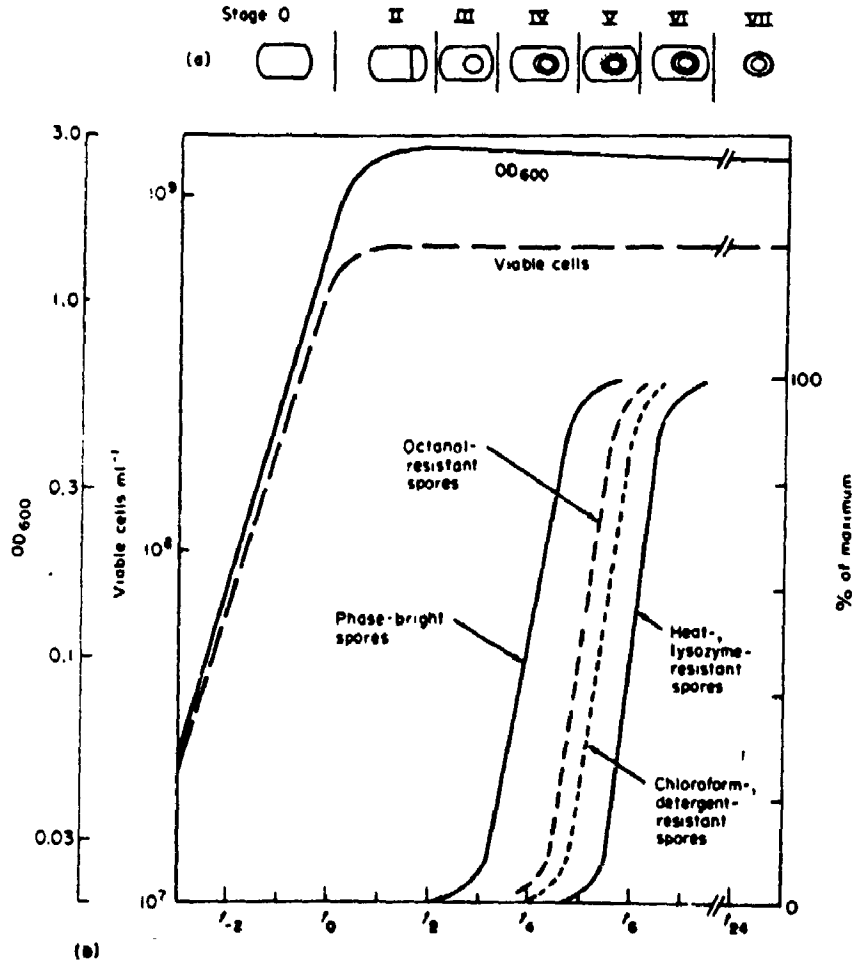

Fig. 2.1: Growth and sporulation of B. subtilis (Freese and Heinze, 1983).

5) stage IV: beginning of spore cell wall primordium and cortex formation;

6) stage V: spore coat deposition;

7) stage VI: maturation of cortex and coat;

8) stage VII: mature spore released by lysis of mother cell.

Completion of stage III marks an irreversible commitment to spore formation: "Most decisive for bacterial differentiation is the ultimate commitment with respect to all compounds, which coincides with the attainment of stage III, that is the complete enclosure of the forespore by a double membrane." (Freese and Heinze, 1983).

Sporulation physiology and parasporal crystal formation in Bacillus thuringiensis are detailed in Fig. 2.2. Crystalline δ-endotoxin is first detectable after stage II (Andrews et al., 1981; Lereclus et al., 1989).

Early sporulation is characterized visually by formation of intracellular granules, apparently composed mainly of PHB (Sect. 2.3). Induction of some or all enzymes of the TCA cycle, with subsequent consumption of organic acids, accompanies the onset of sporulation in bacilli in general (Sect. 2.4). Other metabolic events associated with the transition to sporulation in B. thuringiensis are induction of the glyoxylate cycle (Sect. 2.5), and anaplerotic enzymes ancillary to this and the TCA cycle (Sect. 2.6).

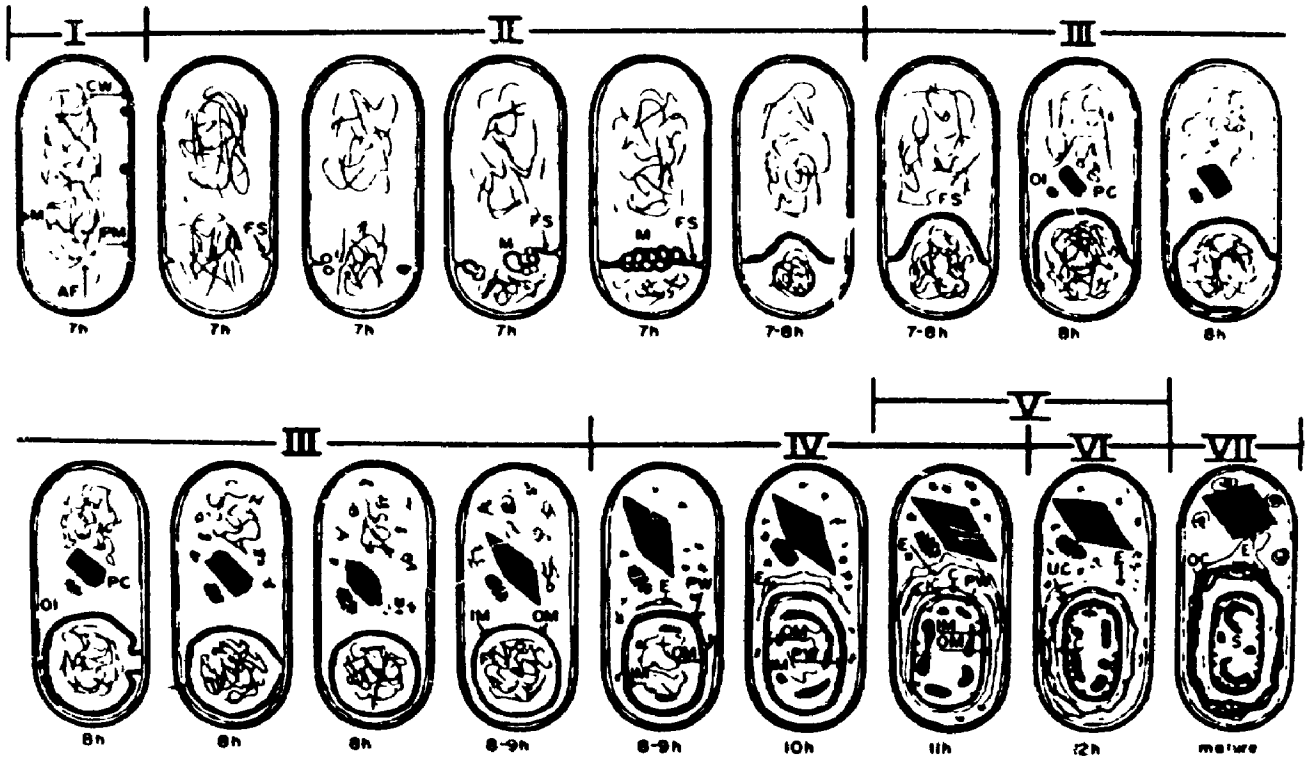

Fig. 2.2: Diagrammatic scheme of sporulation in B. thuringiensis. M ≡ mesosome, CW ≡ cell wall, PM ≡ plasma membrane, AF ≡ axial filament, FS ≡ forespore membrane, IF ≡ incipient forespore, OI ≡ ovoid inclusion, PC ≡ parasporal crystal, F ≡ forespore, IM ≡ inner membrane, OM ≡ outer membrane, PW ≡ primordial cell wall, E ≡ exosporium, LC ≡ lamellar spore, OC ≡ outer spore coat, C ≡ cortex, UC ≡ undercoat, S ≡ mature spore in an unlysed sporangium (Bulla et al., 1980).

The literature in this area is replete with controversy regarding the role of the tricarboxylic acid cycle in sporulation (cf. Sect. 2.4). The older view was that TCA cycle activation is essential for utilization of acetate, etc. for energy production and spore biosynthesis (Gollakota and Halvorson, 1960; Hanson et al., 1964; Yousten and Rogoff, 1969; Ohné, 1975). The opposite view holds that sporulation is not necessarily contingent on TCA cycle activity (Singh, 1970; Yousten and Hanson, 1972; Nickerson et al., 1974). More recent research on artificial inhibition of GTP synthesis has shed light on the relationship between sporulation and glucose catabolite repression of certain TCA cycle enzymes:

> "...catabolite repression of enzyme synthesis is controlled differently from the suppression of sporulation because catabolite-repressible enzymes could not be induced when sporulation was induced by GTP deprivation in the presence of glucose...enzymes specifically made for ATP regeneration via the citrate cycle are needed if sporulation results from carbohydrate limitation but not if it is initiated by deprivation of guanine nucleotides in the presence of glucose." (Freese and Heinze, 1983).

This debate has therefore been resolved against the absolute necessity of TCA cycle activation for sporulation (cf. Sonenshein, 1989).

The onset of sporulation in B. thuringiensis is also accompanied by either a gradual and sustained (Young and Fitz-James, 1959), or rapid and marked (Monro, 1961) decline in cellular free amino acids. This would appear to be related to turnover of endogenous protein, since 80 to 100 per cent of spore protein is formed de novo (Murrell, 1967); and can occur

without exogenous nutrients ("endotrophic" sporulation; cf. Young and Fitz-James, 1959). This was recently confirmed with the HD-1 strain of B. thuringiensis by Anderson (1990): "...protein and ammonia levels remained nearly constant during the later stages of sporulation [after 12 hours] suggesting that nitrogen requirements were largely met by intracellular protein turnover during this phase of development." Thus breakdown or "turnover" of vegetative or mother - cell protein is a major aspect of sporulation metabolism: "...under shift-down conditions, or when growth ceases due to the presence of an inhibitor or to the exhaustion of a nutrient, the rate of [endogenous] protein breakdown increases immediately...to nearly 8 % per hr in Bacillus cereus." (Mandelstam and McQuillen, 1973, p.487). In both B. cereus and B. megaterium the mother cell visibly deteriorates during spore maturation (Freese and Heinze, 1983).

More refined study of protein metabolism in mother - cell and forespore has revealed the importance of protein catabolism in the former:

> "Protein synthesized in the mother - cell compartment at all times during sporulation was subject to extensive breakdown at a rate which increased throughout the sporulation sequence...After t_3, proteins synthesized in the mother-cell compartment are degraded at rates increasingly faster than that for proteins made during vegetative growth." (Ellar et al., 1975).

Although the phenomenon of protein turnover has been known since 1954, its detailed mechanism is not understood (Freese and Heinze, 1983). It is known that cells blocked at stage 0

of sporulation neither produce intracellular protease, nor undergo protein turnover (ibid.; cf. Szulmajster et al., 1975). Thus,

> "Several independent lines of research seem to indicate that the intracellular [protease] enzyme may play a major role in sporulation. Inhibitors of the enzyme do not inhibit vegetative growth but prevent sporulation. All the mutants lacking intracellular serine protease that have been isolated so far failed to sporulate, and were blocked in protein turnover, whereas in revertants both properties were restored." (Keynan and Sandler, 1989).

In B. cereus the enzyme is required for post - translational processing of spore coat precursor, as well as for provision of amino acids (Cheng and Aronson, 1977). The intracellular protease may therefore be involved in formation of δ-endotoxin in B. thuringiensis (cf. Aronson and Fitz-James, 1976; Carroll et al., 1989).

2.2 Glycolysis

Vegetative growth of bacilli is almost universally considered to be primarily at the expense of carbohydrates (Freese and Fujita, 1976); however some catabolism of amino acids during this phase may also occur (Sakharova et al., 1985; Anderson, 1990).

All subspecies of B. thuringiensis use glucose predominantly (93 - 100 per cent) by the EMP pathway, the hexose monophosphate pathway apparently serving biosynthetic needs (Nickerson et al., 1974). Glucose exhaustion, and/or growth inhibition by organic acids (Nakata, 1963), ends the binary

fission process of vegetative growth, although not usually biomass accumulation (Anderson, 1990). Specific growth rate of up to 1.9 hr^{-1} has been reported for B. thuringiensis (Holmberg et al., 1980).

Vegetative growth of B. thuringiensis and B. cereus is accompanied by production of various intermediates such as lactate, pyruvate, acetate, acetoin and 2,3-butanediol (Nakata and Halvorson, 1960; Yousten and Rogoff, 1969). Anderson (1990) found lactate and acetate to be the major intermediates under all conditions of aeration and C:N ratio. Thus, "Lactate formation was tied directly to glucose catabolism and reached peak concentrations in balanced C:N media coincident with maximum glucose utilization." Acetate appeared to arise from both glucose and amino acids; and to be principal intermediate when the rate and/or absolute consumption of glucose were suboptimal (ibid.). The temporal sequence of acetate following pyruvate in B. cereus (Hanson et al., 1963), and radiorespirometry in B. thuringiensis (Bulla et al., 1970b), implicated formation of acetyl-CoA by pyruvate dehydrogenase as a necessary step in acetate production. Formation of acetoin and/or 2,3-butanediol (Sect. 3.1) is apparently dependent on some interaction of pH, acetate concentration and aeration (Anderson, 1990).

Several observations by Anderson (1990) indicate that even during fully aerobic vegetative growth Bacillus thurin-

giensis behaves as a typical facultative anaerobe (cf. Sect. 2.1.1), namely:

1) "...the effects of aeration on vegetative phase biomass and cell formation are nominal under a wide range of aeration conditions. Only under severe oxygen limitations was vegetative phase biomass production affected.";

2) maximum specific growth rate, μ_{max}, was higher (0.83 - 1.11 hr^{-1}) at moderate oxygen transfer rate ($k_{La} \approx 45$ hr^{-1}) than at k_{La} of 120 hr^{-1} ($\mu_{max} \approx 0.63 - 0.70$ hr^{-1});

3) both lactate and acetate accumulated to greater concentrations under conditions of low aeration.

2.3 Poly-β-hydroxybutyrate

Certain microorganisms form poly-β-hydroxybutyric acid (PHB), via acetoacetyl-CoA, under conditions of growth limited by various factors such as oxygen, nitrogen, etc. (Dawes and Senior, 1973). Such formation might benefit the cell in two ways, namely: by acting as an electron sink (ie. regeneration of NAD^+ from NADH); and as an endogenous reserve source of carbon and reducing equivalents (ibid., Sect. 2.3.4). As stated by Dawes and Senior (1973), "Conditions for PHB biosynthesis, namely high $NAD(P)H_2$, high acetyl-CoA and low free coenzyme A concentrations, are produced during oxygen - limitation of growth, which thus stimulates biosynthesis of

the polymer." Macrae and Wilkinson (1958) found a 5 per cent oxygen atmosphere to maximize PHB formation in B. cereus; production of the polymer in hydrogen gas, but not nitrogen, was almost as great as in air.

PHB formation in the B. cereus group has generally been observed to begin in late vegetative growth phase (essentially at t_0), reaching peak concentration at the end of transition phase (Nakata, 1963; Kominek and Halvorson, 1965; Nakata, 1966). Induction of acetoacetyl-CoA reductase is a prerequisite to PHB synthesis (Kominek and Halvorson, 1965). Greatest PHB production by B. cereus strain T occurred in media buffered at pH 6.2 to 6.4 (Nakata, 1963).

Kominek and Halvorson (1965) demonstrated PHB formation to depend on induction of acetoacetyl-CoA reductase. Radiotracer studies showed both acetate and acetoin to be converted to PHB, presumably via acetyl-CoA (ibid.; Nakata, 1966; cf. Sect. 2.3.4). It has been reported that B. megaterium is capable of synthesizing mixed poly-β-hydroxyalkanoates, which include β-hydroxyvalerate and β-hydroxyheptanoate amongst others (Finnerty and White, 1983).

2.4 Tricarboxylic Acid Cycle

The tricarboxylic acid (TCA) cycle is well described in the standard biochemical literature (cf. Lehninger, 1976, p. 443-466). For a more specialized review, dealing especially

with control of bacterial TCA enzyme activity, see Weitzman (1981).

During the vegetative growth phase acetyl-CoA is not appreciably metabolized by the TCA cycle (Hanson et al., 1963; Bulla et al., 1970b), presumably due to catabolite repression (Sect. 2.4). Nevertheless Aronson et al. (1975b) found unexpectedly high levels of second - half TCA cycle enzymes in vegetative cells. Sonenshein (1989) also reported high fumarase activity during vegetative growth on amino acid - rich medium.

In the present context the most important fact about the TCA cycle is that it often does not function as a cycle. Thus in B. thuringiensis subspecies berliner, Aronson et al. (1975a) could not detect α-ketoglutarate dehydrogenase activity by any of three different procedures. This appears to be common amongst facultative anaerobes, at least when grown anaerobically (Gottschalk, 1979, p.154). In the words of Sonenshein (1989):

> "In many respects it is misleading to think of the Krebs [TCA] cycle as a single pathway. The tricarboxylic acid component (citrate to 2-ketoglutarate) has a different role from the dicarboxylic acid component (succinyl coenzyme A [CoA] to oxaloacetate) and seems to be subject to separate, but overlapping, regulation. This is necessary for cell economy. If a cell is supplied with glucose and a good source of 2-ketoglutarate (e.g., glutamate or glutamine), it has little need to express the tricarboxylic acid pathway; under these conditions the enzymes that convert citrate to 2-ketoglutarate are greatly reduced in specific activity."

Induction of early TCA cycle activity has long been associated with the onset of sporulation (Gollakota and Halvorson, 1960; cf. Sect. 1.2). Thus,

> "The citB gene (coding for aconitase)...is transcribed at low level during exponential growth in a nutrient broth medium and becomes induced as cells enter stationary phase...A similar pattern probably holds for citrate synthase (the citA product), although this has only been studied at the level of enzyme activity." (Sonenshein, 1989).

These genes are repressed by glutamate or α-ketoglutarate (Ohné, 1975). They are apparently not transcribed using the major sporulation sigma factor (ie. promoter - recognition subunit of DNA - dependent RNA polymerase), σ^H, as are later TCA cycle enzymes (Sonenshein, 1989). Neither are they strictly necessary for sporulation, in that Ohné and Rutberg (1976) found that mutants of B. subtilis deficient in aconitase or isocitrate dehydrogenase sporulated well if supplied with glutamate (cf. Nickerson et al., 1974, re B. thuringiensis).

Similarity between early TCA cycle enzymes and those of leucine synthesis was noted by Umbarger (1978):

> The leucine pathway uses the same chain-lengthening pattern...which is also the way oxaloacetate is converted to α-ketoglutarate via the tricarboxylic acid cycle. Thus, isopropylmalate isomerase is analagous to aconitase, and β-isopropylmalate dehydrogenase is analagous to isocitrate dehydrogenase."

Furthermore the first TCA enzyme, citrate synthase, catalyzes a very similar reaction to that of α-isopropylmalate synthase, the first enzyme in leucine biosynthesis.

Cells can be divided into two groups based on the regulatory properties of their citrate synthase enzyme (Weitzman, 1981). Gram - positive bacteria (including Bacillus) and all eukaryotic cells are insensitive to inhibition by NADH; citrate synthase of Gram - negative bacteria is inhibited by NADH, with AMP reactivation in some species. Enzyme from the latter organisms is much larger, and composed of more subunits than the former; this appears to reflect the fact that the larger enzyme is subject to allosteric control (ibid.). In facultative anaerobes of the genus Bacillus (viz. B. polymyxa, B. macerans), citrate synthase is also inhibited by α-ketoglutarate; no such inhibition occurs in B. megaterium, a strict aerobe (ibid.).

Isocitrate dehydrogenase in B. thuringiensis, B. stearothermophilus and E. coli is the NADPH - dependent form (ibid., Aronson et al., 1975b). It does not appear to be a regulatory enzyme in bacilli (Weitzman, 1981), unlike in E. coli, where it is subject to complex control via a bifunctional phosphatase/kinase (Holms, 1986). This is necessary to regulate glyoxylate cycle versus TCA cycle flow (ibid.).

Later TCA cycle enzymes, at least succinate dehydrogenase and fumarase, are normally actively expressed only as vegetative growth ends; and are transcribed using a sporulation - associated sigma factor, σ^H (Sonenshein, 1989). However in minimal glucose - casamino acids medium, succinate dehydrogenase, fumarase, and this sigma factor, are expressed early in

vegetative growth (ibid.; Weber and Broadbent, 1975). Aronson et al. (1975a,b) reported high levels of second - half TCA cycle enzymes in vegetative, as well as sporulating, cells of B. thuringiensis grown on glucose/Casamino Acids medium.

Conversion of succinyl-CoA to succinate by succinate thiokinase is the only instance of substrate - level phosphorylation in the TCA cycle. Although most bacteria can phosphorylate either ADP or GDP, bacilli are members of a small group which uses only ADP (Weitzman, 1981). Analagous to citrate synthase, succinate thiokinase of bacilli is the "small", unregulated type:

> "...only Gram - negative bacteria produced the "large" [succinate thiokinase] enzyme, Gram - positive bacteria and eukaryotes producing only the "small" enzyme. There is thus a remarkable correlation between the incidence of "large" and "small" succinate thiokinases and that of "large" and "small" citrate synthases..." (ibid.).

Succinate dehydrogenase is an $FADH_2$ - linked enzyme which passes electrons directly to ubiquinone (cf. Lehninger, 1976, p. 495). It is coded in B. subtilis by the sdh operon (Piggot, 1989), which is strongly repressed by malate (Ohné, 1975). However, in a mutant lacking malate dehydrogenase, this effect was abolished : "...sporulation was completely resistant to repression by malate and partly resistant to repression by glucose. The synthesis of serine [intracellular] protease and DPA [dipicolinic acid] was also resistant to repression by malate." (Ohné and Rutberg, 1976). The same workers found that malate delayed spore formation in wild - type cells if added

by (especially at) t_3, but not if added later. They concluded, "The presence of malate thus affects spore formation as well as the synthesis of enzymes not specifically required for sporulation. This suggests that malate interferes with a general control mechanism governing a number of stationary - phase activities including sporulation." They also found increased malic enzyme (Sect. 2.6) in the mutant lacking malate dehydrogenase.

The activity of succinate dehydrogenase, as in mammals, is strongly inhibited by oxalacetate (Ohné, 1975).

Fumarase is induced by fumarate (ibid.); and the citG gene which codes for it is transcribed by σ^H, the major sporulation - associated sigma factor (Sonenshein, 1989). citG expression appears to be unique amongst σ^H - dependent genes, since it requires only availability of the sigma factor; other genes need an additional, unknown, stationary - phase effector (ibid.). As described above, fumarase, and σ^H itself, are expressed under certain conditions of vegetative growth, as well as during the transition to sporulation (cf. Sect. 9.7).

Malate dehydrogenase seems to be a "weak link" in the TCA cycle. Thus, "...malic [malate] dehydrogenase alone does also not produce oxalacetate at a rate necessary for optimal growth...The equilibrium constant of malic dehydrogenase and the stabilizing effect of NADH favor the production of malate." (Diesterhaft and Freese, 1973). Furthermore,

> "...malate dehydrogenase [of B. subtilis] is strongly inhibited by AMP and shows an energy charge response

> usually observed only for biosynthetic enzymes. The reason for this unexpected behaviour is not clear. The finding that malate dehydrogenase and malic enzyme are differentially controlled by the adenine nucleotides suggests that the energy charge may influence the metabolism of malate. Thus, a drop in the energy charge will result in an increased proportion of malate being metabolized via malic enzyme to pyruvate." (Ohné, 1975).

This is compatible with the finding that a number of bacilli (and a few other bacteria) contain malate dehydrogenase approximately twice as large as that of most cells (Weitzman, 1981). In the words of this reviewer,

> "No special regulatory properties have been attributed to the "large" enzyme and it is interesting that the incidence of the "large" malate dehydrogenase among certain Gram - positive bacteria contrasts with the occurrence of "large" forms of citrate synthase and succinate thiokinase only in Gram - negative bacteria."

Finally, Ohné and Rutberg (1976) reported that a B. subtilis mutant devoid of malate dehydrogenase sporulated normally when supplied with oxalacetate. "This is the first instance of complete restoration of sporulation in a citric acid cycle mutant." (ibid.).

2.5 Glyoxylate Cycle

Glyoxylate cycle enzymes are isocitrate lyase, which produces glyoxylate and succinate from isocitrate; and malate synthase, which adds acetyl-CoA to glyoxylate to form malate (cf. Lehninger, 1976, p.466). Isocitrate lyase is induced in B. cereus T during the phase of most active granulation, ie. during early sporulation (Megraw and Beers, 1964). There is

controversy over whether activity declines during later sporulation (cf. ibid.; Aronson et al., 1975a). Contrary to that found in many organisms, enzyme expression was much greater in amino acid - rich media (Megraw and Beers, 1964). Malate synthase of B. thuringiensis is apparently most active early in sporulation (Aronson et al., 1975a).

Megraw and Beers (1964) demonstrated the possibility of formation of 3-phosphoglyceric acid (PGA) from glyoxylate via the glycerate pathway (cf. Gottschalk, 1979, p.122). This might be used during late sporulation (ie. post stage III) to produce PGA at up to 5 per cent of dry matter (cf. Freese and Heinze, 1983; Setlow, 1983).

2.6 Pyruvate Carboxylase and Malic Enzyme

Pyruvate carboxylase consumes one ATP to add CO_2 to pyruvate, thus producing oxalacetate. The enzyme, which is strongly activated by acetyl-CoA, is constitutive in B. subtilis (Diesterhaft and Freese, 1973). It is necessary for growth on glucose but is not required for sporulation. Rather gluconeogenesis occurs via phospho-enolpyruvate carboxykinase, which is repressed by glucose; this enzyme is normally required for sporulation to occur (ibid.).

Malic enzyme (malate dehydrogenase [decarboxylating]) simultaneously decarboxylates and dehydrogenates malic acid to form pyruvic acid (and in principle the reverse reaction).

Properties of the enzyme, especially from vertebrate sources, were reviewed by Frenkel (1975). Malic enzyme, which occurs in most types of cells, appears to be universally activated by succinate.

In E. coli two forms of the enzyme exist, namely an NAD^+ - dependent and an $NADP^+$ - dependent form (Murai et al., 1971). Both are allosteric, and operate in the direction of conversion of malate to pyruvate (ibid.; Sanwal, 1970; Murai et al., 1972). Both enzymes are also repressed by glucose, although induction of the NAD^+ form by malate overcomes the glucose effect (Murai et al., 1971). The $NADP^+$ - dependent form of malic enzyme is inhibited by acetyl-CoA, oxalacetate, NADPH and NADH (Sanwal and Smando, 1969). The NAD^+ - dependent enzyme is inhibited by ATP and CoA, and activated by aspartate (Sanwal, 1970).

Induction of malic enzyme by malate in B. subtilis is not repressed by glucose (Diesterhaft and Freese, 1973). It is five times more active with NAD^+ as cofactor than with $NADP^+$ (ibid.). The enzyme from B. stearothermophilus also has a much higher affinity for NAD^+ (Kobayashi et al., 1989). The major role of malic enzyme in bacilli thus appears similar to that of the NAD^+ - dependent form in E. coli, namely: "...NAD-enzyme is presumed to play a role in the catabolism of malate, controlling the concentrations of C_4-dicarboxylic acids." (Murai et al., 1972). This function would appear to be regulated by energy availability.

3. Metabolism of Branched - chain Amino Acids in Bacteria

3.1 Biosynthesis of Branched - chain Amino Acids

Most microorganisms are capable of synthesizing the three branched - chain amino acids (BCAA's; viz. isoleucine, valine and leucine) by the sequences of enzymatic reactions shown in Fig. 3.1 and 3.2. The biosynthesis of these amino acids, including its regulation, based mostly on work with E. coli and Salmonella typhimurium, has been reviewed by several authors (Umbarger, 1978; Iaccarino et al., 1978; Meister, 1965, p. 729 et seq.). These should be consulted for a complete discussion and bibliography on this subject; see Sokatch (1986) for a recent general review.

The phenomenon of antagonism of a property of one substance by another is exibited by certain sets of amino acids, and is charteristic of the BCAA's (cf. De Felice et al., 1979). According to Umbarger (1978), "The kinds of antagonism that have been found [in bacteria] are interference with active transport into the cell, interference with end - product control, interference with repression control, and, perhaps, interference with incorporation into protein." Early work on the effect of the BCAA's (and the serine/methionine/threonine/glycine group) with various Bt strains showed the prevalence of such antagonism: "Sensitivity to the particular amino acids studied is apparently common to this group of bacilli [ie. Bt] and also to B. cereus, to which

these crystal - formers are related. The particular patterns of inhibition do, however, vary considerably between strains. Most of the B. thuringiensis strains tested by us to date are sensitive to at least one of the valine/ leucine/isoleucine groupings." (Singer and Rogoff, 1968; cf. Conner and Hansen, 1967).

The three BCAA's are all formed at least partially from pyruvate, as are two other amino acids, alanine and lysine (see Fig. 3.1; lysine pathway not shown). Isoleucine, which obtains only two of its six carbon atoms from pyruvate, has however much in common with valine, sharing most of the enzymes required for their synthesis (Fig. 3.1). Control of carbon flow over the pathway from pyruvate to isoleucine is effected by inhibition of threonine deaminase by isoleucine (Reaction 1, Fig. 3.1). Valine is a positive effector, which reverses inhibition by isoleucine (ibid.). In addition to this biosynthetic threonine deaminase (EC 4.2.1.6), there may be expressed a degradative enzyme (EC 4.2.1.16) not inhibited by isoleucine, as reported for E. coli (Shizuta and Tokushige, 1971) and Clostridium tetranomorphum (Nakazawa, 1971).

Control of carbon flow for the pathway leading to valine and leucine occurs at the first step (ie. acetohydroxy acid synthetase); and may thus also block isoleucine synthesis, giving rise to the phenomenon of antagonism discussed above.

End - product control of carbon flow to leucine is effected at the first step in its synthesis from α-ketoisoval-

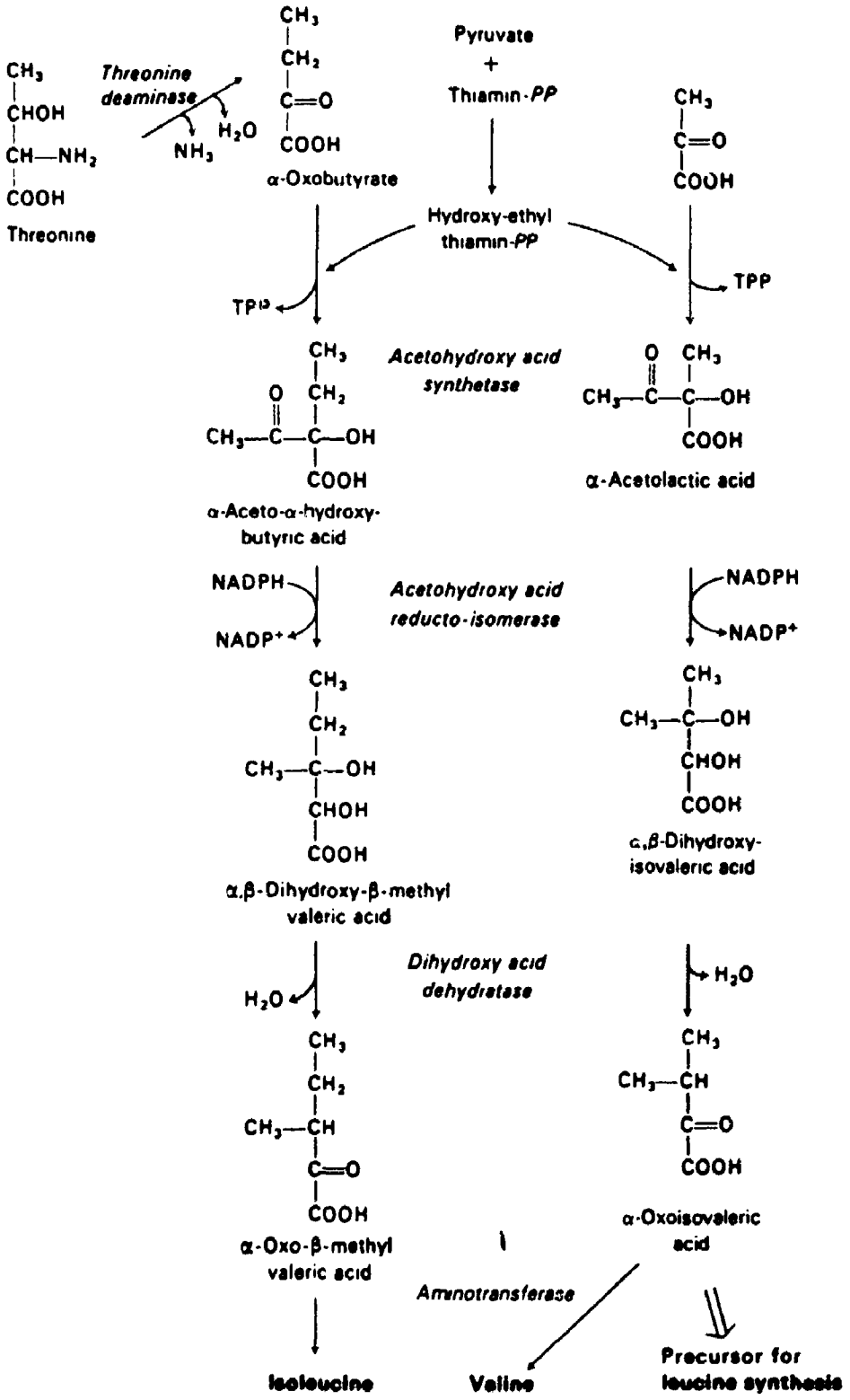

Fig. 3.1: Biosynthesis of isoleucine and valine. Note that valine is formed from two molecules of pyruvate (Bender, 1985).

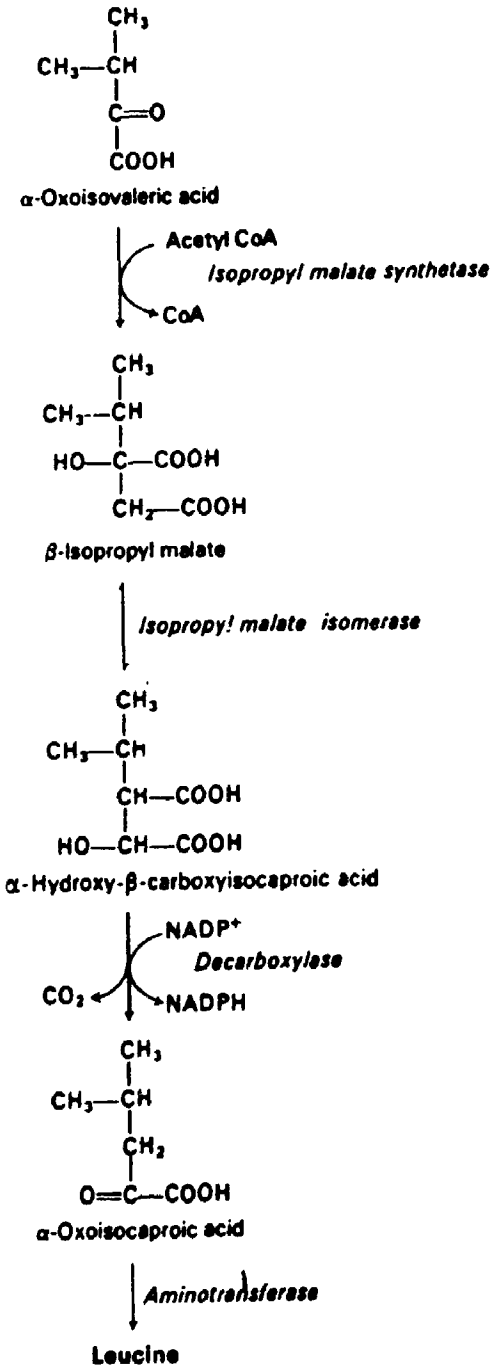

Fig. 3.2: Biosynthesis of leucine. See Fig. 3.1 re synthesis of α-oxoisovaleric acid (Bender, 1985).

erate (α-oxoisovaleric acid, Fig. 3.2). This enzyme, α-isopropylmalate synthetase, possesses broad biosynthetic capabilities: "The enzyme from a variety of sources has been shown to have only a limited specificity; it can transfer the acetyl group not only to α-ketoisovalerate but also to pyruvate, α-ketobutyrate, α-ketovalerate, and even to α-ketoisocaproate itself." (Umbarger, 1978). These alternative pathways are not normally significant, but might function under specific conditions.

At least three BCAA - active transaminase enzymes are found in E. coli (ibid.; Braunstein, 1973; cf. Meister, 1965, p. 338 et seq. for an extensive discussion). Transaminase B catalyzes amino group transfer between glutamate and any of the three BCAA's, as well as methionine and phenylalanine. The enzyme was found to be constitutive in P. aeruginosa, and to have Michaelis constants for amino and keto acid substrates consistent with a possible role in both biosynthesis and catabolism (Massey et al., 1976; cf. Sokatch, 1986, re P. cepacia). The order of activity was leucine > isoleucine > valine, as for transaminase B in E. coli (ibid.). Transaminase C functions in the terminal reaction in valine synthesis, with alanine or α-aminobutyrate as donors; and has leucine, valine and α-ketoisovalerate as effectors. Transaminase A, active between leucine and glutamate, also transaminates aspartate,tyrosine and phenylalanine (Iaccarino et al., 1978).

Regulation of expression of these biosynthetic systems at the genetic level is complex, presumably due to the need to coordinate biosynthesis of three end products using largely common enzymes (Iaccarino et al., 1978). As these authors state, "...isoleucine and valine biosynthesis is a model system for study of the mechanisms by which the cell coordinates different parts of its total metabolism." These amino acids cannot be treated wihout reference to leucine:

> "The question regarding the role of the loci known to affect the leucine biosynthetic pathway can be extended to the isoleucine and valine biosynthetic pathway, for some of the enzymes of isoleucine and valine biosynthesis are repressed by a mechanism that involves leucine as one of the multivalent repressors. Of those that do, all involve a 'leucine excess' signal that is apparently generated in the same way for the ilv regulon [isoleucine, valine] as it is for the leu operon [leucine]." (Umbarger, 1978)

Genetic research has located three structural genes for α-acetolactate synthetase in E. coli K-12: "The best interpretation of current evidence is that there are three isoenzymes: AHAS I, the product of the ilvB gene; AHAS II, the product of the ilvG gene; and AHAS III, the product of the ilvHI genes. AHAS I and AHAS III are sensitive to valine inhibition; AHAS II is resistant to valine inhibition..." (Iaccarino et al., 1978). However according to Umbarger (1978) the latter is multivalently controlled by isoleucine, valine, and leucine.

Both ilvB and ilvG genes are present in S. typhimurium. A. aerogenes possesses an α-acetolactate synthetase active in acetoin formation with pH optimum of 6 (Stormer, 1968), and

another for isoleucine and valine synthesis with pH optimum of 8 (ibid.; acetoin is formed by irreversible decarboxylation of α-acetolactate, cf. Löken and Störmer, 1970). It is interesting that in both A. aerogenes and Neurospora crassa, the product of the "pH 6 acetolactate - forming" enzyme is not available for amino acid biosynthesis (Iaccarino et al., 1978).

In the enterobacteria, wild - type cells grown on complex media exhibit strong repression of all enzymes responsible for BCAA biosynthesis (Rodwell, 1969). In E. coli and S. typhimurium, the enzymes converting α-ketoisovalerate to α-ketoisocaproate are coordinately repressed by leucine (Mandelstam and McQuillen, 1973, p.225).

3.2 Catabolism of Branched - chain Amino Acids

Pathways for the degradation (catabolism, oxidation) of the BCAA's are shown in Fig. 3.3 and 3.4. These enzyme systems have been reported in a wide variety of bacteria (Massey et al., 1976), although most studies have been with Pseudomonas species. The first step in catabolism of the BCAA α-keto acids, catalyzed by branched - chain keto acid dehydrogenase, is performed by a single enzyme (ibid.; transamination is discussed in Sect. 3.1). Some results also suggest that the acyl-CoA dehydrogenase enzyme may be common to all three pathways, and that enoyl-CoA hydratase may be shared at least

Fig. 3.3: Catabolism of isoleucine and valine. Both yield succinyl-CoA; the former also gives acetyl-CoA (Lehninger, 1976).

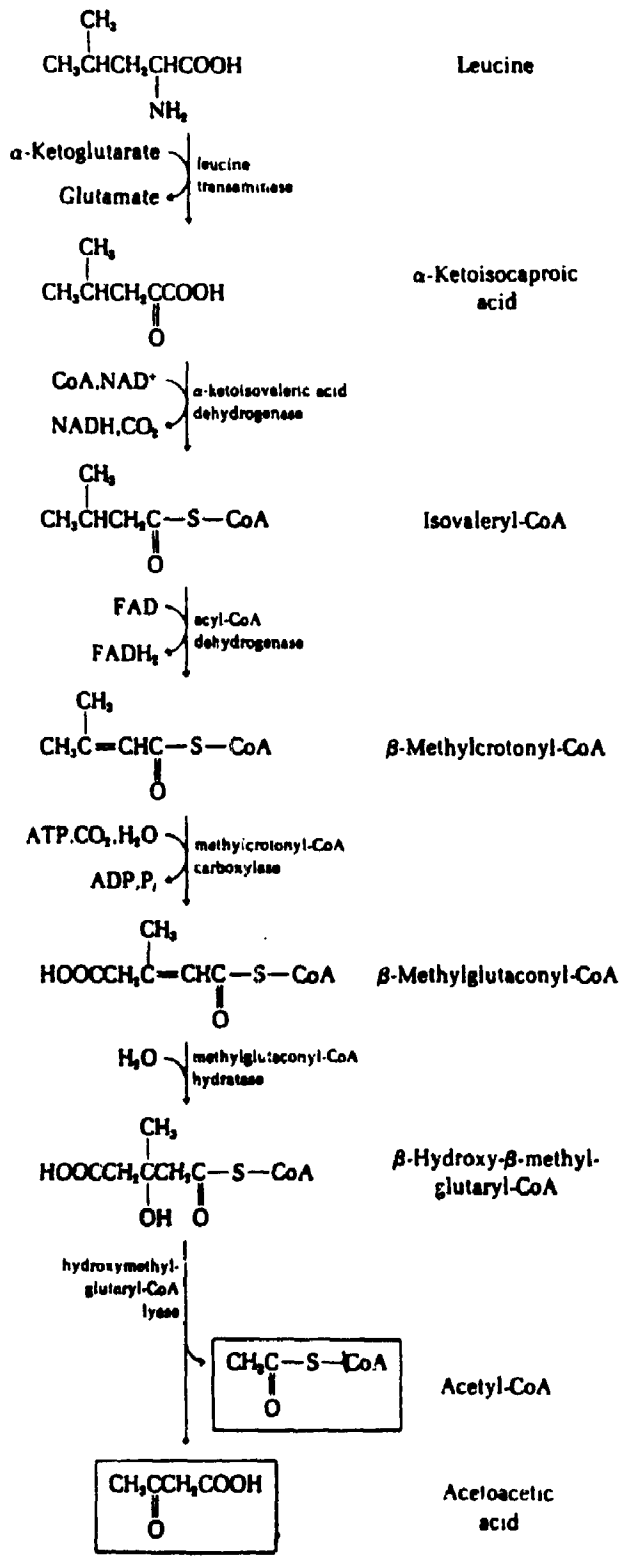

Fig. 3.4: Catabolism of leucine (Lehninger, 1976).

by the valine and isoleucine pathways (ibid.). As these authors state, "This type of branched pathway is unusual in bacterial physiology, since it consists of segments of enzymes common to the catabolism of leucine, isoleucine, and valine followed by three segments with enzymes specific for each amino acid."

Branched - chain keto acid dehydrogenase (BCKA DH; also known as α-ketoisovaleric acid dehydrogenase) catalyzes the first step of the degradation pathways. Since this reaction gives every indication of being irreversible in vivo (cf. Lehninger, 1976, p. 450; Lowe et al., 1983), it is likely to be the primary locus of control for these pathways: "Two generalizations that apply to the regulation of enzyme activity can be made about the reaction catalyzed by the enzyme subject to modulation. It is thermodynamically irreversible and it comes immediately after a branch point of two (or more) metabolic routes." (Mandelstam and McQuillen, 1973, p.457).

This enzyme exhibits several unusual features. Firstly it has been reported that, in B. subtilis, this enzyme and pyruvate dehydrogenase are one and the same (Lowe et al., 1983). In this case pyruvate and α-ketoisovalerate were found to be competitive substrates, with a marked preference for the former. The occurrence and significance of this phenomenon in bacilli in general is not known. BCKA DH is clearly very closely related to pyruvate dehydrogenase (Massey et al.,

1976); and most BCKA dehydrogenases have significant activity with pyruvate (Sokatch, 1986).

The second unusual feature of BCKA DH is its activation by the branched - chain amino acids, as reported by Roberts and Sokatch (1978): "To our knowledge, this is the first time that an amino acid has been demonstrated to be an activator of an enzyme in its own catabolic pathway." These results, for Pseudomonas putida (where the enzyme is distinct from pyruvate dehydrogenase), are shown in Table 3.1. Thus in this organism at least, activation of oxidation of the three α-keto acids is in the same relative order, ie. valine > isoleucine > leucine; the reaction rate is highest with α-ketoisovalerate, and somewhat greater towards α-keto-β-methylvalerate than α-ketoisocaproate. The same relative activities have also been reported for the constitutive enzyme from B. subtilis, and that from S. faecalis (Massey et al., 1976). In P. putida the three BCKA's were equally effective as inducers of the dehydrogenase (ibid.).

The nature of the branched - chain acyl-CoA dehydrogenase enzyme(s) in bacteria, and its (their) possible relationship to similar enzymes active in β - oxidation of fatty acids, are unclear (ibid.). Mitochondria from rat liver cells are reported to contain five distinct acyl-CoA dehydrogenases, including one specific for 2-methylbutyryl-CoA and isobutyryl-CoA, and another specific for isovaleryl-CoA and n-valeryl-CoA (Ikeda et al., 1983).

Additions to Standard Assay	nanomoles NADH/min with		
	aKIV	aKMV	aKIC
None	15.4	10.7	9.4
1 micromole L-VALINE	46.3	24.0	28.3
1 micromole L-ISOLEUCINE	27.0	18.2	16.2
1 micrmole L-LEUCINE	19.5	14.3	12.4

Table 3.1: Stimulation of branched - chain α-ketoacid dehydrogenase by branched - chain amino acids. aKIV ≡ α-ketoisovalerate; aKMV ≡ α-keto-β-methylvalerate; aKIC ≡ α-ketoisocaproate (Roberts and Sokatch, 1978).

Three enzymes beyond the described common pathway are required to complete the catabolism of leucine to acetoacetate, namely: methylcrotonyl-CoA carboxylase, methylglutaconyl-CoA hydratase, and hydroxymethyl-glutaryl-CoA lyase (see Fig. 3.4). All three were induced during growth of P. putida on isovalerate as sole carbon source; the carboxylase and the lyase were repressed by glucose or glutamate in cells grown on leucine (Massey et al., 1976). In this organism and E. coli the acetoacetate produced by leucine degradation can be converted to acetyl-CoA by the combined action of acetoacetyl-CoA : succinyl-CoA transferase and acetoacetyl-CoA thiolase, induced by acetoacetate (ibid., cf. Lehninger, 1976, p. 554).

The three enzymes specific to isoleucine catabolism beyond acyl-CoA dehydrogenase (Fig. 3.3) were induced during growth of P. putida on any of isoleucine, 2-keto-3-methylvalerate, 2-methylbutyrate or tiglate. The catabolic hydratase and dehydrogenase were distinct from similar enzymes involved in fatty acid oxidation. Interestingly the dehydrogenase also oxidized β-hydroxybutyryl-CoA to acetoacetyl-CoA (ibid.). Conversion of propionyl-CoA to succinyl-CoA, the final step in catabolism of both isoleucine and valine (cf. methionine), is performed by propionyl-CoA carboxylase, methylmalonyl-CoA racemase, and methylmalonyl-CoA mutase (Fig. 3.3).

In the valine catabolic pathway at least two enzymatic reactions, and perhaps as many as four, are specific for the

conversion of methylacrylyl-CoA to propionyl-CoA. An enoyl-CoA hydratase was induced in P. fluorescens by growth on BCAA's, BCKA's or short branched - chain fatty acids. However the specificity of this enzyme is unresolved: "There is still no conclusive evidence that methylacrylyl-CoA hydratase (enoyl-CoA hydratase) is unique to the valine catabolic pathway. A hydration step is required for the catabolism of every branched - chain amino acid...[and] isoleucine and leucine catabolic intermediates were more effective than valine as inducers of the hydratase when used as the sole source of carbon." (Massey et al., 1976).

The next enzyme of valine catabolism, 3-hydroxyisobutyryl-CoA hydrolase, was induced in P. fluorescens by growth on valine, α-ketoisovalerate, isobutyrate or 3-hydroxyisobutyrate. The formation of the hydrolase was repressed by several tricarboxylic acid cycle intermediates. The same pattern of induction and repression was observed for 3-hydroxyisobutyrate dehydrogenase. This enzyme was specific to the valine pathway in P. aeruginosa (ibid.).

In the next step methylmalonate semialdehyde is oxidatively decarboxylated to propionyl-CoA by methylmalonate semialdehyde dehydrogenase. In two Pseudomonas species the enzyme was induced coordinately with 3-hydroxyisobutyrate dehydrogenase (ibid.). Conversion of propionyl-CoA to succinyl-CoA has already been described.

3.3 Branched - chain Fatty Acid Metabolism

Our knowledge of fatty acid (FA) metabolism in the genus Bacillus comes mostly from the work of T. Kaneda of the Alberta Research Council (cf. Kaneda, 1977, re bibliography; cf. Kaneda et al., 1983; Kaneda and Smith, 1980). In his words, "Some 48 species of the genus Bacillus are recognized...Of these, 22 species have been examined, all of which were found to contain iso and anteiso saturated fatty acids as major acid components of lipids (60 to 90 % of the total fatty acids)." The relevance of this fact to branched - chain amino acid (BCAA) metabolism is apparent from Fig. 3.5, which shows the conservation of the carbon skeleton of the particular BCAA, in α-keto acid, acyl-CoA and fatty acid. Terminally methyl - branched iso and anteiso fatty acids having 12 to 17 carbon atoms were found in all Bacillus species studied (Kaneda, 1977). [Iso (i) and anteiso (a) refer to a methyl side - chain in the penultimate and antepenultimate positions, respectively, as compared with the normal (n) fatty acids.] Minor amounts of saturated normal and unsaturated fatty acids are also present.

The branched - chain fatty acid synthetase complex found in bacilli differs from that responsible for production of myristic and palmitic acids in most other cells, in that it uses as chain initiators branched, short - chain acyl-CoA esters (isobutyryl-, isovaleryl-, and 2-methylbutyryl-CoA),

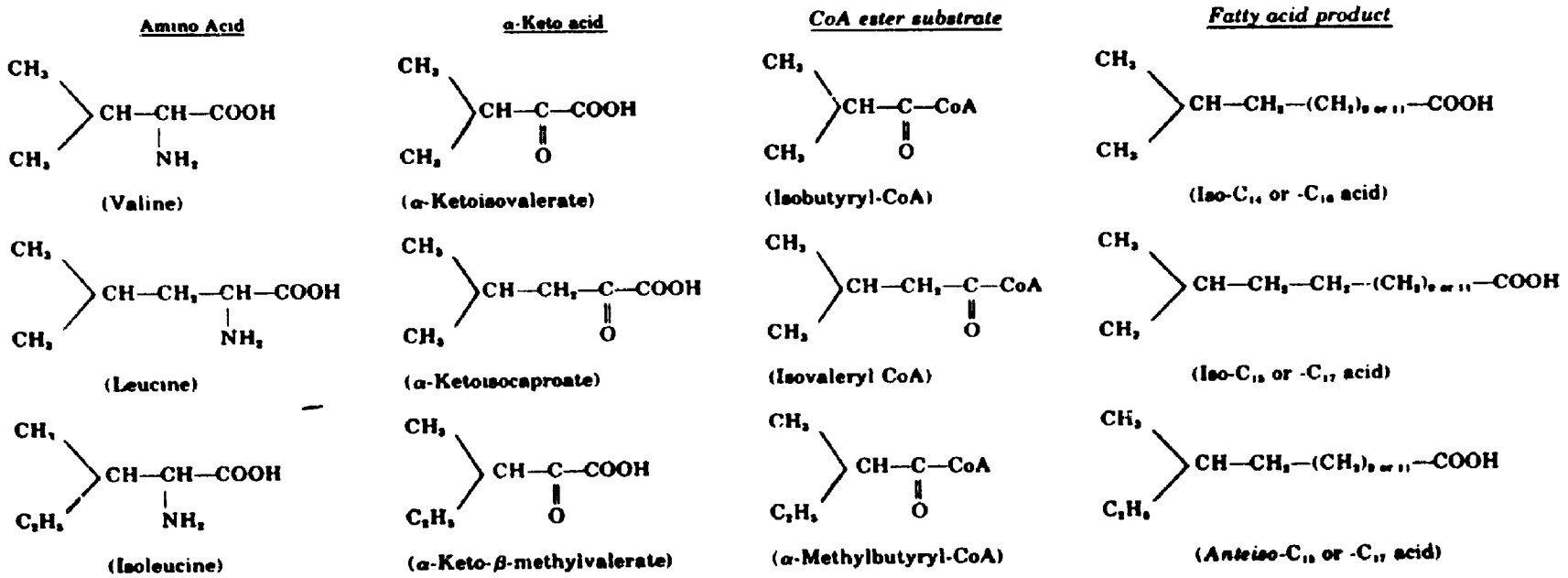

Fig. 3.5: Structural correlation of branched - chain substrates and fatty acid products (Kaneda, 1977).

rather than acetyl-CoA. These properties are discussed in detail in Sect. 5.5. Fatty acid chain elongation is accomplished as usual by adding successive malonyl-CoA units, with NADPH as hydrogen donor (Schweizer, 1989; cf. Lehninger, 1976, p. 663 et seq.).

Fatty acid profiles of two strains of B. thuringiensis (var. thuringiensis, and B-2172) during vegetative growth were found to contain 12 saturated and 4 monounsaturated compounds in the 12 to 17 carbon range (Kaneda, 1968). Branched - chain saturated and unsaturated fatty acids were 70 to 80 % of the total; unsaturated acids comprised 14 to 20 % of the total fatty acids. The pattern in Bt was very similar to those in B. cereus and B. anthracis, ie. some fatty acids with less than 14 carbon atoms, more i-C15 acid than a-C15 acid, and significant proportions of unsaturated fatty acids.

The same study found significant differences in Bt fatty acid composition dependent on the growth medium:

> B. thuringiensis, when grown on glucose - yeast extract medium, produced four classes of fatty acids, the combined odd - numbered iso (related to leucine), the combined anteiso (related to isoleucine), the combined even - numbered iso (related to valine), and the combined normal, in decreasing order of relative abundance...When Pennassay Broth, an amino acid - rich medium, was used to grow B. thuringiensis, in both cases the relative proportion of the combined odd - numbered iso acids increased greatly, to nearly 50 % of the total fatty acids, and that of the combined normal fatty acids also increased slightly; in contrast, the proportions of the combined anteiso fatty acids and of the combined even - numbered iso fatty acids decreased significantly. A similar effect with Pennassay Broth has been observed with the other 10 bacilli [Kaneda, 1967]." (Kaneda, 1968).

A summary of fatty acid composition results for several B. thuringiensis and B. cereus strains grown on different liquid media is shown in Table 3.2. The vegetative cell results show considerable variation amongst the various strain and medium combinations. In order to separate the effects due to strain from those due to the medium, a multivariate analysis of variance (MANOVA) determination was made using the two data sets contributed by Kaneda (Table 3.2). Specifically, using SYSTAT™ (SYSTAT, Inc., Evanston, IL), each of the four fatty acid group (dependent) variables were subjected to bivariate linear regression in terms of the two categorical (independent) variables strain and medium composition. Thus the "strain" category consisted of four members (viz. Bt var. thuringiensis, and B-2172; and B. cereus var. B-17 and B-19), and the "medium" category contained two members (viz. glucose - yeast extract medium, and Pennassay Broth). Post-hoc tests of significance for the categorical variables at the 95 per cent confidence level led to the following conclusions:

1) there was no significant difference amongst the strains with respect to grouped fatty acid content on the same medium (ie. all four values of the F statistic were much lower than that required to indicate a significant effect due to strain); in other words, both B. thuringiensis and B. cereus strains responded identically to a given medium in terms of fatty acids biosynthesis;

Reference	Strain	Medium, g/litre		iso-Even	iso-Odd	anteiso-Odd	Normal
		Glucose	Yeast Extract				
Kaneda (1967)	B cereus B-17	10	1	27	33	22	18
	B cereus B-19	10	1	24	37	22	17
	B cereus B-17	Pennassay broth		10	64	10	16
	B cereus B-19	Pennassay broth		14	55	14	16
Kaneda (1968)	Bt thuringiensis	10	1	23.9	36.9	17.5	18.3
	Bt B-2172	10	1	28.9	35.4	21.4	15.2
	Bt thuringiensis	Pennassay broth		16.6	46.8	14.5	19.6
	Bt B-2172	Pennassay broth		12.0	53.9	14.3	17.4
Bulla et al. (19	Bt B-2172	2	15	10.0	38.3	11.4	40.2
	Bt NRS-996	2	15	12.6	44.8	9.7	32.9
Bulla et al. (19	Bt NRRL B-4027:	1	2				
	vegetative cells			14.9	33.5	40.1	11.3
	mature spores			18.9	45.3	24.1	10.5

Table 3.2: Fatty acid profiles reported for . cereus and B. thuringiensis. Pennassay broth composition, g/litre: glucose, 1.0; yeast extract, 1.5; tryptone, 5.0; beef extract, 1.5.

2) there was a highly significant effect due to growth medium on the relative content of iso - even, iso - odd, and anteiso fatty acids in the four organisms (ie. F statistics ranged from 16.6 to 27.1, much higher than the value of $F_{3,3} = 9.28$ required for significance [cf. Benjamin and Cornell (1970),p. 667]); growth medium was not, however, a good predictor of normal FA content.

To summarize these important findings (admittedly derived from a small data set, yet statistically significant at the 95 per cent confidence level), Bt and B. cereus are indistinguishable in terms of fatty acid profiles on the same medium; furthermore the growth medium has a profound effect on their relative contents of fatty acids formed from the three branched - chain acyl-CoA primers. Thus the observations made by Kaneda (see above) have been verified categorically, and statistically quantified.

It is also noteworthy that the canonical coefficients for the only (highly) significant eigenvector are positive, and approximately equal, for the iso - even, iso - odd, and normal variables; in contrast the canonical coefficient for the anteiso variable is negative, and approximately of the same magnitude as each of the other coefficients. The anteiso FA group thus shows a response to medium opposite to those of the other groups of fatty acids.

The fatty acid data for Bt spores (Bulla et al., 1975), shown in Table 3.2, does not appear to differ significantly from the overall results for vegetative cells. However vegetative cells from which these spores arose were much lower in iso - odd, and higher in anteiso, fatty acid contents.

Scandella and Kornberg (1969) observed substantial alteration in fatty acids of B. megaterium during the cell cycle:

> "Cells in which spore development was underway but in which refractile spores were not yet apparent showed definite changes in fatty acid abundances. There were large increases in br-C14 [i-C14] and br-C16 [i-C16], especially in PG [phosphatidylglycerol]; the ratio of br-C15 [combined i-C15, a-C15] to br-C14 was thus reduced from a value of about 7 in log-phase cells to about 1 in the sporulating cells...It is evident that the major production of br-C14 and br-C16 comes after 4 hr, when the exponential phase of growth is over and the cells are committed [sic] to sporulation..."

These authors also reported large changes in cellular fatty acid content during sporulation, namely:

1) during logarithmic growth: 2.9 ($\pm$0.5) x 10^{-14} g/cell;

2) just before development of refractile forms:

   6.0 ($\pm$1.2) x 10^{-14} g/cell;

3) free spores: 1.7 ($\pm$0.3) x 10^{-14} g/spore (ibid.).

Sporulation was associated with a doubling of fatty acids; spore maturation, conversely, might involve their oxidation.

In contrast with B. megaterium, Scandella and Kornberg (1969) found no change in fatty acids during sporulation of a strain of B. subtilis. However Ishihara et al. (1977) reported progressive increase in i-C14 and i-C16 fatty acids of B.

subtilis from vegetative cell to mature spore. They also observed increasing i-C15, and decreasing a-C15 fatty acids, during evolution from vegetative growth to mid - sporulation; these patterns then reversed as the spore matured.

Bulla et al. (1975; cf. Nickerson et al., 1975) dealt primarily with fatty acid production during spore germination and outgrowth of B. thuringiensis. The significance of these patterns is briefly discussed in Sect. 9.7.

Finally it should be noted in passing that the failure of Bt to grow with glucose as sole carbon source has been attributed to a requirement for a compound capable of stimulating fatty acid biosynthesis (Nickerson and Bulla, 1975).

4. Experimental Methods

4.1 Microorganism, Medium and Inoculum

The microorganism used in all work was *Bacillus thuringiensis* subspecies *kurstaki*, strain HD-1, kindly provided by the United States Department of Agriculture, Insect Pathology Research Unit, Brownsville, Texas. The physiology of this organism was described in detail by Bulla *et al.* (1980); its genetics was recently reviewed by Lereclus *et al.* (1989).

Appropriate pure culture techniques were used throughout; fermentation samples were routinely plated, incubated and examined to verify freedom from contamination.

The lyophilized culture was suspended in TGY broth (see below); and incubated aerobically at 30 °C with rotary agitation at 250 RPM. After about two days the culture was streaked on TGY agar plates, which were incubated at room temperature. After about 3 days a typical colony, apparently derived from a single spore, was used to inoculate two flasks containing TGY broth. These were incubated and plated as before. To each plate was added 3 ml of double strength skim milk, prepared by dissolving 30 ml of instant skim milk powder (Stacey Brothers, Mitchell, Ont.) in 50 ml of distilled water. A spore suspension was made by scraping the agar surface with an inoculating needle; and transferred to ampoules via Pasteur pipet. These were quickly frozen at -20 °C; lyophilized at 8-10 μm Hg for 48 hr; then flame sealed.

Fresh working cultures were prepared from the above master culture ampoules every 2-3 months. Lyophilized culture was revived in TGY broth as described above; and used to inoculate several TGY agar slants. After incubation for two days at room temperature, these were stored in a refrigerator.

Medium for routine culture growth, designated TGY broth, was prepared according to the following recipe (Haynes et al., 1955): Bacto tryptone (Difco Laboratories Inc., Detroit, MI), 5.0 g; yeast extract (Cat. No. Y-4000; Sigma Chemical Co., St. Louis, MO), 5.0 g; D-glucose (USP grade, anhydrous; Corn Products Co., Englewood Cliffs, NJ), 1.0 g; dipotassium hydrogen phosphate (ACS grade; BDH Chemicals Ltd., Toronto, Ont.), 1.0 g; tap water, 1.00 litre. The pH was 7.0 without adjustment. After dissolution, small quantities were autoclaved at 121 °C for 15 to 20 min. For TGY agar, 20 g of agar (Difco Laboratories Inc., Detroit, MI) was suspended in the above; and gently heated with occasional stirring to dissolve.

Fermentations were performed using complex media designed to provide carbon and nitrogen in balanced ratio, with other required elements in slight excess, as shown in Table 4.1. Buffered tryptone/yeast extract medium had the following composition (per litre): D-glucose, 10.00 g; Bacto tryptone, 3.20 g; yeast extract, 3.20 g; pH 7.0 phosphate buffer (see below), 100 ml; mineral salts solution (see below), 100 ml. Buffered Casamino Acids/yeast extract medium was identical except that Casamino Acids (Cat. No. 0230-01; Difco Labora-

Component	Medium Concentration, g/litre
D-glucose	10.00
Bacto tryptone or Casamino Acids	3.20
yeast extract	3.20
sodium dihydrogen phosphate monohydrate	1.153
disodium hydrogen phosphate	1.856
potassium chloride	0.500
magnesium sulfate septahydrate	0.300
calcium chloride dihydrate	0.106
ferric citrate n-hydrate	0.075
manganous sulfate	0.050
zinc sulfate septahydrate	0.0075
cupric sulfate	0.0045

Table 4.1: Composition of fermentation media.

tories Inc., Detroit, MI) was used in place of Bacto tryptone. With the exception of the nitrogen sources, which were combined, each ingredient above was autoclaved separately, cooled, and mixed. This prccedure was followed with the last two inoculum stages, as well as the main fermenter. The pH of the latter was always slightly acidic after initial reparation, and was adjusted to 7.0 with 3 M sodium hydroxide before inoculation.

Phosphate buffer, pH 7.0, also containing a source of potassium, had the following composition (per litre; all chemicals: ACS grade; BDH Chemicals Ltd., Toronto, Ont.): sodium dihydrogen phosphate monohydrate, 11.53 g; disodium nydrogen phosphate, 18.56 g; potassium chloride, 5.00 g. Mineral salts solution had the following composition (per litre; all chemicals, except ferric citrate: Fisher Chemical Co., Fairlawn, NJ; ferric citrate: J.T. Baker Chemical Co., Phillipsburg, NJ): $MgSO_4.7H_2O$ (ACS grade), 3.00 g; $MnSO_4$ (ACS grade), 0.50 g; $CaCl_2.2H_2O$ (ACS grade), 1.06 g; $ZnSO_4.7H_2O$ (ACS grade), 0.075 g; $CuSO_4$ (Fisher certified grade), 0.045 g; ferric citrate, n-hydrate (Baker grade), 0.75 g. This composition was based on a recalculation (not shown) of proportions given by Nickerson and Bulla (1974) of the "minimal" trace elemental needs of Bt. Ferric citrate was selected as an iron source which did not precipitate on sterilization. It was first dissolved by heating and stirring for several hours; the

solution was cooled, and the remaining salts added with stirring.

Nearly synchronous growth and sporulation were obtained using the "active culture" technique pioneered by Halvorson (1957). A spore slant was heat - shocked at 80 to 85 °C for 20 minutes, then used to inoculate two 300 ml shake flasks each containing 15 ml of TGY broth. These were incubated at 30.0 °C while agitating at 250 RPM for 3.0 to 3.5 hours. Broth (3.0 ml) from one of these was used at 10 %V/V to inoculate the next stage. Thus duplicate wide - mouth 500 ml flasks were seeded, each containing 30 ml of the same medium to be used in the main fermentation. These were incubated as above for 2.0 hours, then one was used to inoculate the final stage, again at 10 %V/V. The latter consisted of two 500 ml baffled erlenmeyer flasks, each containing 72 ml of the same medium as stages before and after it. The final inoculum stage, incubated as above, lasted 2.5 to 3.5 hours, ie. until a reasonably dense culture of rapidly dividing cells had been obtained.

4.2 Fermentation Methods

Fermentations were performed in a two litre bioreactor with a post - inoculation liquid volume of 1600 ml. The vessel was a 112 mm ID x 225 mm high, jacketed, borosilicate glass, tempering beaker (Duran-Schott; Cole-Parmer Instrument Co., Chicago, IL). Its 316 stainless steel (SS) headplate was

fitted with dissolved oxygen (DO) and pH probes, an enclosed - bearing impeller shaft, and ports for inoculation, aeration and sampling. The single impeller had 6 blades (57 mm diameter x 16 mm high), each inclined at 45°; the bottom of the impeller was positioned about 1 cm from the vessel bottom. The fermenter contained 4 baffles (each 10 mm wide x 152 mm high), offset at 90 degrees.

Temperature was controlled at 30.0 (±0.1) °C in all fermentations by circulating water from a bath through the fermenter jacket. It was measured by an accurate mercury thermometer (Cat. No. T-2025-3C; Canlab, Toronto, Ont.) in a water - filled well through the fermenter headplate.

Aeration rate in all fermentations was 1.4 VVM (volume of air [at S.T.P.]/volume of broth/minute), controlled with an air flow meter (Lab-Crest Century; Canlab, Toronto, Ont.) calibrated as shown in Fig. 4.1. Calibration was performed by the volume displacement method, ie. by partial displacement of water from an inverted 500 ml or 1,000 ml graduated cylinder during an accurately measured time interval. Flowrate was periodically lowered slightly to account for volume decrease due to sampling. Air was sterilized by filtration through a 150 x 15 mm ID glass tube packed with glass wool; then sparged through a 15 hole, circular (68 mm diameter), 316 SS ring located just beneath the impeller. Mixing by means of a Fisher Dyna-Mix stirrer (Fisher Scientific Co., Fairlawn, NJ) was at 500 RPM in Run 10, and 530 RPM in Run 11 and 12. These were

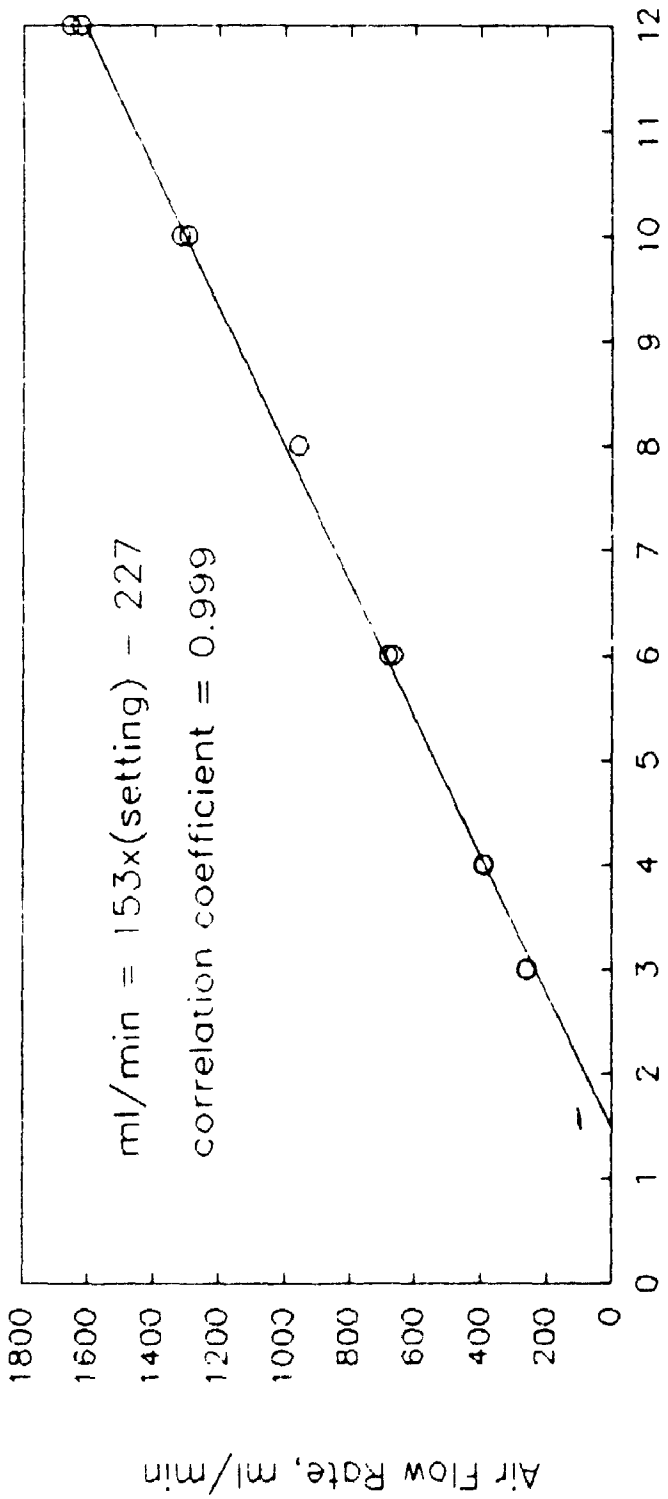

Fig. 4.1: Air flowmeter calibration.

calibrated with a stroboscope (Strobotac Type 1531-A; General Radio Co., Concord, MA) prior to fermentation. Foaming was controlled by addition of a solution of 1 part Antifoam B (BDH Chemicals Ltd., Toronto, Ont.) and 5 parts distilled water; this was added as required using a peristaltic pump (Cat. No. N-07521-35; Cole-Parmer Scientific Co., Chicago, IL).

An autoclavable, galvanic type DO electrode (Model MG-2; LSL Biolafitte, Princeton, NJ) was connected to a dissolved oxygen analyzer (Model DO-40; New Brunswick Scientific Co., Edison, NJ); whose output drove a strip - chart recorder (Model 285; Canlab, Toronto, Ont.). Meter and recorder baselines were set after sparging the medium with oxygen - free nitrogen (Canox Ltd., London, Ont.) for ten minutes. Full scale (ie. 0-100 % saturation) was set after similar sparging with air produced a stable reading.

Broth pH was monitored by an autoclavable glass electrode (Cat. No. 465-35-K9; Ingold Electrodes Inc., Andover, MA). This was connected to a pH meter/controller (Model 5997-20; Horizon Ecology Co., Chicago, IL), attached to the strip - chart recorder above. The system was calibrated after autoclaving, using pH 4.00 and 7.00 buffer solutions (BDH Chemicals Ltd., Toronto, Ont.), using a standard internal reference - type electrode (Canlab, Toronto, Ont.) connected to the meter. In Run 11 the meter was inadvertently left on "Monitor" during much of the fermentation. Sample pH in this case was measured with a standard internal reference electrode (Canlab, Toronto,

Ont.) connected to a Fisher Accumet™ meter (Fisher Scientific Co., Toronto, Ont.).

4.3 Anaerobic Incubation Experiments

This procedure was intended to block oxidative metabolism in order to measure catabolic flux through branched - chain α-ketoacid dehydrogenase (Sect. 5.4). Chloramphenicol (Cat. No. 44204; BDH Chemicals Ltd., Toronto, Ont.) was used to ensure that any changes during incubation were not due to expression of new enzyme systems. Since chloramphenicol in sufficient concentration is bactericidal to bacilli (Brock, 1961), a range of concentrations was tested to find one which would inhibit protein synthesis without killing the cells. The procedures used, each in duplicate, were as follows:

1) three - stage inoculum was prepared as usual (ie. 10 %V/V inoculum; Sect. 4.1), but with only 10 and 30 ml of tryptone/yeast extract medium in stages 2 and 3 respectively;

2) chloramphenicol solution (40 mg/l) and/or distilled water were added to each of four wide mouth 500 ml flasks (coded "X1" to "X4") to give initial volume of 5.0 ml, and final chloramphenicol concentrations (ie. after inoculum addition) of 0, 5.0, 10 or 20 mg/l;

3) to each "X" flask was added 5.0 ml of inoculum; these were incubated as usual (ie. 30.0 °C, 250 RPM); a sample

of inoculum was filtered and frozen for subsequent analysis;

4) after 8.2 hr, 1.0 ml from each "X" flask was added as inoculum into 25 ml of tryptone/yeast extract medium in a 500 ml shake flask (coded "G1" to "G4"); the latter were incubated as usual;

5) the contents of each "X" flask were filtered (Sect. 4.4.1), and analyzed for acetoin content (Sect. 4.4.6);

6) the "G" flasks were examined for growth after 8.2 hr of incubation.

The 1:25 dilution factor at step 4 was designed to reduce chloramphenicol concentration below 1 mg/l, which does not inhibit bacterial growth (ibid.).

Examination of the "G" flasks revealed that all cultures had grown, and were beginning to sporulate. Thus apparently none of the chloramphenicol treatments were significantly bactericidal. Analysis for acetoin showed none in the initial inoculum, or in the "X" flasks containing chloramphenicol at 10 or 20 mg/l. Acetoin concentration was 9.8 mg/l at 5 mg/l chloramphenicol, and 86.5 mg/l in the absence of the inhibitor. Thus chloramphenicol at 10 or 20 mg/l prevented expression of enzyme(s) necessary for acetoin formation, but did not kill the cells.

A second test was done to determine the time needed for measurable amounts of metabolites to accumulate in the broth due to anaerobic incubation. The procedure was as follows:

1) three - stage inoculum was prepared as usual (Sect. 4.1), except that the final stage was grown for either 6.3 or 13.2 hours;

2) nine 250 ml flasks were prepared, each containing 1.0 ml of 200 mg/l chloramphenicol solution;

3) to each was added 10.0 ml of inoculum; flasks were mixed by swirling, and oxygen - free nitrogen gas (Canox Ltd., London, Ont.) passed through the headspace, at about 2 l/min for two minutes, to displace all oxygen;

4) the flasks were tightly sealed with a rubber stopper, then incubated without agitation in a water bath at 30.0 °C for 30, 60 or 90 minutes;

5) broth was filtered (Sect. 4.4.1), and analyzed for non - volatile organic acids content (Sect. 4.4.7; the inoculum was similarly analyzed).

As indicated in step 1, anaerobic production of intermediates (especially α-keto acids) was tested with vegetative (6.3 hr) cells, and those (13.2 hr) just starting to sporulate. The result was that, after 30 to 60 minutes, the former had released measurable pyruvate and α-ketoisocaproate; the latter had excreted substantial lactate, α-hydroxyisovalerate and α-keto-3-methylvalerate.

Thus the method adopted for anaerobic incubation (in duplicate) was as follows:

1) 1.0 ml of 200 mg/l chloramphenicol solution was placed in a 250 ml flask;

2) sample (10.0 ml) was added, the flask mixed by swirling, and oxygen - free nitrogen gas passed through the headspace, at about 2 l/min for one minute;

3) the flask was tightly stoppered, and incubated without agitation in a water bath at 30.0 °C for 40 minutes;

4) the sample was filtered and analyzed as usual.

4.4 Analytical Methods

All procedures were performed in duplicate unless noted otherwise. Broth filtrate was prepared as described in Sect. 4.4.1.

4.4.1 Biomass

Biomass concentration, as g dry matter (BDM) per litre of fermentation broth, was determined by vacuum filtering 5.0 to 10.0 ml of broth through a tared cellulose nitrate filter (0.45 μm pore size; Sartorius GmbH, Gottingen, W. Germany). The filter paper was then rinsed with 2 ml of stabilized saline solution (0.82 %W/V NaCl, and 0.01 %W/V merthiolate, ie. ethylmercurithiosalicylic acid, disodium salt; Eastman Kodak Co., Rochester, NY), and 2 ml of distilled water, before drying at least 24 hours at 100 to 105 °C. Typical coefficient

of variation (ie. standard deviation divided by the mean) for the analysis was about 2 per cent.

4.4.2 Viable Cell and Spore Count

Viable cell count in broth was measured, after appropriate serial dilution in 0.82 %W/V NaCl solution, by uniformly applying 0.1 ml to a 100 mm x 15 mm petri dish containing TGY agar (in triplicate). These were incubated at 25 °C for 12 to 24 hours before counting colonies. Only plates containing between 30 and 300 colonies were used for calculation. Viable cell count per ml was taken as the average number of colonies, multiplied by 10, and by the appropriate initial dilution factor.

Viable spore count was measured as above, except that the final saline dilution tube was heated at about 85 °C for 30 minutes before plating. Typical coefficient of variation for either cell or spore count was about 24 per cent.

4.4.3 Glucose

Reducing sugars, as glucose, were measured using a slight modification of the method of Miller et al. (1960; cf. Miller, 1959). The dinitrosalicylic acid (DNS) reagent was prepared by first dissolving 5.00 g of sodium hydroxide (reagent grade; J.T. Baker Chemical Co., Phillipsburg, NJ) in about 250 ml of

distilled water in a 500 ml volumetric flask. To this was added with stirring 5.00 g of 3,5-dinitrosalicylic acid (reagent grade; Fisher Scientific Co., Fairlawn, NJ), 1.00 g of phenol (reagent grade; Mallinckrodt Chemical Works, St. Louis, MO), 0.25 g of sodium sulfite (ACS grade; J.T. Baker Chemical Co., Phillipsburg, NJ), and 100.0 g of sodium potassium tartrate (Cat. No. B29657; BDH Chemicals Ltd., Toronto, Ont.). The solution was made up to volume with distilled water, and placed in a light-protected dispenser bottle.

For analysis 1.00 ml aliquots of broth filtrate (containing 0.3 - 1.5 g/l of reducing sugars) were placed in 25 x 150 mm test tubes; and 3.00 ml of DNS reagent added. A distilled water blank was similarly treated. The tubes were vortexed for five seconds, then placed in boiling water for exactly ten minutes. They were then placed in ice-water for one minute, then 20.00 ml of distilled water added to each. The tubes were again vortexed for five seconds. The absorbance of each solution was read at once in 1.0 cm cells at 600 nm, using distilled water to zero the spectrophotometer (Model PU 8610; Pye Unicam Ltd., Cambridge, England).

The method was calibrated using known glucose solutions of about 0.3 to 1.2 g/l concentration. Net absorbance versus concentration was calculated by linear regression through the origin using SYSTAT™ (SYSTAT, Inc., Evanston, IL). Typical

with a Teflon™ - lined cap, and stored in the freezer until analyzed.

Gas chromatography was performed as described in Sect. 4.4.6, with the following exceptions:

1) the column used was 6 ft x 4 mm ID glass, packed with 10 % OV-101 on 80/100 mesh Supelcoport (Supelco Canada Ltd., Oakville, Ont.);

2) a separate insert, containing plain glass wool, was used in the injection port;

3) operating conditions were as follows: injector: 200 °C; detector: 250 °C; attenuation: 8 x 10^{-11}; temperature program: 70 °C for 10 min, then 2 C°/min to 140 °C.

The peaks eluted were identified by a combination of coupled gas chromatography - mass spectroscopy (GC-MS); comparison of retention times relative to normal alkanes with tabulated values; and comparison of retention times with those of known standards.

GC-MS analysis of several samples was performed by Mr. Doug Hairsine, Department of Chemistry, University of Western Ontario. Comparison of these mass spectra with standard spectra (cf. Chalmers and Lawson, 1982, p. 447-495) allowed positive identification of lactic acid, α-ketoisocaproic (2-oxo-4-methylpentanoic) acid, succinic acid, and peak 2 of α-keto-3-methylvaleric (2-oxo-3-methylpentanoic) acid. Tentative identification of 2,3-butanediol was also possible.

lost completely during hydrolysis; recovery of serine and threonine was estimated to be 90 and 95 per cent respectively (cf. Ambler, 1981; Blackburn, 1978).

4.4.5 Ammonia

Liquid - phase ammonia concentration, in the range 0 to 40 mg/l, was measured in duplicate by the phenol - hypochlorite reaction (Weatherburn, 1967).

For sample analysis 200 µl of broth filtrate was measured (Oxford Sampler; Canlab, Toronto, Ont.) into a 20 mm x 150 mm test tube; and 5.00 ml of phenol/nitroprusside reagent added (Oxford Pipettor, 0 - 10 ml scale; Canlab, Toronto, Ont.) with vortexing (Vortex-Genie, Scientific Industries, Inc., Bohemia, NY; setting "4"). Similarly 5.00 ml of alkaline hypochlorite reagent was added (L/I Repipet, 0 - 20 ml scale; Labindustries, Berkeley, CA). The tube was covered with Parafilm "M" (American Can Co., Dixie/Marathon, Greenwich, CT), and allowed to stand at room temperature for 1.0 to 24 hr. Tubes standing for longer than about two hours were vortexed before reading. Duplicate distilled water blanks were similarly treated. The absorbance was read at 625 nm (Model PU 8610; Pye Unicam Ltd., Cambridge, England) in a 1.00 cm cell zeroed with distilled water. A daily calibration check was also performed using two standard ammonia solutions (see below).

The method was calibrated for each batch of reagents using at least three known solutions of ammonium sulfate (ACS grade; Fisher Scientific Co., Fairlawn, NJ). These were prepared by dilution of a 1.94 g/l solution of ammoniun sulfate stabilized with 0.01 %W/V merthiolate (ethylmercurithiosalicylic acid disodium salt; Eastman Kodak Co., Rochester, NY), and stored under refrigeration. Merthiolate was demonstrated to have no effect on the analysis, which had typical standard error of about 1.4 per cent.

The reagents were prepared as follows:

Phenol/Nitroprusside Reagent: To a 500 ml volumetric flask was added about 250 ml of distilled water, 5.00 g of phenol (ACS grade; Mallinckrodt Chemical Works, St. Louis, MO), and 25 mg of sodium nitroferricyanide dihydrate (sodium nitroprusside; reagent grade; J.T. Baker Chemical Co., Phillipsburg, NJ). These were dissolved; and the flask made to volume with distilled water. The reagent was placed in a dispenser (see above), and stored in the refrigerator.

Alkaline Hypochlorite Reagent: To a 500 ml volumetric flask was added about 250 ml of distilled water, 2.50 g of sodium hydroxide (ACS grade; J.T. Baker Chemical Co., Phillipsburg, NJ), and 4.20 ml of Javex™ (6% sodium hypochlorite; Bristol - Meyers Canada Inc., Toronto, Ont.). After dissolution, the flask was made to volume with distilled water. The reagent was stored as above.

4.4.6 Volatile Organic Products

Volatile organics were measured using a modification of the method suggested in Supelco Bulletin No. 751 (Supelco Canada Ltd., Oakville, Ont.). Sample preparation consisted simply of adding 100 µl of 2 %V/V formic acid solution (ACS grade; BDH Chemicals Ltd., Toronto, Ont.) to 1.00 ml of broth filtrate, and mixing well.

Analysis was performed using a Varian Model 3700 gas - liquid chromatograph (Varian Associates Inc., Palo Alto, CA) with a flame - ionization detector connected to a digital integrator (Chromatopac Model C-R6A; Shimadzu Corp., Kyoto, Japan). Flash injection into a glass insert, whose lower third was loosely packed with o-phosphoric acid - treated glass wool, was used to protect the column. Sample volume of 1.00 µl was measured and injected with a 0-10 µl syringe fitted with a Chaney adapter (Cat. No. 701; Hamilton Co., Reno, NE). The column used was 3 ft x 4 mm ID glass, packed with 0.3 % Carbowax 20M / 0.1 % H_3PO_4 on 60/80 mesh Carbopack C (Supelco Canada Ltd., Oakville, Ont.). Oxygen - free nitrogen (Canox Ltd., London, Ont.) at a flow rate of 50 ml/min was used as carrier gas.

For analysis of acetic acid and acetoin, the following operating conditions were used: injector: 120 °C; detector: 200 °C; attenuation: 2 x 10^{-11}; temperature program: 90 °C for 2 min, then 2 °C/min to 100 °C. Because of a tendency of acetic

acid to adsorb on the column, a distilled water blank was injected between each sample injection. Traces of propionic acid were also detected by this assay but were not quantitated.

The method was calibrated for acetate by weighing acetic acid (ACS grade; Fisher Scientific Co., Fairlawn, NJ) into 100 ml volumetric flasks to obtain three concentrations between 100 and 500 mg/l. These standard solutions and a distilled water blank were acidified as above, and injected in quadruplicate. The blank produced about 3100 counts on average due to a small amount of acetic acid impurity in the formic acid. This blank correction was subtracted from the acetate peak area before further calculation. Thus calibration was accomplished by linear regression through the origin of net acetate counts versus concentration, giving standard error of about 3.2 per cent.

Acetoin was calibrated similarly, after initial purification as follows:

1) acetoin (3-hydroxy-2-butanone, containing 5-10 % water; Aldrich Chemical Co., Milwaukee, WI) was warmed in an oil bath to melt the solids;

2) about half this volume of anhydrous sodium suphate (reagent grade; J.T. Baker Co., Phillipsburg, NJ) was added to combine with most of the water;

3) the bulk of the dried liquid was poured into a vial, and allowed to recrystallize in the refrigerator.

Three standard solutions between 100 and 700 mg/l were prepared from the purified crystals, and analyzed in quadruplicate as above. Regression through the origin gave a calibration with standard error of about 1.2 per cent.

For analysis of isobutyric, 2-methylbutyric and isovaleric (3-methylbutyric) acid, higher temperature operation was required for satisfactory peak resolution. These conditions were as follows: injector: 120 °C; detector: 200 °C; attenuation: 2×10^{-11}; column temperature: 120 °C. Traces of n-butyric acid were detected but not quantitated.

The branched short - chain acids were calibrated as for acetate, by weighing isobutyric acid (certified grade; Fisher Scientific Co., Fairlawn, NJ) or (±)-2-methylbutyric acid (Cat. No. 19,307-0; Aldrich Chemical Co., Milwaukee, WI) into a vial, then rinsing into a 1 litre volumetric flask to give three different concentrations between 15 and 45 mg/l. These were injected in quadruplicate, and absolute response factors for each calculated as above. Calibration standard error for isobutyrate was 1.6 per cent, and for 2-methylbutyrate, 1.5 per cent. It was assumed that the flame did not discriminate between the latter and 3-methylbutyrate, and their response factors were taken to be identical.

4.4.7 Non - volatile Organic Products

This analysis required by far the greatest investment of effort both to develop, and to arrive at reasonably consistent results. Several factors contributed to this situation. In order to quantitatively detect the 3 - to 6 - carbon α-keto and hydroxy acids which were believed to be present, it was necessary to use a rather complex procedure developed for clinical analysis. Furthermore it was not possible for lack of equipment to use the recommended method (Chalmers and Lawson, 1982, p. 20). The evaporation step of the method chosen proved to be very difficult to control (as reported, ibid.), often forcing analysis of a large number of replicates, and rejection of poorly derivitized samples. Finally it was necessary to identify and calibrate the relatively large number of peaks present.

The method used was developed from those of Jakobs et al. (1977) and Chalmers et al. (1977). Thus to 1.00 ml of broth filtrate in a 13 mm x 100 mm screw - cap tube was added 1.0 ml of saturated NaCl solution, and one drop of concentrated HCl; then vortexed (Vortex-Genie; Scientific Industries, Inc., Bohemia, NY) briefly to mix. Ethyl acetate (1.0 ml, ACS grade; BDH Chemicals Ltd., Toronto, Ont.) was added; and the tube capped and vortexed at setting "5" for 15 sec. After phase separation, aided if necessary by mild centrifugation, most of the upper layer was removed via pasteur pipet, and placed in

a 25 ml pear - shaped boiling flask (Pyrex; Canlab, Toronto, Ont.). Extraction with 1.0 ml of ethyl acetate was repeated twice more, pooling the extracts, and attempting definitive separation in the final stage.

Evaporation to complete dryness generally required between 4 and 7 minutes using a rotary evaporator (Rotavapor <R>; Büchi, Switzerland) attached to a water aspirator capable of drawing a vacuum of below -20 PSIG. The next step produced an ethoxime derivative, required to avoid mutiple peaks and decomposition due to carbonyl group reactivity (cf. Chalmers and Lawson, 1982, p. 39-45).

The residue from evaporation was first dissolved in 100 µl of acetonitrile (Omnisolv grade; BDH Chemicals Ltd., Toronto, Ont.), then 50 µl of ethoxime reagent added and mixed. The latter consisted of 20 mg/ml solution of O-ethylhydroxylamine HCl (98 %; Aldrich Chemical Co., Milwaukee, WI) in pyridine (Omnisolv grade; BDH Chemicals Ltd., Toronto, Ont.), prepared fresh at least every two months. The flask was covered with Parafilm "M" (American Can Co., Dixie/Marathon Div., Greenwich, CT), and allowed to stand in a fume hood for 30 minutes. The econd derivitization step, to make the substances olatile, consisted of treatment of the reacticn mixture with the contents (100 µl) of an ampoule of BSTFA (bis-[trimethylsilyl]-trifluoroacetamide; Cat. No. 3-3084; Supelco Canada Ltd., Oakville, Ont.). After 30 minutes of reaction, the mixture was placed by pasteur pipet into an injection vial

with a Teflon™ - lined cap, and stored in the freezer until analyzed.

Gas chromatography was performed as described in Sect. 4.4.6, with the following exceptions:

1) the column used was 6 ft x 4 mm ID glass, packed with 10 % OV-101 on 80/100 mesh Supelcoport (Supelco Canada Ltd., Oakville, Ont.);

2) a separate insert, containing plain glass wool, was used in the injection port;

3) operating conditions were as follows: injector: 200 °C; detector: 250 °C; attenuation: 8 x 10^{-11}; temperature program: 70 °C for 10 min, then 2 C°/min to 140 °C.

The peaks eluted were identified by a combination of coupled gas chromatography - mass spectroscopy (GC-MS); comparison of retention times relative to normal alkanes with tabulated values; and comparison of retention times with those of known standards.

GC-MS analysis of several samples was performed by Mr. Doug Hairsine, Department of Chemistry, University of Western Ontario. Comparison of these mass spectra with standard spectra (cf. Chalmers and Lawson, 1982, p. 447-495) allowed positive identification of lactic acid, α-ketoisocaproic (2-oxo-4-methylpentanoic) acid, succinic acid, and peak 2 of α-keto-3-methylvaleric (2-oxo-3-methylpentanoic) acid. Tentative identification of 2,3-butanediol was also possible.

Since linear temperature programming was used for analysis, a retention index (RI) system based on linear interpolation between adjacent normal alkanes was used in peak identification (ibid., p. 61). Thus a mixture of nine normal alkanes (ie. n-nonane, C9, to n-heptadecane, C17) in hexane was prepared, and injected under sample analysis conditions. Sample peak retention times were indexed to these; for example, a peak eluted midway between C11 and C12 would have RI of 1150. Sample peak retention indices were compared with tabulated values (ibid., p. 447-495), permitting identification of pyruvic acid; and confirmation of lactic, α-ketoisocaproic and succinic acids.

Other significant sample peaks were tentatively identified on the basis of similar retention times to those of known compounds. Peaks for α-ketoisovaleric (2-oxo-3-methylbutanoic) acid, α-hydroxyisovaleric (2-hydroxy-3-methylbutanoic) acid, and α-keto-3-methylvaleric (2-oxo-3-methylpentanoic) acid were identified in this manner.

Three minor peaks which were present in various samples were not sufficiently identified to warrant quantitation. A peak at about 28.9 min (RI ≈ 1135) was evident especially under conditions of limited oxygen (not shown). A likely candidate is 2-hydroxybutyric acid, which has a retention index of 1128. A peak at about 39.5 min (RI ≈ 1272) was present throughout the fermentations, increasing considerably during granulation and sporulation. Finally a substantial peak

at about 43.4 min (RI ≈ 1342) appeared as the spores became refractile.

Quantitative calibration was achieved by at least duplicate derivitization and injection of 3 or more concentrations of pure standard. Response factors were obtained as before by linear regression through the origin of peak area versus concentration. A summary of identification and calibration results is given below. All chemicals were the highest purity available, obtained from Aldrich Chemical Co., Milwaukee, WI, unless noted otherwise.

The peak at about 22.3 min (RI ≈ 1047) was tentatively identified as 2,3-butanediol based on co-elution with authentic (2R,3R)-(-)-2,3-butanediol (Aldrich Cat. No. 23,763-9). Standard error of the calibration was 7.5 per cent.

The strong peak at 23.9 min was identified as lactic acid from its fragmentation pattern. Its calculated RI of 1067 was quite close to the published value of 1074. Calibration, as performed with L-(+)-lactic acid (Cat. No. L-1750; Sigma Chemical Co., St. Louis, MO), had standard error of 2.0 per cent.

Pyruvic acid, eluting at about 26.7 min, was identified based on its RI value of 1103 compared to the published value of 1104. It was calibrated using sodium pyruvate (Biochemical grade; BDH Chemicals Ltd., Toronto, Ont.), giving standard error of 6.7 per cent.

α-Ketoisovaleric acid (αKIV) was identified by co-elution of its two peaks with those of the known compound, although the single published retention index of 1140 did not correspond to those found (ie. RI ≈ 1159, 1187). Identifi ation and calibration were done using 3-methyl-2-oxo-butanoic acid, calcium salt dihydrate (Aldrich Cat. No. 24,643-3). The sum of counts for both peaks (ie. at about 30.9 and 33.0 min) was used for quantitation; the calibration factor had standard error of 7.0 per cent.

The reduced form of αKIV, namely α-hydroxyisovaleric acid (αOHIV), was identified similarly; its calculated RI of 1172 was considerably less than the literature value of 1194. This peak, eluting at about 31.6 min, was generally not resolved from peak 1 of αKIV. Calibration, done with (±)-2-hydroxy-3-methylbutyric acid (Aldrich Cat. No. 21,983-5), gave a response factor (standard error ≈ 2.8 per cent) about 1.11 times that of αKIV. In practice, since αKIV and αOHIV could not be consistently separated, they were calculated together using the sum of their peak areas.

One of the two peaks of α-keto-3-methylvaleric acid (αK3MV, αKMV) was identified by its GC-MS fragmentation pattern. This was augmented by co-elution of both peaks, at about 35.8 and 37.0 min, with those of the known compound. Again experimental RI values (1231, 1244) were higher than those tabulated in Chalmers and Lawson (1982; ie. 1186, 1228). Calibration, done using (±)-3-methyl-2-oxopentanoic acid

(Aldrich Cat. No. 28,097-6), gave standard error of 8.8 per cent. Quantitation used total counts of the two peaks, after subtracting out interference with peak 1 from the first peak of α-ketoisocaproate (see below).

α-Ketoisocaproic acid (αKIC), which was identified from its GC-MS mass - ion pattern, produced peaks at about 36.1 and 38.6 minutes. Their experimental retention indices (about 1233 and 1267 respectively) bracketed the single published RI value of 1256 for both peaks. The identity of the two peaks was confirmed using an authentic sample of αKIC. The method was calibrated using 4-methyl-2-oxopentanoic acid, calcium salt dihydrate (Aldrich Cat. No. 24,644-1); standard error of the calibration was 3.9 per cent. Quantitation of αKIC employed only peak 2; since peak 1 counts were highly correlated with this (correlation coefficient ≈ 0.987), counts at about 36 min due to αKIC were subtracted out to allow determination of αKMV (see above).

Succinic acid was identified by its GC-MS fragmentation pattern. The single peak at 41.6 min (RI ≈ 1311) was close to the expected retention index of 1300. Succinic acid calibration (with Aldrich Cat. No. 23,968-2) gave a standard error of 2.8 per cent.

4.4.8 Fatty Acids and Poly-β-hydroxyalkanoates

This group of biomass constituents was measured by a modified gas chromatographic method for poly-β-hydroxybutyrate (PHB), as its methyl ester, adapted from Braunegg et al. (1978).

Sample derivitization began with centrifugation for 10 minutes at 12,000 RPM of 10.0 ml of broth in a 25 ml screw - cap Pyrex™ centrifuge tube (Cat. No. 8446; Corning Glass Works, Corning, NY), fitted with a Teflon™ - lined cap. The supernatant was poured off, and 2.00 ml of acidic methanol (containing internal standard ,see below) and 2.00 ml of chloroform (Omnisolv grade; BDH Chemicals Ltd., Toronto, Ont.) were added. The tube was heated in an oil bath at 100 ± 2 °C for 3.5 hr to form the methyl esters of the organic acids. After cooling to room temperature, 1.00 ml of distilled water was added and the tube shaken vigorously by hand for one minute to extract the esters into the chloroform phase. The two phases were allowed to separate, during which cell detritus gathered at the interface; if necessary the tube was centrifuged at 5,000 RPM for 5 min. The lower chloroform layer was placed by pasteur pipet in an injection vial, and stored in the freezer.

The acidic methanol derivitizing solution was prepared by accurately weighing about 70 mg of benzoic acid (Analar grade; BDH Chemicals Ltd., Toronto, Ont.) into a 100 ml

volumetric flask, and dissolving it in about 50 ml of absolute methanol (Omnisolv grade; BDH Chemicals Ltd., Toronto, Ont.). Concentrated sulfuric acid (3.1 ml , ACS grade; J.T. Baker Chemical Co., Phillipsburg, NJ) was added and mixed. The flask was brought to volume with methanol, and well mixed.

Gas - liquid chromatography was performed as described in Sect. 4.4.6, with the following exceptions:

1) the column used was 6 ft x 2 mm ID glass, packed with 10 % Carbowax 20M TPA on 80/100 mesh Chromosorb WHP (Supelco Canada, Oakville, Ont.);

2) operating conditions were as follows: injector: 220 °C; detector: 230 °C; attenuation: 8 x 10^{-11}; temperature program: 160 °C for 8 min, then 1 C°/min to 177 °C.

Peaks were identified by use of a homologous series of normal fatty acids (viz. n-decanoic acid, n-C10, and the six normal fatty acids from n-dodecanoic, n-C12, to n-heptadecanoic acid, n-C17). Since GLC was isothermal for the first 8 minutes, logarithmic interpolation was used for calculation of a Kovats - type retention index (equivalent chain length, ECL; Kates, 1986; cf. Handbook of Chromatography, 1972). Since a linear temperature gradient was used during the last 17 minutes of aralysis, ECL was calculated by linear interpolation (cf. Sect. 4.4.7). Results from the above GLC column, summarized in Table 4.2, show excellent agreement with the set of ECL values reported by Kaneda (1977) on a stationary phase of similar polarity (viz. EGA ≡ ethylene glycol adipate). Standard fatty

Retention Time, min	Calculated ECL	Presumed Identity	ECL on EGA Column
3.050	11.51	i-C12	11.62
3.598	11.96	n-C12	12.00
3.942	12.19		
4.467	12.52	i-C13	12.58
4.717	12.66	a-C13	12.72
5.082	12.85		
6.583	13.52	i-C14	13.60
7.450	13.83		
7.932	13.99	n-C14	14.00
9.732	14.49	i-C15	14.60
10.258	14.63	a-C15	14.74
11.565	14.99	n-C15	15.00
13.958	15.51	i-C16	15.57
15.332	15.80	i-C16=	15.90
16.267	16.00	n-C16	16.00
17.848	16.29	n-C16=	16.32
19.038	16.5	i-C17	16.58
19.800	16.64	a-C17	16.73
21.183	16.89	i-C17=	16.88

Table 4.2: Identification of fatty acids on Carbowax 20M column. See text for definition of terms.

acid notation (cf. Kaneda, 1967, 1977) is used throughout, as exemplified below:

i-C13 ≡ 11-methyldodecanoic acid (ie. penultimate methyl branch);

a-C15 ≡ 12-methyltetradecanoic acid (ie. antepenultimate methyl branch);

n-C14 ≡ normal tetradecanoic acid;

i-C16$^{:}$ ≡ cis-Δ^{10}-14-methylpentadecenoic acid.

Peak identity was confirmed by chromatography of the above homologous series of normal fatty acids, and samples, on a column of much lower polarity (ibid.). Thus the OV-101 column, described in Sect. 4.4.7, was used under the following operating conditions: injector: 200 °C; detector: 250 °C; attenuation: 8 x 10^{-11}; temperature program: 160 °C to 220 °C at 2 C°/min. These results (Table 4.3), with RI values found by linear interpolation, greed well with those of Kaneda (1977) on a similar silicone stationary phase (viz. SE-30).

Poly-β-hydroxybutyric acid (PHB) was identified by co-elution of an authentic sample on the Carbowax column under both the above conditions (retention time, RT ≈ 1.13 min), and those specified by Braunegg et al. (1978; RT ≈ 5.90 min). Poly-β-hydroxyvaleric acid (PHV) was tentatively identified by its RT relative to PHB, since an authentic sample of 3-hydroxypentanoic acid was not available. Thus RT of the unknown peak at 1.71 min (Carbowax column) was about 1.45 times that of 3-hydroxybutyrate; and Findlay and White (1983)

2

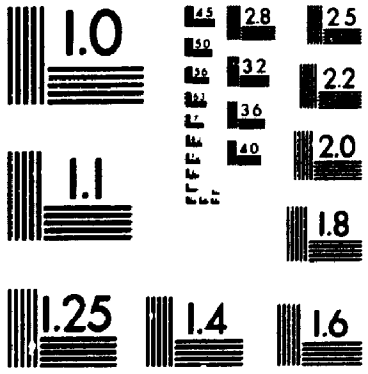

MICROCOPY RESOLUTION TEST CHART
NATIONAL BUREAU OF STANDARDS
STANDARD REFERENCE MATERIAL 1010a
(ANSI and ISO TEST CHART No 2)

Retention Time, min	Calculated ECL	Presumed Identity	ECL on SE-30 Column
4.598	10.21		
6.753	11.27		
7.473	11.63	i-C12	11.6
8.426	12.07	n-C12	12.0
10.233	12.69	i-C13	12.6
		a-C13	12.7
13.433	13.68	i-C14	13.6
14.717	14.05	n-C14	14.0
17.317	14.74	i-C15	14.6
		a-C15	14.7
20.268	15.48	i-C16=	15.4
21.055	15.68	i-C16	15.6
21.732	15.84	n-C16=	15.8
22.538	16.04	n-C16	16.0
24.417	16.49	i-C17	16.6
25.308	16.7	a-C17	16.7

Table 4.3: Identification of fatty acids on OV-101 column. See text for definition of terms.

reported that the ethyl esters of the two β-hydroxyalkanoates had a retention time ratio of about 1.43 on an SE-30 column.

During and after stage IV of sporulation, a large peak was observed at RT ≈ 17.1 min operating isothermally at 180 °C. This retention relative to n-C17 indicated about an n-C20 fatty acid, or more likely a diterpene.

This analysis differed from the GLC methods described in Sect. 4.4.6 and 4.4.7 in that sample response was normalized to the response of an internal standard (viz. benzoic acid). Concentration of each analyte in the fermentation broth, ie. C_j (t_i), mmol/litre, was calculated as follows:

$$C_j\ (t_i) \approx \frac{(\text{mmol benzoate}) \times (\text{area of peak } j)}{(\text{sample volume, 1}) \times R_j \times (\text{benzoate peak area})} \qquad (4.1)$$

where:

t_i ≡ time of sample i, hr;

R_j ≡ molar response factor for component j,

$$\equiv \frac{(\text{area of peak } j) \times (\text{mmol benzoate})}{(\text{benzoate peak area}) \times (\text{mmol of analyte } j)}$$

Molar response factors were measured for β-hydroxybutyrate and each normal fatty acid from dodecanoic (C12) to heptadecanoic acid (C17). Standards for derivitization were prepared in duplicate as follows:

1) hydroxybutyric acid (DL-3-hydroxybutyric acid, sodium salt; Cat. No. 23,389-7; Aldrich Chemical Co., Milwaukee, WI) was dried at 105 °C for 2 hours, and cooled in a

dessicator before weighing; fatty acids (all 99+ % purity; Sigma Chemical Co., St. Louis, MO) were stored in a dessicator in the freezer;

2) the compound was accurately weighed (Model H51-V40; Sartorius GMBH, Gottingen, W. Germany) into an 11 ml vial with Teflon™ - lined screw cap; this was dissolved by addition of 10.00 ml of chloroform (Omnisolv grade; BDH Chemicals Ltd., Toronto, Ont.);

3) to a 25 ml centrifuge tube (see above) was added 0.50, 1.00 or 1.50 ml of this solution; chloroform was added to bring the volume to 2.00 ml.

These solutions were treated with acidic methanol (containing benzoic acid internal standard), derivitized and chromatographed as described above. Response factors, calculated by linear regression through the origin using SYSTAT™, had standard errors of 0.6 to 2.6 per cent for the fatty acids, and 2.4 per cent for 3-hydroxybutyrate. The molar response factor for 3-hydroxyvalerate was assumed to be greater than that of the latter substance in proportion to their molecular weights, ie. 132.16/118.13 ≈ 1.12.

5. Metabolic Model Structure and Solution Methodology

5.1 Model Structure and General Assumptions

The metabolic model of *B. thuringiensis* elaborated is determined primarily by the set of metabolic flows permitted in principle. Other necessary assumptions were made regarding the following:

1) flows to cell (*ie.* VDM, viable dry matter) biosynthesis, discussed in Sect. 5.3;

2) resolution of several minor ambiguities, *viz.* source of propionyl-CoA; catabolism of acetoin and 2,3-butanediol; catabolism of glutamate;

3) imposition of molar flux balance at pyruvate.

The latter issues will be addressed after introduction of the model structure and solution mechanics. Throughout the text the term "flux" will be used as employed by Holms (1986) as shorthand for specific reaction rate, in units of mmol/g VDM/hr.

The actual model (META.WK1) was constructed in a LOTUS™ spreadsheet with a cell for each molar flux (all in mmol/g VDM/hr). A set of possible metabolic pathways was configured, based on the literature reviewed in Sect. 2 and 3. This approach, and the "flux" nomenclature, are adapted from Holms (1986). A representation of this model, simplified by grouping certain flows, and omitting others, is shown in Fig. 5.1.

There are three distinct classes of chemical substance in this diagram, namely:

1) intracellular intermediates of central metabolism, ie. any substance having both inflow and outflow, eg. pyruvate, acetyl-CoA;

2) extracellular substrates or excreted products, eg. glucose, lactate;

3) viable biomass content of certain amino acids, viz. valine, leucine, isoleucine, aspartate and glutamate.

This group of amino acids was of interest for display, although all amino acids were considered in the calculations (Sect. 5.3). Note that several compounds are members of more than one of the above classes.

The following groupings were made in Fig. 5.1 and similar model solution diagrams:

1) lactate ≡ lactate + pyruvate;

2) acetoin ≡ acetoin + 2,3-butanediol;

3) acetate, PHB ≡ acetate + PHB + PHV.

No flows to viable biomass are shown, except for the five amino acids listed above; these were subtracted "at source" (Sect. 5.3). Also not shown are several substances excreted in low amounts, namely the three short - chain branched fatty acids and corresponding 2-keto acids (BCKA's).

Propionyl-CoA for synthesis of poly-β-hydroxyvaleric acid (PHV) and n-C15 fatty acid was generally assumed to come from the valine catabolic pathway (Sect. 3.2). In Sect. 7.2, this

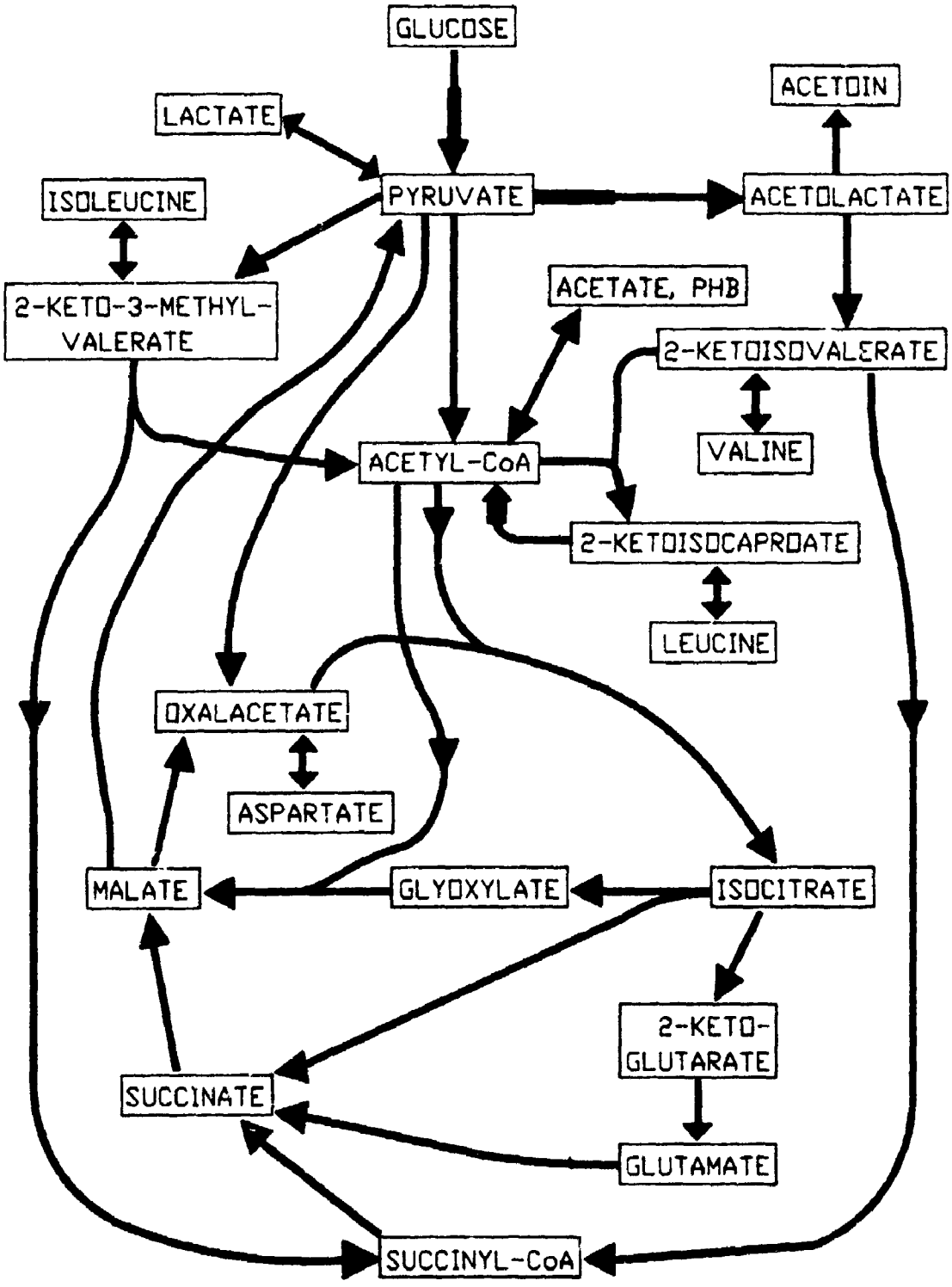

Fig. 5.1: Main permissible model pathways. See text for flows not shown and/or grouped.

source was insufficient, and it was assumed to come from α-ketobutyrate (Fig. 3.3).

Only net flux of acetoin plus 2,3-butanediol was used in model calculations. Furthermore simultaneous formation and catabolism of acetoin/butanediol was not considered permissible. Consumption of these compounds occurred via the 2,3-butanediol cycle to acetate (Juni and Heym, 1956); for clarity this is not shown in Fig. 5.1, etc.

Because dehydrogenation of isocitric acid to 2-ketoglutarate is highly exothermic (Lehninger, 1976, p.456), catabolism of glutamate, when it occurred, was via the gamma-aminobutyric acid (GABA) pathway to succinate (Aronson et al., 1975a,b). Conversion of isocitrate to succinate by simultaneous formation and catabolism of glutamate was not allowed, since competition with isocitrate lyase (Sect. 2.5) was not considered realistic.

To solve the model, all calculated fluxes (Sect. 5.2 - 5.5) were first entered in their respective cells. The actual process of flux balancing started by calculation of the three BCAA catabolic (ie. acyl-CoA dehydrogenase) flows. This gave the flows to succinyl-CoA and acetyl-CoA from BCAA degradation. In the vegetative - phase solutions, it was then possible to calculate balances around isocitrate and oxalacetate, assuming the necessary pyruvate carboxylase flux to the latter. Thus pyruvate dehydrogenase flux was calculated from a balance around acetyl-CoA; which permitted testing flux

balance at pyruvate (see below). In transition - and sporulation - phase solutions, pyruvate dehydrogenase was considered inactive (Sect. 6.3.2); and acetyl-CoA balance allowed calculation of glyoxylate cycle flux, after subtracting flux to glutamate. Pyruvate production by malic enzyme was then derived from malate balance. This again permitted a test of pyruvate balance.

Flux balance around pyruvate was not generally achieved by these calculations. Since such a balance is theoretically required, it was imposed by varying the apparent mass of viable dry matter present. Generally it was necessary to reduce same to achieve balance. The expediency of decreasing apparent viable biomass formation rate effectively decreased pyruvate demand relative to measured substrate consumption rate. This appeared to be the most straightforward and equitable solution, given that conservation of matter requires a molar balance. By this device a consistent set of fluxes was obtained whose numerical values are indicative of the various flows in a relative sense. Apparent biomass formation rate was adjusted via factor BMF, used as a multiplier of all flows to cell biosynthesis.

The errors involved in the model solution process are described quantitatively in Appendix H.

For the mid - sporulation case on tryptone/yeast extract medium (Sect. 6.4), a completely different solution method was necessary.

5.2 Basic Calculation Methods

Calculations were done in general using various LOTUS 123™ worksheets. These were selectively verified with a hand - held calculator.

For biomass components which were measured, namely, PHB, PHV and 15 fatty acids, the volumetric concentration (mmol/ litre total liquid) was found as described in Sect. 4.8. Molar concentration of each component, j, on a biomass basis (C_{Mj}, mmol/g BDM) was calculated as follows:

$$C_{Mj} = C_j(t_i)/X(t_i) \qquad (5.1)$$

where:

t_i ≡ time of sample i, hr;

$C_j(t_i)$ ≡ broth concentration of component j in sample i, mmol/litre;

$X(t_i)$ ≡ broth biomass concentration, g BDM/litre;

Based on the molecular weight (MW_j, g/mol), weight concentation in biomass (C_{Wj}, g/g BDM) was calculated as follows:

$$C_{Wj} = C_{Mj} * MW_j/1000 \qquad (5.2)$$

Values for C_{Wj} were summed over the 15 fatty acids measured, giving typical total cellular concentrations during growth and sporulation of 2.7 to 3.0 per cent of BDM. These levels are in agreement with those reported by Bulla et al. (1970a), and reflect the cell's needs for FA's for membrane formation. Values of C_{Wj} for PHB and PHV were also calculated. While their vegetative phase levels were low, during sporu-

lation over seven per cent of biomass dry matter (BDM) consisted of the two inert storage polymers. These were treated as solid - phase products, in a separate compartment from the metabolic processes per se; and specific rates were based on the reduced mass of this "viable" compartment. Thus all specific rates were calculated on the basis of viable dry matter concentration (VDM, g/l) as follows:

$$\text{VDM, g/l} \equiv (\text{BDM, g/l})*[1-(\text{PHB} + \text{PHV})] \quad (5.3)$$

where:

BDM ≡ total biomass dry matter concentration, g/l;

(PHB + PHV) ≡ $C_{WPHB} + C_{WPHV}$, g/g BDM.

The specific rate of consumption or production of each biomass and liquid - phase component, j, was calculated as follows:

1) the volumetric molar consumption/production rate (R_{Vj}, mmol /litre/hr) at the temporal mid - point between consecutive samples was approximated as follows:

$$R_{Vj}(t_k) \approx [C_{Mj}(t_{i+1}) - C_{Mj}(t_i)]/(t_{i+1} - t_i) \quad (5.4)$$

2) the viable biomass dry matter concentration [$X'(t_k)$, g VDM/ litre] at the temporal mid - point was estimated as follows:

$$X'(t_k) \approx \exp(\{\ln[X'(t_{i+1})]+\ln[X'(t_i)]\}/2) \quad (5.5)$$

This quantity is herein designated as the "log mean" biomass concentration, although this term is often used elsewhere in engineering in a different sense.

3) the specific rate of consumption or production ($R_{mj}(t_k)$, mmol/g VDM/hr) was calculated by dividing the volumetric rate by the log mean viable biomass concentration, namely:

$$R_{mj}(t_k) \equiv R_{vj}(t_k) / X'(t_k) \qquad (5.6)$$

An example specific rate calculation is given in App. G.

As stated above, specific rates so calculated were considered to apply at the temporal mid - point between samples. Since the anaerobic incubation results (Sect. 4.3, 5.4) were considered representative of the time of sampling, it was necessary to interpolate specific rates to coincide with the latter. This was performed using a published natural cubic spline program (Press et al., 1986, p. 88). The resulting values were entered into their respective cells in the metabolic flowchart described in Sect. 5.1.

5.3 Calculation of Carbon Flows to Biosynthesis of Viable Dry Matter

Flows of coenzyme A (CoA) esters (viz. acetyl-, isobutyryl-, isovaleryl- and 2-methylbutyryl-CoA) to fatty acid (FA) biosynthesis were calculated as follows:

1) for each FA measured, the CoA esters required for its synthesis were determined (Kaneda, 1977); these are shown in Table 5.1;

2) these factors were multiplied by the rate of individual FA production ($R_{FAm}(t_k)$, mmol/g VDM/hr; see Sect. 5.2), and the values for each CoA ester summed to give its overall rate of production (or consumption);

These rat s were entered into their respective cells in the metabolic flowchart described in Sect. 5.1.

Detailed amino acid analyses were performed (Sect. 4.4.4) on biomass from three phases of growth on tryptone / yeast extract medium (Sect.4.1). Mean values and standard deviations are given in App. A. The three biomass samples were as follows:

1) vegetative growth phase (6.15 hr; 2.05 [±0.014] g BDM/l): pairs and chains of 4 rods with faint internal (nuclear?) structure;

2) early sporulation phase (11.0 hr; 5.94 [±0.064] g BDM/l): short single and paired rods with pronounced internal granulation;

Fatty Acid	Moles CoA Ester per mole Fatty Acid			
	acetyl-	isobutyryl-	isovaleryl-	2-methyl-butyryl-
i-C12	4	1	0	0
n-C12	6	0	0	0
i-C13	4	0	1	0
a-C13	4	0	0	1
i-C14	5	1	0	0
n-C14	7	0	0	0
i-C15	5	0	1	0
a-C15	5	0	0	1
n-C15 *	6	0	0	0
i-C16	6	1	0	0
n-C16	8	0	0	0
i-C16=	6	1	0	0
n-C16=	8	0	0	0
i-C17	6	0	1	0
a-C17	6	0	0	1

Table 5.1: Co-enzyme A esters required for fatty acid biosynthesis. * Note that n-C15 also requires 1 mole of propionyl-CoA.

3) late sporulation phase (20.9 hr; 3.76 [±0.028] g BDM/l): free, refractile spores, crystals, cell debris, and a very few unlysed cells containing refractile spores.

Since this analytical data was considered accurate only regarding relative amounts of individual amino acids, it was converted to absolute concentrations in biomass as described below.

A detailed composition for viable bacterial biomass (Morowitz, 1968) is shown in Table 5.2. Although this amino acid profile differs from that found in B. thuringiensis, the total α-amino nitrogen (N) content calculated from it (viz. 6.7 %) is reasonable. For example, Murrell (1969) reported average vegetative phase α-amino N of 7.4 % in four strains of B. subtilis and B. cereus var. mycoides, with total N as low as 6.3 % in B. megaterium, and 6.8 % in B. anthracis. I therefore assumed that the Morowitz (1968) data was correct in regard to total amino acid content. The procedure for adjustment of my raw biomass amino acid data to an absolute concentration basis was thus as follows:

1) since the analytical method used destroyed cysteine, proline and tryptophan (Sect. 4.4.4), total amino acid content with exception of these was found from Morowitz to be 4.382 mmol/ g VDM;

2) total amino acid content of vegetative cells from the raw data (App. A) was calculated to be 2.078 mmol/g VDM;

Compound	mmoles/g VDM
alanine	0.454
arginine	0.252
aspartic acid	0.201
asparagine	0.101
cysteine	0.101
glutamic acid	0.353
glutamine	0.201
glycine	0.403
histidine	0.050
isoleucine	0.252
leucine	0.403
lysine	0.403
methionine	0.201
phenylalanine	0.151
proline	0.252
serine	0.302
threonine	0.252
tryptophan	0.050
tyrosine	0.101
valine	0.302
hexose	1.026
ribose	0.447
deoxyribose	0.096
thymine	0.024
adenine	0.140
guanine	0.140
cytosine	0.140
uracil	0.115

Table 5.2: Simplified chemical composition of a microbial cell (adapted from Morowitz, 1968).

3) raw data was multiplied by 2.109 (ie. 4.382/2.078). Biomass concentrations of cysteine, proline and tryptophan were taken from Morowitz (1968), as were those for hexose, ribose, deoxyribose, thymine, adenine, guanine, cytosine and uracil (Table 5.2). The vegetative cell composition employed contained about 11.2 % total N, compared to about 10.6 % for B. cereus var. mycoides and B. subtilis (Murrell, 1969). Biomass concentration of fatty acids was measured (Sect. 4.4.8), and glycerol required for lipid synthesis calculated therefrom (see below).

Several assumptions were made to simplify the anabolic aspects of the model, specifically:

1) requirements for hexose, ribose and deoxyribose were assumed to come directly from glucose (Lehninger, 1976, p. 467-472, 729-739);

2) serine and glycine were treated as a single amino acid (ibid., p. 697);

3) derivatives of tetrahydrofolate, interconverted in several biosynthetic reactions (cf. ibid., p. 568, 697, 730, 731, 739, 939), were omitted from the carbon balance; Stouthamer (1975) justified such omission as follows: "...no allowance has been made for the ATP needed for the generation of formyl - and methenyl - tetrahydrofolates. These are formed in sufficient amounts during the conversion of serine into glycine to make

possible the formation of methionine, purines and thymine."

4) conversion of aspartate to fumarate during synthesis of adenylic and guanylic acids (ibid., p. 730-733) was ignored;

5) glycerol for lipid synthesis was assumed to come directly from glucose (Mandelstam and McQuillen, 1973, p. 163); and to exist in lipids, on average as a diester (Morowitz, 1968);

6) conversion of succinyl-CoA to succinate during synthesis of lysine and methionine (Lehninger, p. 700-702) was ignored.

Based on these assumptions and the data of Table 5.2, precursor fluxes to non - amino acid biosynthesis ($R_{PNj}(t_k)$, mmol/g VDM/hr), at the midpoint between consecutive samples, were calculated as follows:

1) glucose (to hexose, ribose, deoxyribose and glycerol):

$$R_{PNglc}(t_k) \approx (1.026 + 0.447 + 0.096)*[\mu_A(t_k)] + (0.25)*(R_{FA}(t_k) \qquad (5.7)$$

where:

$\mu_A(t_k)$ ≡ apparent specific growth rate, hr^{-1}

$$\equiv [X'(t_{i+1})-X'(t_i)]/\ [(t_{i+1})-(t_i)]/\ X'(t_k) \qquad (5.8)$$

$t_k \equiv (t_{i+1} + t_i)/\ 2$

$R_{FA}\ (t_k)$ ≡ rate of fatty acids production, mmol/g VDM /hr;

2) aspartate (to thymine, cytosine and uracil):

$$R_{PNasp}(t_k) \approx (0.024 + 0.140 + 0.115)*[\mu_A(t_k)] \quad (5.9)$$

3) serine (to adenine and guanine):

$$R_{PNser}(t_k) \approx (0.140 + 0.140)*[\mu_A(t_k)] \quad (5.10)$$

Precursors, stoichiometry and references for amino acid biosynthesis are given in Table 5.3. The total cellular requirement for each amino acid ($R_{TAj}(t_k)$, mmol/g VDM/hr), at the midpoint between consecutive samples, was calculated as follows:

$$R_{TAj}(t_k) \approx [\mu_A(t_k)]*(C'_{Mj}) \quad (5.11)$$

where:

C'_{Mj} ≡ cellular concentration of amino acid j, mmol/g VDM.

Rates of individual amino acid biosynthesis or catabolism ($R_{AAj}(t_k)$, mmol/g VDM/hr) were thus calculated as,

$$R_{AAj}(t_k) \approx R_{TAj}(t_k) - R_{Mj}(t_k) \quad (5.12)$$

where:

$R_{Mj}(t_k)$ ≡ specific rate of consumption or production of amino acid j, mmol/g VDM/hr (Sect. 5.2).

Since cysteine, proline and tryptophan were not measured by the amino acid analysis (Sect. 4.4.4), they were assumed to be synthesized (or catabolized) at the average rate of amino acid biosynthesis.

The cellular intermediates assumed to be formed by possible net catabolism of amino acids are shown in Table 5.4,

Amino Acid	Precursor	mol precursor/ mol amino acid	Reference Page
alanine	pyruvate	1	696
arginine	glutamate	1	705
asparagine	aspartate	1	696
cysteine	serine	1	698
glutamine	glutamate	1	695
glycine	serine	1	697
histidine	glucose	1	707
	glycine	1	730
lysine	aspartate	1	702
	pyruvate	1	702
methionine	(see text)		701
phenylalanine	glucose	1.67	708
proline	glutamate	1	695
serine	glucose	0.5	697
threonine	aspartate	1	700
tryptophan	glucose	0.667	708
	serine	1	708
tyrosine	glucose	1.67	708

Table 5.3: Intermediates of amino acid biosynthesis. Conversion of cysteine to methionine requires conversion of aspartate to pyruvate, and serine to glycine (Lehninger, 1976).

Amino Acid	Product	mol product/ mol amino acid	Ref. Page
alanine	pyruvate	1	696
arginine	glutamate	1	575
asparagine	aspartate	1	578
cysteine	pyruvate	1	568
glutamine	glutamate	1	575
glycine	(see text)		567
histidine	glutamate	1	575
lysine	acetyl-CoA	2	572
methionine	succinyl-CoA	1	577
phenylalanine	malate	1	569
	acetyl-CoA	2	569
proline	glutamate	1	576
serine	pyruvate	1	568
threonine	2-ketobutyrate	1	574
tryptophan	alanine	1	573
	acetyl-CoA	2	573
tyrosine	malate	1	569
	acetyl-CoA	2	569

Table 5.4: Intermediates of amino acid catabolism (Lehninger, 1976).

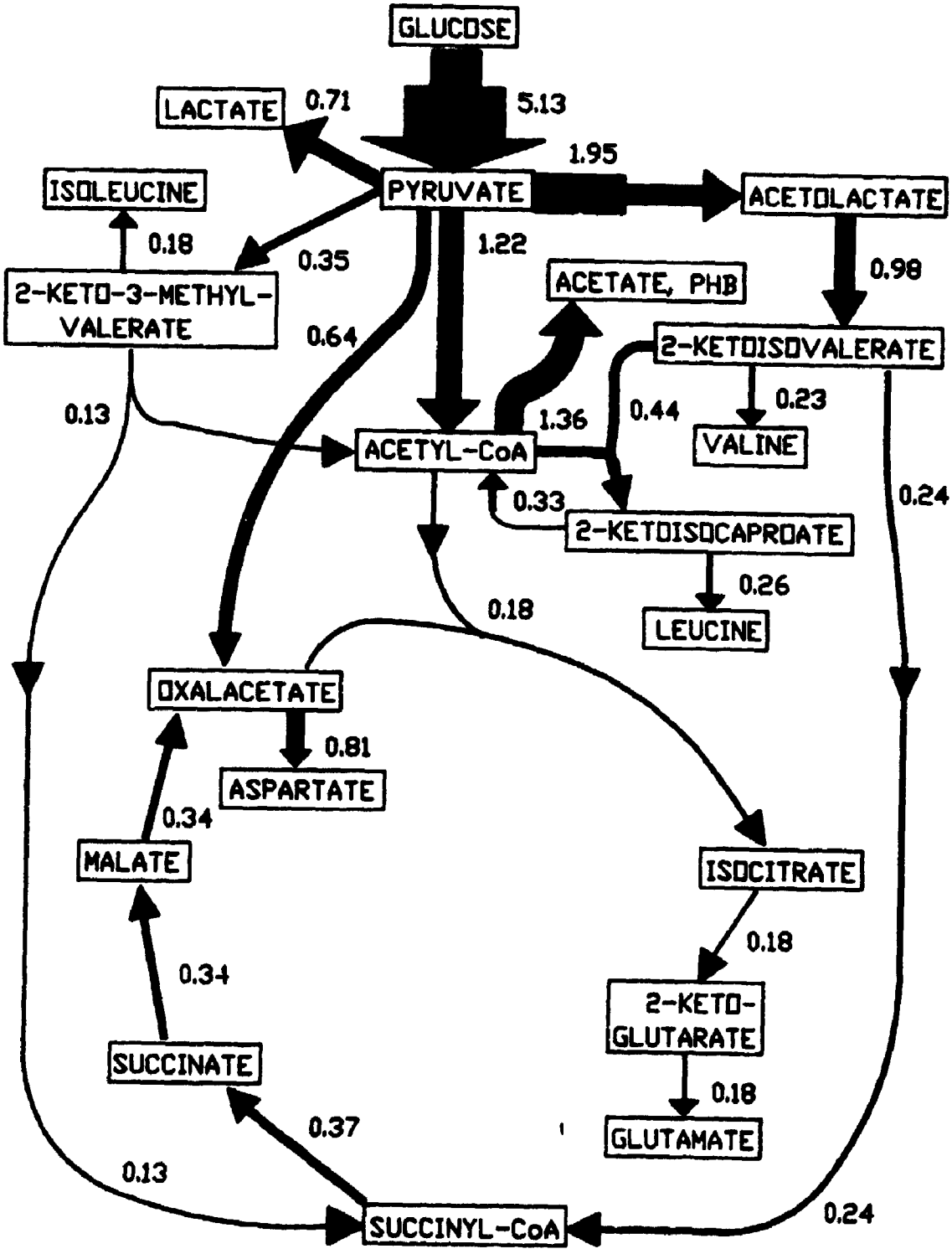

Fig. 5.4: Model solution for energy analysis case, P/O set to 1.60. Flux in mmol/g VDM/hr proportional to line width.

+ NADH + H^+). In aerobes subjected to anaerobic conditions, transfer of electrons to oxygen cannot occur, and the intracellular concentration of reduced coenzyme rapidly increases (Harrison, 1976). This effectively inhibits most, if not all, dehydrogenases: "The expected relative increase of NADH [/NAD^+ ratio] in anaerobically grown cells from 0.19 to 0.34 substantiates a regulatory mechanism found earlier, where anaerobiosis rapidly and completely blocks the pyruvate dehydrogenase activity in E. coli." (Hansen and Henning, 1966). Furthermore, "It can be concluded that NADH inhibition of the overall [pyruvate dehydrogenase] reaction is localized at the lipoamide dehydrogenase component of the enzyme complex." (ibid.). This is significant since this component is common to various dehydrogenases, as summarized by Lowe et al. (1983):

> "Our conclusion is that a single E3 gene codes for the dihydrolipoamide [lipoamide] dehydrogenase needed in the pyruvate dehydrogenase, 2-oxoglutarate dehydrogenase and branched-chain 2-oxo acid dehydrogenase activities of B. subtilis. The dihydrolipoamide dehydrogenase of E. coli pyruvate dehydrogenase and 2-oxoglutarate dehydrogenase complexes (there is no branched-chain 2-oxo acid dehydrogenase complex) is coded for by a single structural gene...[I]n Pseudomonas putida there are two different dihydrolipoamide dehydrogenases...This appears to be the only instance of functionally different dihydrolipoamide dehydrogenases occurring in the same organism."

Thus the common branched - chain keto acid dehydrogenase will be inhibited by anaerobic conditions. Furthermore the acyl-CoA dehydrogenase (likely common to the three BCAA pathways; see Sect. 3.2) is expected to be inhibited, since it

is a flavin - linked enzyme similar to lipoamide dehydrogenase (Lehninger, 1976, p. 486). Imposed anaerobiosis was therefore used to block the catabolic segments of the BCAA pathways, in an attempt to infer quantitative flow rates through them, as indicated by liquid - phase accumulation of metabolic intermediates. The method used for aseptic, anaerobic incubation of broth samples is described in Sect. 4.3.

A schematic diagram of part of the valine pathway is shown in Fig. 5.2. With the exception of 2-ketoisocaproate synthesis, a similar flux balance can be applied to each of the three BCAA pathways (see Sect. 3). The "control volume" for molar balance calculations is also shown; the flows crossing its boundaries are as follows:

1) biosynthesis of α-keto acid from endogenous precursors (ie. pyruvate, etc.; Sect. 3.1);

2) reversible transamination of α-keto acid to BCAA for protein synthesis (Sect. 3.1);

3) reversible transamination of α-keto acid to/from exogenous (extracellular) BCAA;

4) excretion/assimilation of α-keto acid (cf. αOHIV; Sect 4.4.7);

5) reversible interconversion of acyl-CoA and corresponding exogenous acid;

6) reversible interconversion of acyl-CoA and corresponding fatty acids (Sect. 3.3);

7) dehydrogenation of acyl-CoA (Sect. 3.2);

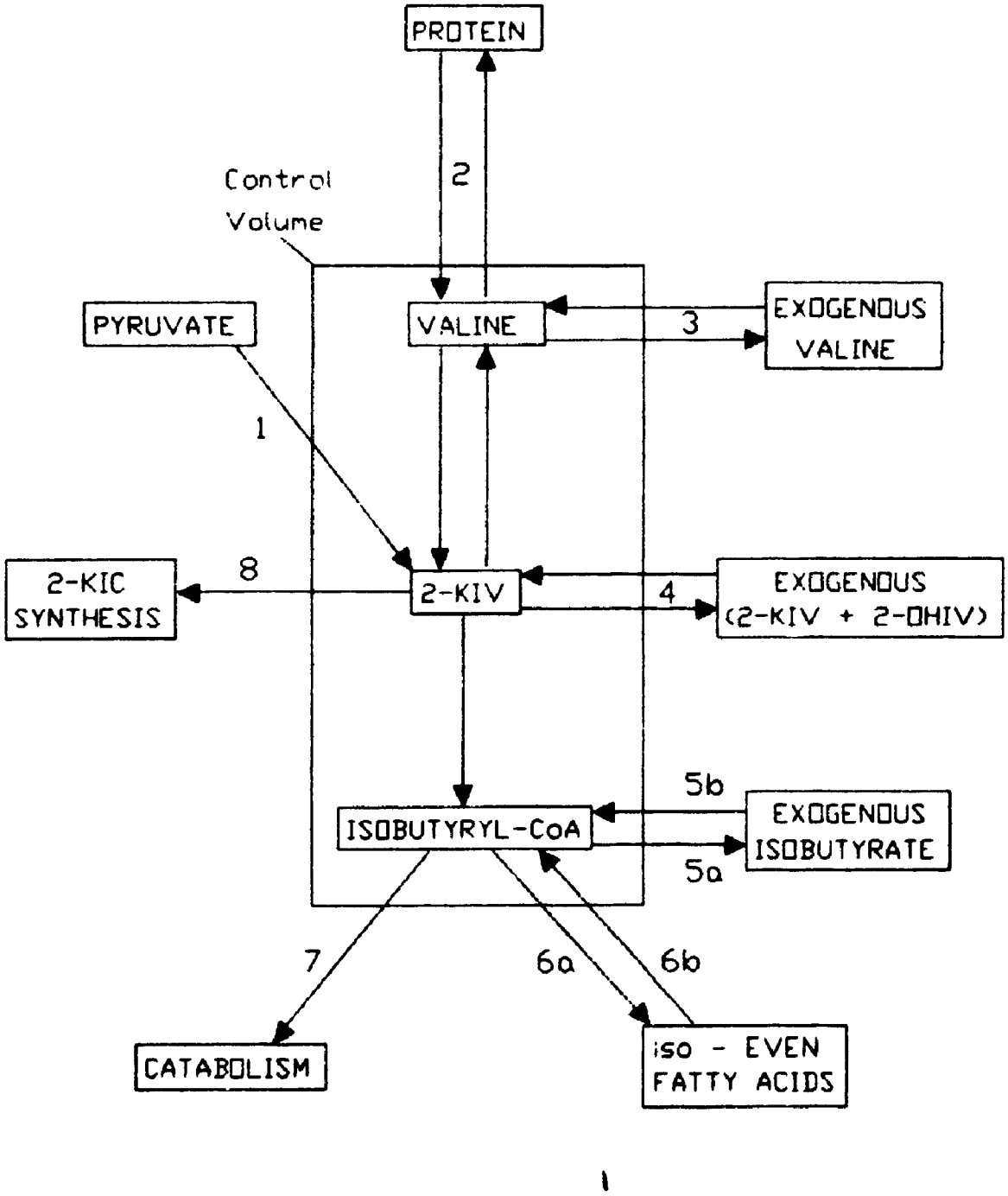

Fig. 5.2: Valine pathway molar flux balance. 2-KIV = 2-ketoisovaleric acid; 2-OHIV = 2-hydroxyisovaleric acid; 2-KIC = 2-ketoisocaproic acid.

8) synthesis of αKIC from αKIV (Sect. 3.1).

The strategy employed was to calculate the first flow above as the sum of the other flows. The nature of the latter under the test conditions (viz. anaerobiosis, protein synthesis blocked; see Sect. 4.3) will now be described.

Transamination of α-keto acid to amino acid for protein synthesis (flow #2) is effectively blocked as follows:

1) chloramphenicol inhibits incorporation of amino acid into protein (Brock, 1961);

2) intracellular amino acid concentration increases rapidly (Mandelstam, 1958);

3) transamination, being highly reversible, effectively stops due to the law of mass action, ie. forward and reverse reaction rates become equal.

Transamination of α-keto acid to/from exogenous amino acid (flow #3) was quantified by measuring the change, if any, in broth concentration of the latter.

Export of α-keto acid (flow #4) was measured as the rate of change in its concentration in the broth.

Conversion of acyl-CoA to the corresponding branched, short - chain fatty acid (flow #5a) is catalyzed by an acyl-CoA hydrolase (Kaneda, 1977). Conversion of free acid to its acyl-CoA ester (flow #5b) is effected by medium - chain acyl-CoA synthetase (Lehninger, 1976, p. 546; Barman, 1969, p.

876). The resultant of these flows was measured as the rate of change in the broth concentration of free acid.

As discussed fully in Sect. 3.3, formation of branched - chain fatty acids from acyl-CoA ester (flow #6a) is catalyzed by branched - chain fatty acid synthetase. Oxidation of fatty acids via the corresponding acyl-CoA ester (flow #6b), if it occurs in B. thuringiensis, would presumably be catalyzed by one or more acyl-CoA synthetase enzymes (Lehninger, 1976, p. 546; cf. Moat and Foster, 1988, p. 240). However no change in the fatty acid composition of the cells could be detected under the conditions of this test.

Catabolism of acyl-CoA by acyl-CoA dehydrogenase (flow #7; see Sect. 3.2) is effectively blocked as discussed above.

Flow #8 was calculated first by a similar molar balance on the leucine pathway.

It would appear in principle that accumulation of α-keto acid under the present conditions could result from inhibition of protein biosynthesis and/or acyl-CoA catabolism (flows #2 and #7 respectively, Fig. 5.2). I will now attempt to establish that only the latter can be a significant cause of such accumulation.

As described in Sect. 3.1, B. thuringiensis may well in general contain two types of α-acetolactate synthase enzyme (viz. degradative and biosynthetic), of which only the latter is inhibited by any BCAA (specifically valine). Similarly, of the two types of threonine deaminase likely present, only the

biosynthetic enzyme is inhibited by any BCAA (specifically isoleucine). A major effect of chloramphenicol is to increase intracellular amino acid levels:

> "...in cultures of Escherichia coli growing in glucose - salts medium, such that all essential amino acids must be synthesized, there is a marked increase in the amount of all free amino acids upon addition of chloramphenicol, presumably because synthesis of these continues while incorporation into protein is blocked. This leads to an increase in amino acid concentration within the cellular pool and also an excretion of amino acids into the medium." (Brock, 1961).

Results by Mandelstam (1958) show that within 40 minutes of chloramphenicol addition, and probably much sooner, intracellular amino acid concentrations reach saturation levels. Thus both the biosynthetic acetolactate synthase and threonine deaminase would be rapidly inhibited; and any products formed by these pathways would result predominantly from the degradative enzyme systems. That ADP or AMP activate the degradative threonine deaminase (Nakazawa, 1971; Shizuta and Tokushige, 1971) implies subsequent catabolism, at least via the isoleucine pathway. It is therefore plausible that intermediates accumulated under the test conditions were destined for catabolism by BCKA dehydrogenase, acyl-CoA dehydrogenase, etc. This conclusion is substantiated by the fact that much greater amounts of keto acid than amino acid were always released.

Flux balances on the three BCAA pathways for each of the seven anaerobic incubation experiments are given in App. B. Specific rates of release (R_{Mj}, mmol/g VDM/hr) of the branched - chain amino acid, 2-keto acid and short - chain fatty acid

for each pathway (flows 3, 4 and 5 respectively, Fig. 5.2) were calculated as described in Sect. 5.2. A time period of 40 minutes was used for these calculations (Sect. 4.3). The sum of these flow rates (ie. net pathway release rate, Table B.1) was assumed to be identical to the acyl-CoA flux from BCKA dehydrogenase for the pathway [ie. FT(x), Sect. 5.5, Equation (5.13)] at the time that the actual fermentation sample was taken.

Anaerobic incubation resulted in accumulation of intermediates of the isoleucine pathway in all but one case (viz. GR10X5; see Sect. 6.4.1). Intermediates of the valine pathway also accumulated in several samples, raising the possibility of calculating two separate absolute fluxes. However three samples gave net depletion of valine and leucine pathway intermediates, implying at least partial operation of the catabolic section of these two pathways under certain anaerobic, as well as aerobic, conditions. This was corroborated by the fact that absolute BCKA dehydrogenase flows calculated from valine pathway accumulation data were consistently less (generally 3 to 20 times lower) than the same flows calculated from isoleucine pathway accumulation data. Thus all absolute flux calculations (GR10X5 excepted) were performed using the latter.

5.5 Estimation of Relative Fluxes of BCAA Pathways

Research by Kaneda (1966) on fatty acids in *B. subtilis* provided the conceptual basis for calculation of flux through the branched - chain amino acid pathways relative to each other. Thus,

> Any one of the branched-chain amino acids...or of the branched short-chain fatty acids...added to the glucose - yeast extract medium increased the synthesis of the specific pairs [*sic.*] of fatty acids structurally related to the added substrate and decreased the synthesis of other fatty acids. This indicates that the relative abundance of branched-chain fatty acids in *B. subtilis* is a function of the relative availability of the precursors of the terminal portions of the fatty acids..." (*ibid.*)

A similar phenomenon was demonstrated in *B. cereus* (Kaneda, 1971), and no doubt represents the reason for marked dependence on growth medium of fatty acid composition observed in bacilli (Kaneda, 1967; Sect. 3.3).

Kaneda (1977) described the variables involved in the present determination:

> "Factors affecting the relative proportions of the branched fatty acid series may be grouped into three categories: (i) the relative activity of the three chain initiators toward fatty acid synthetase...;(ii) the relative availability of chain initiators...; and (iii) the amount of chain extender...Factor (i) is characteristic of the fatty acid synthetase and is fixed for a given microorganism. Factors (ii) and (iii) are variable, depending upon physiological and culture conditions."

By summing over all fatty acids derived from each of the three chain initiators (acyl-CoA's), factor (iii) becomes irrelevant. It follows that knowledge of the "specificity", if any, of the operant fatty acid synthetase complex would allow

calculation from fatty acid data of the relative availability of acyl-CoA esters.

The intracellular concentration of each acyl-CoA ester is expected to be a complex function of BCKA dehydrogenase flux and the rates of flows #5, 6 and 7 of Fig. 5.2. However it is clear from basic principles and experimental results (*cf.* Kaneda, 1973; Naik and Kaneda, 1974) that acyl-CoA availability is a direct function (*per se*) of the rate of its formation. Thus two observations made with *B. subtilis* indicate the nature of the major factors affecting acyl-CoA ester availability, namely:

1) the activity of BCKA dehydrogenase is about 50,000 times greater than that of fatty acid synthetase (Kaneda, 1973);

2) branched, short - chain fatty acids, formed by reaction #5a (Fig. 5.2), are produced only on amino acid - rich media (Kaneda, 1977).

The latter observation indicates that release or uptake of these free acids serves merely to modulate acyl-CoA concentration under certain conditions. The former observation implies that flux through BCKA dehydrogenase is normally much greater than that to fatty acid synthesis. It therefore appears justified to consider availability of each acyl-CoA as a function of flux through BCKA dehydrogenase.

Equations for specific rates of branched - chain fatty acid synthesis were thus assumed to be of the following form:

$$FA(x) = k_x * [FT(x) + SA(x)] \qquad (5.13)$$

where:

FA(x) ≡ acyl-CoA flux to fatty acid synthesis for branched - chain pathway x, mmol/g VDM/hr;

x ≡ isoleucine (I), leucine (L) or valine (V);

k_x ≡ fatty acid synthetase activity constant for acyl-CoA primer of pathway x;

FT(x) ≡ acyl-CoA flux from BCKA dehydrogenase for pathway x, mmol/g VDM/hr;

SA(x) ≡ specific rate of acyl-CoA formation from the corresponding short chain acid for pathway x (flow #5b, Fig. 5.2), mmol/g VDM/hr.

Note: To simplify the notation explicit reference to time has been omitted in the case of FA(x), FT(x) and SA(x); all three are time - dependent.

The specificity, if any, of the fatty acid synthetase enzyme (of which k_x, above, is a measure) remains to be determined. Kaneda (1977) summarized his conclusions in this regard as follows:

> "The relative activity of the three branched α-keto acid substrates used as the source of chain initiators to the B. subtilis fatty acid synthetase is 5:2:1 in the order α-keto-β-methylvalerate, α-ketoisocaproate, and α-ketoisovalerate, whereas toward B. cereus synthetase it is 4:3:1."

In my opinion these conclusions are questionable, since they are based on non - steady state experiments in which relative fatty acid biosynthesis was measured after addition of individual BCKA's to crude cell extracts (Kaneda, 1973; Naik and Kaneda, 1974). Under these conditions any fatty acid synthetase specificity which might exist is confounded with the acyl-CoA availability factor.

More specifically, under non - steady state conditions assumption of a constant and identical relationship between the concentration of each α-keto acid and its corresponding acyl-CoA is not warranted. In isolated rat liver cells (hepatocytes), addition of 1 mM α-ketoisocaproate led to a constant intracellular concentration (about 360 nmol/g DM) of isovaleryl-CoA during five minutes; 1 mM α-ketoisovalerate produced a brief peak in isobutyryl-CoA concentration (about 360 nmol/g DM), which declined to about 150 nmol/g DM by five minutes (Corkey et al., 1982). Not only was the response to α-ketoisovalerate addition time - varying, but more significantly the average concentration of isobutyryl-CoA produced was much lower than that of isovaleryl-CoA, in response to the same level of α-keto acid addition.

The reason for such a differential response to α-ketoisovalerate (αKIV) compared to α-ketoisocaproate (αKIC) probably lies in their effect on BCKA dehydrogenase and subsequent catabolic enzymes. In mammals BCKA dehydrogenase activity ratios are 1.5-1.8:1.0:0.6-0.7 in the order αKIV:α-KIC:α-keto-3-methylvalerate (αKMV; Odessey, 1986). In B. subtilis, S. faecalis and P. putida the enzyme has an order of activity of αKIV > αKMV > αKIC (Massey et al., 1976; Roberts and Sokatch, 1978). Furthermore in the latter organism valine activated BCKA dehydrogenase (Sect. 3.2), suggesting a catabolic role for such regulation (ibid.). Since transamination of α-ketoisovalerate to valine is certain to occur (Sect.

3.1), the former would also be at least an indirect activator of its own catabolism. As such it would tend to depress the concentration of isobutyryl-CoA, which Corkey *et al.* (1982) observed. The result in bacilli would be less formation of the corresponding branched - chain fatty acids for a given concentration of added α-keto acid, especially α-ketoisovalerate. This is exactly what Kaneda found, but interpreted as a measure of fatty acid synthetase specificity.

Research by Butterworth and Bloch (1970) on the cell - free fatty acid synthesizing system of *B. subtilis* showed that if specificity exists it must lie in the initial step, *ie.* the priming reaction catalyzed by acyl-CoA:acyl carrier protein transacylase (ACP-acyl transferase; *cf.* Lehninger, 1976, p.664). Results obtained by Willecke and Pardee (1971) with a *B. subtilis* mutant apparently lacking BCKA dehydrogenase activity were consistent with lack of ACP-acyl transferase specificity. Thus, "One of the three mentioned short branched chain acids was enough to support growth of *B. subtilis* 626. The doubling time was always found to be about 175 min regardless of whether the mutant was growing in the presence of only one or all three short branched chain acids." Boudreaux *et al.* (1981) made a similar finding with a *B. subtilis* mutant having altered ACP-acyl transferase enzyme, and requiring a short - chain branched fatty acid as growth factor. Again identical growth was observed with any of isobutyrate, isovalerate or 2-methylbutyrate.

In spite of considerable research in this area, briefly reviewed above, it appears that none has definitively addressed the question of the relative rates of the three branched - chain acyl-CoA esters in the ACP-acyl transferase reaction which initiates fatty acid synthesis in bacilli.

Metabolic energy balance calculations were performed on a vegetative growth - phase sample to attempt to further resolve this question; details of the fermentation and calculation procedure are given in Appendix C. The metabolic flows which result for the base case (viz. no FA synthetase specificity; FT(I) = 0.0036 mmol/g VDM/hr) are summarized in Fig. 5.3, in which line width is proportional to molar flow rate.

The two independent variables studied in the energy analysis were absolute flux through BCKA dehydrogenase (Sect. 5.4), and specificity of branched - chain fatty acid synthetase. The decision variables which result are the apparent relative flux of carbon to cell biosynthesis (ie. parameter BMF, Sect. 5.1); and the apparent P/O ratio (g-mol of ADP phosphorylated per g-atom of oxygen reduced), a measure of the efficiency of oxidative phosphorylation (cf. Jones, 1979).

Results for the six cases tested (Table 5.5) show that for an identical set of metabolic inputs and non - biomass outputs (including PHB and PHV) absence of fatty acid synthetase specificity is consistent with greater carbon flux to biosynthesis and more efficient oxidative phosphorylation.

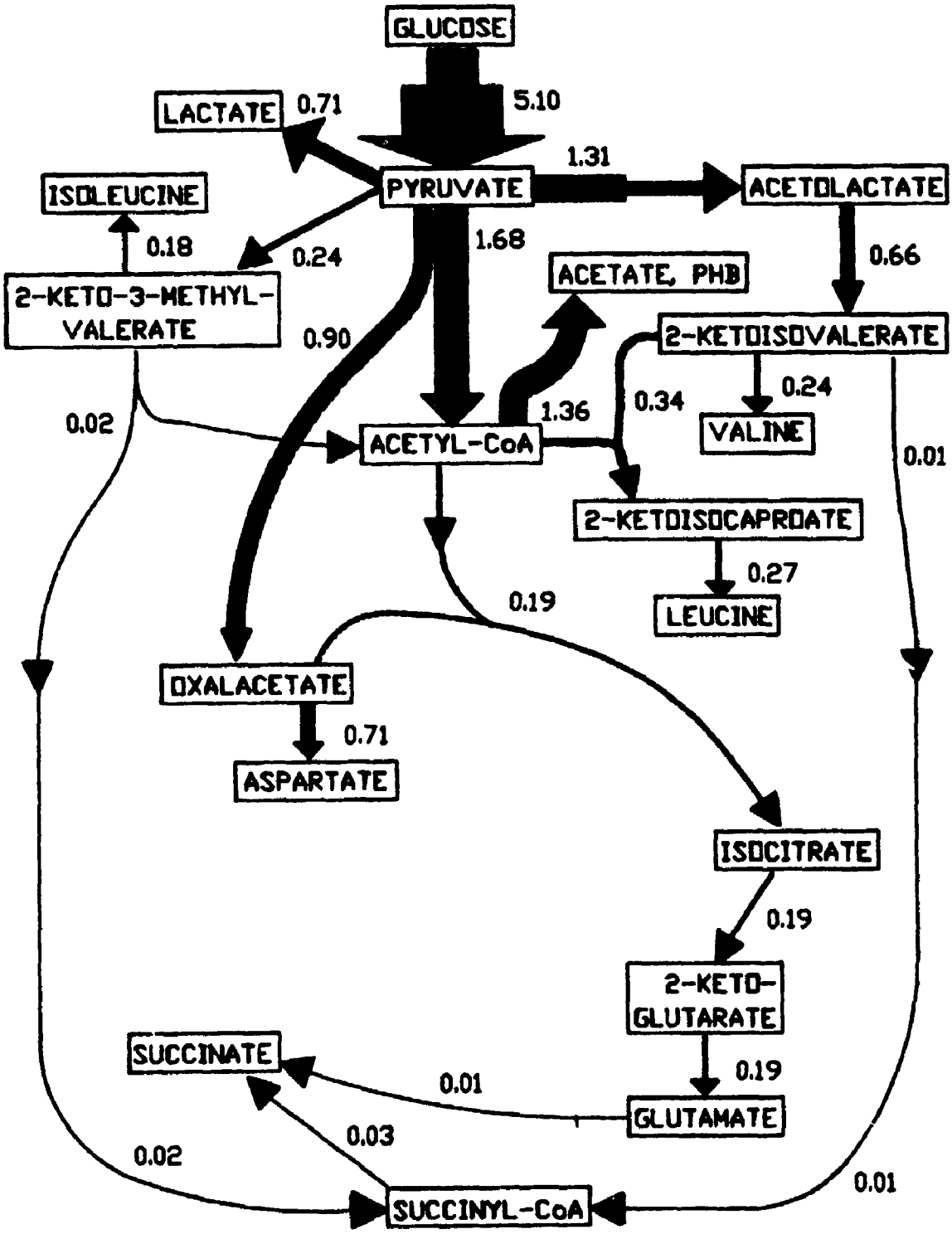

Fig. 5.3: Model solution for energy analysis case. Flux in mmol/g VDM/hr proportional to line width.

FT (I)	K(I) : K(L) : K(V) = 1 : 1 : 1		K(I) : K(L) : K(V) = 4 : 3 : 1	
	BMF at balance	P/O	BMF at balance	P/O
0.0018	0.7124	1.988	0.6900	1.744
0.0036	0.7129	1.990	0.6871	1.717
0.0072	0.7129	1.985	0.6821	1.667

Table 5.5: Apparent P/O ratio as a function of fatty acid synthetase specificity. See text for definition of terms.

Furthermore the result is quite insensitive to uncertainty in the absolute flux value through BCKA dehydrogenase used in the calculation.

The P/O ratio derived for the case of no FA synthetase specificity is about 1.99, compared to 1.67-1.74 in the other case. These values are at or approaching the theoretical maximum efficiency of oxidative phosphorylation in bacilli, as indicated by the following references:

1) Jones (1977) gives maximum P/O for three species of Bacillus as 1.95 to 1.98, ie. two phosphorylation sites;

2) according to Stouthamer (1979),

> "From the measurement of aerobic growth yields, a P:O ratio of 1.46 was calculated for wild - type E. coli. During the complete oxidation of glucose we expect an overall P:O ratio of 1.83 for complete oxidation of glucose when 2 phosphorylation sites are present...The agreement between these two values is reasonable."

3) Roels (1983) considers the maximum operational P/O ratio to be about 1.5.

Based on this evidence the calculated P/O ratios appear to be somewhat too high. To determine if greater inaccuracy in the experimentally estimated value of FT(I) could be responsible, a model simulation was performed in which P/O was set at 1.60; thus values of FT(I) and BMF were calculated to satisfy both carbon and energy balances (Sect. 5.1, App. C respectively). This was achieved for FT(I) $\approx$ 0.12 mmol/g VDM/hr, and BMF $\approx$ 0.690. The metabolic flows which result, as shown in Fig. 5.4, do not differ greatly from those of Fig.

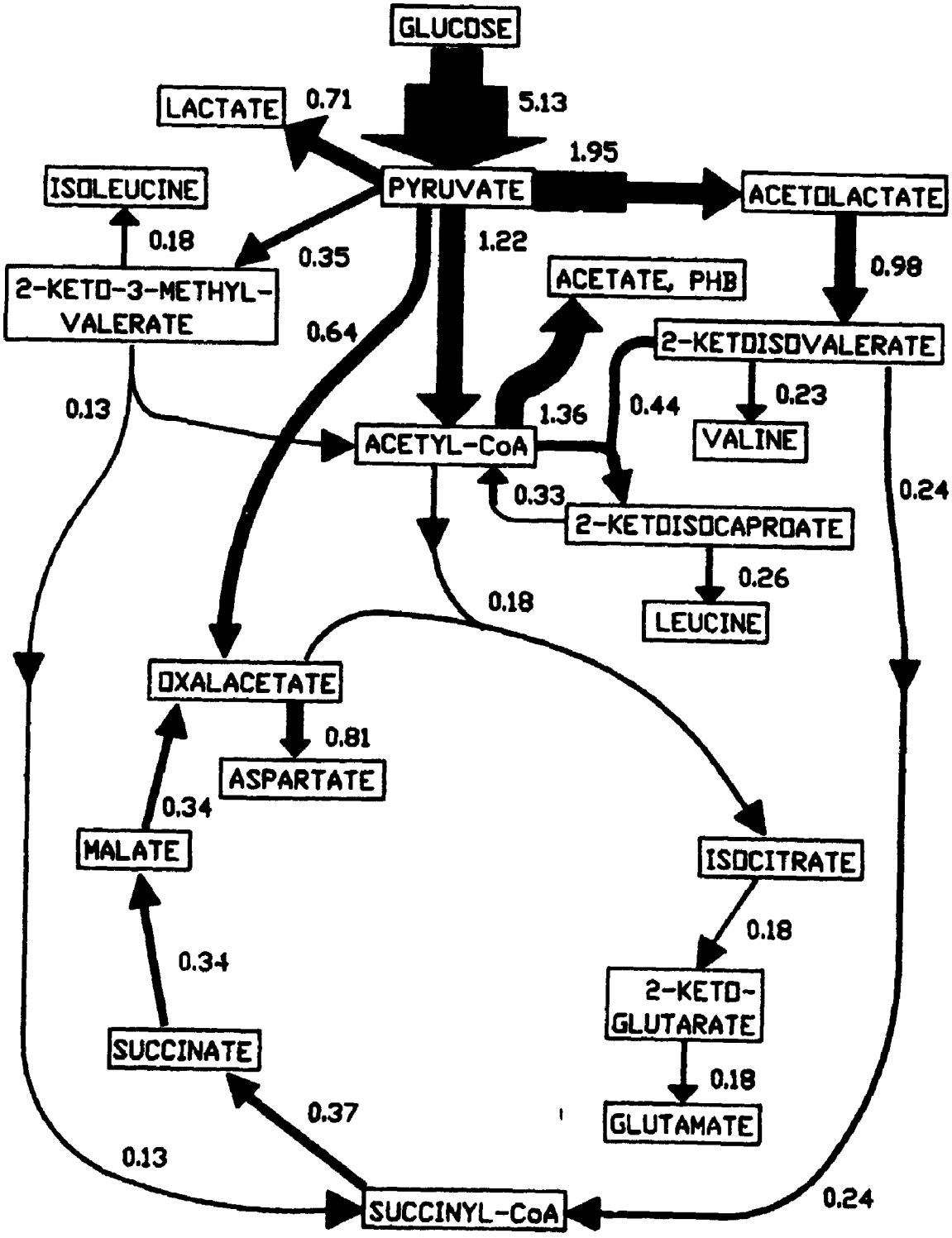

Fig. 5.4: Model solution for energy analysis case, P/O set to 1.60. Flux in mmol/g VDM/hr proportional to line width.

5.3. This explanation, that BCKA DH flux was underestimated, appears plausible for the following reasons:

1) estimates of FT(I) represent the lower bound on flux of αKMV through BCKA dehydrogenase (Sect. 5.4);

2) the higher value of FT(I) required is well within the range found in other fermentations (Table 5.6);

3) the overall metabolic pattern which results is very similar to that of vegetative phase in other fermentations (Fig. 6.16, 8.11).

It is justified to conclude, therefore, that the results of these calculations are reasonable; and that lack of fatty acid synthease specificity implies both greater biomass yield and oxidative phosphorylation efficiency. Since the latter appear to be in fact achievable, evolution would surely have arrived at the more efficient growth and energetic alternative. This follows from a teleological argument, to wit:

> "...we might imagine that a bacterium must have acquired, through selection in the environments to which it is adapted, two main features of metabolic control: the ability to utilize as efficiently as possible (as regards both growth rate and yield) the nutrients normally available in those environments, and the capacity to respond rapidly to environmental changes." (Mandelstam and McQuillen, 1973,p. 423).

On the basis of the evidence presented above I am led to conclude that the activity of branched - chain fatty acid synthetase of B. thuringiensis with each of isobutyryl-, isovaleryl-CoA and 2-methylbutyryl-CoA as substrate is

Sample	FT(I)	FT(V)	FT(L)
GR10X1	0.0574	0.202	0.156
GR10X3	0.186	1.382	0.561
GR10X5	0. 1	0.0352	0.0612
GR11X1	0.0247	0.0763	0.0362
GR11X3	0.168	0.207	0.413
GR12X1	0.220	0.490	0.241
GR12X3	0.187	2.449	0.785

Table 5.6: Calculated fluxes, mmol/g VDM/hr, through branched - chain α-ketoacid dehydrogenase.

essentially identical under physiological conditions. In terms of the notation introduced above,

$$k_I : k_L : k_V = 1:1:1 \qquad (5.14).$$

Given one value of FT(x), for example FT(I), fluxes in the other two branched - chain pathways can be calculated from equation (5.13), as follows:

$$FA(I) = k_I * [FT(I) + SA(I)] \qquad (5.13a);$$

$$FA(L) = k_L * [FT(L) + SA(L)] \qquad (5.13b);$$

dividing (5.13b) by (5.13a),

$$FT(L) = [FT(I) + SA(I)]*[FA(L)/FA(I)] - SA(L) \qquad (5.15a);$$

similarly,

$$FT(V) = [FT(I) + SA(I)]*[FA(V)/FA(I)] - SA(V) \qquad (5.15b).$$

The calculated values of FT(I), FT(V) and FT(L) used for model solution are summarized in Table 5.6.

6. Results and Discussion: Run 10

Complete results for this fermentation are tabulated in Appendix D.

6.1 General Fermentation Characteristics

Run 10 was performed using buffered tryptone/yeast extract medium (Sect. 4.1) with high aeration (1.4 VVM). Patterns of growth and glucose consumption are shown in Fig. 6.1; and ln VDM (viable dry matter; Sect. 5.2) versus time is plotted in Fig. 6.2. Maximum specific growth rate of about 0.49 hr^{-1} was observed between 3.0 and 4.1 hours.

Vegetative growth was accompanied by decreasing pH and dissolved oxygen (DO) concentration, as shown in Fig. 6.3. Although minimum pH of 5.55 appeared to coincide with the end of vegetative growth at about 4.25 hours (t_0 of sporulation; Sect. 2.1.2), minimum DO of approximately 14 % of saturation occurred at about 5.5 hr. Dissolved oxygen and pH then rose rapidly and simultaneously until 7.75 hr, at which time the former reached 78 % sat'n., and the latter peaked at 6.77. At about the same time (viz. 8.0 hr) maximum biomass concentration was reached; and glucose consumption almost ceased, as forespore septation was observed in some cells. Viable cell count at 6 hr was 1.3×10^9 /ml.

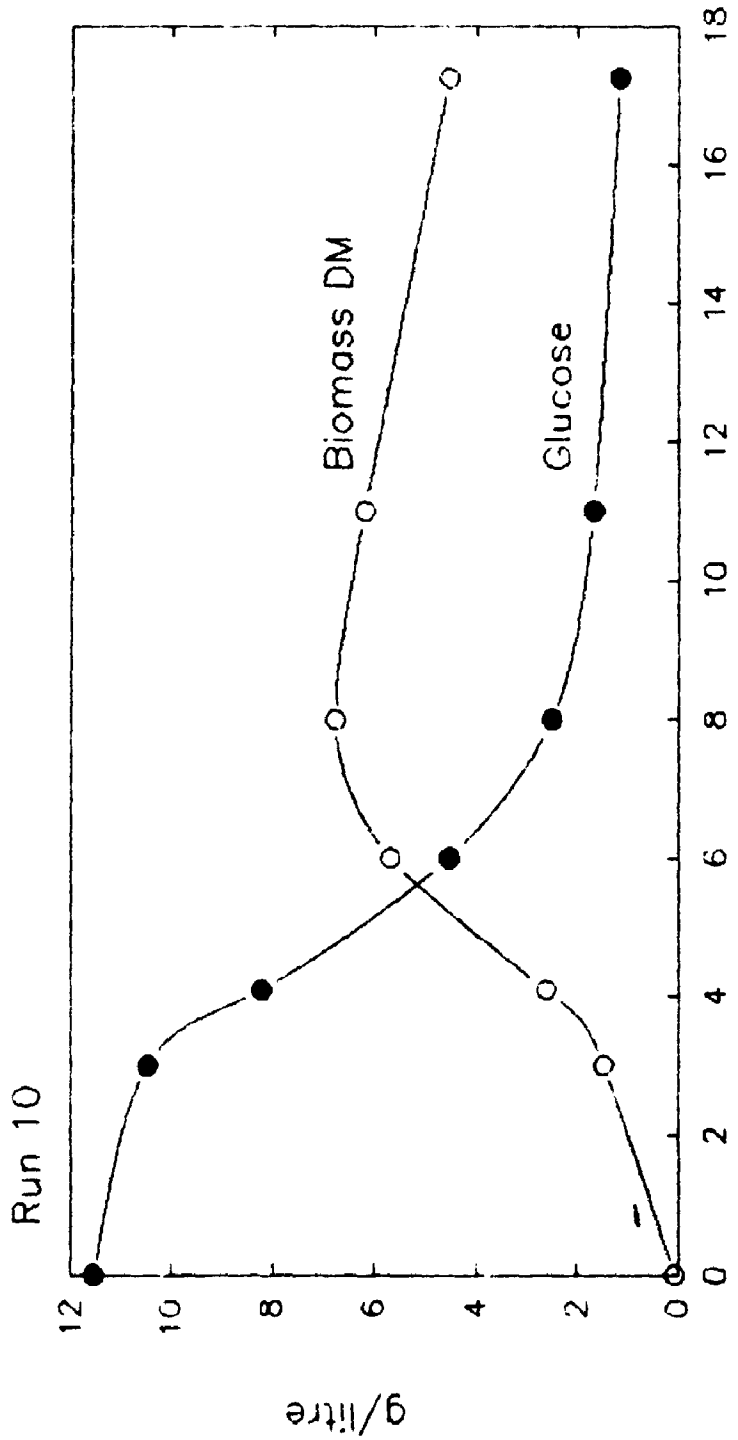

Fig. 6.1: Biomass dry matter and glucose concentration vs. time, Run 10.

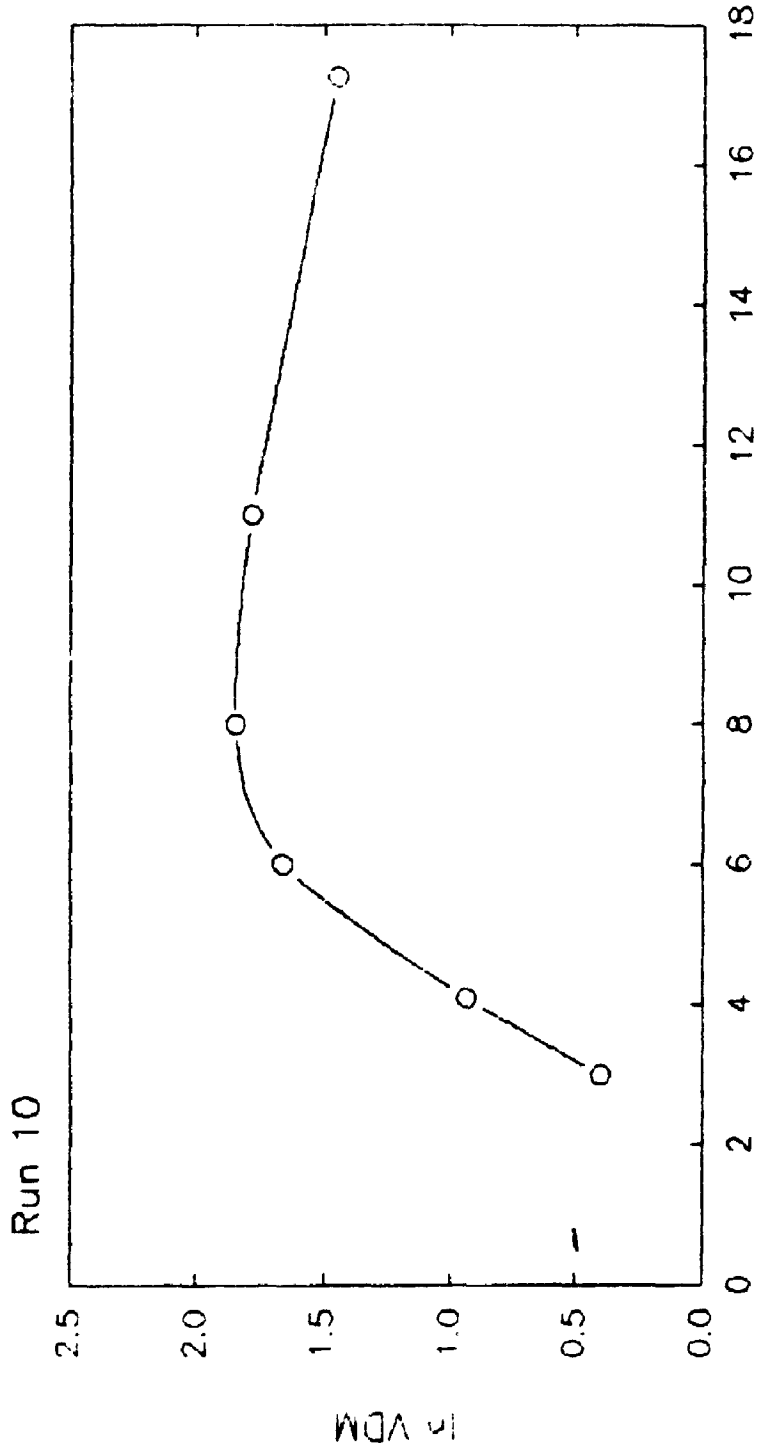

Fig. 6.2: Natural logarithm of viable dry matter vs. time, Run 10.

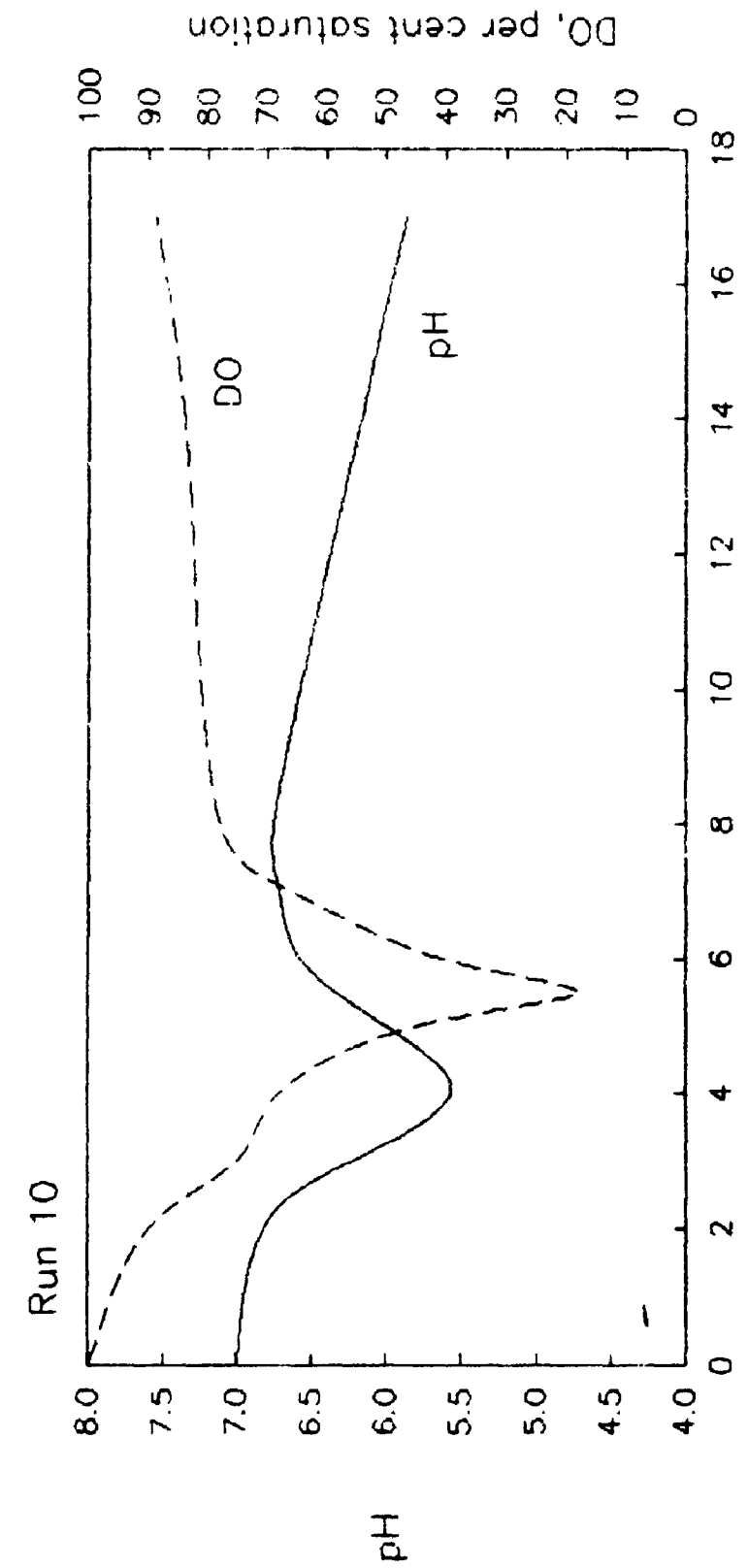

Fig. 6.3: Dissolved oxygen and pH vs. time, Run 10.

During sporulation per se (ie. stages IV to VII; after 8 hours) DO continued to rise slowly, reaching 88 % sat'n. at 17 hr, as biomass concentration and pH decreased in parallel. Early crystal formation was seen at 10.5 hr, and was extensive by 11 hr. Early development of spore cortex was observed at this time (presumably stage IV); no refractility was as yet evident. By 17.25 hr the broth contained mostly free spores and crystals, as well as a few pairs of cells containing refractile spores and crystals. Final yield of spores (heat - resistant colony - forming units) was 1.5 (±0.5) x 10^9 /ml.

Profiles of individual amino acid concentrations (after hydrolysis; Sect. 4.4) versus time are shown in Fig. 6.4 to 6.8. Proline and tryptophan were presumably present in the medium but lost in sample hydrolysis; no cysteine was detected, although a trace amount was presumably present in yeast extract. Amino acid use was generally greatest during early transition phase (ie. 4.1 to 6.0 hr), and ceased after 8.0 hr The concentration of some amino acids may have slightly increased later in sporulation.

The majority of biomass was formed between 4.1 and 8 hr (ie. stages I to III of sporulation), during which time considerable amounts of refractile granules appeared within the cells. Fig. 6.9 shows total fatty acids, PHB and PHV as a percentage of biomass dry matter (BDM) versus time; and implicates PHB as a major constituent of the observed granules. This graph also demonstrates consumption of PHB, and to

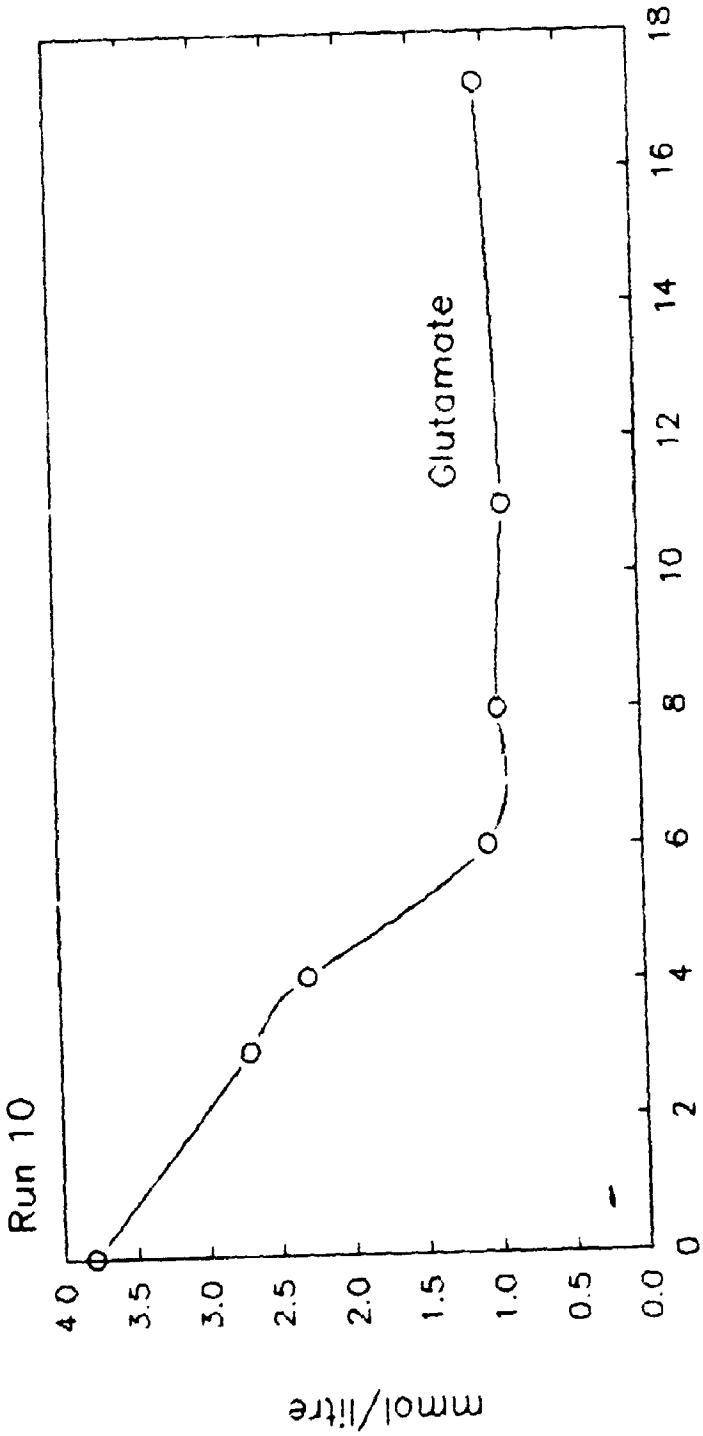

Fig. 6.4: Glutamic acid concentration vs. time, Run 10.

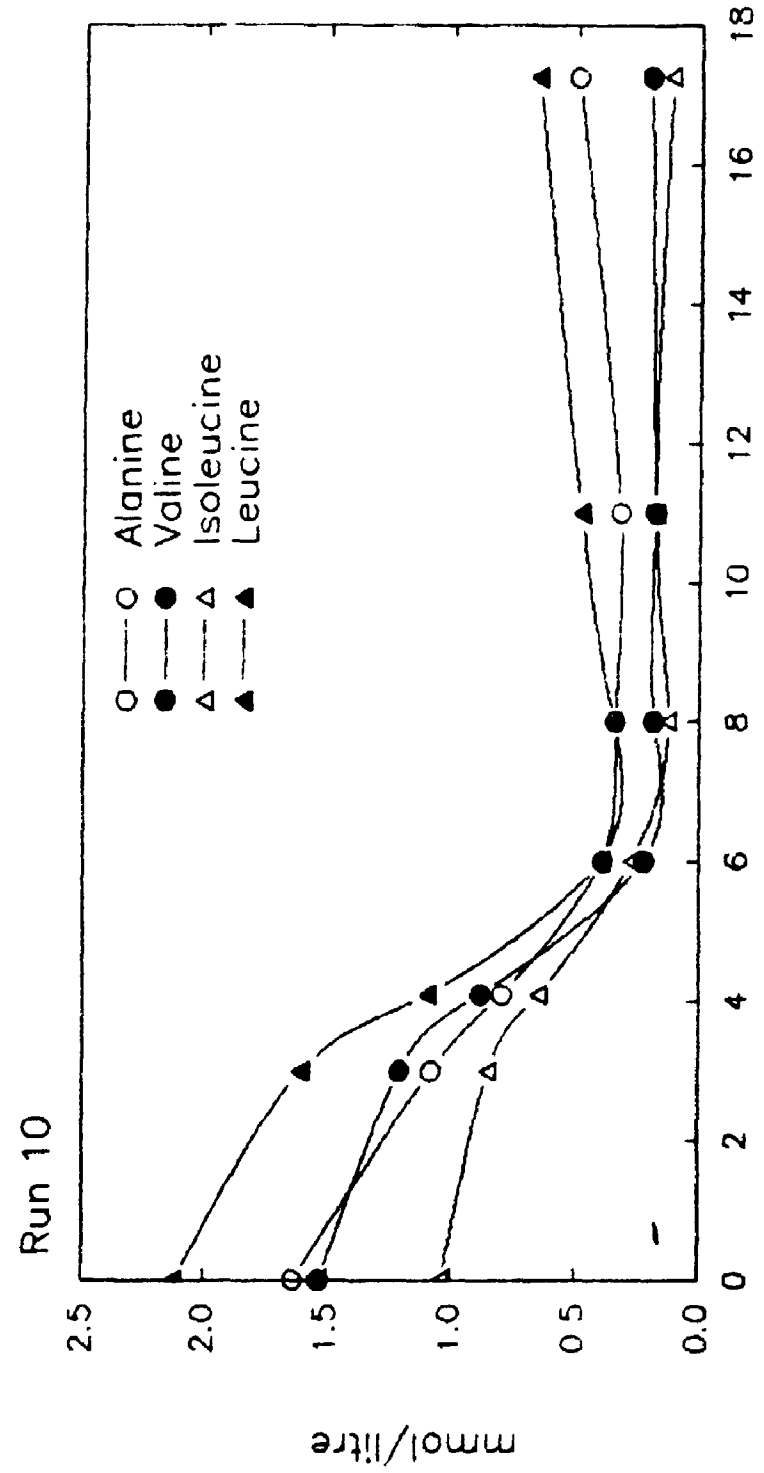

Fig. 6.5: Alanine, valine, isoleucine and leucine concentration vs. time, Run 10.

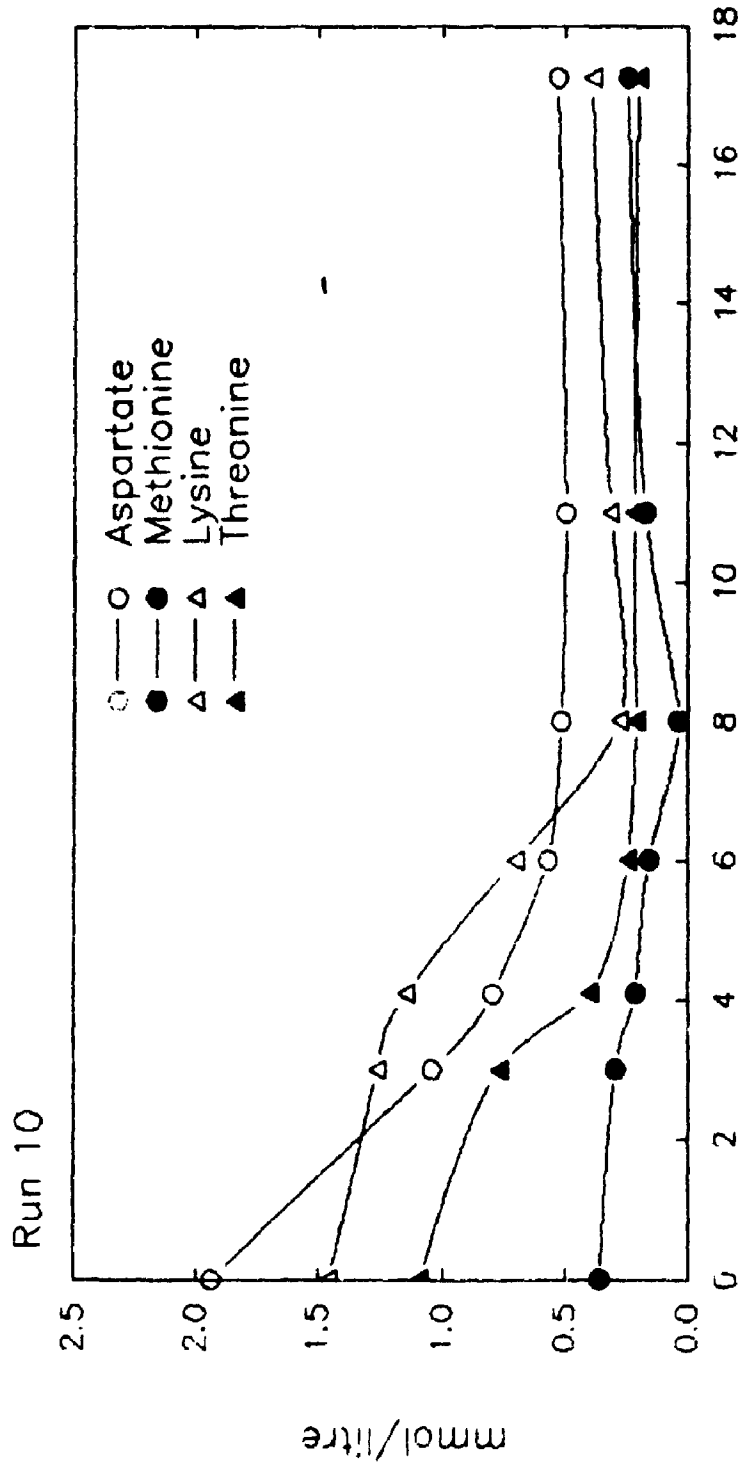

Fig. 6.6: Aspartic acid, methionine, lysine and threonine concentration vs. time, Run 10.

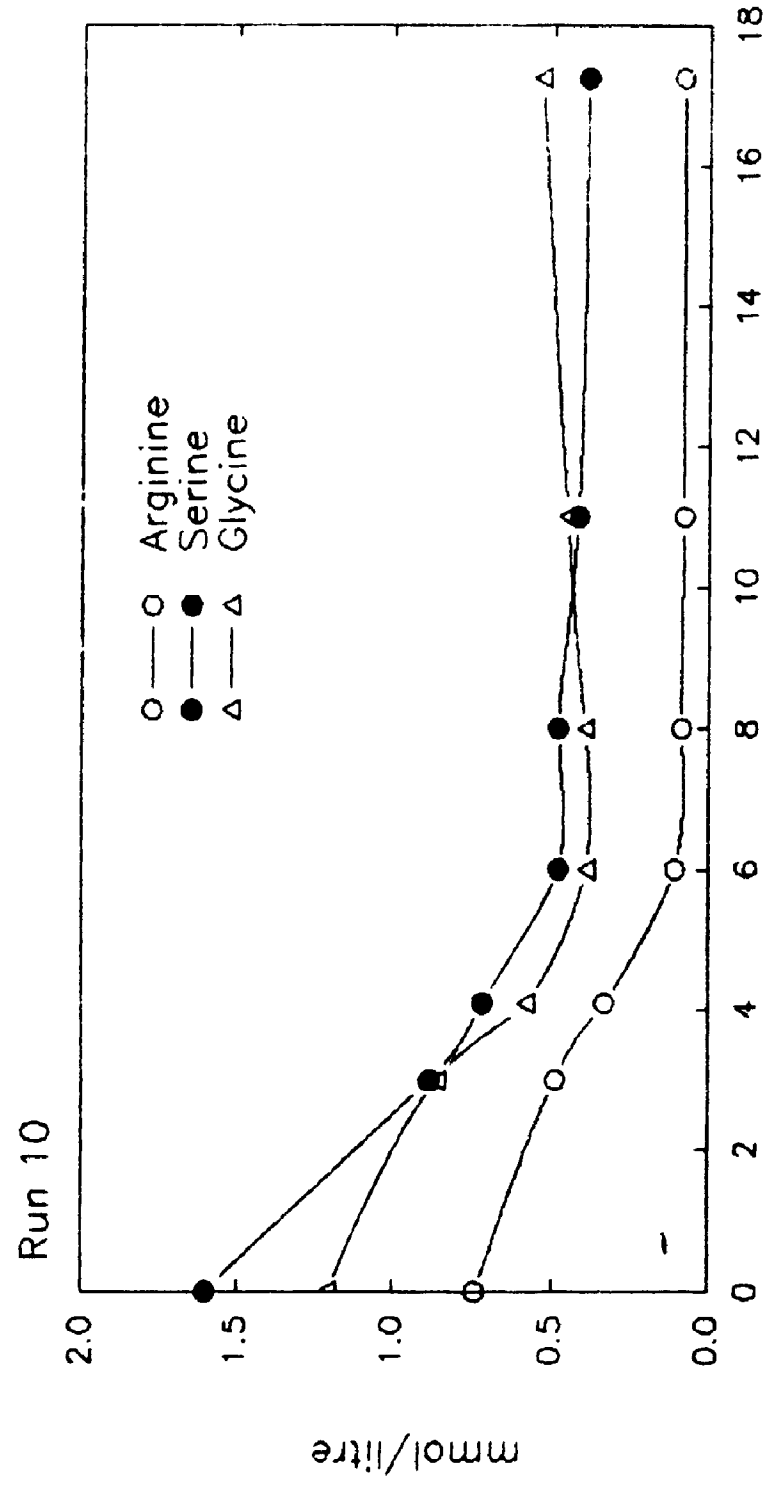

Fig. 6.7: Arginine, serine and glycine concentration vs. time, Run 10.

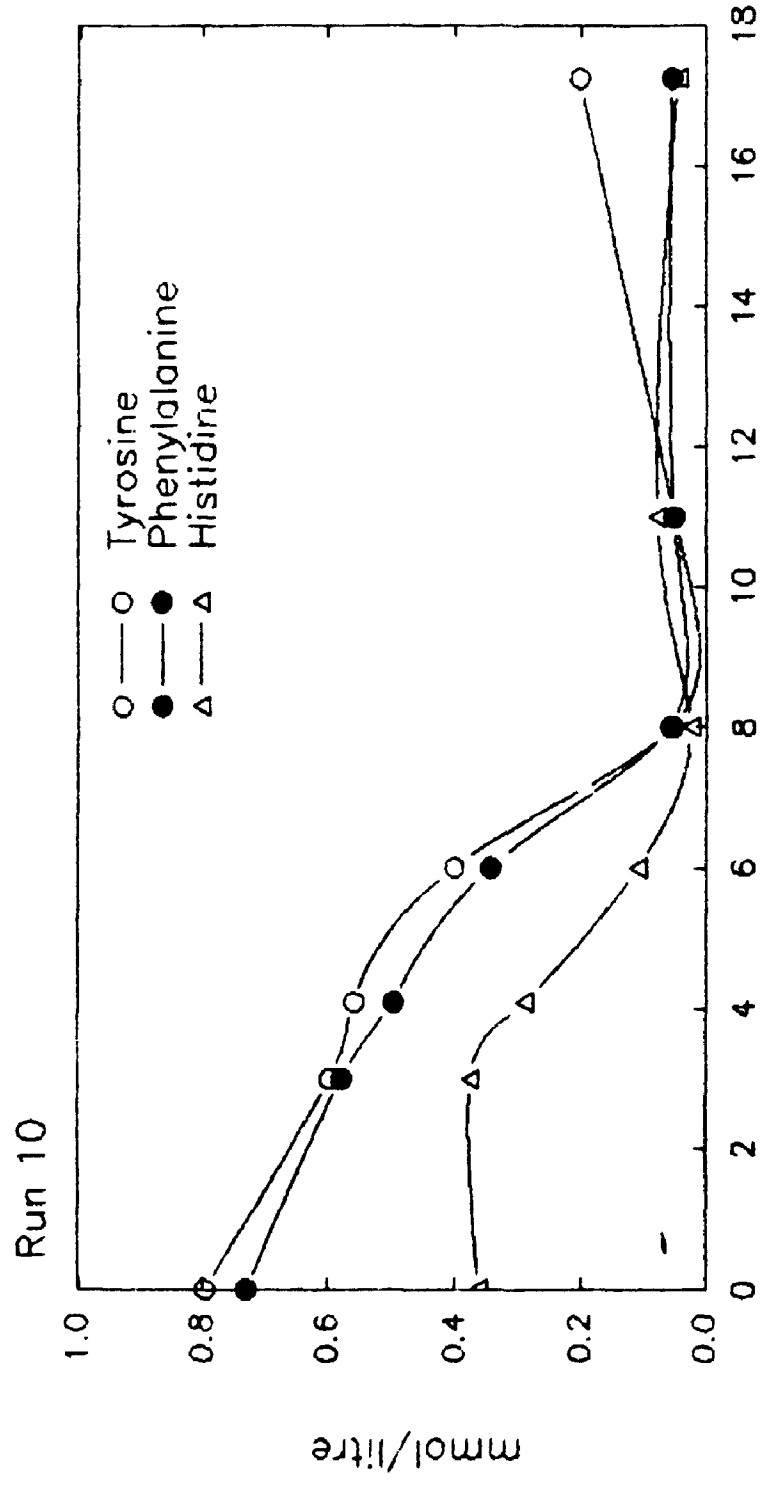

Fig. 6.8: Tyrosine, phenylalanine and histidine concentration vs. time, Run 10.

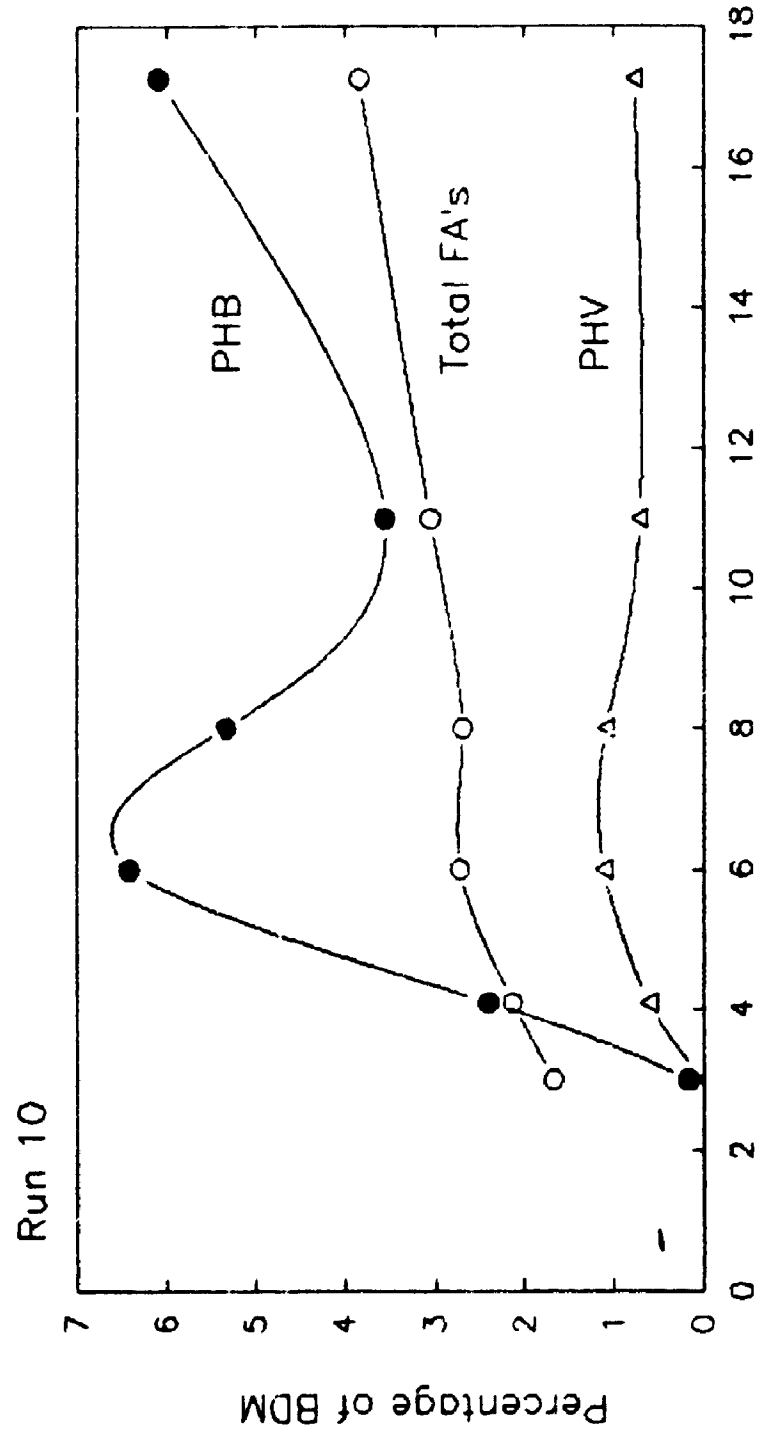

Fig. 6.9: PHB, PHV and total fatty acids as a weight percentage of biomass dry matter vs. time, Run 10.

a much lesser extent PHV, as a carbon and/or energy source during early to mid - sporulation as reported for PHB in B. cereus (Kominek and Halvorson, 1965). Increases in both fatty acids and PHB during later sporulation, concomitant with high and rising DO, suggest that these reduced substances may be acting as electron sinks. Changes in the three major biomass fatty acids versus time, shown in Fig. 6.10, demonstrate the importance of valine - related fatty acids during early sporulation, as reported in B. megaterium by Scandella and Kornberg (1969; Sect. 3.3). Both valine - and leucine - related fatty acids accumulated substantially in biomass during later sporulation.

Pyruvate, lactate and acetate were released and reached maxima by the end of the vegetative growth phase, as reported by Anderson (1990). Acetate was the major intermediate, followed by lactate. As shown in Fig. 6.11, acetate was consumed extremely rapidly after about 4 hr; this event may functionally define the onset of transition phase (Sect. 2.1.2). Broth pyruvate and succinate concentrations versus time are plotted in Fig. 6.12. The profile observed for pyruvate is very similar to that of acetate. Succinic acid formation was greatest during stage IV of sporulation.

Acetoin and 2,3-butanediol, as shown in Fig. 6.13, began to be formed during late vegetative growth phase, reaching maxima at 8 and 6 hours respectively. Both were essentially completely consumed by 11 hours.

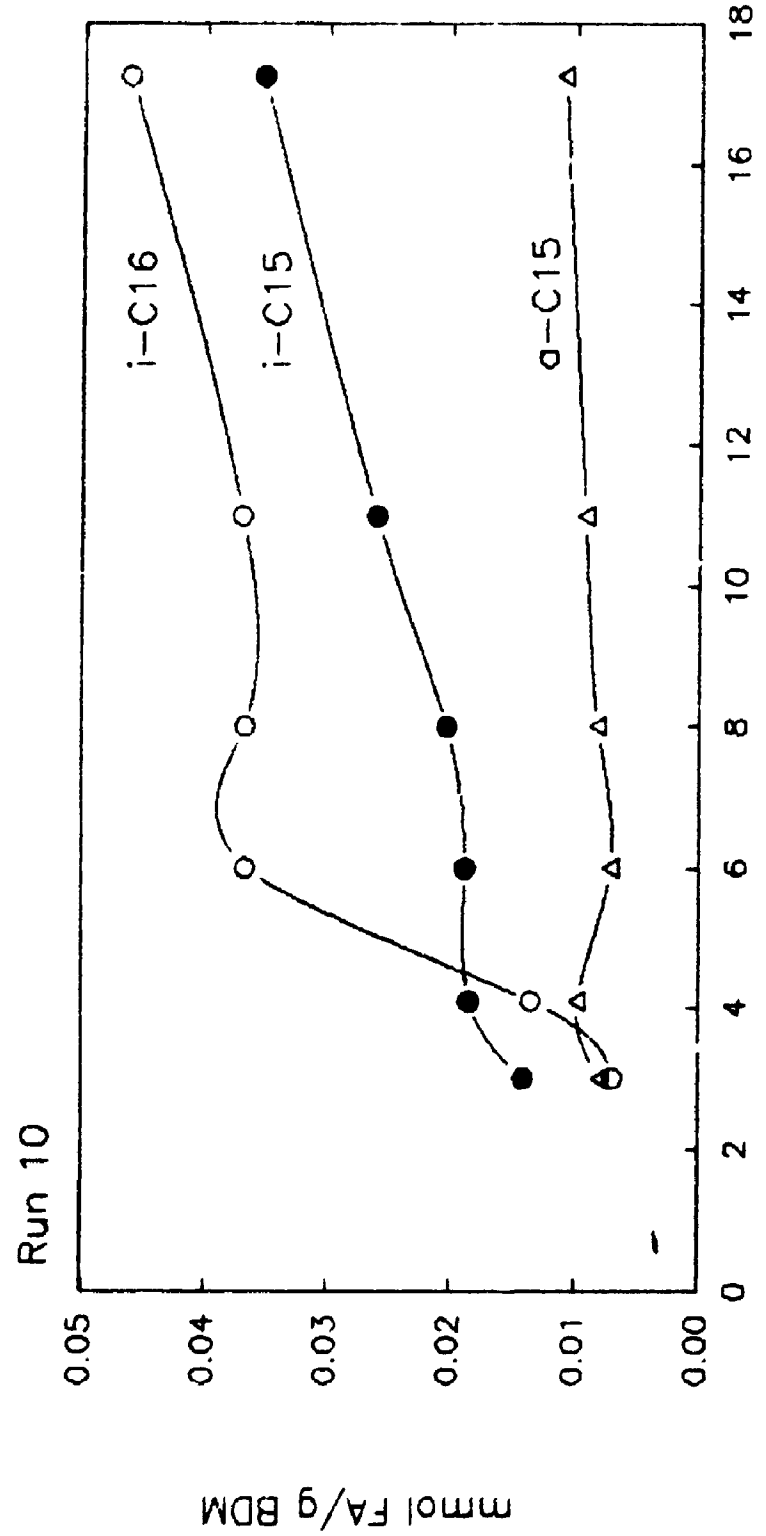

Fig. 6.10: Concentration of major fatty acids in biomass vs. time, Run 10.

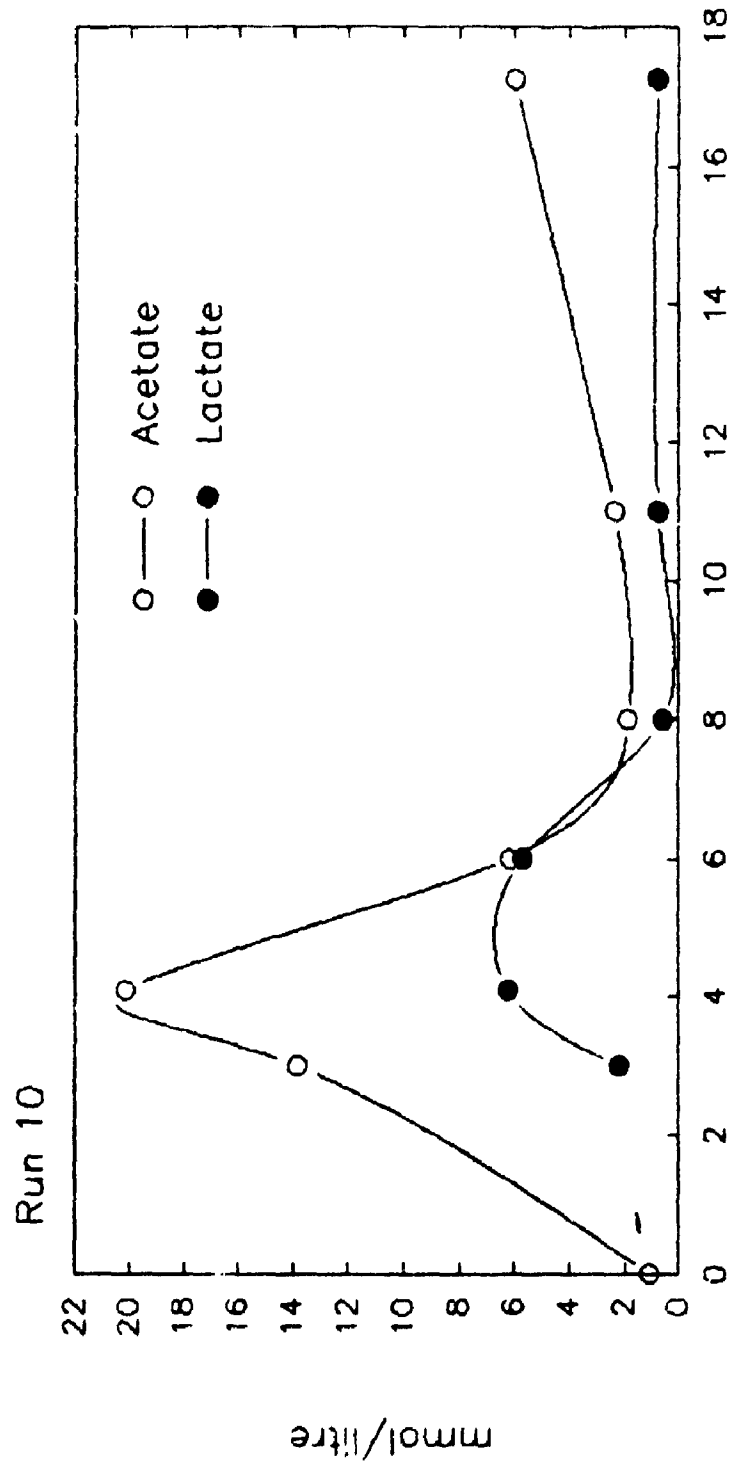

Fig. 6.11: Lactate and acetate concentration vs. time, Run 10.

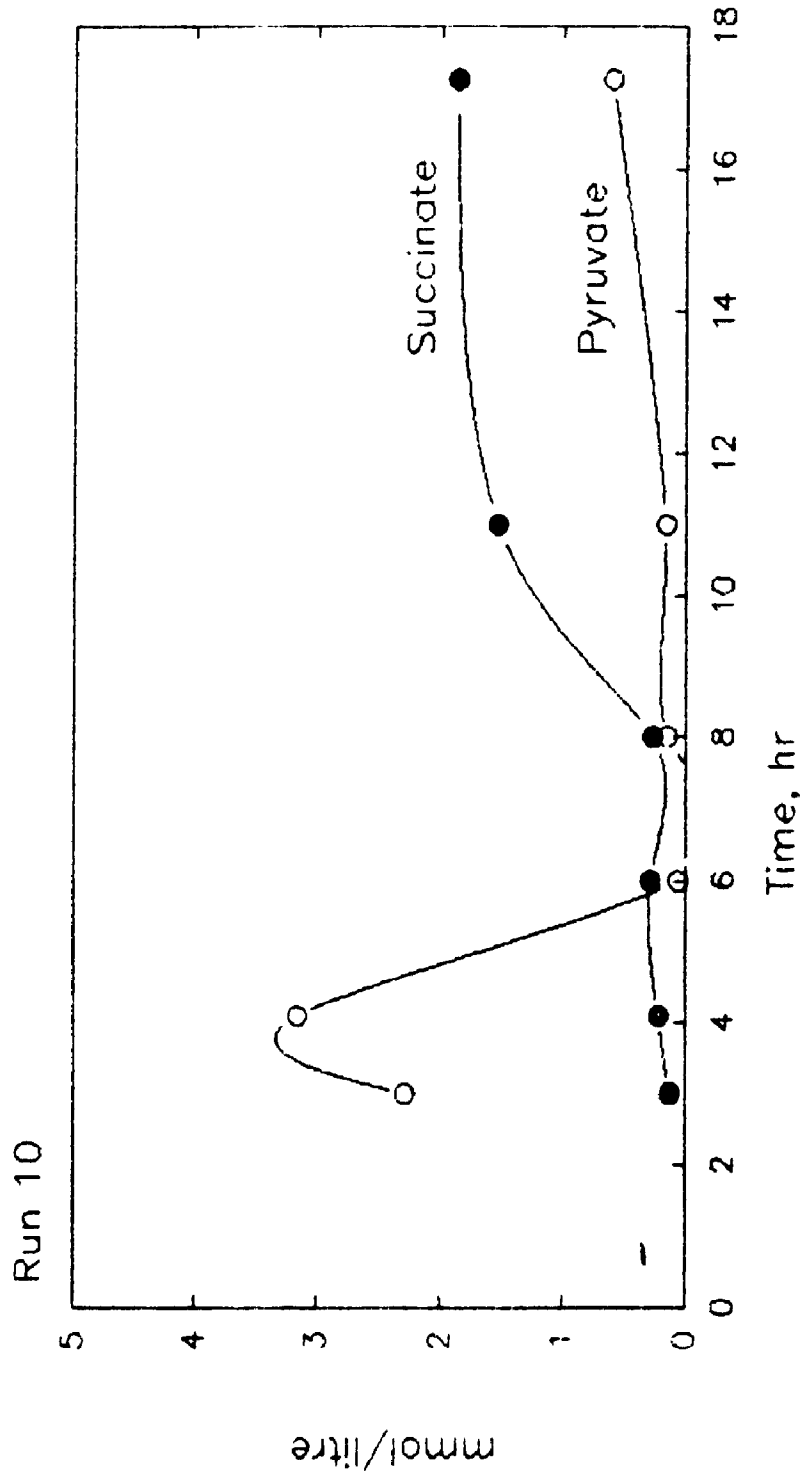

Fig. 6.12: Pyruvate and succinate concentration vs. time, Run 10.

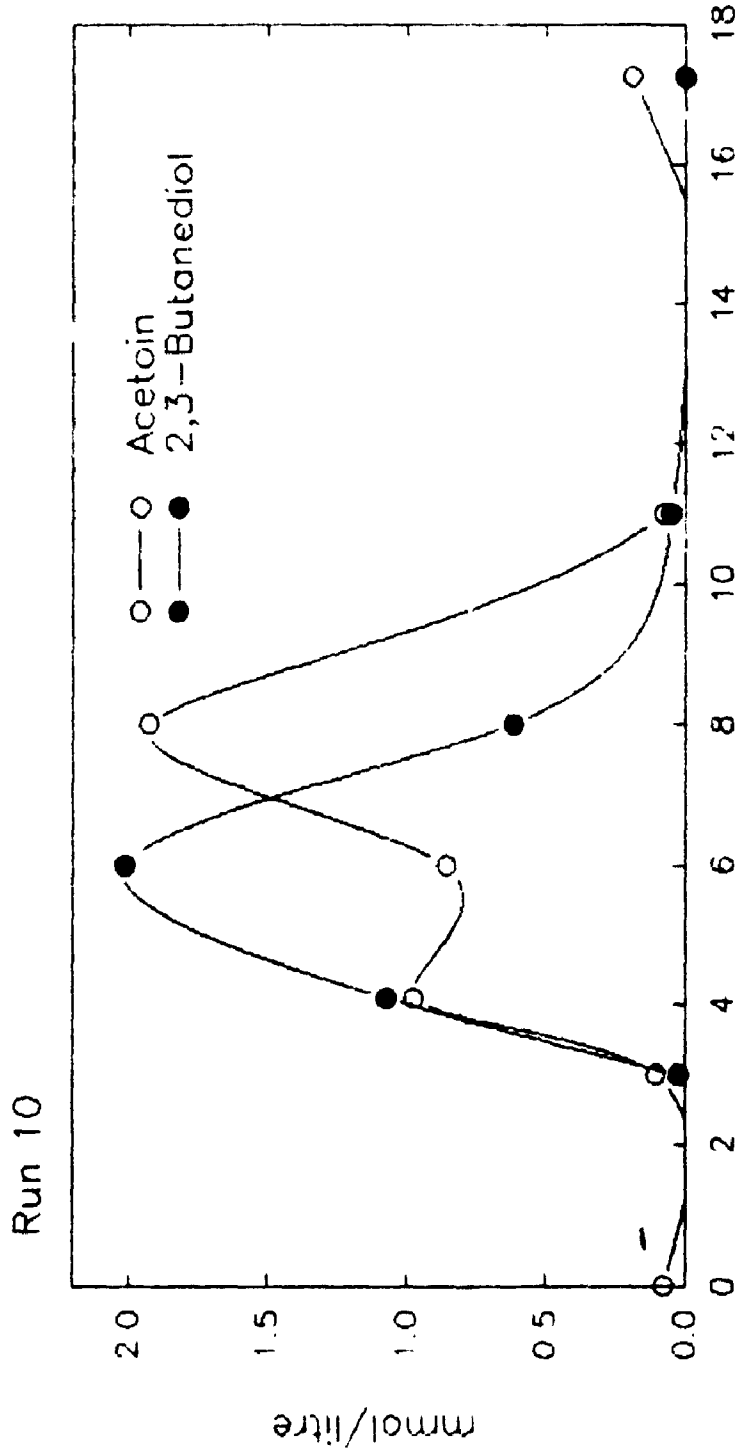

Fig. 6.13: Acetoin and 2,3-butanediol concentration vs. time, Run 10.

The branched short - chain fatty acids, isobutyrate, 2-methylbutyrate and isovalerate, were released in relatively small amounts during vegetative growth; and consumed to some extent during transition phase (Fig. 6.14). Isovalerate was also formed during spore maturation (cf. Sect. 9.5). The three branched - chain α-keto acids accumulated from late vegetative growth to mid - transition phase, as shown in Fig. 6.15. α-Keto-3-methylvalerate especially was rapidly consumed during late transition phase.

Several of the above compounds have not, to my knowledge, been previously reported in B. thuringiensis fermentations, namely: isobutyrate, 2-methylbutyrate, isovalerate, 2,3-butanediol, PHV, α-ketoisovalerate, α-hydroxyisovalerate, α-keto-β-methylvalerate, α-ketoisocaproate and succinate. Apparently neither succinate nor the BCKA's have been previously identified as products of any species of the genus Bacillus.

6.2 Vegetative Phase Model Solution

The flux of α-keto-β-methylvalerate through BCKA dehydrogenase for this case (ie. sample GR10X1; 4.1 hr) was calculated to be 0.0574 mmol/g VDM/hr (Table 5.6). Dehydrogenation rates of α-ketoisovalerate and α-ketoisocaproate were calculated from equations 5.15b and 5.15a (Sect. 5.5) respectively, using data summarized in App. B as follows:

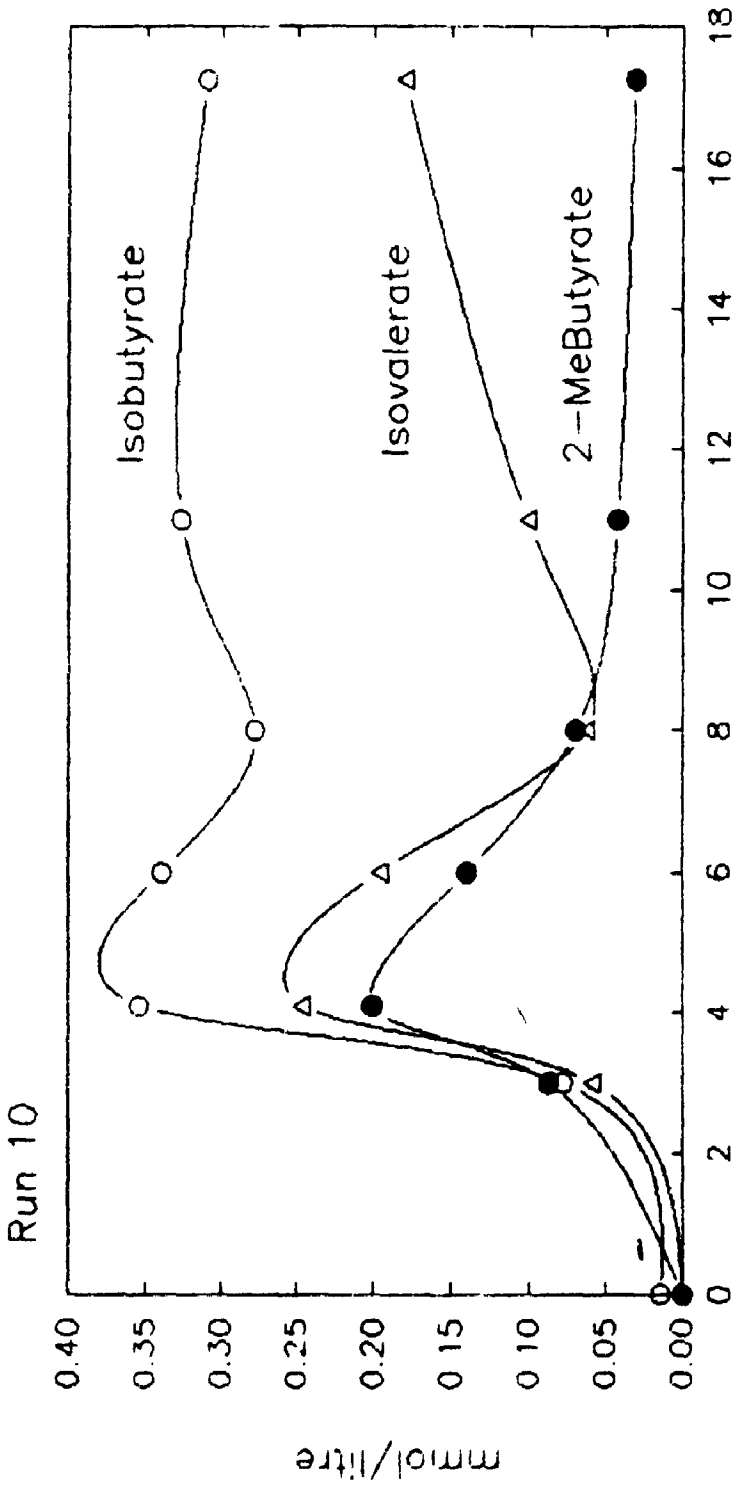

Fig. 6.14: Isobutyrate, isovalerate and 2-methylbutyrate concentration vs. time, Run 10.

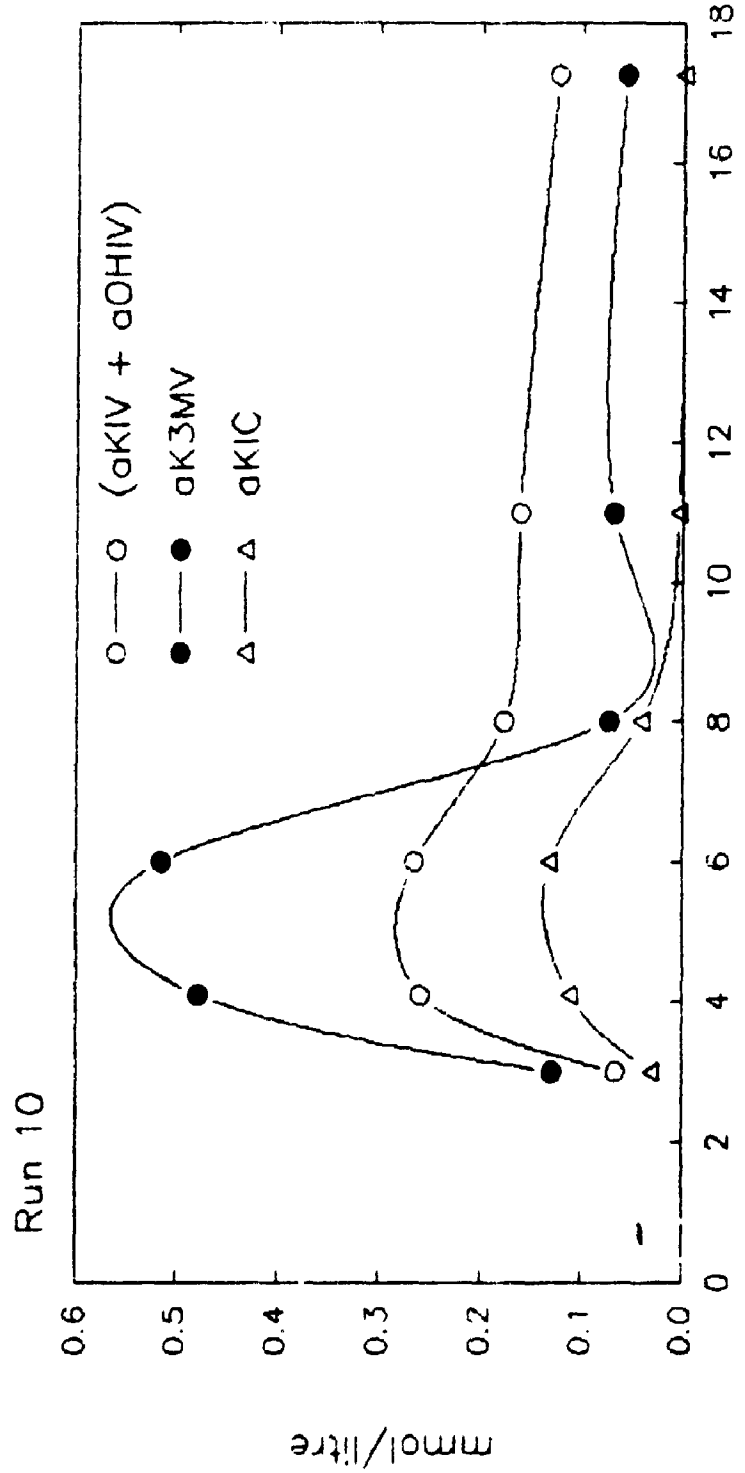

Fig. 6.15: Concentration of branched - chain α-ketoacids vs. time, Run 10. (aKIV + aOHIV) = combined α-ketoisovalerate and α-hydroxyisovalerate; aK3MV = α-keto-β-methylvalerate; aKIC = α-ketoisocaproate.

$$FT(V) = [FT(I) + SA(I)]*[FA(V)/FA(I)] - SA(V)$$

$$\approx (0.05741)*(0.02569/0.007304)$$

$$\approx 0.202 \text{ mmol/g VDM/hr}$$

$$FT(L) = [FT(I) + SA(I)]*[FA(L)/FA(I)] - SA(L)$$

$$\approx (0.05741)*(0.01990/0.007304)$$

$$\approx 0.156 \text{ mmol/g VDM/hr}$$

Substitution of the calculated values of FT(I), FT(V) and FT(L) into the metabolic model described in Sect. 5.1 led to an apparent pyruvate deficit of about 100 %. This could arise from either or both of unmeasured substrate consumption, or overestimated biomass production; and was resolved by adjusting the apparent rate of cell biosynthesis via factor BMF (Sect. 5.1). In the present case pyruvate balance was achieved for BMF equal to 0.5005.

Bacterial metabolism during (or at the end of) the vegetative growth phase (4.1 hr; samples GR1004/GR10X1) of Run 10, as summarized in Fig. 6.16, exhibits the following characteristics:

1) large glycolytic flux to pyruvate;

2) substantial conversion of pyruvate to acetyl-CoA via pyruvate dehydrogenase;

3) production of lactate, and lesser amounts of 2,3-butanediol and acetoin, from pyruvate;

4) vigorous production of PHB from acetyl-CoA (acetate formation has just ceased; Fig. 6.11);

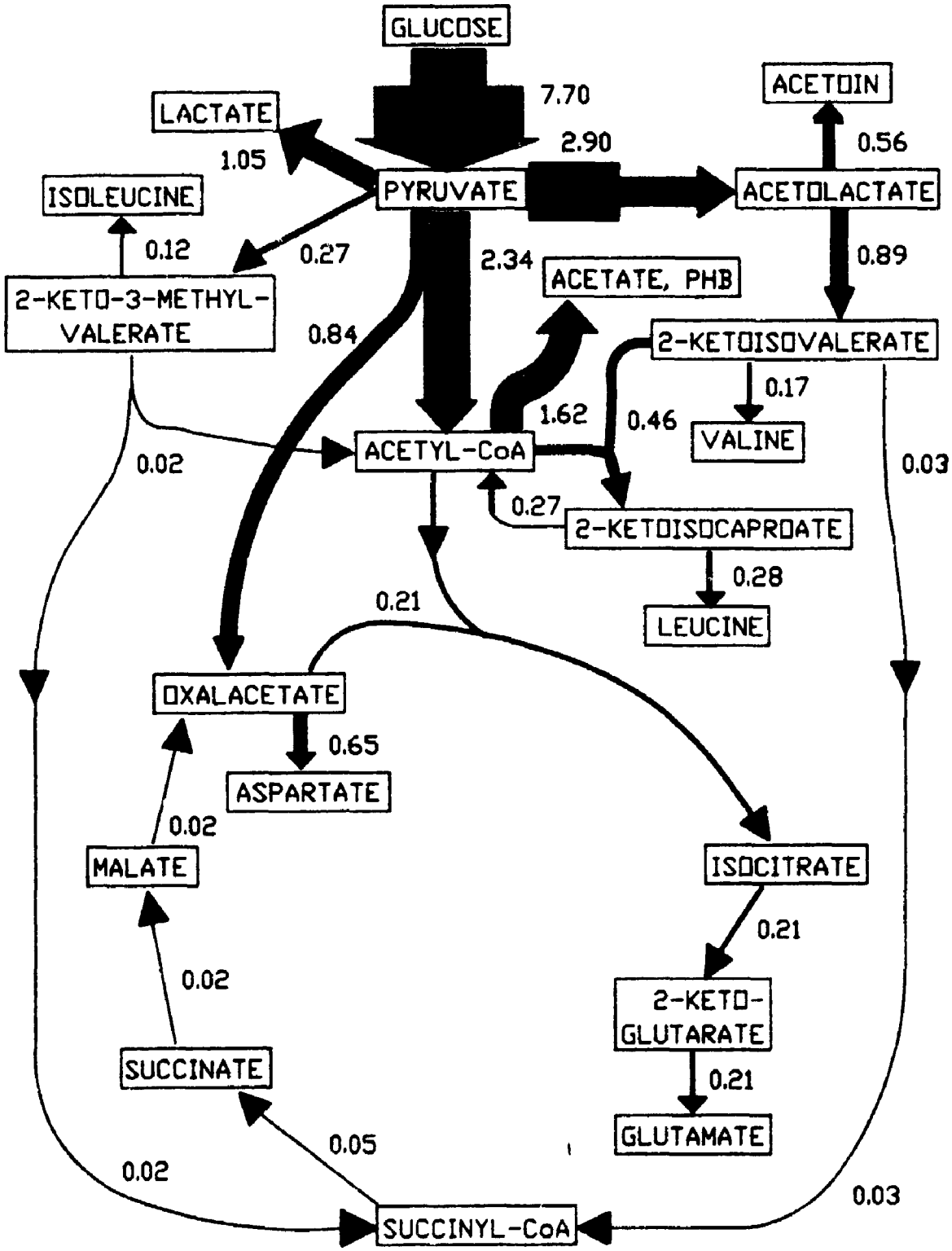

Fig. 6.16: Model solution for vegetative phase (4.1 hr) of Run 10. Flux in mmol/g VDM/hr proportional to line width.

5) conversion of pyruvate to oxalacetate via pyruvate carboxylase;

6) biosynthetic flows to specific amino acids (viz. isoleucine, valine, leucine, glutamate and aspartate);

7) minor catabolism of the three branched - chain α-keto acids to acetyl-CoA and succinyl-CoA, thence to oxalacetate.

The last item is the only metabolic feature which is remarkable in light of current knowledge. Although these fluxes are small (eg. less than 12 per cent of acetyl-CoA could derive from catabolism of 2-ketoisocaproate), they will prove significant (Sect. 6.3). This is foreshadowed in the accumulation of the three BCKA's (Fig. 6.15), and short - chain fatty acids (Fig. 6.14) resulting from their dehydrogenation and deesterification (Sect. 3.2).

6.3 Early Sporulation Phase Model Solution

6.3.1 Calculation Results

The flux of α-keto-β-methylvalerate through BCKA dehydrogenase for this case (ie. sample GR10X3; 6.0 hr) was calculated to be 0.1857 mmol/g VDM/hr (Table 5.6). Dehydrogenation rates of α-ketoisovalerate and α-ketoisocaproate were again calculated from equations 5.15b and 5.15a (Sect. 5.5) respectively, using data summarized in App. B as follows:

$$FT(V) = [FT(I) + SA(I)]*[FA(V)/FA(I)] - SA(V)$$

$\approx$ [0.1857 + 0.150)*(0.01954/0.002798) - 0.0190

$\approx$ 1.382 mmol/g VDM/hr

FT(L) = [FT(I) + SA(I)]*[FA(L)/FA(I)] - SA(L)

$\approx$ (0.1857 = 0.0150)*(0.008120/0.002798) - 0.0210

$\approx$ 0.561 mmol/g VDM/hr

These values resulted in pyruvate balance at BMF equal to 0.7608 for this metabolic system.

Bacterial metabolism during early sporulation phase (6.0 hr; samples GR1005/GR10X3) of Run 10, as summarized in Fig. 6.17, exhibits the following major characteristics:

1) moderate glycolytic flux to pyruvate;

2) presumed absence of pyruvate dehydrogenase activity;

3) substantial consumption of acetate, lactate and pyruvate (Fig. 6.11, 12), although PHB formation continues (Fig. 6.9);

4) greatly increased flux through the valine pathway to succinyl-CoA;

5) greatly increased flux through second half TCA cycle enzymes, ie. from succinyl-CoA to oxalacetate;

6) substantial flux from acetyl-CoA through the glyoxylate cycle to succinate and malate;

7) presumed absence of pyruvate carboxylase activity;

8) substantial decarboxylation of malate to pyruvate by malic enzyme.

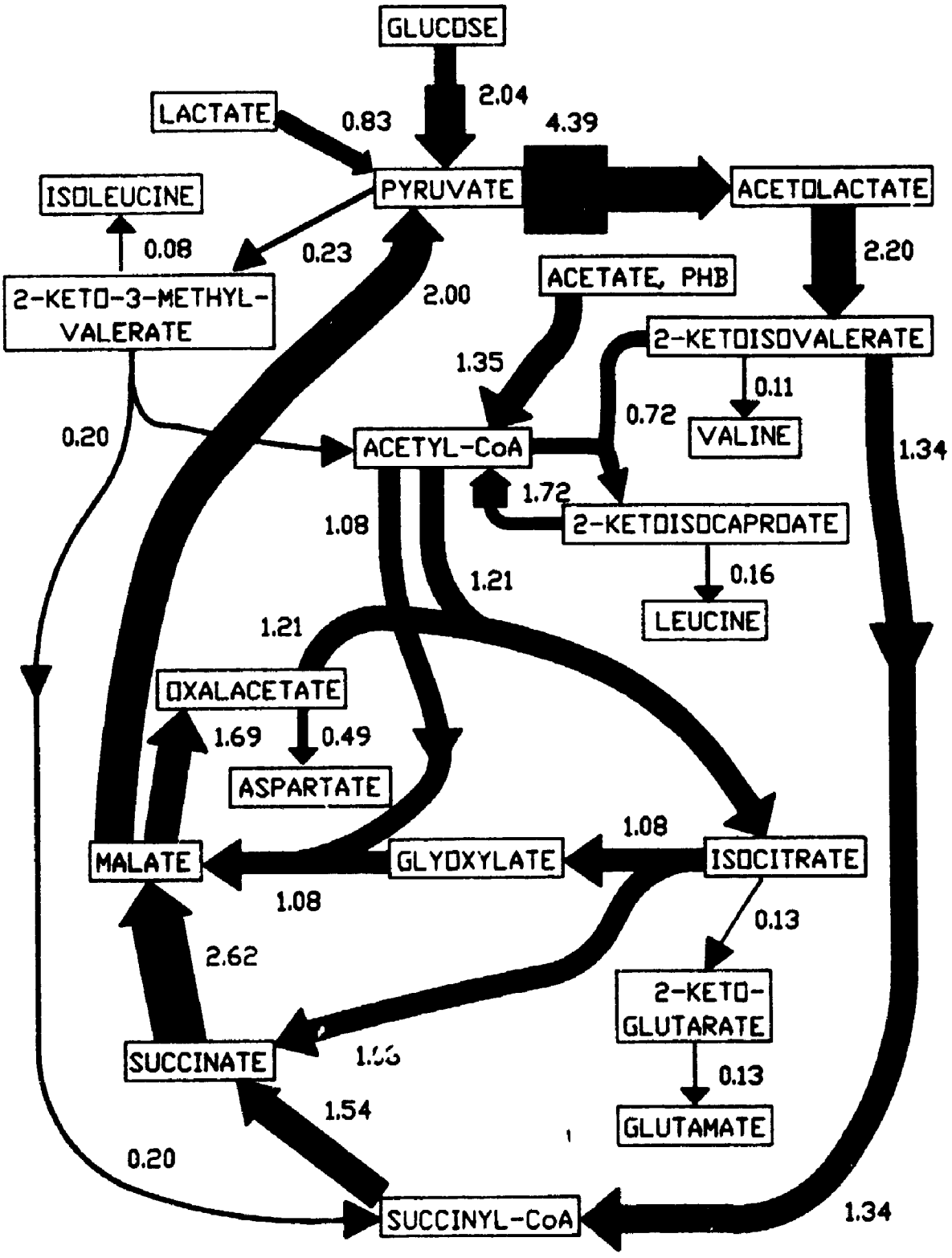

Fig. 6.17: Model solution for early sporulation phase (6 hr) of Run 10. Flux in mmol/g VDM/hr proportional to line width.

A striking result of the latter pathway is its completion of several cycles, of which the three branched - chain amino acid pathways are integral parts. Increased flux through the catabolic segments of these pathways is accompanied by consumption of the respective short - chain fatty acids (Fig. 6.14). The corresponding 2-keto acids have just begun to be consumed at this time (Fig. 6.15). Also noteworthy is the absence of acetoin or 2,3-butanediol formation (Fig. 6.13). Selected aspects of this metabolic system are discussed below.

6.3.2 Inhibition of Pyruvate Dehydrogenase

Flux through pyruvate dehydrogenase was assumed to be zero for the following reasons:

1) acetyl-CoA is being formed from acetate and catabolism of α-ketoisocaproate (*ie.* leucine pathway) at a rate greater than its earlier production from pyruvate;

2) insufficient pyruvate appears to be available for other demands.

As would be expected pyruvate dehydrogenase (*E. coli*) is potently inhibited by acetyl-CoA, or more accurately by acetyl-CoA:CoA ratio (Schwartz *et al.*, 1968). It is also germane that several intermediates of the valine (and isoleucine) catabolic pathway(s) (*viz.* isobutyryl-, propionyl-, and methylmalonyl-CoA) are strongly inhibitory to pyruvate dehydrogenase of pig heart (Martin-Requero *et al.*, 1983).

Valine pathway flux *per se* inhibits pyruvate dehydrogenase by decreasing CoA availability, since all but two of the eight intermediates between α-ketoisovalerate (αKIV) and succinyl-CoA are CoA esters (Sect. 3.2). Further inhibition of the enzyme due to αKIV catabolism is likely from the relatively large amounts of reducing equivalents produced, *ie.* three NADH, one $FADH_2$ (*cf.* Hansen and Henning, 1966, re inhibition by NADH in *E. coli*). That the cell interior becomes more reduced (*ie.* NADH:NAD^+ increases) during this metabolic phase is substantiated by both the rapid increase observed in dissolved oxygen concentration (Fig. 6.3); and marked formation of granules containing reduced substances, namely PHB, PHV and lipids (Fig. 6.9, 6.10; *cf.* Macrae and Wilkinson, 1958; Nickerson *et al.*, 1981).

6.3.3 Valine Pathway Activation

Fatty acid results (Fig. 6.10) leave no doubt that this "transitional growth" phase is characterized by induction and/or activation of the valine pathway from pyruvate via α-ketoisovalerate (αKIV) at least to isobutyryl-CoA. One explanation is induction of AHAS II (pH 6 acetolactate synthetase); the product of which is not destined for biosynthesis; and whose activity is thus not specifically inhibited by valine (Sect. 3.1). Acetate both induces and activates this enzyme, which is associated with acetoin and

2,3-butanediol formation in Aerobacter aerogenes (Johansen et al., 1975; Störmer, 1977; Iaccarino et al., 1978). However Fig. 6.13 shows that in the present fermentation combined acetoin and 2,3-butanediol were formed most actively during mid- to late vegetative growth phase, ie. AHAS II induction occurred at 3 hours. Another explanation is activation of enzymes of the catabolic segment of the valine pathway.

The properties of branched - chain keto acid dehydrogenase (BCKA DH) were thoroughly discussed in Sect. 3.2. Its activation by valine (Table 3.1) is unusual; such "precursor activation" substantiates a key role in an amphibolic pathway, ie. one fulfilling both anabolic and catabolic functions (Sanwal, 1970). Thus, "From the physiological point of view, a control mechanism unique so far to amphibolic pathways is precursor activation." (ibid.).

The remaining enzymes of the valine catabolic pathway are induced, apparently co-ordinately, by some or all of valine, αKIV, isobutyrate, 3-hydroxyisobutyrate, β-hydroxybutyrate, and isoleucine and leucine catabolic intermediates (Massey et al., 1976; Marshall and Sokatch, 1972).

6.3.4 Inhibition of Pyruvate Carboxylase and Induction of Malic Enzyme

Unlike the vegetative growth phase, when oxalacetate demand requires pyruvate carboxylase as an anaplerotic pathway

(Sect. 6.2), early sporulation is characterized by an excess of dicarboxylic acids due to operation of the valine pathway (Sect. 6.3.3) and glyoxylate cycle (Sect. 2.5). For this reason, as well as the existence of a pyruvate deficit, pyruvate carboxylase activity was set to zero. This is compatible with literature results that, while necessary for vegetative growth of B. subtilis on glucose, the enzyme is not required for sporulation (Sect. 2.6). Although pyruvate carboxylase is strongly activated by acetyl-CoA, its operation in the present circumstances may be inhibited by an effective shortage of two of its substrates, pyruvate and/or ATP (Diesterhaft and Freese, 1973).

That pyruvate carboxylase is inhibited in vivo during sporulation of bacilli is clearly evident from the fact that a mutant of B. subtilis devoid of malate dehydrogenase sporulated only if supplied with oxalacetate (Sect. 2.4); although in vitro pyruvate carboxylase activity is essentially constant throughout growth and sporulation of this species (Diesterhaft and Freese, 1973).

It appears relevant here that catabolism of α-ketoisovalerate in rat hepatocytes (liver cells) causes inhibition of pyruvate carboxylase (Martin-Requero et al., 1983). Although this was attributed mainly to a decrease in acetyl-CoA concentration (due to pyruvate dehydrogenase inhibition; Sect. 6.3.2), inhibition by methylmalonyl-CoA, an intermediate of αKIV catabolism, also contributed.

For the same reasons that pyruvate carboxylase flux was set to zero, a pathway was sought for conversion of excess dicarboxylic acids to pyruvate. As mentioned in Sect. 2.6, malic enzyme, activated during sporulation of B. thuringiensis (Aronson et al., 1975), appears to serve this function. Furthermore control of enzyme activity in the latter organism by acetyl-CoA:CoA ratio (Sanwal, 1970) could well be amplified and refined in bacilli, which, apparently unlike E. coli (Lowe et al., 1983), are able to catabolize branched - chain α-keto acids. Specifically, the predominance of acyl-CoA esters as intermediates of the catabolic sections of each of the BCAA pathways would ensure low CoA availability (and low CoA:acyl-CoA ratio) upon activation of these pathways. This in turn could activate the catabolic malic enzyme as observed in E. coli.

6.4 Mid - sporulation Phase Model Solution

6.4.1 Calculation Method

Calculation of flux through BCKA dehydrogenase for this case (ie. GR10X5; 11.0 hr), using the standard method described in Sect. 5.4, gave negative values for each of the three BCAA pathways (App. B). Thus it was necessary to perform a complete molar balance solution on the anaerobic incubation results, as follows:

1) specific rates of uptake or release for each measured variable were calculated for the anaerobic incubation period (Sect. 4.3; samples GR1007, GR10X5), and entered into the metabolic model worksheet (Sect. 5.1);

2) since the only flows from pyruvate during early sporulation - phase (Sect. 6.3) were to the BCAA pathways and biosynthesis; and since this appeared to be true in the present case also, except that no cell synthesis was occurring (Sect. 6.1); it was assumed that the net difference between flux to and flux from, pyruvate was equal to the sum of the three fluxes through BCKA dehydrogenase; this gave the following result:

$$FT(I) + FT(L) + FT(V) \approx 0.1185 \text{ mmol/g VDM/hr};$$

3) since both isoleucine and α-keto-β-methylvalerate were consumed during anaerobic incubation, a lower bound on FT(I) was calculated as follows:

$$FT(I) \geq 0.0154 + 0.0067 \approx 0.0221 \text{ mmol/g VDM/hr};$$

4) thus [FT(L) + FT(V)] was calculated as follows:

$$FT(L) + FT(V) \approx 0.1185 - 0.0221$$
$$\approx 0.0964 \text{ mmol/g VDM/hr};$$

5) since neither isobutyrate nor isovalerate were being consumed in the actual fermentation, it follows that the fluxes to fatty acid synthesis from the leucine and valine pathways are proportional to FT(L) and FT(V) respectively (cf. equations 5.15a and 5.15b, Sect. 5.5); thus,

$$FT(L) = [FT(L) + FT(V)]*(FA(L)/[FA(L) + FA(V)]) \quad (6.1a)$$

$$\approx (0.0964)*(0.002311)/(0.002311 + 0.001331)$$

$$\approx 0.0612 \text{ mmol/g VDM/hr;}$$

$$FT(V) = [FT(L) + FT(V)]*(FA(V)/[FA(L) + FA(V)]) \quad (6.1b)$$

$$\approx (0.0964)*(0.001331)/(0.002311 + 0.001331)$$

$$\approx 0.0352 \text{ mmol/g VDM/hr.}$$

6.4.2 Calculation Results

Incorporation of these values of FT(I), FT(L) and FT(V) into the metabolic model resulted (for the first time· see Sect. 6.2, 6.3) in an apparent excess of pyruvate of approximately 0.65 mmol/g VDM/hr. This could arise from underestimation of either or both of biosynthetic or catabolic activities. Although there was no net biomass formation at this time (Fig. 6.1), it is possible that significant formation of sporulation - specific materials (eg. dipicolinic acid, 3-phosphoglyceric acid) was occurring. However, since dipicolinic acid (DPA) appears to be formed after cortex development (Freese and Heinze, 1983), it is likely that no appreciable synthesis of DPA was occurring. On the other hand 3-phosphoglyceric acid (phosphoglycerate, PGA) is formed, apparently in the forespore, before accumulation of DPA (ibid.). However, since PGA comprises only 3 to 5 per cent of

the dry weight of B. cereus spores regardless of medium composition (Setlow, 1984), its synthesis was not considered in the present calculations (cf. discussion below). Thus it was assumed that the apparent pyruvate excess was due solely to underestimation of pyruvate catabolism.

Since there was net consumption of 2-methylbutyryl-CoA (derived from isoleucine - pathway fatty acids), while isobutyryl- and isovaleryl-CoA were still being formed, it was decided to increase apparent pyruvate catabolism rate by proportionally increasing the values of FT(L) and FT(V). [Note that consistency requires that isoleucine - derived fatty acids are simultaneously formed and oxidized, the latter at a greater rate than the former.] By this means pyruvate balance was achieved at values of FT(L) and FT(V) 7.730 times greater than those calculated above.

The pattern of bacterial metabolism which resulted, as summarized in Fig. 6.18, is similar to that for early sporulation phase (Fig. 6.17), differing as follows:

1) much smaller glycolytic flux to pyruvate;

2) reduced flow from pyruvate to succinyl-CoA, via the valine pathway, and thence back to pyruvate via malate;

3) net consumption, rather than production, of glutamate, aspartate, leucine and isoleucine;

4) slight net production, rather than consumption, of lactate.

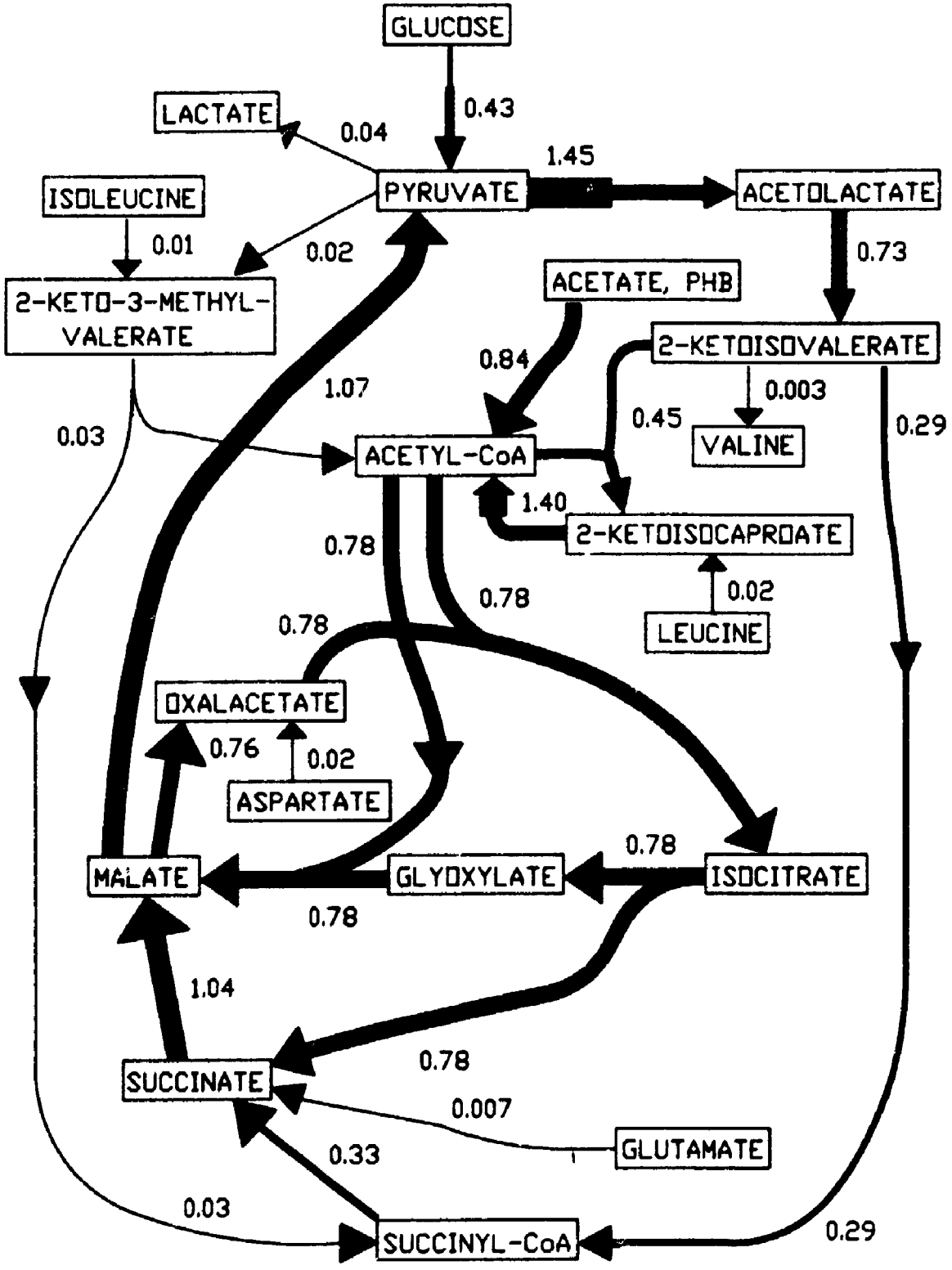

Fig. 6.18: Model solution for mid - sporulation phase (11 hr) of Run 10. Flux in mmol/g VDM/hr proportional to line width.

While catabolic flux through the valine pathway decreased by about 78 per cent from its early sporulation value, catabolism of α-ketoisocaproate decreased by only about 19 per cent. This relative increase in leucine pathway flux is believed to be functionally related to turnover of intracellular protein (Sect. 2.1.2). Catabolism of biomass (*ie.* mother cell) components is indicated by decreasing biomass concentration (Fig. 6.1) in the absence of observable lysis; this process appears to be associated with broth acidification (Fig. 6.3; *cf.* Fig. 6.11 re acetate production).

If 3-phosphoglyceric acid (PGA) is being formed at this time, it would appear to arise from glyoxylate via tartronic semialdehyde and glyceric acid, as in *B. cereus* T (Megraw and Beers, 1964). That isocitrate lyase activity does not peak until late sporulation, whereas malate synthase is most active during early sporulation (Aronson *et al.*, 1975a), lends indirect support to this assertion.

7. Results and Discussion: Run 11

Complete results for this fermentation are tabulated in Appendix E.

7.1 General Fermentation Characteristics

Run 11 was performed identically to Run 10 (Sect. 6) except that a Casamino Acids mixture was used in place of tryptone (Sect. 4.1); thus buffered Casamino Acids/yeast extract medium was aerated at 1.4 VVM. Biomass and glucose concentrations versus time are shown in Fig. 7.1. Natural logarithm of viable dry matter (VDM; Sect. 5.2), plotted versus time in Fig. 7.2, shows maximum specific growth rate of about 0.48 hr^{-1} during vegetative phase. In spite of similar vegetative growth kinetics, the present fermentation reached only 6.05 g BDM/l compared to 6.77 g BDM/l for Run 10. Comparison of the curves (Fig. 6.1, 7.1) reveals that the additional biomass was formed during late transition phase (6 to 8 hr) of Run 10.

Growth was again accompanied by decreasing pH and dissolved oxygen (DO) concentration, as shown in Fig. 7.3. Their temporal pattern was similar to Run 10 (Fig. 6.3), although certain DO variations were more pronounced than previously. Thus a decrease in oxygen consumption occurred for about two hours (3 to 5 hr), centred on the pH minimum.

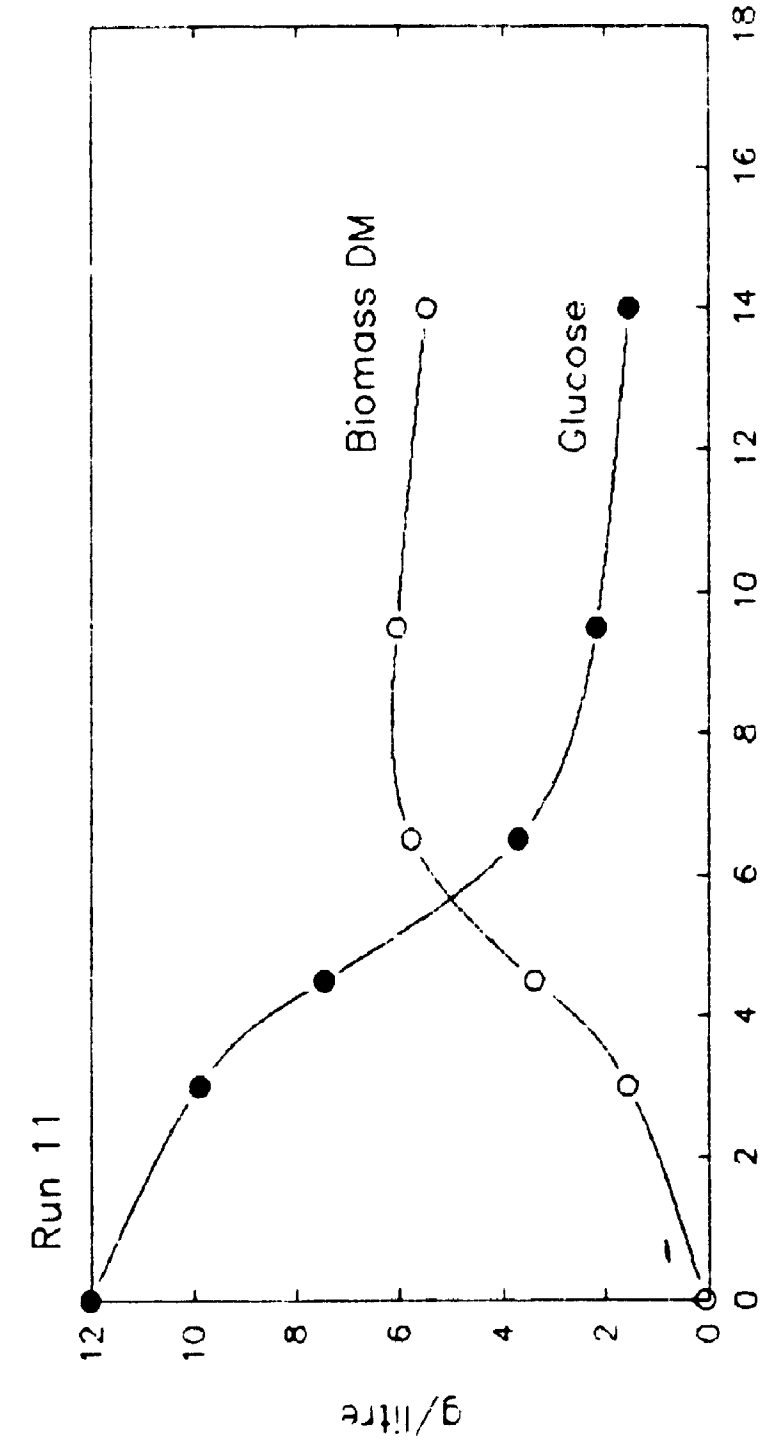

Fig. 7.1: Biomass dry matter and glucose concentration vs. time, Run 11.

Fig. 7.2: Natural logarithm of viable dry matter vs. time, Run 11.

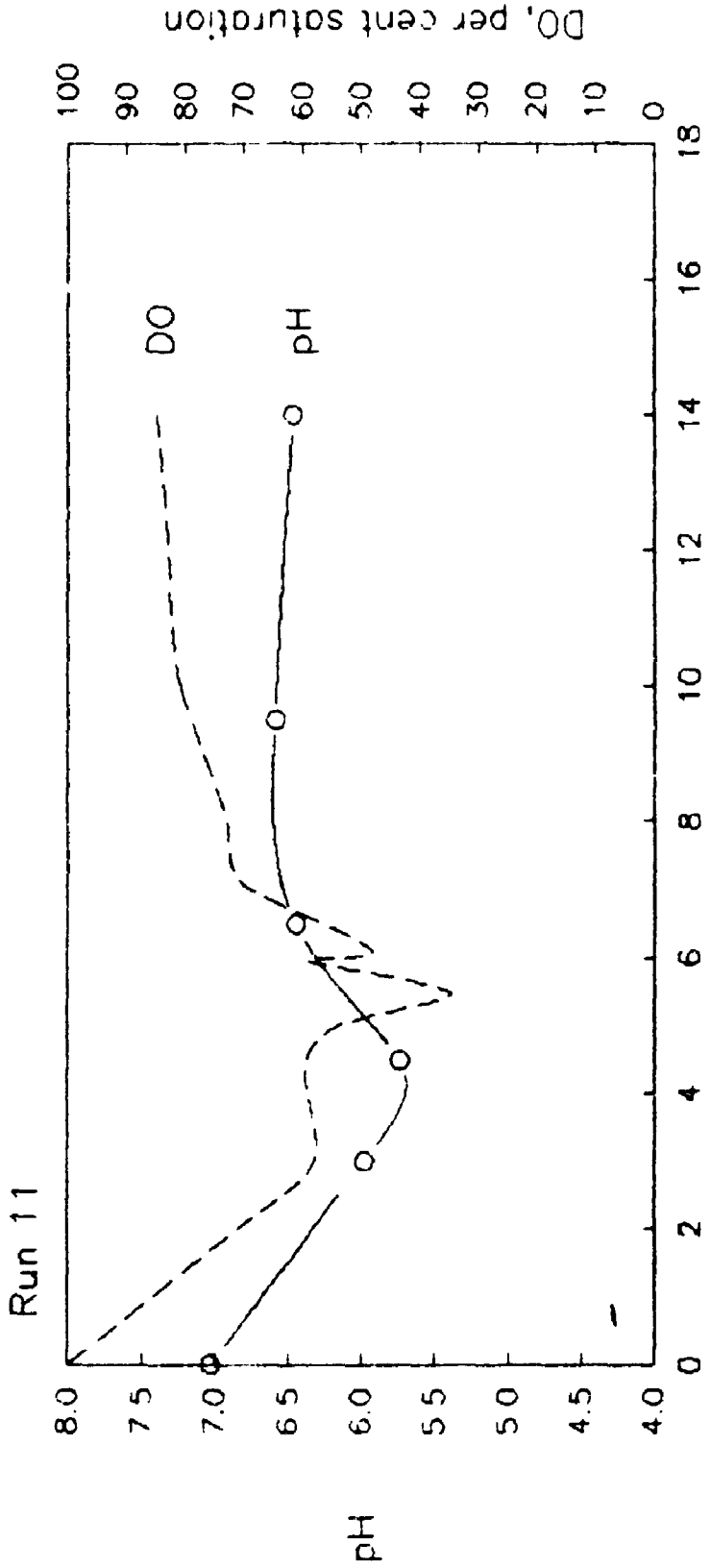

Fig. 7.3: Dissolved oxygen and pH vs. time, Run 11.

Similarly there was a sharp DO peak at about 6 hr, followed by a brief but rapid decline; in Run 10 only a change in slope was seen at apparently the same point in the fermentation. Timing of DO and pH minima corresponded closely to those observed in Run 10, but neither reached as low a value (viz. Run 10 minima: pH: 5.55; DO: 18%; Run 11 minima: pH: 5.7; DO: 34%).

Stage IV of sporulation (ie. cortex formation) again began at about 8 hr as biomass peaked. Unlike Run 10 there was only slight subsequent decrease in biomass and pH. By 14 hr most cells contained refractile spores, granules and, to a lesser extent, crystals; free spores and crystals were also present. Final spore yield was 2.2×10^9 /ml, identical within experimental error to Run 10 (Sect. 6.1).

Patterns of use of individual amino acids were for the most part very similar to those of Run 10 (see tabulated data, App. E).

As in Run 10, the majority of biomass was produced during transition phase, accompanied by substantial formation of intracellular granules. Fig. 7.4 shows total fatty acids, PHB and PHV as a percentage of BDM versus time. PHB accumulation was again temporally associated with late vegetative/early transition - phase granulation. The present fermentation differed from Run 10, however, in both producing and consuming less PHB; and in failing to continue net fatty acid synthesis during the sporulation phase. Thus Run 11 cellular PHB content

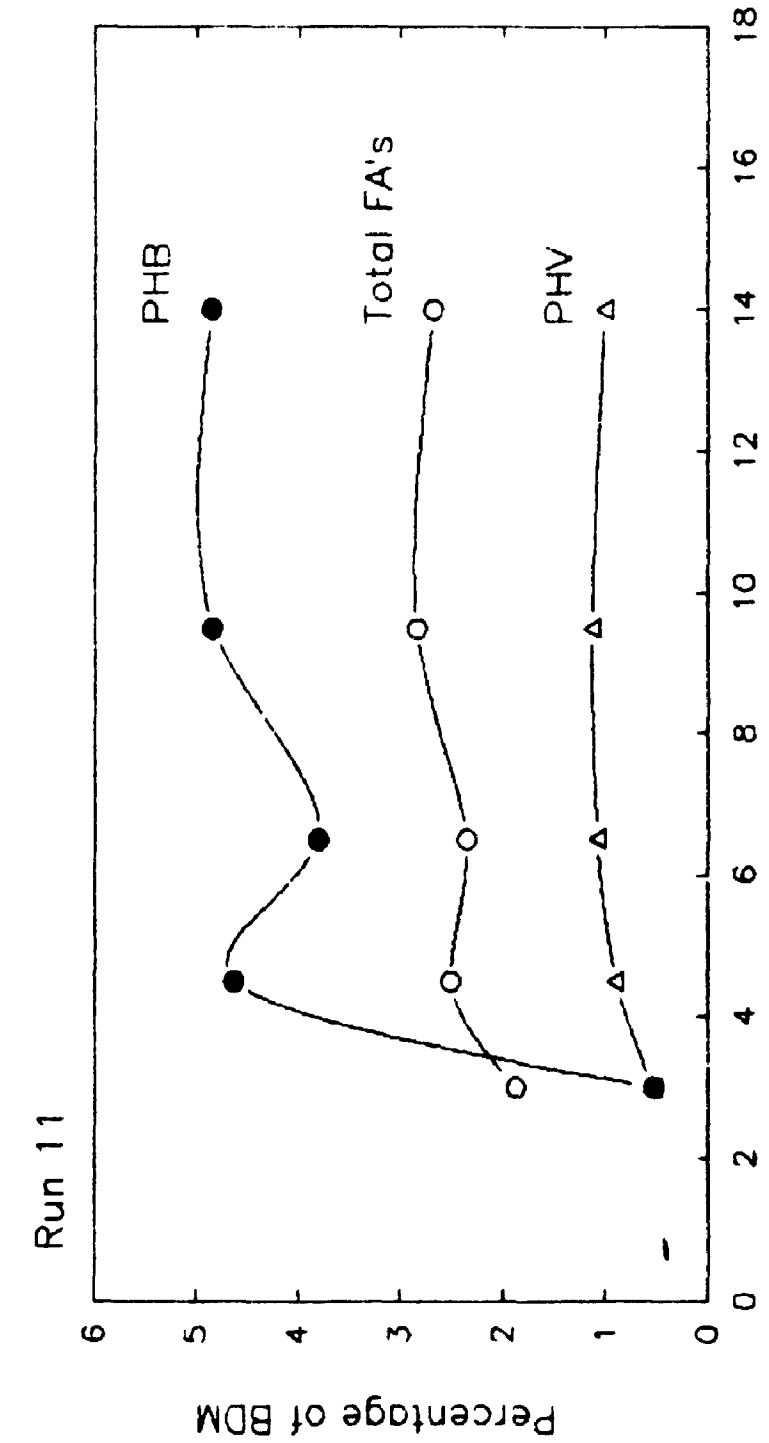

Fig. 7.4: PHB, PHV and total fatty acids as a weight percentage of biomass dry matter vs. time, Run 11.

peaked at about 4.8 per cent of BDM at 4.5 hr, while Run 10 reached about 6.7 per cent at 6.5 hr. Interestingly during both fermentations PHB subsequently decreased to slightly less than 4.0 per cent of BDM before rising again. This sporulation - phase increase was much less pronounced in the present run.

Concentrations of the three major fatty acids in biomass versus time, shown in Fig. 7.5, exhibit a generally similar pattern to Run 10. In the present case, however, less i-C16 was formed during transition phase; and no fatty acids were formed during sporulation, in contrast to Run 10 where i-C15 (leucine - related) and i-C16 (valine - related) fatty acids increased markedly (Fig. 6.10).

Kinetics of production and consumption of acetate, lactate and pyruvate, as shown in Fig. 7.6 and 7.7, were also generally similar to those of the previous fermentation. Again there were apparent differences, namely:

1) in Run 10, but not Run 11, acetate was produced during late sporulation phase;

2) the lactate peak in the present case decreased sooner, ie. during early rather than late transition phase;

3) vegetative - phase pyruvate formation was greater than in Run 10 (about 4.4 versus 3.3 mmol/litre), but its production during late sporulation was less.

Succinate concentration profiles (Fig. 7.7, 6.12) were basically similar, with somewhat lower sporulation - associated formation here.

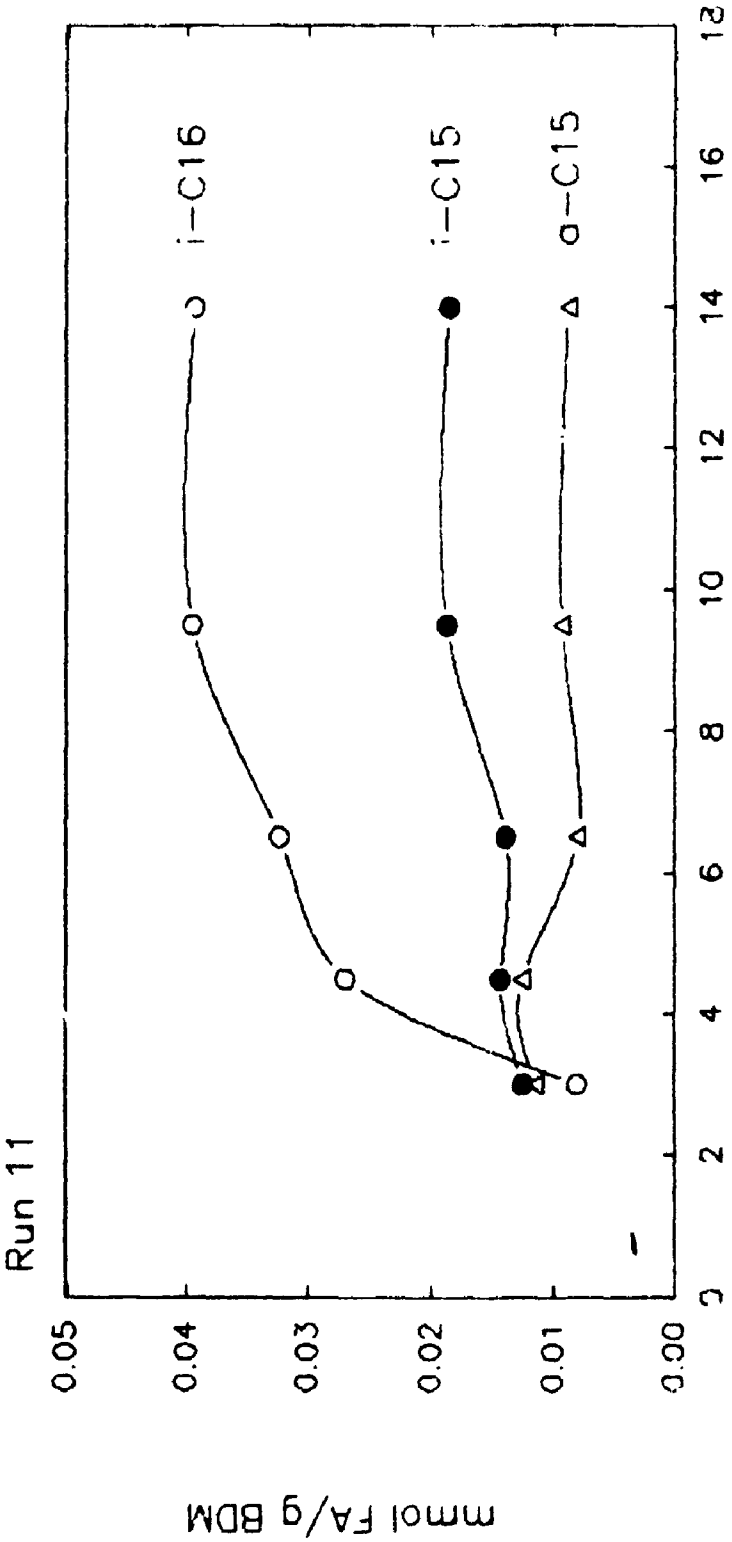

Fig. 7.5: Concentration of major fatty acids in biomass vs. time, Run 11.

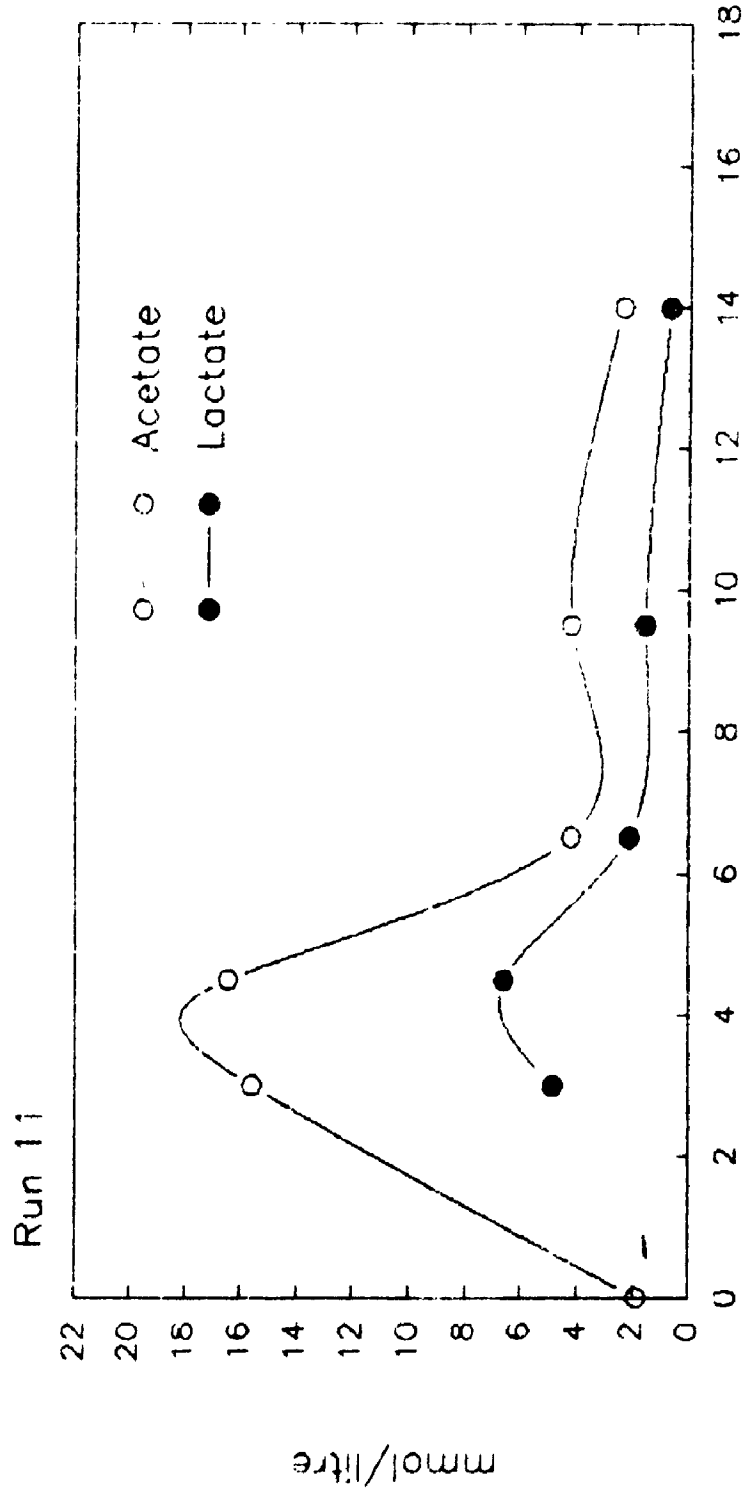

Fig. 7.6: Lactate and acetate concentration vs. time, Run 11.

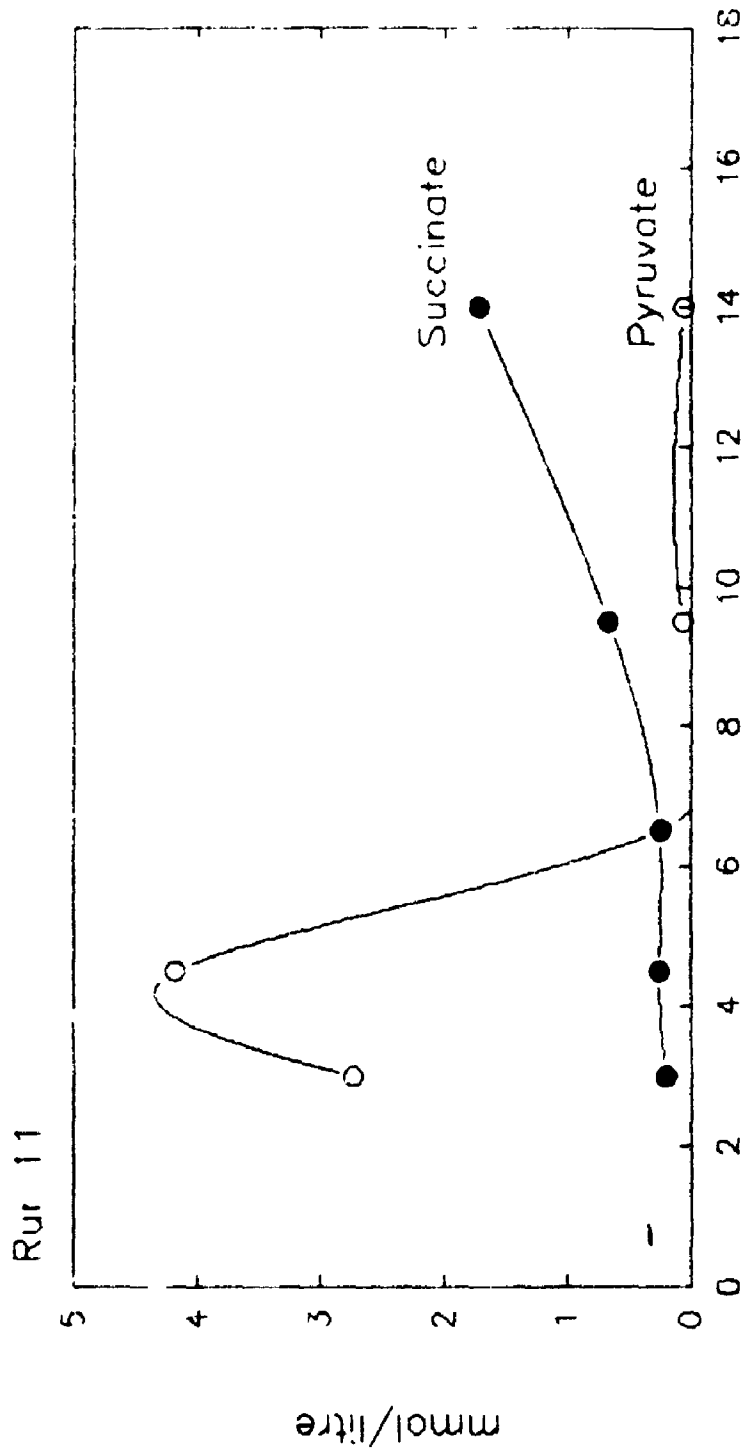

Fig. 7.7: Pyruvate and succinate concentration vs. time, Run 11.

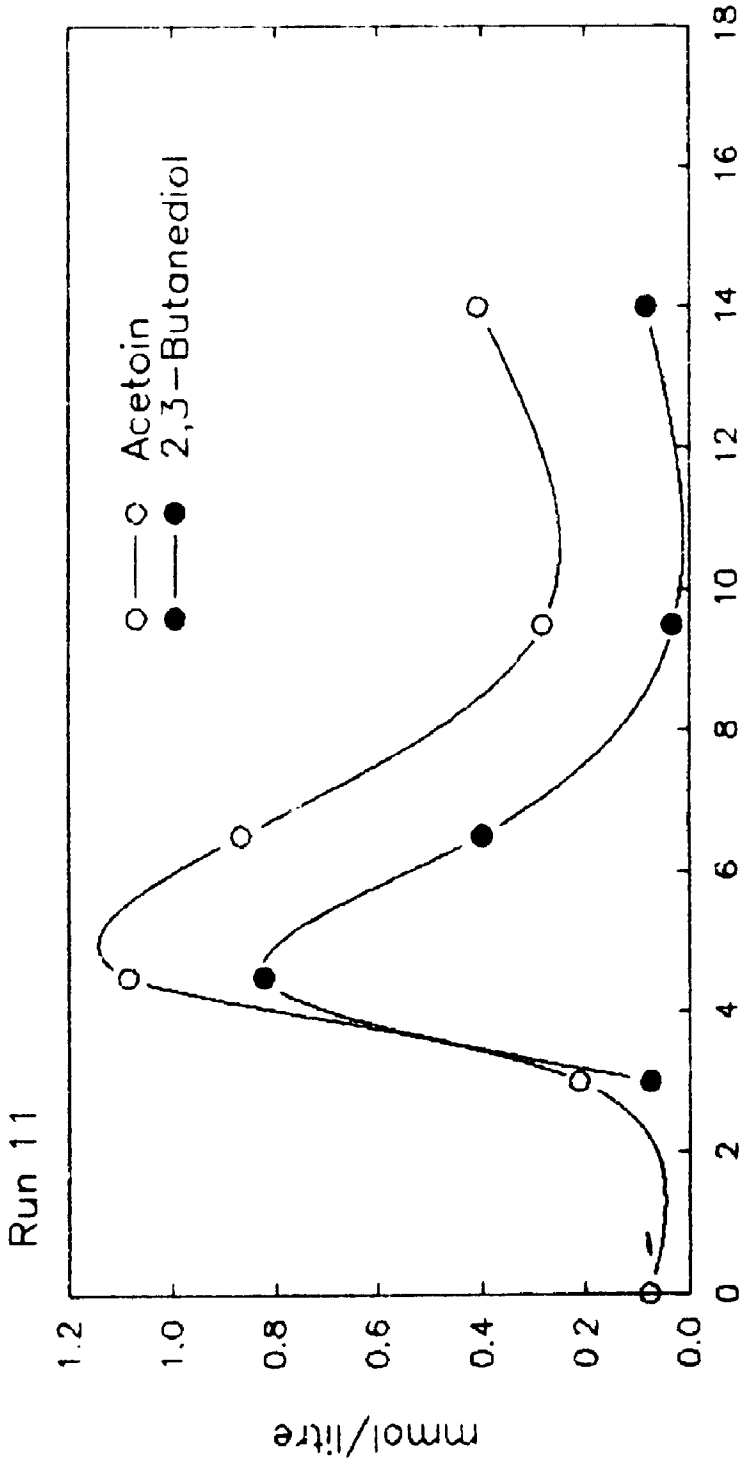

Fig. 7.8: Acetoin and 2,3-butanediol concentration vs. time, Run 11.

As shown in Fig. 7.8, less acetoin and 2,3-butanediol were formed in the present run; and more of the former remained in the sporulation broth. The diauxic pattern of acetoin production observed in Run 10 (Fig. 6.13) did not recur.

Profiles of isovalerate and 2-methylbutyrate concentrations versus time (Fig. 7.9) are very similar to those observed previously (Fig. 6.14). Isobutyrate, however, accumulated to a much greater extent (about 0.65 vs. 0.38 mM) by 5 hours, before dropping to about 0.3 mM in both cases. In further contrast, spore maturation in Run 11 was accompanied by sustained production of isobutyric acid (as well as isovaleric acid). Conversely, release of branched - chain α-keto acids (BCKA's) in the present fermentation (Fig. 7.10) was less than in the previous case (Fig. 6.15).

7.2 Vegetative Phase Model Solution

Flux of α-keto-β-methylvalerate through BCKA dehydrogenase for sample GR11X1 (4.5 hr) was calculated to be 0.0247 mmol/g VDM/hr (Table 5.6). Dehydrogenation rates of the other BCKA's were calculated via equation 5.15, using data from App. B, as follows:

$$FT(V) = [FT(I) + SA(I)]*[FA(V)/FA(I)] - SA(V)$$

$$\approx (0.02468)*(0.02209/0.007148)$$

$$\approx 0.0763 \text{ mmol/g VDM/hr}$$

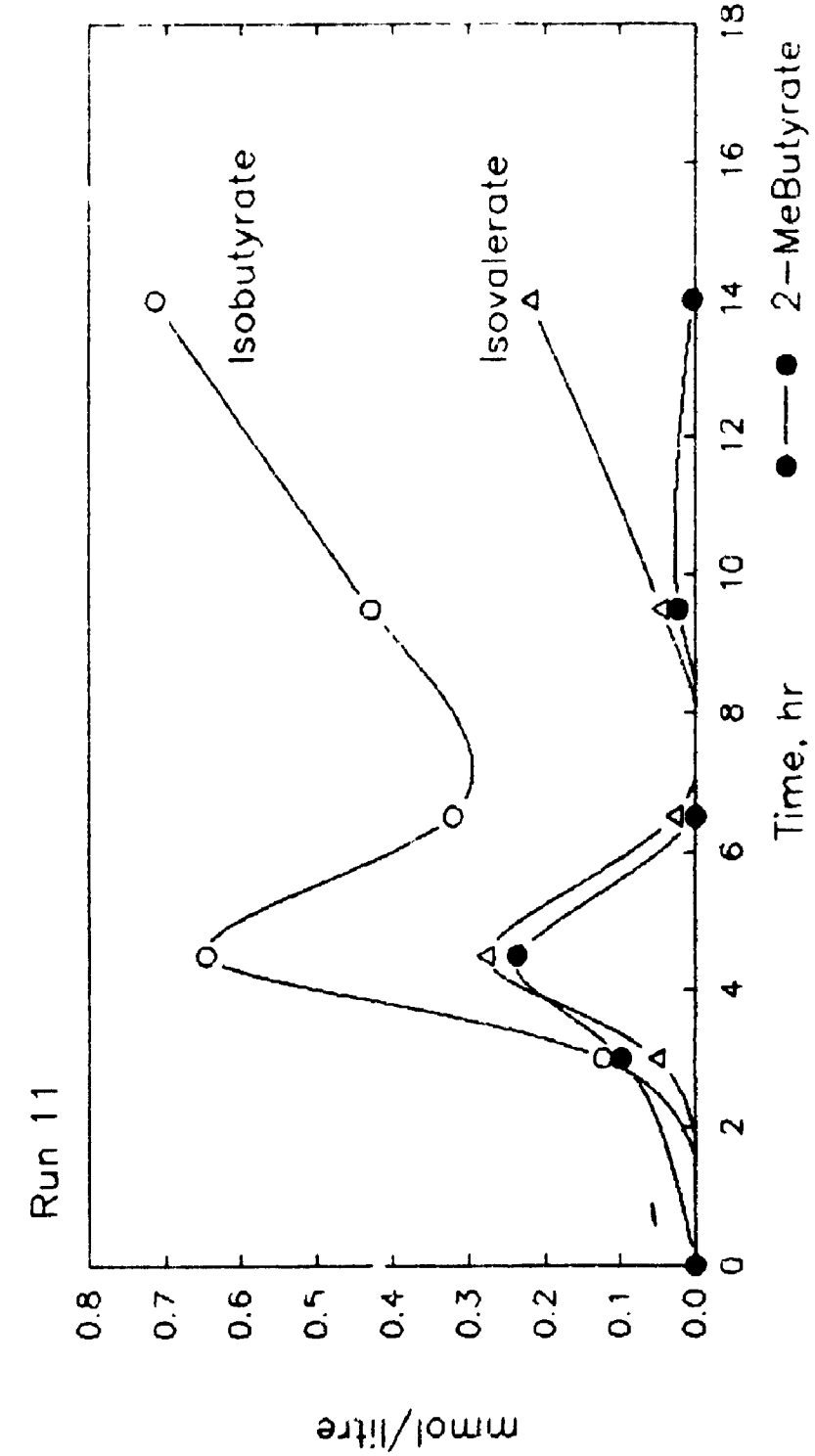

Fig. 7.9: Isobutyrate, isovalerate and 2-methylbutyrate concentration vs. time, Run 11.

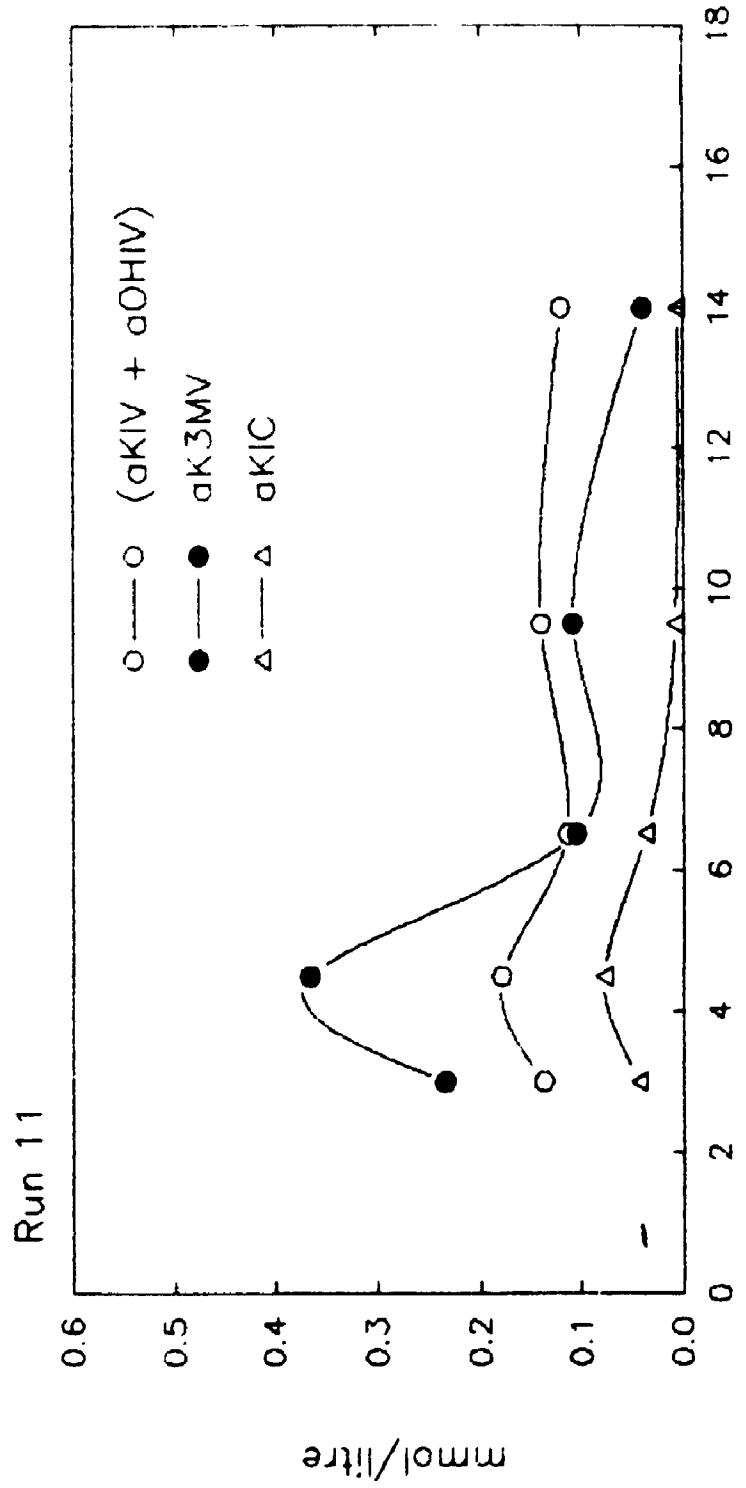

Fig. 7.10: Concentration of branched - chain α-ketoacids vs. time, Run 11. (aKIV + aOHIV) = combined α-ketoisovalerate and α-hydroxyisovalerate; aK3MV = α-keto-β-methylvalerate; aKIC = α-ketoisocaproate.

$$FT(L) = [FT(I) + SA(I)]*[FA(L)/FA(I)] - SA(L)$$

$$\approx (0.02468)*(0.01049/0.007148)$$

$$\approx 0.0362 \text{ mmol/g VDM/hr}$$

Substitution of these values into the metabolic model (Sect. 5.1) gave a dehydrogenation rate for α-ketoisovalerate (αKIV) just sufficient for fatty acids and isobutyrate formation, ie. not sufficient for propionyl-CoA production (for PHV and n-C15 fatty acid) from this pathway. Since isoleucine pathway flux was also insufficient to meet this demand, the required propionyl-CoA was assumed to arise by decarboxylation of α-ketobutyrate (Fig. 3.3).

The model solution shown in Fig. 7.11 was obtained with BMF equal to 0.9821. This metabolic pattern is similar to the vegetative phase of Run 10 (Fig. 6.16), differing basically as follows:

1) flows through glycolysis, pyruvate dehydrogenase and acetolactate synthetase are considerably smaller;

2) there is no flux from αKIV to succinyl-CoA (flux was only 0.03 mmol/g VDM/hr in Run 10);

3) whereas before lactate and PHB were being actively formed, here both have already reached their maxima.

The present case appears to show metabolism essentially at the point of switching from vegetative growth to the first stage of sporulation. This is substantiated by inflections in the pH and DO profiles (Fig. 7.3). On the other hand i-C16 fatty acid

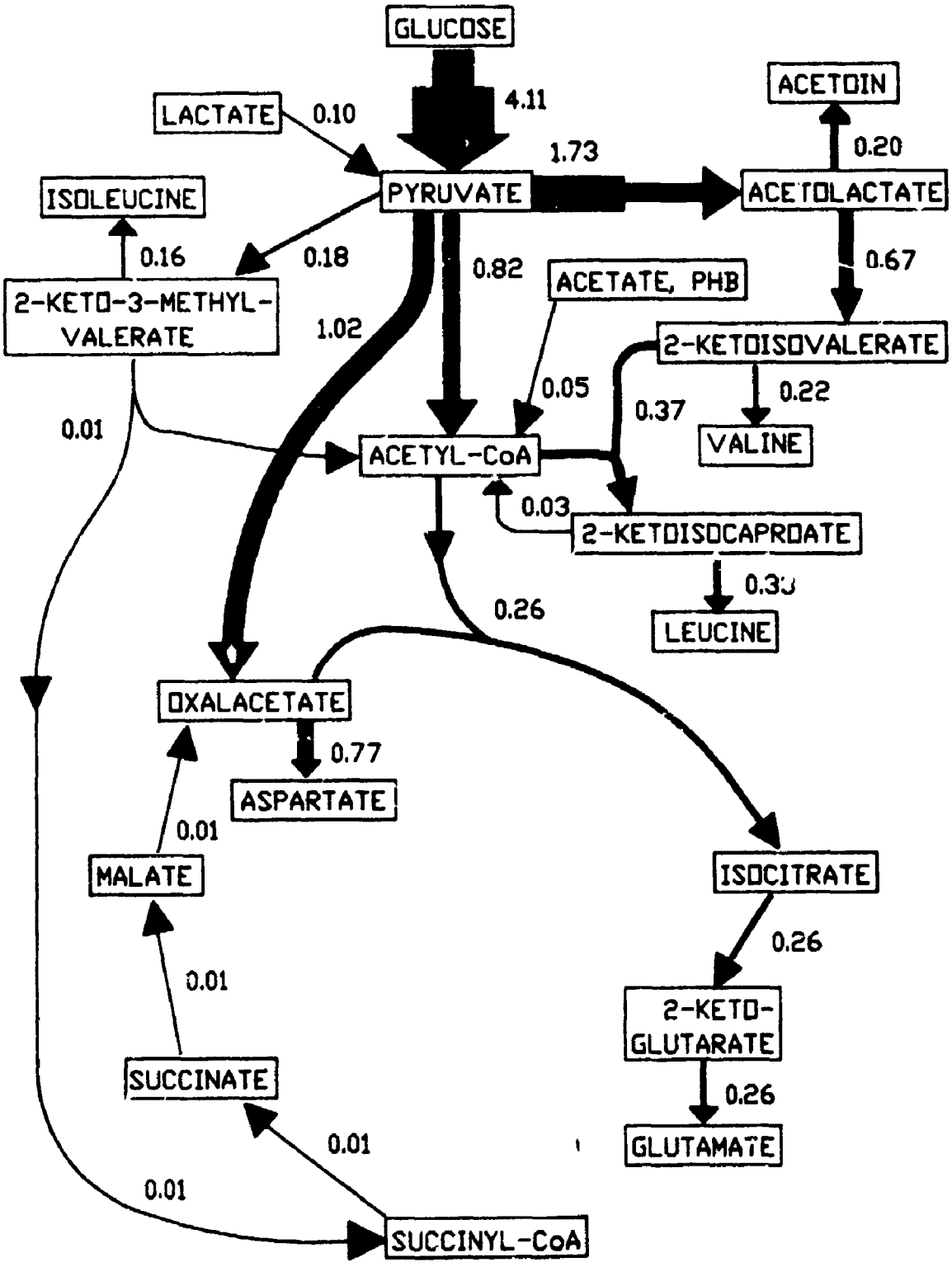

Fig. 7.11: Model solution for vegetative phase (4.5 hr) of Run 11. Flux in mmol/g VDM/hr proportional to line width.

content has already increased considerably (Fig. 7.5), whereas this occurred mostly during early transition phase of Run 10 (Fig. 6.10). Maxima of the BCKA's also occurred earlier in the present case (compare Fig. 7.10 with Fig. 6.15).

7.3 Mid - sporulation Phase Model Solution

For this case (ie. sample GR11X3; 9.5 hr) flux of α-keto-β-methylvalerate through BCKA dehydrogenase was calculated to be 0.168 mmol/g VDM/hr (Table 5.6). As before the other dehydrogenation rates were calculated from data in App. B using equation 5.15 as follows:

$$FT(V) = [FT(I) + SA(I)]*[FA(V)/FA(I)] - SA(V)$$

$$\approx (0.1677)*(0.000995/0.000808)$$

$$\approx 0.207 \text{ mmol/g VDM/hr}$$

$$FT(L) = [FT(I) + SA(I)]*[FA(L)/FA(I)] - SA(L)$$

$$\approx (0.1677)*(0.001992/0.000808)$$

$$\approx 0.413 \text{ mmol/g VDM/hr}$$

Substitution of these values into the metabolic model (Sect. 5.1) led to an apparent deficit of pyruvate. Because biomass breakdown was occurring (see Fig. 7.1), intermediates such as pyruvate were produced partially from such breakdown ("turnover"); and it was necessary to increase factor BMF. Thus pyruvate balance was achieved for BMF equal to 4.217, resulting in the metabolic flows summarized in Fig. 7.12.

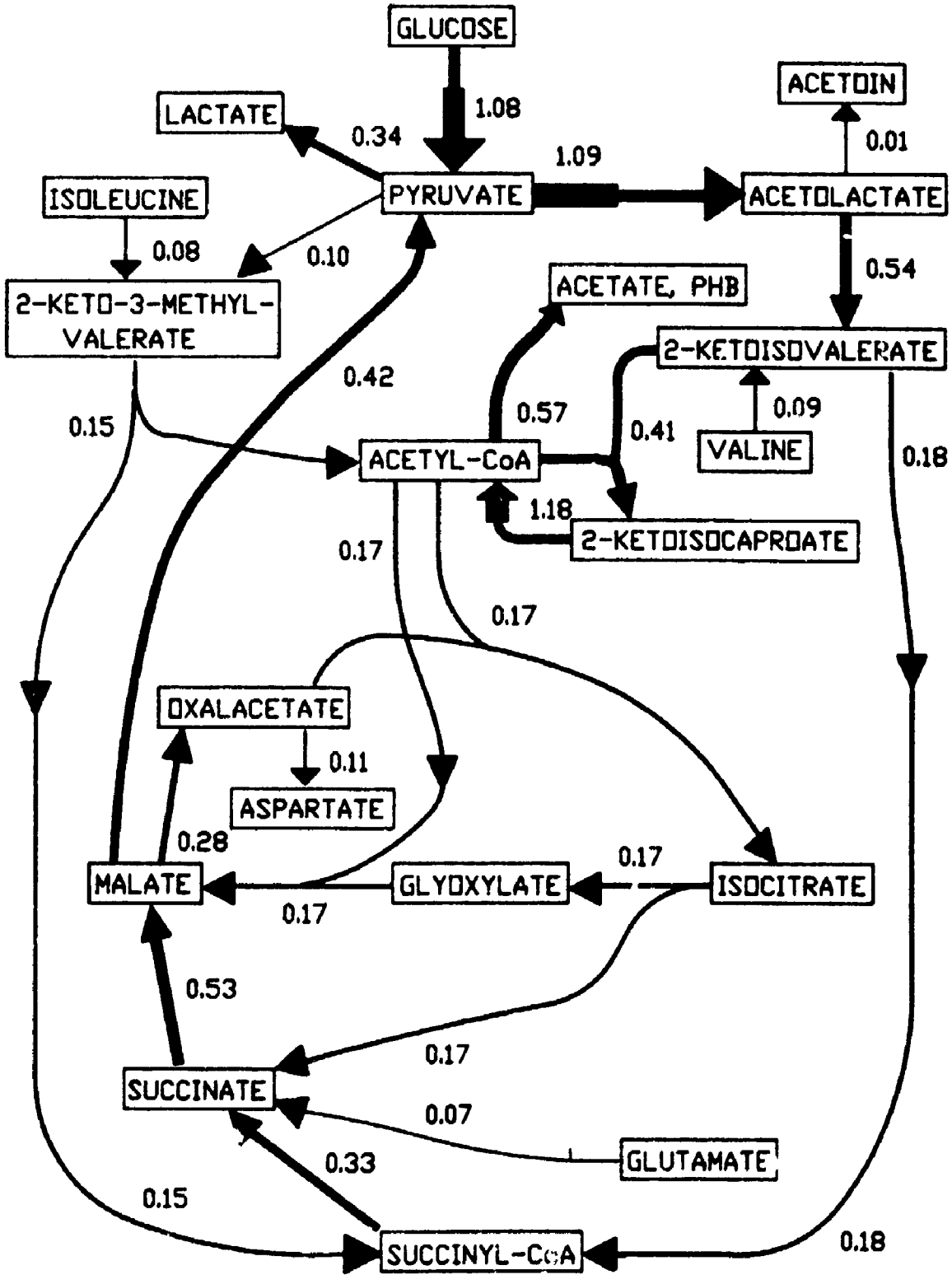

Fig. 7.12: Model solution for mid - sporulation phase (9.5 hr) of Run 11. Flux in mmol/g VDM/hr proportional to line width.

About 44 per cent of the glycolytic flux to pyruvate arose from biomass turnover. As for the mid - sporulation sample of Run 10 no specific allowance was made for synthesis of phosphoglycerate or dipicolinate (*cf.* Sect. 6.4.2).

The observed metabolic system is generally similar to that found at 11 hr in Run 10 (Fig. 6.18). Biomass turnover was in progress in both cases, although to a lesser degree here. The following major differences are observable in the present case:

1) greater glycolytic flux, of which a larger proportion derives from biomass turnover;

2) much lower glyoxylate cycle and malic enzyme activity;

3) greater activity of the isoleucine pathway, including α-ketobutyrate formation via aspartate.

The present case did not differ substantially from the corresponding Run 10 sample in regard to acetate and PHB formation (*ie.* there was slight formation in both cases). However, whereas here PHB formation is ending (Fig. 7.4), it began anew in the previous fermentation (Fig. 6.9). Comparison of Fig. 7.5 with Fig. 6.10 shows a similar pattern for the major cellular fatty acids and acetic acid (Fig. 7.6, 6.11). This pattern is opposite to that shown by isobutyrate, which was substantially produced during later sporulation of Run 11 (Fig. 7.9), but not in Run 10 (Fig. 6.14).

8. Results and Discussion: Run 12

Complete results for this fermentation are tabulated in Appendix F.

8.1 General Fermentation Characteristics

Run 12 was performed identically to Run 11 (Sect. 7). Biomass (BDM) and glucose concentrations versus time are shown in Fig. 8.1, and ln VDM versus time in Fig. 8.2. The latter gives specific growth rate of 0.51 hr^{-1} during vegetative phase, similar to Runs 10 and 11 (Sect. 6, 7 respectively). The present fermentation reached the same biomass concentration, 6.77 g BDM/litre, as Run 10.

Early uptake of several amino acids practically ceased between 3.0 and 4.5 hr (App. F) when glucose consumption began in earnest (Fig. 8.1). This substrate utilization pattern is quite similar to that reported by Sakharova *et al.* (1985).

Although growth was again accompanied by falling pH and dissolved oxygen (DO; Fig. 8.3), their decrease was less than in Run 10 (Fig. 6.3). Thus pH here reached only 5.80 compared to 5.55 previously; dissolved oxygen fell only to about 46 % sat'n. versus the previous 14 % sat'n. Both minima also occurred later in the present fermentation, namely: pH at about 5.0 hr; DO at about 6.5 hr. These are 45 and 60 minutes later than corresponding events of the tryptone - grown cells,

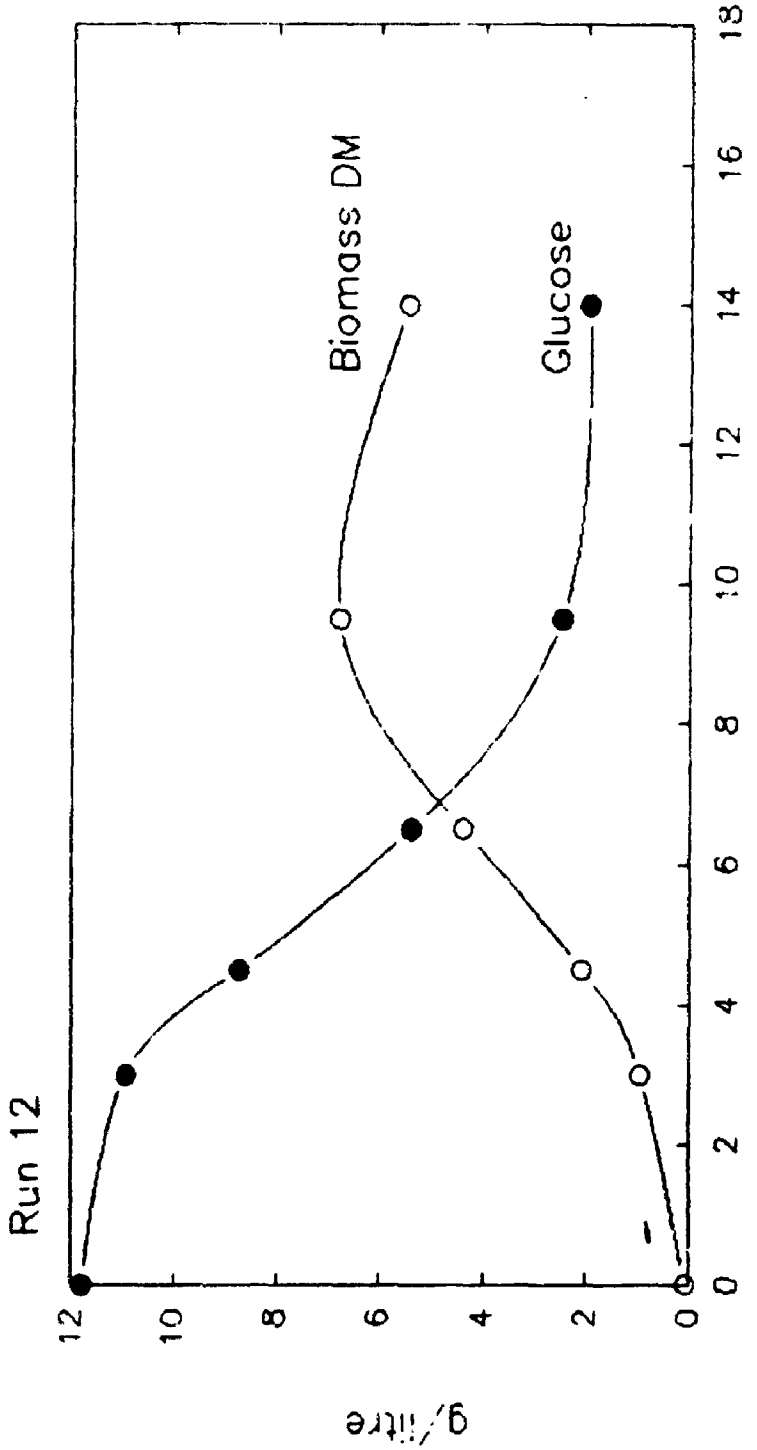

Fig. 8.1: Biomass dry matter and glucose concentration vs. time, Run 12.

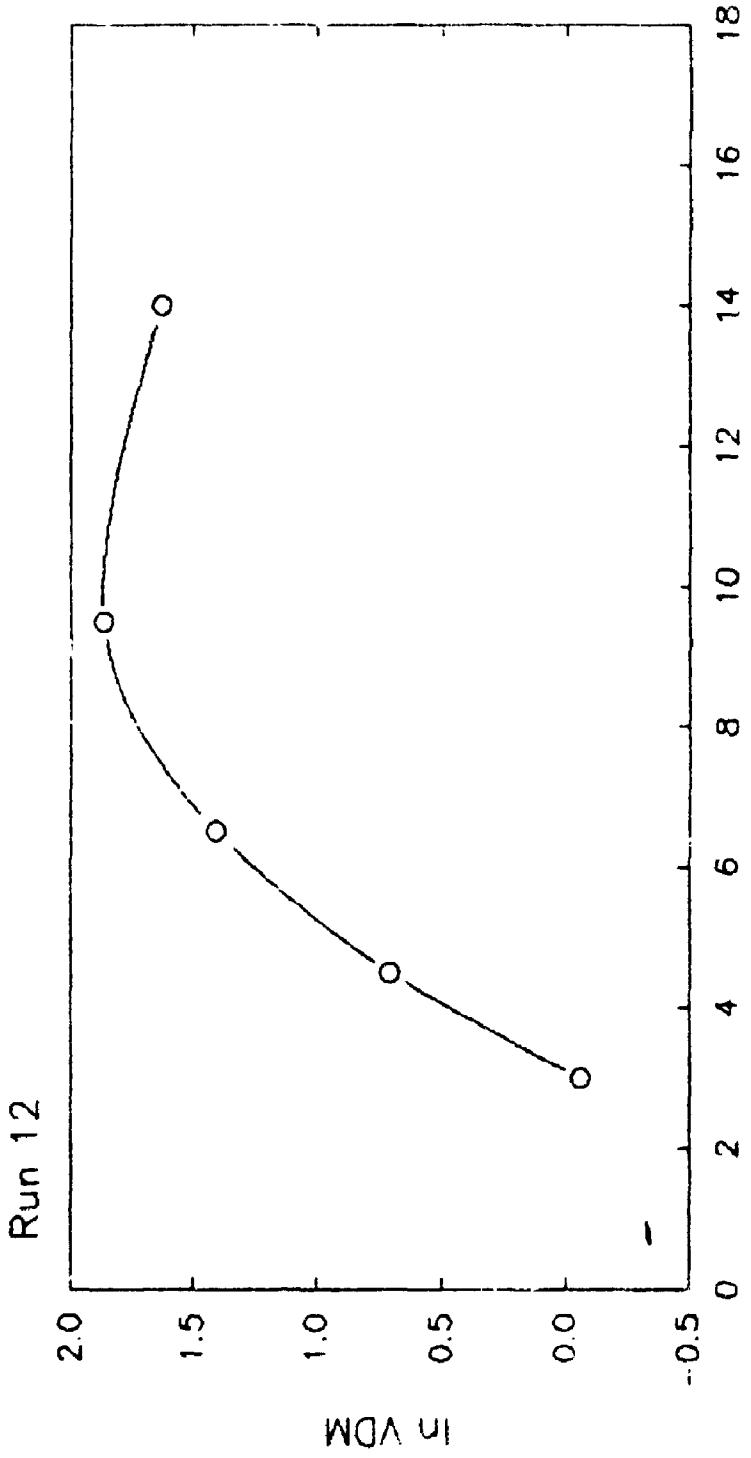

Fig. 8.2: Natural logarithm of viable dry matter vs. time, Run 12.

3

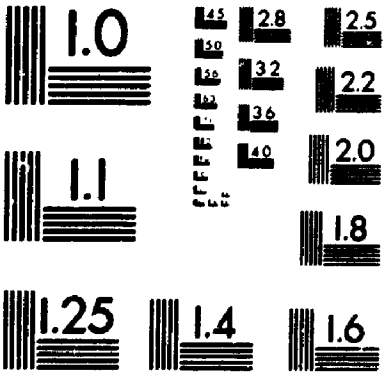

MICROCOPY RESOLUTION TEST CHART
NATIONAL BUREAU OF STANDARDS
STANDARD REFERENCE MATERIAL 1010a
(ANSI and ISO TEST CHART No 2)

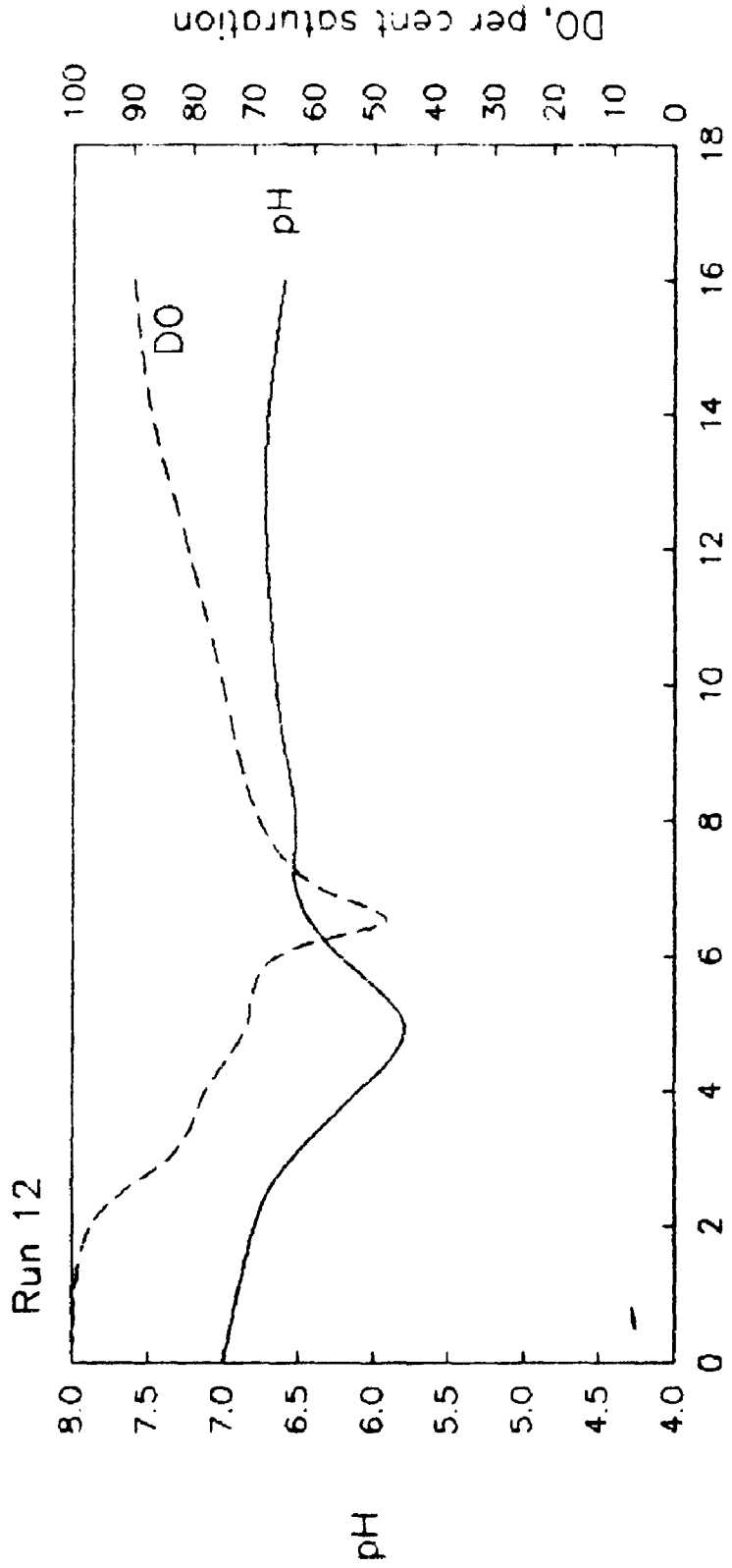

Fig 8.3: Dissolved oxygen and pH vs. time, Run 12.

ie. Run 10. Minima in Run 11 were intermediate, ie. pH: about 5.7; DO: 34 % sat'n. (Sect. 7.1).

Granulation occurred after 4.5 hr, and was very pronounced by 9.5 hr when crystals but not refractile spores were visible, ie. about stage IV of sporulation. By 14.0 hr most of the cells contained refractile spores and crystals. The broth contained about 1.5×10^9 cells/ml at 6.5 hr; but apparently only $4.9 (\pm 0.2) \times 10^8$ viable spores/ml after lysis. However since Run 11 formed as high a spore concentration as Run 10, no significant difference in either cell or spore production seems likely amongst the three runs.

As previously, most biomass was formed during stages I to III of sporulation. The pattern of formation and use of PHB (Fig. 8.4) was very similar to that of Run 10 (Fig.6.9). As observed in the other two runs, cellular i-C16 fatty acid concentration increased greatly during transition - phase growth (Fig. 8.5). The present fermentation also gave clear evidence of oxidation of this fatty acid between 7 and 10 hr (stages III to IV of sporulation). However, in contrast to Run 10, total fatty acids did not increase after 6.5 hr (compare Fig. 8.4 with Fig. 6.9).

Kinetics and amount of acetate produced were very similar to Run 10 (Fig.6.11), but rapid uptake ended after about two hours in the present case (Fig. 8.6). Again the period of most intense oxygen use coincided with disappearance of acetate.

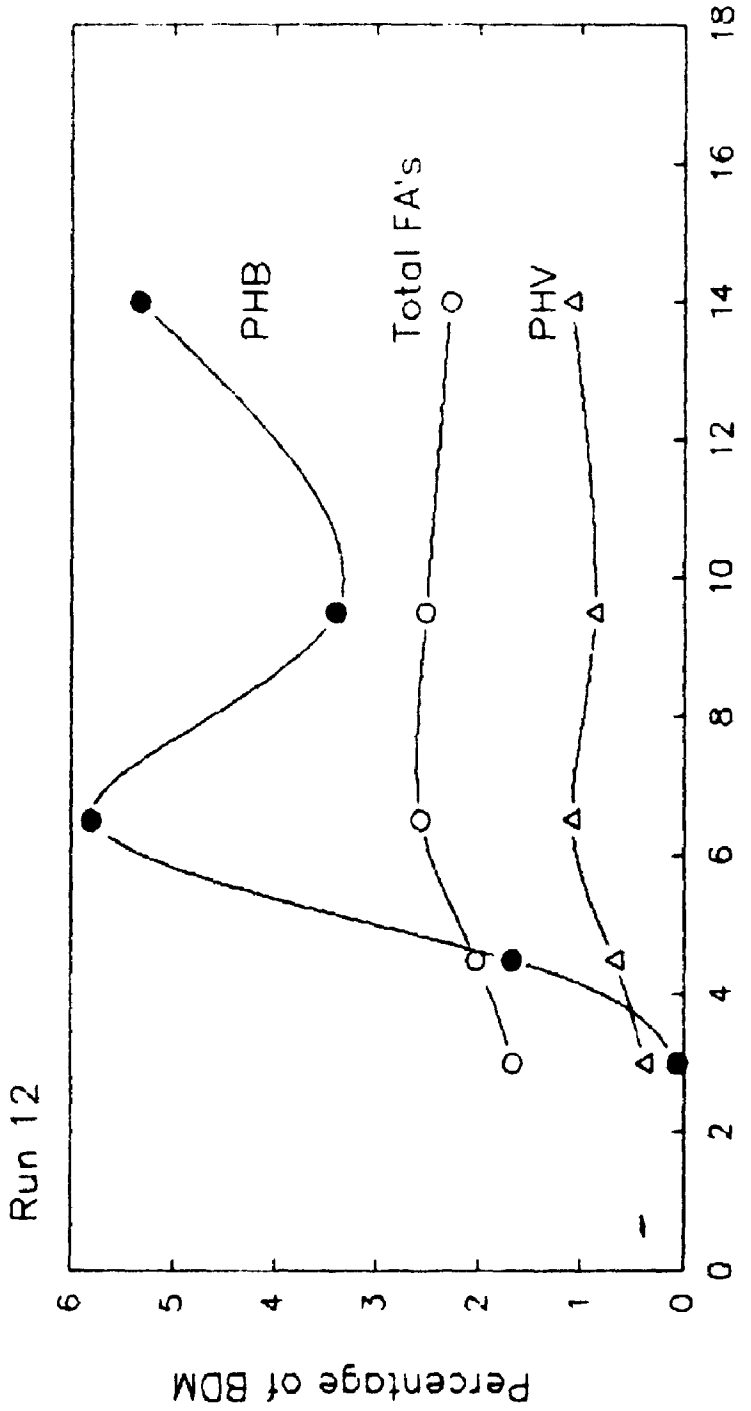

Fig. 8.4: PHB, PHV and total fatty acids as a weight percentage of biomass dry matter vs. time, Run 12.

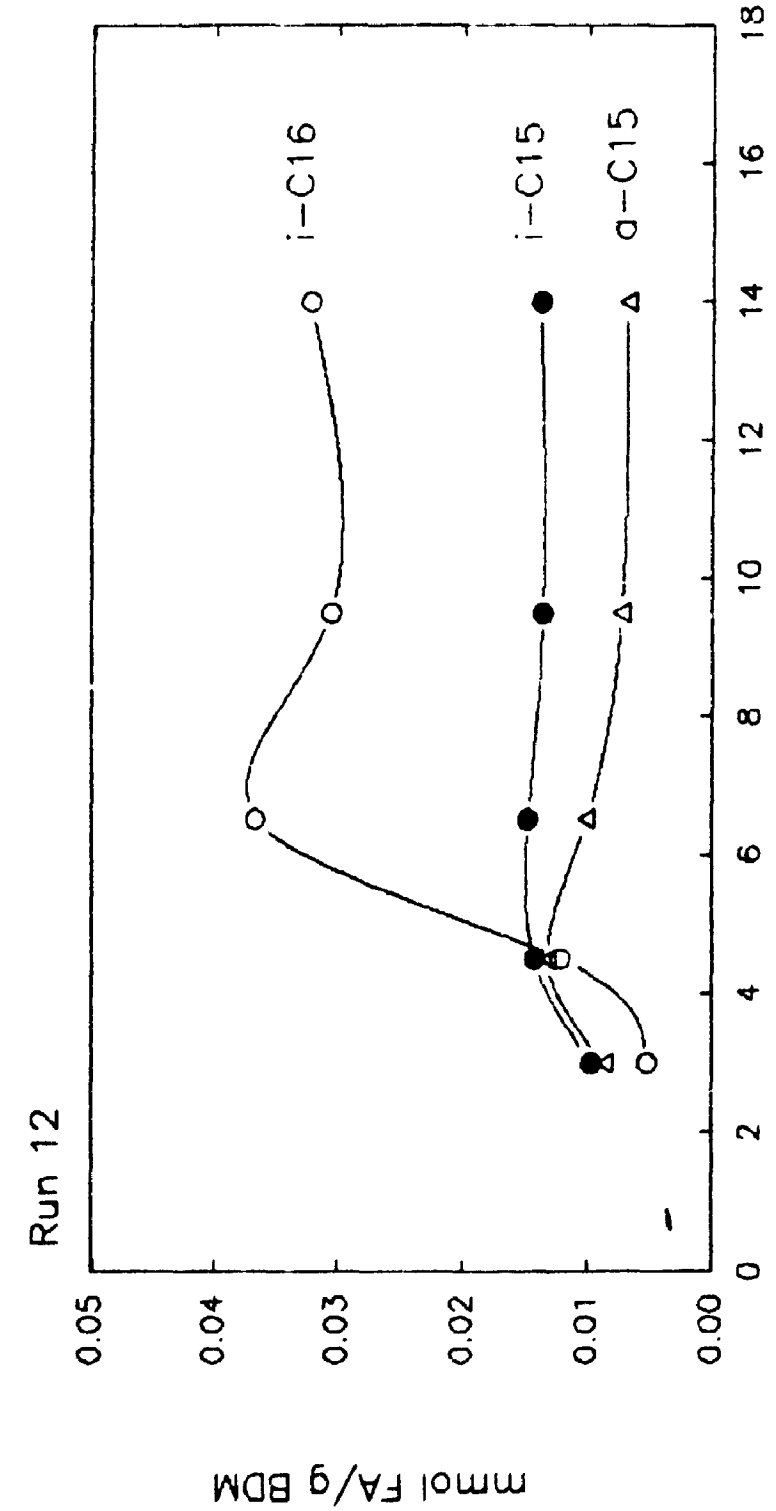

Fig. 8.5: Concentration of major fatty acids in biomass vs. time, Run 12.

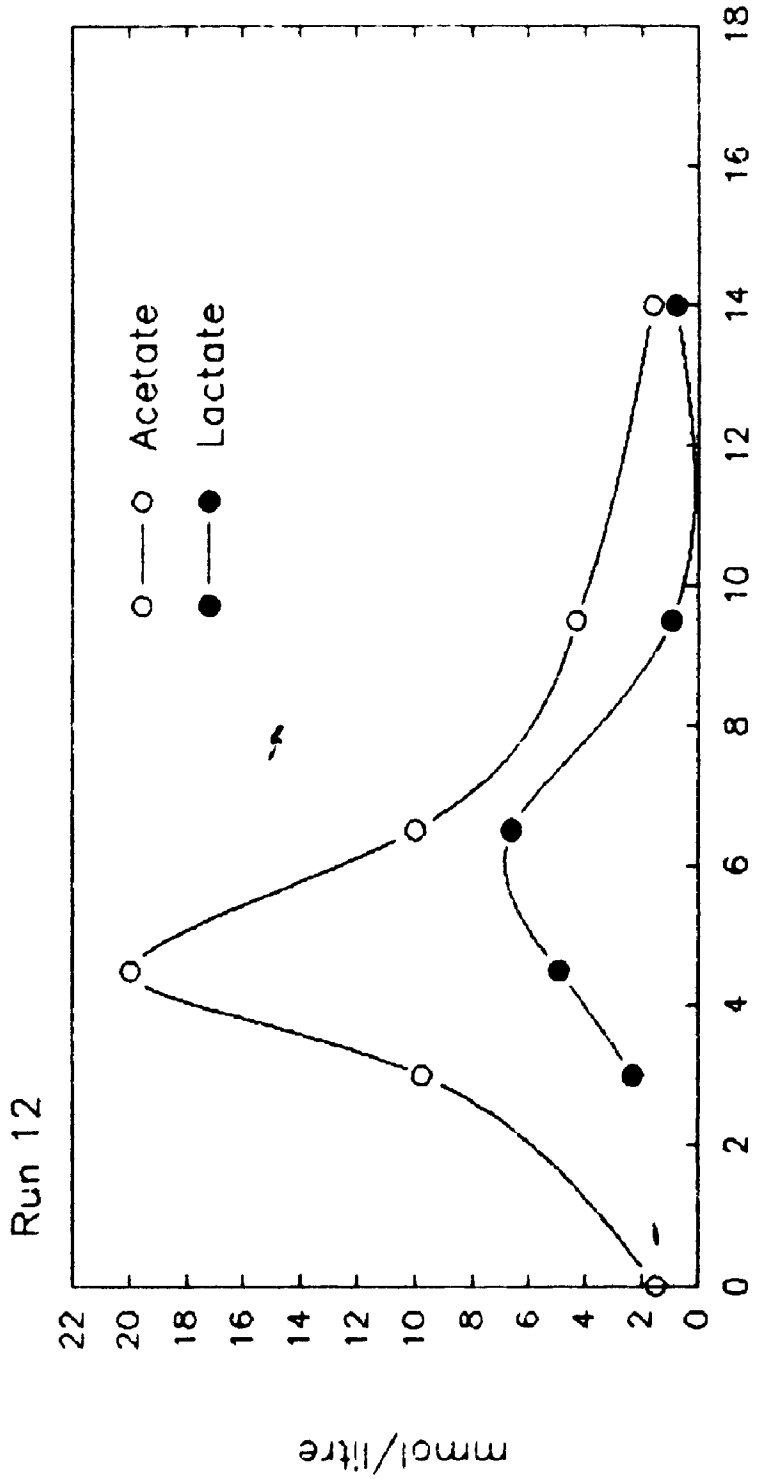

Fig. 8.6: Lactate and acetate concentration vs. time, Run 12.

Contrary to Run 10, no acetate was formed during sporulation phase.

Lactate production was more gradual (Fig. 8.6), peaking at about 6.0 hr, ie. during early sporulation rather than at the end of vegetative growth as in Run 11 (Fig. 7.6). Thus, as in Run 10 but not Run 11, pyruvate reached a maximum before lactate (Fig. 8.7). Pyruvate formation was less than in either previous fermentation, and did not occur during sporulation as in Run 10 (cf. acetate above).

Acetoin and 2,3-butanediol profiles versus time (Fig. 8.8) generally resembled those of Run 11.

This was also true for the short - chain branched fatty acids (Fig. 8.9); except that both formation and uptake of isobutyrate were much more gradual than in either previous case. Thus maximum isobutyrate occurred here at about 6.25 hr (versus 4.5 hr previously), and minimum at about 9.75 hr (versus 7 to 8 hr before). Similarly maximum concentration of valine and leucine - associated 2-oxoacids (viz. [αKIV + αOHIV], αKIC; Fig. 8.10) is delayed about two hours relative to the isoleucine - associated acid (αK3MV). Run 12 differs further in that αKIC accumulates almost as much as (αKIV + αOHIV), before being consumed.

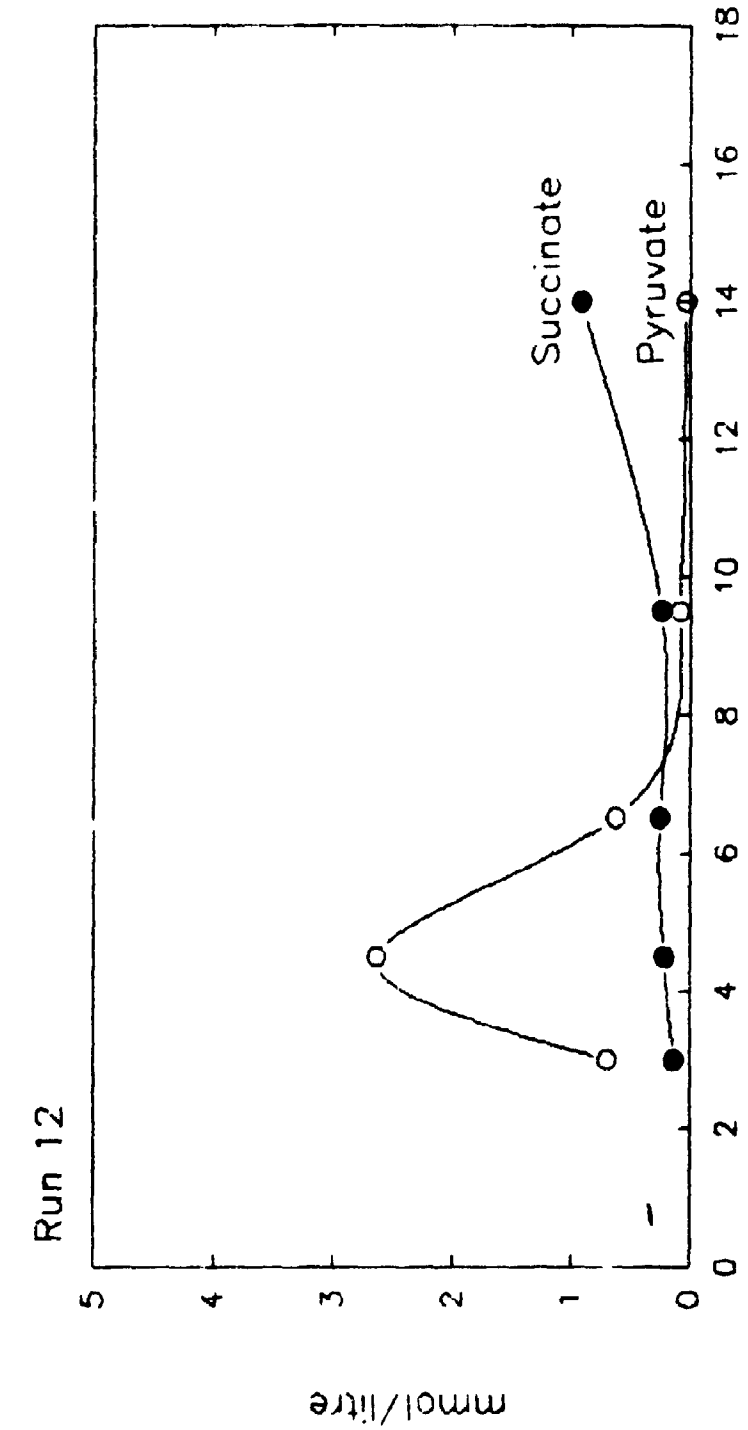

Fig. 8.7: Pyruvate and succinate concentration vs. time, Run 12.

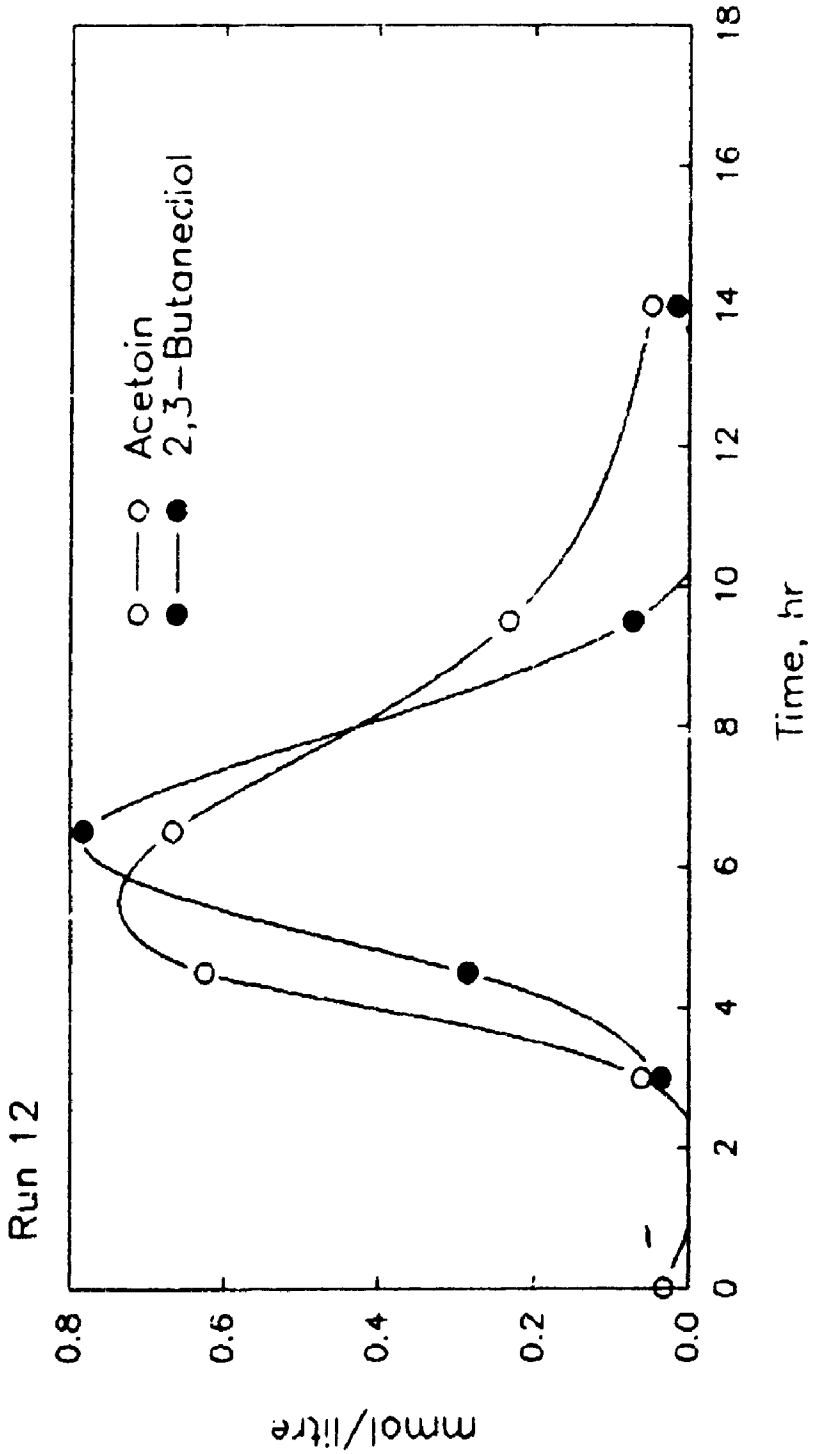

Fig. 8.8: Acetoin and 2,3-butanediol concentration vs. time, Run 12.

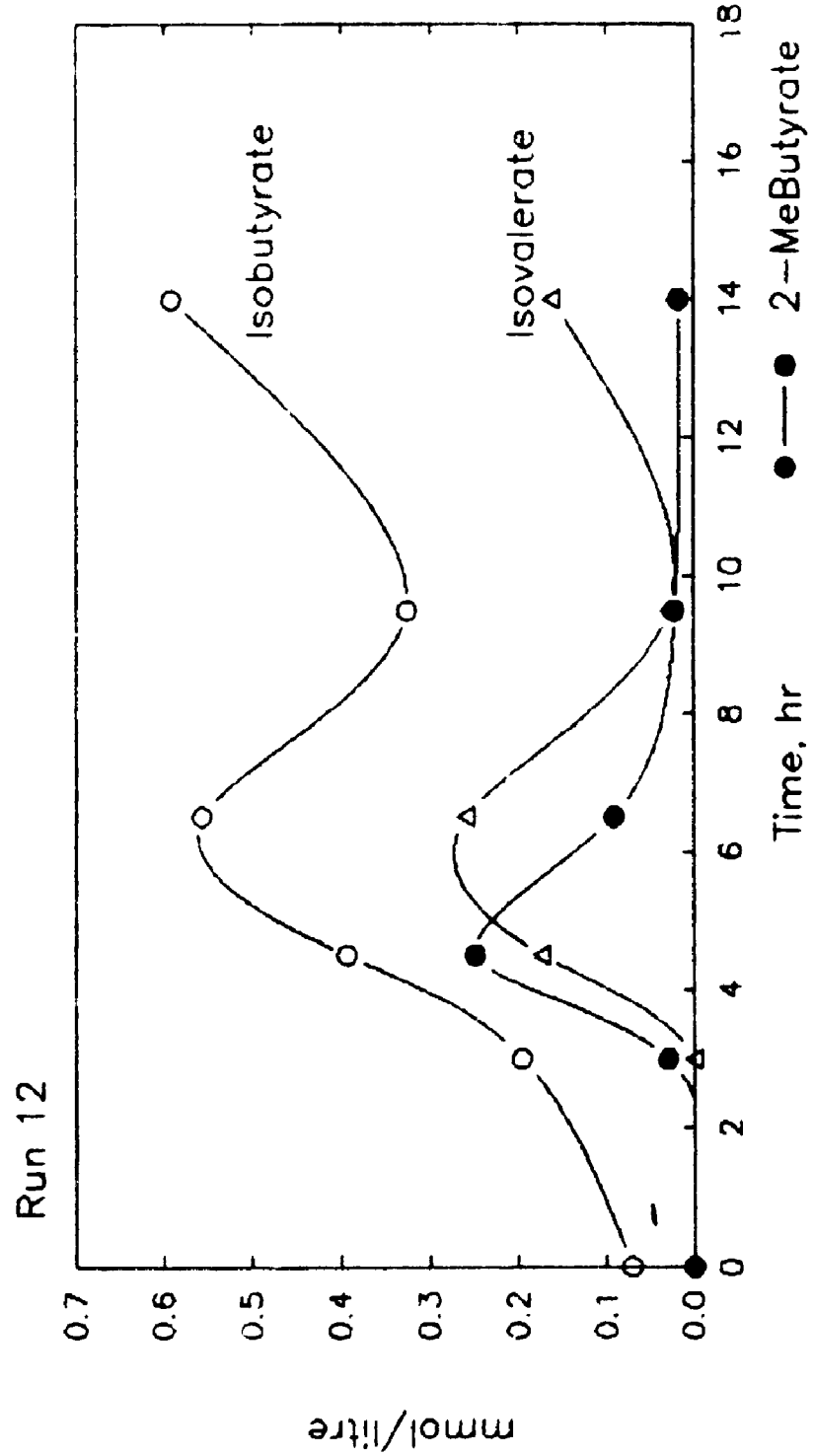

Fig. 8.9: Isobutyrate, isovalerate and 2-methylbutyrate concentration vs. time, Run 12.

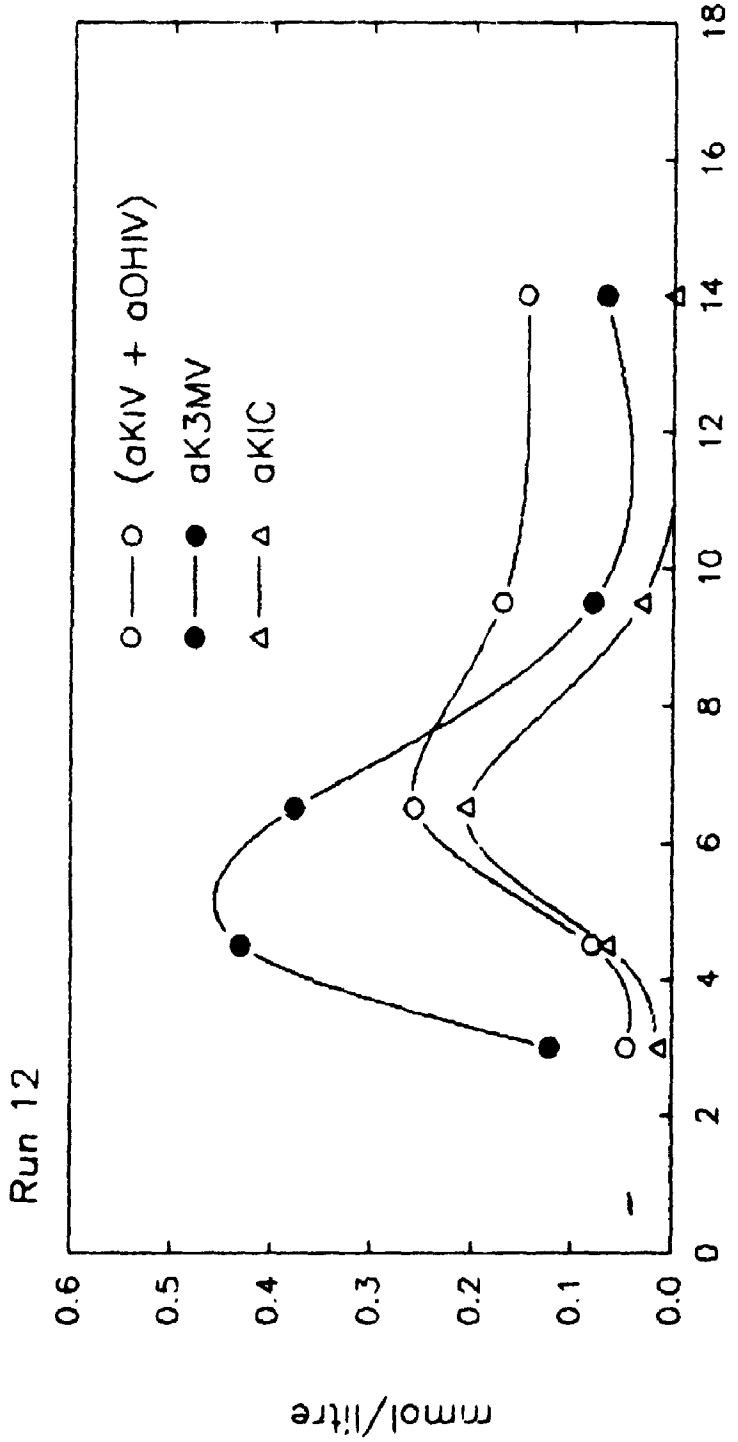

Fig. 8.10: Concentration of branched - chain α-ketoacids vs. time, Run 12. (aKIV + aOHIV) = combined α-ketoisovalerate and α-hydroxyisovalerate; aK3MV = α-keto-β-methylvalerate; aKIC = α-ketoisocaproate.

8.2 Vegetative Phase Model Solution

Flux of α-keto-β-methylvalerate (αK3MV) through BCKA dehydrogenase for this case (*ie.* sample GR12X1; 4.5 hr) was calculated to be 0.220 mmol/g VDM/hr (Table 5.6). Thus dehydrogenation rates of αKIV and αKIC were calculated via equation 5.15 as follows (Sect.5.5; *cf.* App. B):

$$FT(V) = [FT(I) + SA(I)]*[FA(V)/FA(I)] - SA(V)$$

$$\approx (0.2200)*(0.02378/0.01067)$$

$$\approx 0.490 \text{ mmol/g VDM/hr}$$

$$FT(L) = [FT(I) + SA(I)]*[FA(L)/FA(I)] - SA(L)$$

$$\approx (0.2200)*(0.01171/0.01067)$$

$$\approx 0.241 \text{ mmol/g VDM/hr}$$

Substitution of these values into the metabolic model of Sect. 5.1 led to pyruvate balance at BMF equal to 0.6552, and the system of metabolic flows shown in Fig. 8.11. This diagram resembles closely that of vegetative phase in Run 10 (Fig. 6.16). The apparently significant differences in the present pattern are as follows:

1) increased flux through all three BCAA catabolic pathways, and later TCA cycle enzymes;

2) decreased anaplerotic flux via pyruvate carboxylase;

3) decreased rate of production of acetoin and 2,3-butanediol.

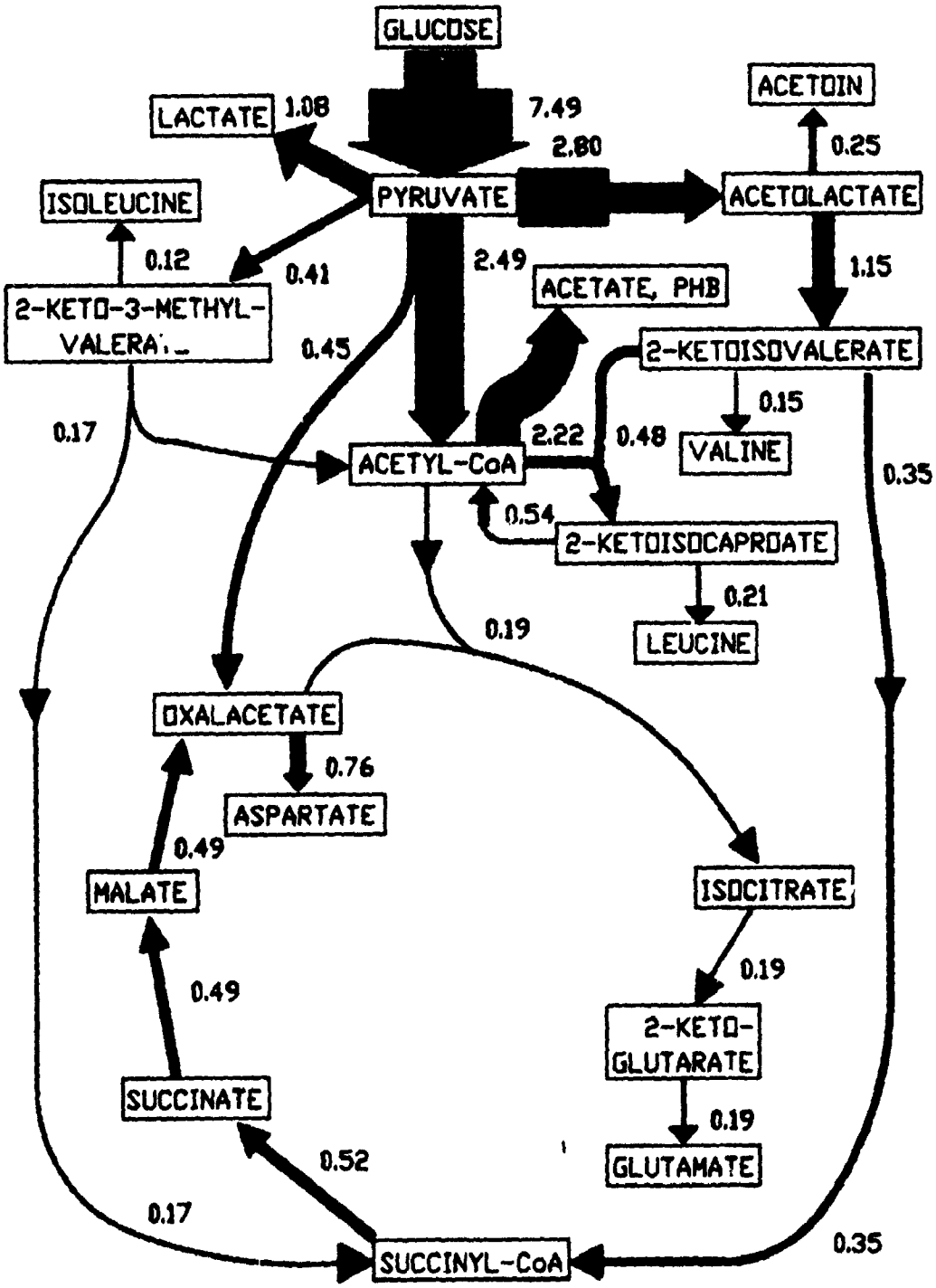

Fig. 8.11: Model solution for vegetative phase (4.5 hr) of Run 12. Flux in mmol/g VDM/hr proportional to line width.

8.3 Early Sporulation Phase Model Solution

Flux of α-keto-β-methylvalerate (αK3MV) through BCKA dehydrogenase for this case (ie. sample GR12X3; 6.5 hr) was calculated to be 0.187 mmol/g VDM/hr (Table 5.6). Thus dehydrogenation rates of aKIV and aKIC were calculated as follows (Sect.5.5; cf. App. B):

$$FT(V) = [FT(I) + SA(I)]*[FA(V)/FA(I)] - SA(V)$$
$$\approx (0.18700 + 0.03814)*(0.02296/0.002111)$$
$$\approx 2.449 \text{ mmol/g VDM/hr}$$
$$FT(L) = [FT(I) + SA(I)]*[FA(L)/FA(I)] - SA(L)$$
$$\approx (0.18700 + 0.03814)*(0.007412/0.002111) - 0.00583$$
$$\approx 0.785 \text{ mmol/g VDM/hr}$$

Substitution of these values into the metabolic model of Sect. 5.1 led to pyruvate balance at BMF equal to 0.4755. The system of metabolic flows which results (Fig. 8.12) is similar to that at 6.0 hr in Run 10 (Fig. 6.17). The present case exhibits somewhat greater flow rates in the central metabolic pathways of glycolysis, the glyoxylate cycle, valine and leucine pathways, and malic enzyme. This difference may reflect simply a more intense stage of transition - phase growth, ie. the middle rather than end of this unbalanced growth process (compare Fig. 8.1 with Fig. 6.1). This interpretation is supported by the dissolved oxygen profiles;

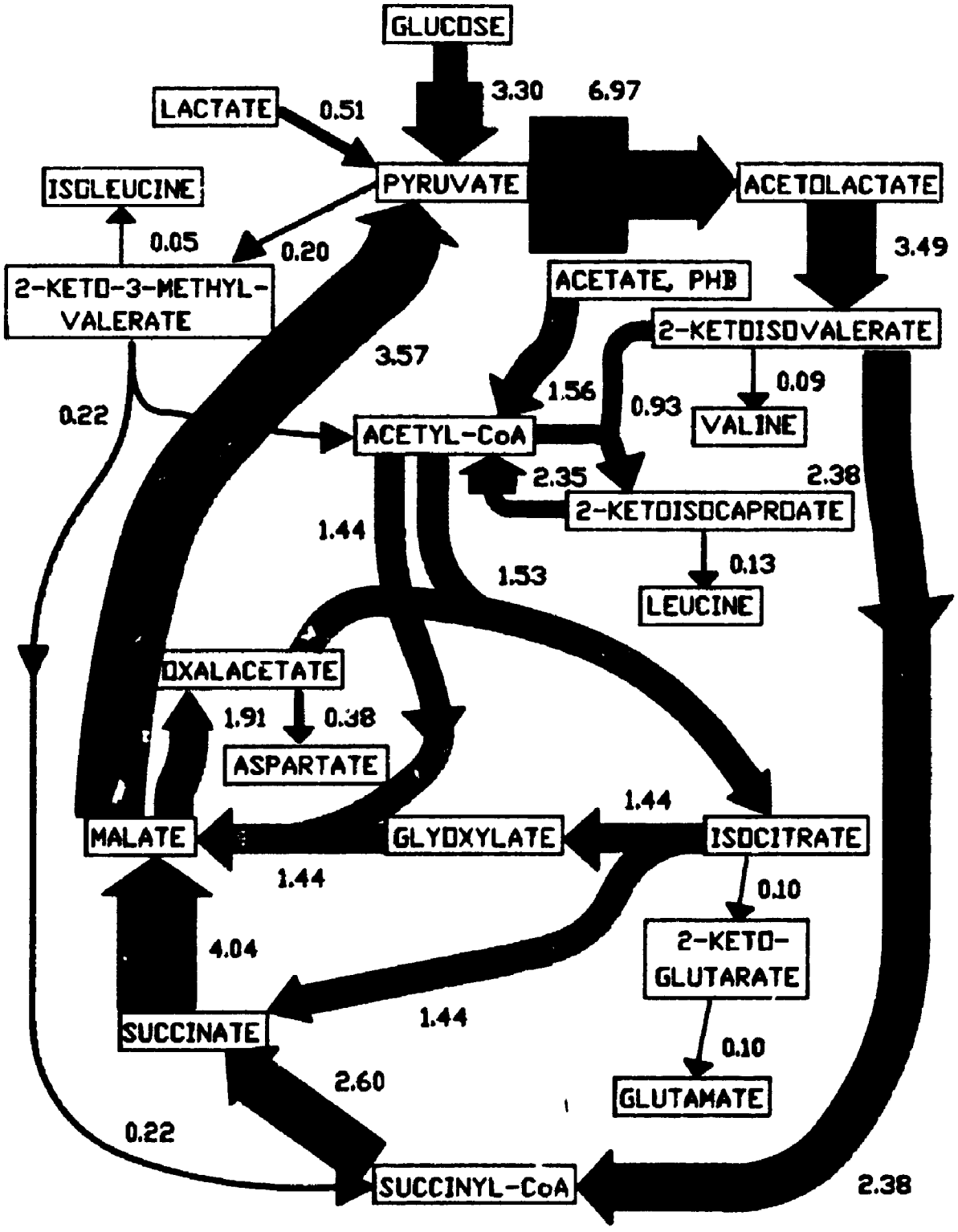

Fig. 8.12: Model solution for early sporulation phase (6.5 hr) of Run 12. Flux in mmol/g VDM/hr proportional to line width.

specifically minimum DO coincides with this sample in Run 12 (Fig. 8.3), but has already occurred in Run 10 (Fig. 6.3). Consumption of lactate, isobutyrate and isovalerate is also less advanced in the present case (compare Fig. 8.6 with Fig. 6.11; Fig. 8.9 versus Fig. 6.14).

9. Comparative Analysis and Synthesis of Results

9.1 Early Vegetative Growth Phase

Simultaneous use of carbohydrates and amino acids for both energy generation and biosynthesis appears to characterize vegetative growth in B. thuringiensis. Thus ammonia was excreted from 0 to 4 hr at essentially the same rate in each run (ie. about 5.2 mg/l/hr; Fig. 9.1), implying catabolism of at least certain amino acids. Those most strongly consumed in all fermentations were serine, alanine, aspartate, glutamate and leucine (App. D to F).

Early uptake of glucose and oxygen, and production of acidic intermediates varied amongst the fermentations. Thus 0 to 3 hr glucose uptake rates were 0.36, 0.71 and 0.29 g/l/hr in Run 10 to 12 respectively. Run 11 also had by far the greatest initial rates of broth acidification and oxygen consumption. Yet Run 11 produced only 6 per cent more biomass during this period than Run 10, demonstrating lower growth efficiency (based on glucose or oxygen) with increased carbohydrate to amino acid consumption ratio.

Major differences in early vegetative metabolism were observed between Run 11 and 12, performed "identically". These are presumed to arise from inocula in different metabolic states; and were reflected in higher zero - time concentrations of acetate and acetoin in Run 11, and significant

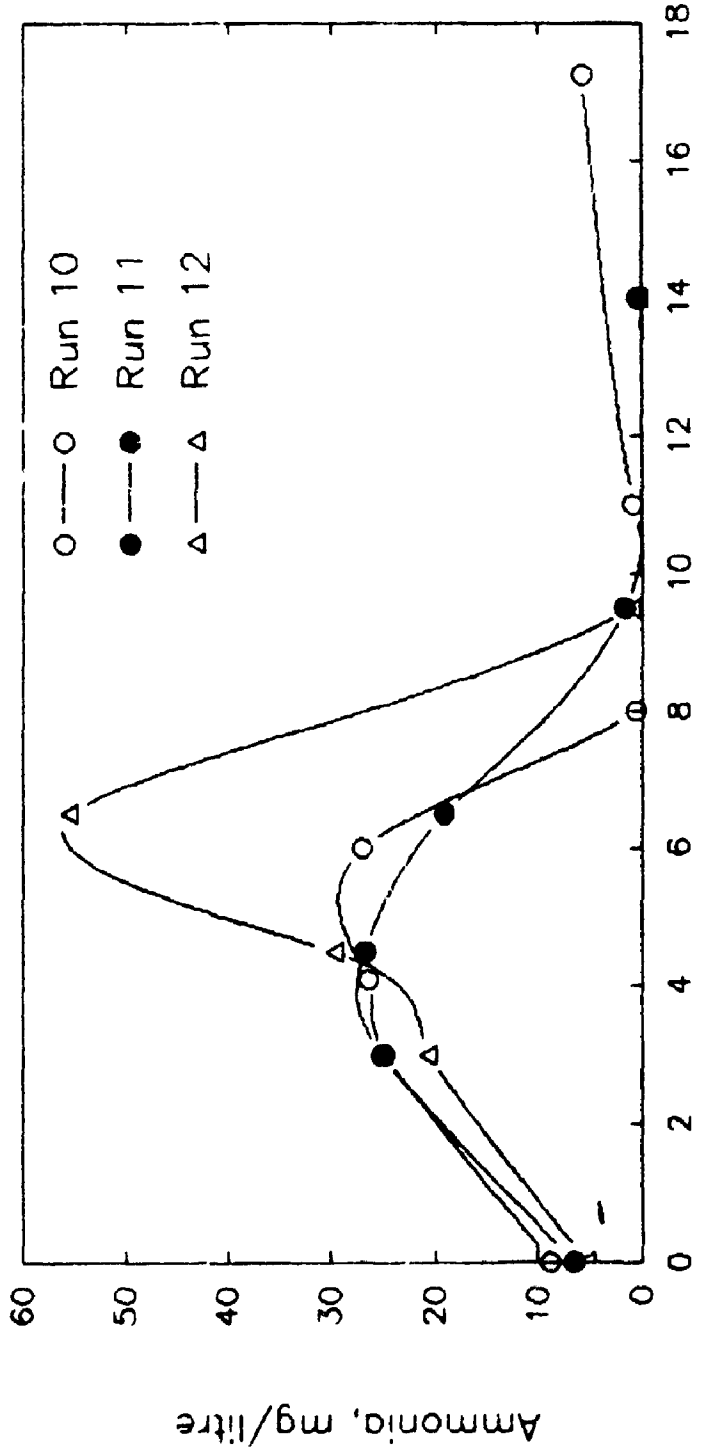

Fig. 9.1: Ammonia concentration vs. time in the three fermentations.

isobutyrate only in Run 12. After three hours of growth, cells in Run 11 contained about 14 per cent more fatty acids, but over eight times as much PHB as those of Run 12. Comparison of fatty acid composition at 3 hr (Table 9.1) reveals more anteiso and iso - even, and fewer iso - odd, fatty acids in Run 11. Thus it appears that isoleucine and valine pathways were more active early in Run 11, whereas the leucine pathway was relatively more important in Run 12.

Thus in many respects Run 11 appeared to be in the same stage which occurred only after 3 hours in the other fermentations (Sect. 9.2), showing relatively high rates of formation of iso - even (valine pathway) fatty acids, as well as PHB and a typical range of acidic intermediates. Thus during the first three hours of fermentation, Run 11 produced more acetate, lactate, pyruvate, α-keto-3-methylvalerate and α-ketoisovalerate (plus α-hydroxyisovalerate) than the other fermentations, especially Run 12.

9.2 Late Vegetative Growth Phase

After about three hours, each fermentation showed a pronounced increase in glucose uptake, and more or less severe restriction of oxygen uptake. At the same time consumption of several amino acids increased in Run 10 and 11. In Run 12, however, the same AA's ceased to be used (for about an hour), and broth acidification increased markedly.

Fermentation	Anteiso	Iso - odd	Iso - even
Run 10	25.8	26.6	25.8
Run 11	27.3	26.6	27.2
Run 12	22.1	29.2	25.3

Table 9.1: Early vegetative phase fatty acid pattern in the three fermentations.

This induction process resulted in greater synthesis of valine - related fatty acids in all fermentations, as can be seen in flow to fatty acid biosynthesis of each acyl-CoA relative to acetyl-CoA, plotted versus time for the three runs in Fig. 9.2 to 9.4. Between 4 and 6 hr flux of isobutyryl-CoA (IBCoA) to fatty acids relative to acetyl-CoA (AcCoA) increased to about 0.1 in each run. Thus flux of α-ketoisovalerate through branched - chain α-ketoacid dehydrogenase appears to have been somehow activated at about 3 hr in each fermentation.

Although oxygen consumption decreased at this time in all runs, the change was very pronounced in Run 11 (Fig. 7.3). As seen in Fig. 9.5, this fermentation also produced by far the most isobutyrate between 3 and 4 hr; and showed the least catabolism of isobutyryl-CoA (Fig. 7.11). One is led to conclude that oxygen consumption in this particular case is highly dependent on valine pathway catabolic activity, presumably due to the large number of reducing equivalents produced in same (Sect. 3.2).

Fig. 9.5 also shows that Run 12 had the lowest vegetative - phase rate of isobutyrate formation, which was accompanied by the highest rate of catabolism of α-ketoisovalerate to succinyl-CoA (Fig. 8.11). Thus it would appear that catabolic operation of the valine pathway somehow inhibits consumption of a number of amino acids (see above).

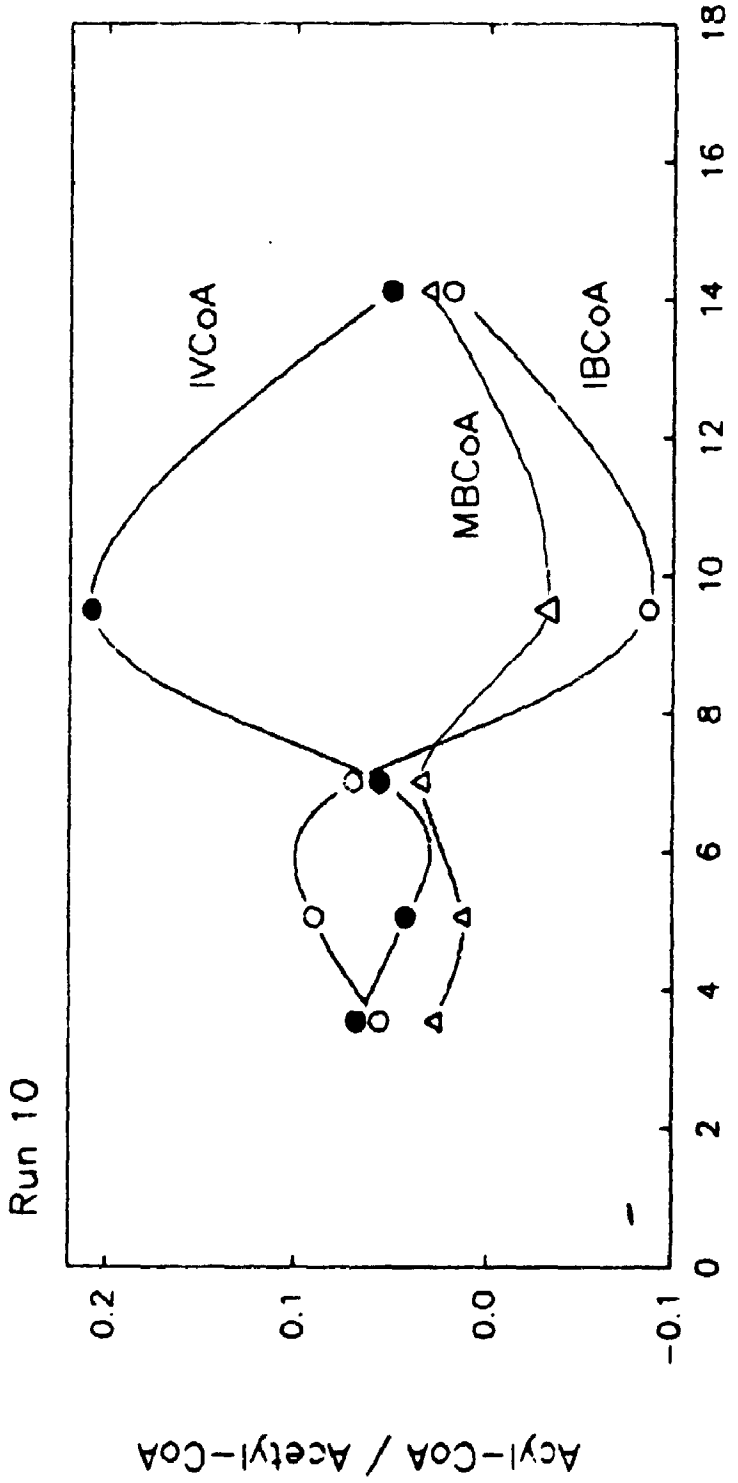

Fig. 9.2: Relative flux of co-enzyme A esters to fatty acid biosynthesis vs. time, Run 10.

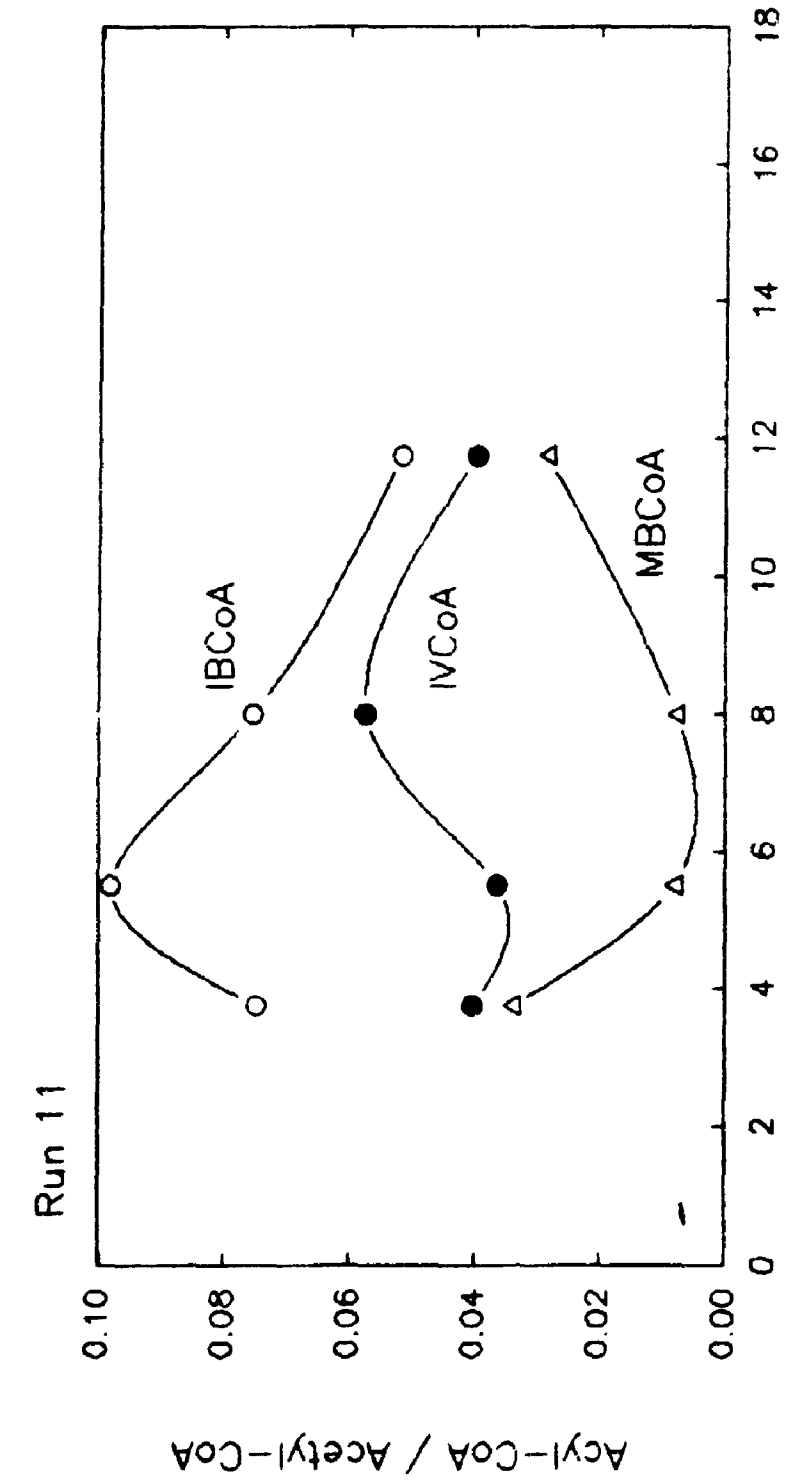

Fig. 9.3: Relative flux of co-enzyme A esters to fatty acid biosynthesis vs. time, Run 11.

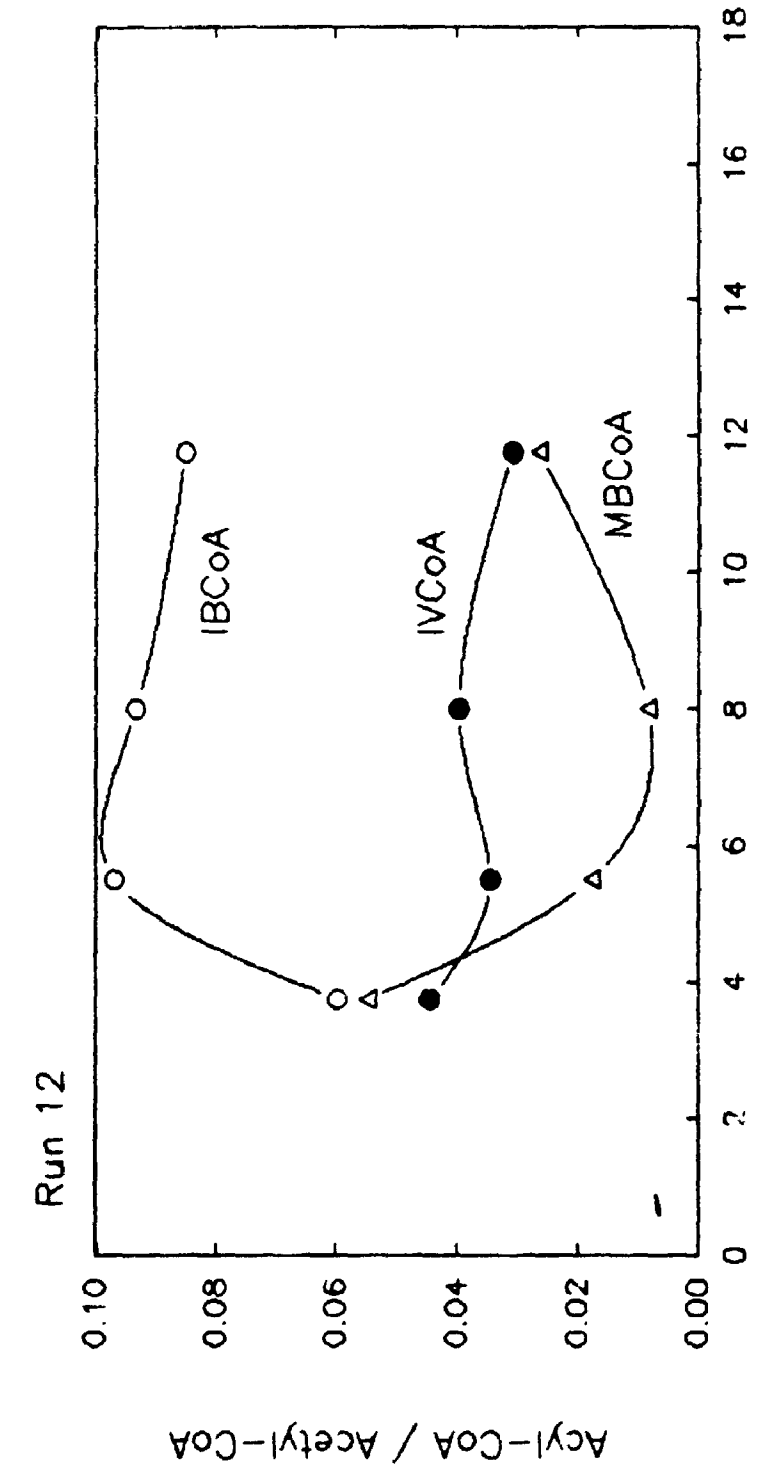

Fig. 9.4: Relative flux of co-enzyme A esters to fatty acid biosynthesis vs. time, Run 12.

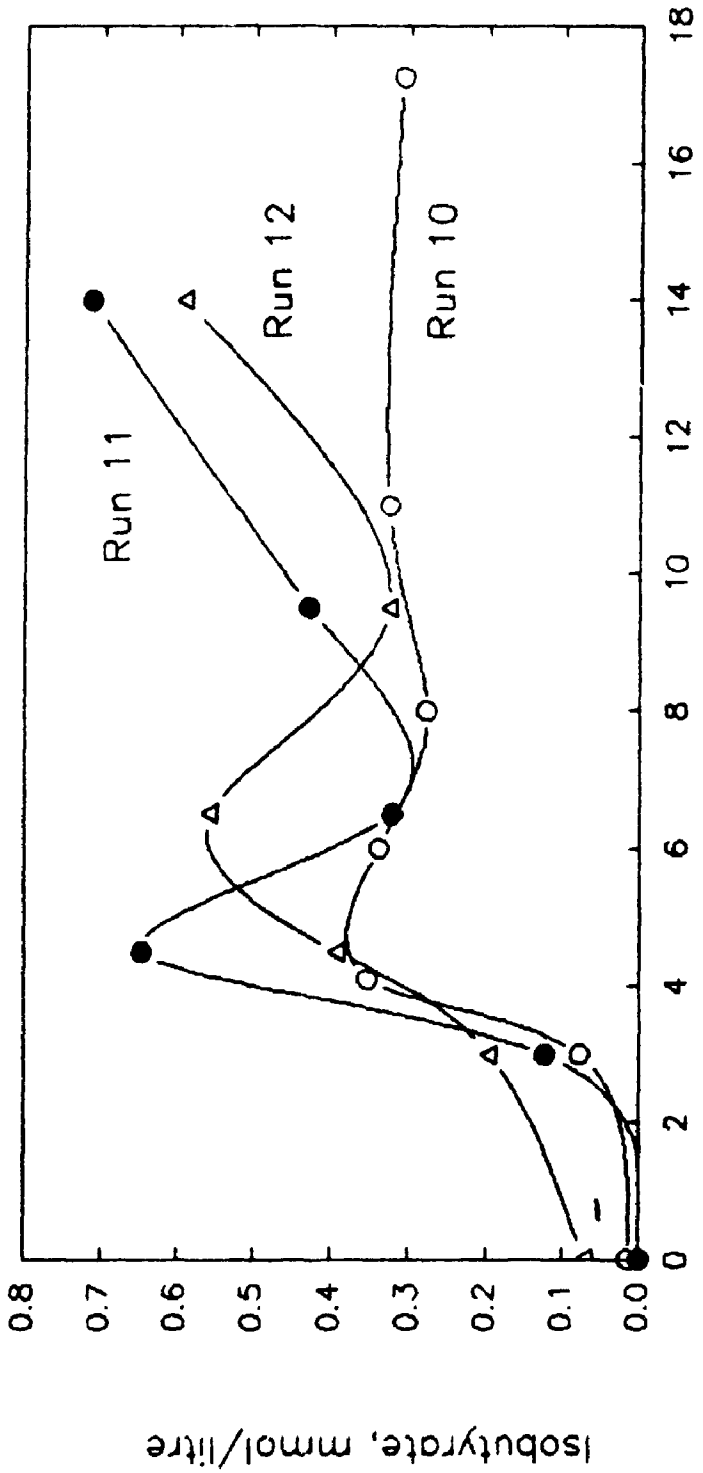

Fig. 9.5: Isobutyric acid concentration vs. time in the three fermentations.

In spite of these differences, between 3.0 and 4.1-4.5 hr all three fermentations reached very similar maximum specific growth rates (viz. 0.48 to 0.51 hr^{-1}). During the same period intra - cellular concentration of PHB and the major fatty acids increased as well. Formation of PHB and i-C16 fatty acid was especially strong in Run 11, anticipating events in the other fermentations.

This period also witnessed substantial release of acetoin, 2,3-butanediol, isobutyrate, isovalerate, 2-methyl-butyrate and the three α-keto acids, in addition to continuing formation of acetate, lactate and pyruvate.

9.3 Early Transition Phase

Between 4 and 5 hr all three fermentations reached t_0, defined by a decrease in growth rate, and the start of consumption of acidic intermediates (Sect. 2.1.2). The transition phase, as indicated by peak broth acetate concentration, began at about 4.0 hr in Run 10 and 11, and at about 4.5 hr in Run 12. Thus early transition - phase (ie. about 4.0 to 5.5 hr in Run 10 and 11; about 5.0 to 6.5 hr in Run 12) was characterized by rising pH, due to strong consumption of acetate and pyruvate, and rapidly decreasing dissolved oxygen concentration.

These phenomena have classically been associated with induction or activation of aconitase and other TCA cycle

enzymes (Sect. 2.4). That such activation does occur at this time is supported by the large early TCA cycle flows shown in Fig. 6.17 and Fig. 8.12. The same figures also show the importance of flux through the catabolic segment of the valine pathway during this stage. In fact, as Fig. 9.2 to 9.4 demonstrate, early transition phase was characterized in all fermentations by increasing flux of isobutyryl-CoA to fatty acids, relative to acetyl-CoA and the other two branched - chain acyl-CoA esters. Bulla *et al.* (1971) reported that production of carbon dioxide from pyruvate or acetate was markedly decreased if amino acids were available for catabolism (*cf.* below). Oxidation of succinate or glutamate was not so affected (*ibid.*). Anderson (1990) reported that lactate use also deterred consumption of acetate.

Acetate (and PHB) utilization has long been known to be greatly enhanced by good aeration (Vinter, 1969). Increased oxygen use may be due largely to demand for oxidation of NADH and $FADH_2$ produced in the valine catabolic pathway (*cf.* Sect. 9.2). Thus, "...the rate - limiting step in the electron transport system during sporulation [of *B. subtilis*] is not the concentration of cytochromes *per se*, but is in the activities of the NADH and succinate dehydrogenase." (Weber and Broadbent, 1975).

Biomass formation by *B. thuringiensis* during transition phase was found by Anderson (1990) to be strongly promoted by aeration. In spite of greater oxygen use, the rate of biomass

increase during this stage was slightly less than during vegetative growth.

A pronounced acceleration during this stage was observed in the uptake rate of most amino acids (viz. glutamate, alanine, valine, isoleucine, leucine, lysine, arginine, glycine, serine, tyrosine and phenylalanine). Significant catabolism of these, as evidenced by ammonia release, appeared to occur only in Run 12 (Fig. 9.1). Anderson (1990) also observed ammonia production during early transition phase growth on peptide - rich media. Given transition - phase increases in cellular content of glutamate, aspartate and serine of about 25 per cent (App. A), substantial accumulation of intracellular protein appears likely during this period.

Consumption of 2-methylbutyrate and a-C15 fatty acid began at the outset of this stage. These phenomena, and cessation of α-keto-3-methylvalerate release, imply activation of the catabolic segment of the isoleucine pathway, likely co-ordinately with the catabolic valine pathway (Sect. 3.2). In fact the onset of consumption of all three branched short - chain fatty acids in Run 10 and 11 implies co-ordinate induction/activation of the leucine catabolic pathway as well (cf. Fig. 6.17 and 8.12).

Small amounts of PHV continued to accumulate; however, although strong formation of PHB occurred in Run 10 and 12, this substance had already started to decline in Run 11. In this sense at least, the latter fermentation appeared to

already have advanced to the next metabolic regime (Sect. 9.4). Total cellular fatty acids content behaved similarly to PHB.

Maximum concentrations, or plateaus, for acetoin and 2,3-butanediol were observed during this stage.

Formation of intracellular granules is an obvious morphological characteristic of this stage in the B. cereus group (Hanson et al., 1963). The present results indicate that such structures are likely to be composed of some combination of poly-β-hydroxyalkanoates (eg. PHB, PHV), fatty acids and protein.

9.4 Late Transition Phase

During an approximately 30 minute period in each fermentation (viz. about 5.5 to 6.0 hr in Run 10 and 11; about 6.5 to 7.0 hr in Run 12) dissolved oxygen concentration rose rapidly, as pH continued to increase. During this short period certain changes occurred in all three fermentations, namely:

1) uptake of most amino acids essentially ceased;

2) ammonia uptake began;

3) pyruvate was exhausted from the medium;

4) flux of isobutyryl-CoA to fatty acid synthesis reached a maximum, as that to isovaleryl-CoA reached a minimum (2-methylbutyryl-CoA use was also low);

5) formation of PHV ceased.

These changes, in conjunction with decreased oxygen use, imply the occurrence of an induction process. Since flux of isovaleryl-CoA to fatty acids increased at this time in all runs, one is led to surmise that one or more enzymes of the leucine pathway are being expressed or activated. It appears that exhaustion of pyruvate and/or specific amino acids may trigger this event.

During the following two hour period (ie. about 6 to 8 hr in Run 10 and 11; about 7 to 9 hr in Run 12), dissolved oxygen, pH and biomass continued to rise. This is the final stage of net biomass formation with the exception of Run 11, wherein this process ceased by about 6 hr (Fig. 7.1). Although uptake of most amino acids has ended, such biomass increase may reflect continuing protein synthesis (Sect. 9.3), since ammonia is now being assimilated (Fig. 9.1). That transition - phase ammonia consumption is increased with better aeration (Anderson, 1990) supports this contention, ie. greater energy production would enhance energy - intensive protein synthesis. Further evidence of ongoing protein synthesis is the fact that some combination of phenylalanine, tyrosine, histidine and/or lysine was taken up during this stage of all fermentations.

Acetate use decreased during this stage, ending with completion of the forespore membrane (ie. at the end of stage III). Such consumption of isobutyrate, isovalerate and 2-methylbutyrate as occurred also ended at this time. Butanediol

was taken up during this stage; acetoin was released in Run 10, but consumed in the other fermentations.

In Run 10 and 12, PHB, lactate and the three branched - chain α-keto acids were consumed during this period. In contrast these had already been utilized (between 4.5 and 6.5 hr) in Run 11; and phenomena associated with spore maturation per se, such as release of isobutyrate (Sect. 9.5), were already underway. In fact by 8 hours flux of isovaleryl-CoA to fatty acids had already peaked in Run 11 and 12, preceding Run 10 in this regard by almost two hours.

9.5 Spore Maturation Phase

During the spore maturation phase (8+ hr in Run 10, 11; 9+ hr in Run 12, ie. after completion of the forespore membrane, ending stage III of sporulation), rates of viable biomass (VDM) decrease were 0.054, 0.022, and 0.053 hr^{-1} in Run 10 to 12 respectively. This biomass degradation or turnover process (Sect. 2.1.2) was accompanied in all fermentations by decreasing oxygen use, and release of isovalerate, isobutyrate and succinate. Although not measured in the present study, gamma-aminobutyric acid is reported to be strongly excreted during this phase (Aronson et al., 1975b).

In Run 10, leucine - related fatty acids accumulated in biomass until about 9.5 hr (Fig. 9.2); and total fatty acids rose at about 0.12 % of BDM /hr during the remainder of the

fermentation. In contrast total FA's rose only slightly in Run 11, and declined slightly in Run 12. This appears to be related to decreasing isovaleryl-CoA flux to fatty acid biosynthesis in these two fermentations (cf. Sect. 9.4). Furthermore, although isobutyryl-CoA flux to fatty acid biosynthesis decreased at least until about 10 hours in all runs, only in these latter two did 2-methylbutyryl-CoA flux relative to acetyl-CoA increase (Fig. 9.3, 9.4). Substantial isoleucine also may have been released late in Run 11 (App. E).

Between 8 and 11 hr in Run 10, PHB declined from 6.43 to 4.27 % of BDM, before rising again to 6.87 % of BDM at 17.25 hr. Run 11 PHB showed a slight rise and plateau, in parallel with its fatty acids. In Run 12 however, intense PHB use has just ended, declining from 6.91 to 4.27 % of BDM between 6.5 and 9.5 hr; thereafter vigorous formation resumes, yielding 6.45 % of BDM by 14 hours. Such PHB formation was not coupled to production of fatty acids, pyruvate and ammonia, as was observed in Run 10.

Broth pH decreased strongly in Run 10, mainly due to acetate accumulation, especially after 11 hours. Large pH changes did not occur in the other fermentations, although acetate continued to be consumed in Run 12. Excretion of succinate and isobutyrate appeared to be closely related. In Run 10 both were released from 8 to 11 hr; isobutyrate then gradually declined, as succinate was released more slowly. The

same acids were released in parallel in Run 11 (from about 7 hr) and Run 12 (from 9.5 hr); production of both was higher in the former fermentation.

During the final hours of each fermentation, release or consumption of acetate varied roughly inversely with that of isobutyrate. This may be due to exchange of coenzyme A (CoA) between isobutyryl-CoA and acetate, or acetyl-CoA and isobutyrate. It is also likely to reflect competition for carbon between the valine and leucine catabolic pathways, producing isobutyrate and acetate (via acetoacetate) respectively.

Acetoin, and lesser amounts of 2,3-butanediol, were completely consumed from 8 to 11 hr of Run 10, and by 14 hr in Run 12. Small amounts of both were released in Run 11.

Leucine, alanine, glycine, tyrosine, and smaller amounts of lysine and methionine appeared to be released throughout this stage of Run 10. Conversely Run 11 more likely consumed leucine, and released isoleucine as well as some lysine. These results tend to confirm those based on fatty acid analysis, namely that the leucine pathway was most active in Run 10 (at least until about 10 hr), and the isoleucine pathway was activated after 8 hours in Run 11 (and Run 12). There appeared to be no net amino acid exchange between Run 12 biomass and its environment after stage III of sporulation.

9.6 Synthesis of Results: Central Metabolism during Growth and Sporulation

The main hypothesis of the present work is that the pathways for synthesis and degradation of the three branched - chain amino acids (BCAA's) function as an integral part of metabolism throughout the cell cycle of bacilli. It appears plausible, furthermore, that the mechanisms which regulate activity in these pathways thus indirectly control central cellular metabolism. In the discussion below, Run 10 has been taken as representing a "normal" (ie. balanced, complex medium) fermentation; results from the other runs are used to substantiate selected assertions.

Early vegetative growth consumes glucose and amino acids, apparently as sources of carbon and energy. As shown in Table 9.1, 3 hr cells contain nearly equal amounts of anteiso, iso - odd and iso - even fatty acids. Fatty acid complement is known to be strongly medium - dependent (Sect. 3.3). High valine - related fatty acids early in Run 11 imply that these cells are metabolically more "advanqed" than those of Run 10, which forms substantial amounts of such acids only after an induction process starting at 3 hr. The reason for high leucine - related fatty acids early in Run 12 is not clear, but may be associated with catabolism of otherwise inhibitory concentrations of amino acids. High initial isobuyrate in this run would appear to result from inhibition of isobutyryl-CoA

oxidation during a period of high flux through α-ketoisovalerate (αKIV). One or more amino acids (eg. valine, leucine) may selectively inhibit the common acyl-CoA dehydrogenase.

The single branched - chain α-ketoacid (BCKA) dehydrogenase is constitutive in bacilli; furthermore it may well be identical with pyruvate dehydrogenase (Sect. 3.2). The latter enzyme is strongly affected by acetyl-CoA:CoA ratio in E. coli (Sect. 6.3.2). It thus appears possible that BCKA dehydrogenase of bacilli is multivalently controlled by the three acyl-CoA:CoA ratios. If the same enzyme is also responsible for conversion of pyruvate to acetyl-CoA, four separate activities could in principle be regulated by acetyl-CoA:CoA, and the three acyl-CoA:CoA ratios.

Induction of one or more enzyme systems, most probably α-acetohydroxyacid synthetase (viz. AHAS II, Sect. 3.1), occurs at about 3 hours. This can be surmised from simultaneous initiation of production of all three BCKA's (Fig. 6.15); and formation of acetoin (Fig. 6.13), which is associated with AHAS II (Sect. 3.1). Enzymes for PHB synthesis are also induced at this time (Fig. 6.9). These changes, which start an unbalanced growth process ultimately leading to sporulation (Sonenshein, 1989), occur 1.0 to 1.5 hours before t_0.

A major result of these changes is a greatly increased rate of dehydrogenation of αKIV. Since glucose uptake also increases at this time, one concludes that this additional substrate is channeled into the valine pathway. This cor-

roborates the earlier finding of simultaneously high glucose use and valine - related fatty acids production (Sect. 9.2).

Late vegetative growth marks the beginning of a granulation process in which PHB, PHV, fatty acids (especially i-C16), and protein accumulate within the cell. Thus are formed the lipid granules classically observed in bacilli (cf. Macrae and Wilkinson, 1958). That increased production of reducing equivalents by αKIV oxidation is associated with decreased oxygen use, and formation of reduced intracellular substances, implies that the electron transport chain was also altered in conjunction with AHAS II induction.

The extensive metabolic changes which occur after t_0 at about 4 hours appear to include the following:

1) activation of the catabolic segment of each BCAA pathway;

2) activation of citrate synthase and aconitase, ie. early TCA cycle enzymes;

3) activation of isocitrate lyase and malate synthase, ie. glyoxylate cycle enzymes;

4) activation of second - half TCA cycle enzymes from succinyl-CoA synthetase to malate dehydrogenase;

5) activation of malic enzyme;

6) inhibition of pyruvate dehydrogenase and pyruvate carboxylase.

That all three BCAA catabolic pathways are activated is seen in Fig. 6.14 and 6.15; and branched short - chain fatty and α-keto acids which had accumulated are largely consumed. As discussed in Sect. 6.3.2, catabolic flow through the valine pathway is known to inhibit pyruvate dehydrogenase activity by several mechanisms. The most potent of these is likely to be by deprivation of coenzyme A. Not counting the products (ie. succinyl-CoA and acetyl-CoA), valine is degraded via six CoA intermediates, isoleucine via seven, and leucine via four. Thus accumulation of variuous CoA esters, especially derived from valine and leucine here, can produce a high acetyl-CoA:CoA ratio by consuming CoA. Formation of acetyl-CoA from acetoacetate derived from αKIC catabolism also contributes to inhibition of pyruvate dehydrogenase activity.

Early transition phase is thus characterized by rapid consumption of acetate via acetyl-CoA and the glyoxylate cycle. Malate so produced flows via malic enzyme to pyruvate, activated by low CoA and ATP concentrations (Sect. 6.3.4). This carbon then enters valine and leucine biosynthetic pathways; active catabolic segments of these yield succinyl-CoA and acetyl-CoA. Thus are formed amphibolic cycles, capable of terminal oxidation of any intermediate, and strategically integrated with glycolysis, TCA cycle and glyoxylate cycle. This conclusion was presaged by Ohné (1975), describing the anomalous regulation of malate dehydrogenase (cf. Sect. 2.4): "...a drop in the energy charge will result in an increasing

proportion of malate being metabolized via malic enzyme to pyruvate." The present results dispel this anomaly by demonstrating the energetic rationalization for such control.

This metabolic stage is characterized by continued formation of reduced cell components, especially PHB and i-C16 fatty acid, as well as protein. Maximum oxygen use during the cell cycle also occurs at this time. Reducing equivalents arise mainly as follows:

1) catabolism of αKIV ($FADH_2$ and three NADH);
2) catabolism of αKIC ($FADH_2$ and one NADH);
3) succinate dehydrogenase ($FADH_2$);
4) malic enzyme (NADH);
5) glycolysis (NADH).

Thus it is clear why high flux through the valine catabolic pathway coincides with both granulation and high oxygen use.

At about 6 hours a transition begins in which more leucine - related fatty acids are formed relative to valine - related FA's (Fig. 9.2). This change corresponds to exhaustion of broth pyruvate, and near - depletion of most amino acids, either or both of which may be precipitating factors. One possible rationalization is the need to mainain intracellular leucine concentration to allow protein synthesis to continue, as observed in various types of vertebrate muscle (Goldberg and Tischler, 1981; Li and Odessey, 1986). Leucine pathway activation is sufficiently intense to markedly decrease oxygen uptake, apparently due to temporary inhibition of αKIV catabolism.

At about 7 hours, especially in Run 12 (Fig. 8.5), i-C16 fatty acids appear to be partially oxidized. This may be related to significant turnover of phosphatidyl- and diphosphatidylglycerol observed by Bulla and St. Julian (1972) during early sporulation of B. thuringiensis. Turnover of phosphatidylglycerol during sporulation has also been reported in B. cereus (Lang and Lundgren, 1970) and B. megaterium (Scandella and Kornberg, 1969).

Progressive switch - over from αKIV dehydrogenation to synthesis of αKIC persists throughout late transition phase (ie. about 6 to 8 hours). Oxygen consumption continues to decline in parallel with αKIV catabolism. Fatty acids and PHV are constant, and PHB is consumed during this stage; biomass increases presumably because of net protein synthesis, evidenced by ammonia uptake. This protein may be formed only for subsequent hydrolysis (Eliar et al., 1975), and/or subsequent processing into spore coat (Freese and Heinze, 1983). Branched - chain α-keto acids, consumed simultaneously with ammonia, may be transaminated for incorporation into protein.

The reason for decreased acetate uptake in late transition phase, which has baffled researchers for thirty years, is now apparent. Activation of the leucine catabolic pathway, about two hours after t_0, produces acetoacetatic acid which is converted to two molecules of acetyl-CoA. Oxidation of a certain amount of fatty acid also yields the latter intermedi-

ate. Thus exogenous acetate must compete with these new endogenous sources of acetyl-CoA.

At about 8 hours the forespore membrane is completed, and an intense process of biomass (especially protein) turnover begins. The rate of protein degradation in B. cereus is reported to be up to 8 per cent/hour (Sect. 2.1.2); biomass was consumed at over 5 per cent/hour in the present study. This process is likely iniatiated by decreased intracellular leucine concentration, although its mechanism is unknown (Li and Odessey, 1986). Exhaustion of broth ammonia, causing nitrogen limitation, would decrease leucine relative to α-ketoisocaproate (αKIC), and trigger massive protein degradation in the mother cell.

Another process which may be initiated at this time is formation of 3-phosphoglyceric acid, presumably from glyoxylate via the glycerate pathway (Sect. 6.4.2). Some catabolism of glutamate by way of gamma-aminobutyric acid (GABA) may also begin (Fig. 6.18).

The entire phase of spore maturation is characterized by release of leucine and isovalerate. Controlled release of the former is apparently used to maintain αKIC concentration relative to leucine such as to favour protein degradation in the mother cell. High intracellular leucine may also serve to inhibit pyruvate decarboxylation, as in muscle (Goldberg and Tischler, 1981). Dehydrogenation rate of αKIC appears to be controlled by isovaleryl-CoA:CoA ratio, which is modulated by

excretion of isovalerate. Interestingly BCKA dehydrogenase from various mammalian sources is inhibited by isovaleryl-CoA (Randle *et al.*, 1981). These suppositions are of necessity highly speculative.

During early spore maturation (*ie.* stage IV, 8 to 11 hr) succinic acid is released; the most likely cause is the continuing shift from catabolism of αKIV to αKIC (Fig. 9.2), as follows:

1) αKIV catabolism produces succinyl-CoA;

2) catabolism of αKIC produces acetoacetate;

3) CoA transfer from the former to the latter, yielding succinate and acetoacetyl-CoA, is effected by 3-ketoacid CoA transferase (Lehninger, 1976, p.554);

4) thus increased flux through acetoacetate requires greater production of succinate;

5) succinate, in excess of that which can be oxidized by succinate dehydrogenase, is excreted.

Two other sources of succinate are possible, namely: formation via GABA from glutamate; and formation by isocitrate lyase. The latter enzyme increases in activity during later sporulation, both absolutely and relative to malate synthase (Aronson *et al.*, 1975a), presumably associated with synthesis of 3-phosphoglycerate from glyoxylate (Sect. 6.4.2).

During this stage (*cf.* Fig. 6.18), production of fatty acids, especially i-C15, resumes (Fig. 6.9, 6.10). PHB,

acetoin and 2,3-butanediol are consumed (Fig. 6.9, 6.13 respectively), presumably via acetyl-CoA.

A final transition occurs at about 11 hours (ie. end of stage IV), as αKIV is again channeled away from αKIC synthesis, and toward catabolism (Fig. 9.2). Thus formation of i-C16 fatty acid resumes, such that it accumulates at the same rate as the i-C15 acid (Fig. 6.10).

In late sporulation phase leucine, isovalerate, and i-C15 fatty acid continue to be formed at roughly similar rates as before. This reflects ongoing flux through the leucine catabolic pathway; continued protein turnover is indicated by renewed excretion of ammonia (Fig. 9.1). Increased dehydrogenation of αKIV yields i-C16 fatty acid, and consumes a small amount of isobutyrate (Fig. 6.14). Valine and leucine pathway flows thus become "balanced" in terms of fatty acid production; this balance is reflected in gradual cessation of succinate release (Fig. 6.12).

Formation of PHB (Fig. 6.9) and acetate (Fig. 6.11) resumes during this stage, presumably as a result of leucine catabolic pathway activity. PHB would thus function as an electron sink for excess reducing equivalents produced by increased valine pathway activity. Renewed excretion of pyruvate (Fig. 6.12) implies continued operation of malic enzyme; in fact Aronson et al. (1975a) reported a large increase in activity of this enzyme in late sporulation. It thus appears that residual excess carbon is utilized in a

terminal oxidative cycle based on the valine pathway, and driven by malic enzyme.

9.7 Discussion of Major Implications

Although metabolism of bacilli during growth and sporulation has received intense study for over thirty years (Sect. 2), major aspects of central metabolism remain unresolved. Thus, "...there is little or no information available at present as to the mechanism regulating metabolism of carbon, nitrogen, or phosphorus compounds in Bacillus spp. or any other gram - positive organism..."(Sonenshein, 1985). Fundamentals, such as the mechanism of catabolite repression (ibid.), and even the direction of flow of half the tricarboxylic acid (TCA) cycle (Sonenshein, 1989), are unresolved. Thus the present tentative conclusions may have far - reaching implications for understanding of metabolism in bacilli.

Although only a single strain of Bacillus thuringiensis was studied experimentally, the findings in general are likely relevant to all members of the genus Bacillus, due to their obligatory dependence on branched - chain amino acid metabolism for lipid formation (Kaneda, 1977). However variations on the mechanisms described herein are to be expected given interspecies differences. Thus B. subtilis and B. megaterium, unlike the B. cereus group, are strict aerobes (Bergey's, 1974). Such differences will be reflected in the details of

metabolism of a particular organism, including use of the three BCAA pathways relative to each other. It is not entirely surprising, therefore, that unlike the B. cereus group, all other bacilli studied by Kaneda contained more a-C15 than i-C15 fatty acid.

The most general finding has been that the three branched - chain amino acid (BCAA) pathways function as complete amphibolic units throughout the cell cycle. This observation, from which arise numerous implications, has apparently not been previously made. The significance of this putative fact derives from the strategic placement of substrates and products of the BCAA pathways. Specifically, pyruvate is the direct product of glycolysis, and a key metabolic intermediate. The other true substrate, α-ketobutyrate, has been proposed as an "alarmone", ie. a metabolic activator of stress response (Daniel et al., 1983). The two products, acetyl-CoA and succinyl-CoA, occupy strategic locations at the top and bottom respectively of the TCA cycle; the former also mediates between pyruvate and the TCA cycle. It is not surprising to find, therefore, that the BCAA pathways operate in conjunction with glycolysis, and TCA and glyoxylate cycles.

Furthermore it appears quite likely that operation of the BCAA pathways at least partially regulates certain key enzyme activities and intermediate concentrations. For example, flux through the valine catabolic pathway regulates pyruvate dehydrogenase activity, apparently by a number of mechanisms

(Sect. 6.3.2). Since catabolism of leucine can readily produce acetyl-CoA, it appears that BCAA metabolism can regulate, at least partially, availability of acetyl-CoA (see below).

Another general conclusion is that the three BCAA pathways, in conjunction with malic enzyme and several TCA cycle enzymes, comprise potential cycles for terminal oxidation of metabolic intermediates. The TCA cycle appears to be the only presently known terminal oxidative cycle of significance to cellular metabolism (Weitzman, 1981). If the present thesis proves substantially true, our understanding of the energetics of intermediary metabolism will be fundamentally altered.

Thus completion of at least one amphibolic cycle by activation of one or more BCAA pathways appears to be essential to the success of sporulation in bacilli. This conclusion is consistent with observations of Scandella and Kornberg (1969) that, although addition of isoleucine or valine to the medium did not affect growth of B. megaterium, it delayed sporulation, and reduced its success. A similar phenomenon was found in a B. subtilis mutant auxotrophic for branched fatty acid primers (Boudreaux and Freese, 1981). Although growth rate and biomass formed were equivalent at initial isobutyrate concentrations of 50 or 100 μM, spore titre by t_{18} was 200 times higher in the latter case.

Compulsory utilization of a BCAA oxidative cycle also appears to rationalize observations arising from induction of

sporulation by blockage of GTP synthesis in the presence of glucose. Under such conditions, induction of early TCA cycle enzymes is unnecessary since glucose can be metabolized via, for example, the valine pathway. This interpretation appears more consonant with the facts (viz. lactate consumption, strong oxygen demand) than does substrate - level ATP formation by glycolysis, as proposed by Sonenshein (1989).

Following are the major apparent implications of the present study for metabolism in the B. cereus group of organisms, viewed particularly from a developmental perspective. In other words the discussion which follows will focus on implications for the metabolic basis of differentiation, especially sporulation.

Activation of the valine biosynthetic pathway, which occurs 1.0 to 1.5 hours before t_0, appears to be the initial metabolic event in the unbalanced growth process leading normally to sporulation (Sonenshein, 1989). Induction of "pH 6 acetolactate synthetase" (AHAS II, Sect. 3.1), and possibly other "non - biosynthetic" enzymes of valine/isoleucine biosynthesis, is the probable cause of such activation. Valine formation would be favoured over that of isoleucine by inhibition of threonine deaminase (ibid.).

The panoply of changes which start at t_0 appear to result from expression of the spo0H gene: "The product of the spo0H gene, σ^H..., is necessary for the transcription of many genes that become expressed during the transition from growth to

stationary phase...In fact, most of the genes known to be expressed in stationary phase depend directly or indirectly on σ^H..." (Sonenshein, 1989). Enzymes normally expressed at this time include those of the TCA cycle (except apparently α-ketoglutarate dehydrogenase), glyoxylate cycle, and malic enzyme. The present work shows that enzymes of the BCAA catabolic pathways are also activated at this time.

The discussion in Sonenshein (1989) makes it clear that the relationship of expression and regulation of TCA cycle enzymes to sporulation is not well understood (cf. Sect. 1.2, 2.1.2). Furthermore it is well - known that the TCA cycle is not unitary under all conditions (Sect. 2.4). Specifically, it operates in certain facultative anaerobes as a branched non - cyclic pathway (from oxalacetate) to meet biosynthetic demands for α-ketoglutarate and succinyl-CoA (cf. Weitzman, 1981). This has led to the hypothesis that, during vegetative growth of bacilli on certain media, as well as during sporulation, flux in the dicarboxylic acid segment of the TCA is reversed, ie. succinyl-CoA is made from oxalacetate (Ohné, 1975; Sonenshein, 1989). In any case it is clear that first - and second - half TCA cycle enzymes are independently regulated. Thus, "...induction of citB [coding for aconitase] is independent of the products of spo0A, spo0B, and spo0H"; whereas the sigma factor produced by spo0H (viz. σ^H) is necessary for expression of citG, coding for fumarase (ibid.).

Examination of fumarase expression shows the relevance of activation of BCAA catabolism to sporulation. Thus, "The gene for fumarase (citG) is...induced from a very low basal level when cells exhaust a nutrient broth medium...However, citG is derepressed during exponential growth in minimal - glucose - Casamino Acids medium..." (ibid.). It is this type of amino acids - rich medium in which the catabolic valine pathway showed high activity during vegetative growth (ie. Run 11, 12; Sect. 9.1, 9.2). Since the product of this pathway, succinyl-CoA, would require fumarase for its further metabolism, it is logical that these activities be expressed simultaneously. This also provides indirect evidence that the activation of BCAA catabolism which normally occurs at t_0 is dependent on σ^H (or possibly vice - versa). Thus, "...intracellular concentration of σ^H is low during growth in nutrient broth and increases in stationary phase; in minimal - glucose [Casamino Acids] medium a high level of σ^H is present all the time." (Sonenshein, 1989).

To conclude discussion of the metabolic transition which occurs in bacilli at t_0, it appears probable that these changes are driven in a metabolic sense by activation of isobutyryl-CoA catabolism. This interpretation seems to be fully compatible with other metabolic phenomena occurring under the same conditions, especially induction of glyoxylate cycle enzymes and malic enzyme (Sect. 6.3). Conversely, the current hypothesis of reversed flow in the dicarboxylate

segment of the TCA cycle seems much less plausible as an explanation of the totality of events.

About two hours after t_0, activation of the leucine pathway occurs, ie. production of isovaleryl-CoA and derived fatty acids increases (Sect. 9.4). During the following two hours, intracellular protein appears to accumulate in the absence of cell division. This bears a striking similarity to findings regarding effects of leucine on protein metabolism in muscle (Goldberg and Tischler, 1981; Li and Odessey, 1986). As the latter authors state, "The evidence to date has established that leucine (or its metabolites) have a specific anabolic effect on the processes of protein synthesis and degradation in muscle." This phenomenon appears not to have been studied in procaryotes.

Endogenous protein turnover is apparently obligatory for spore maturation processes after completion of the forespore membrane (Sect. 2.1.2). This event was found to be temporally associated with increasing flux through the entire leucine pathway; and probable deficiency of leucine relative to α-ketoisocaproate (αKIC; Sect. 9.5, 9.6). As mentioned above, clinical cytologists have reported these substances to strongly affect protein metabolism. Thus in muscle, leucine stimulates protein synthesis, and reduces protein breakdown; αKIC does only the latter (Goldberg and Tischler, 1981). In adipose tissue, leucine stimulates BCAA oxidation, a process inhibited by αKIC (Goodman and Frick, 1986). It therefore

appears probable that the ratio of leucine to αKIC controls the balance between protein synthesis and degradation. In any case it is likely that modulation of the leucine pathway is causatively associated with protein turnover during spore maturation.

Metabolism after completion of spore cortex is characterized by balanced operation of the leucine and valine pathways, at least in terms of fatty acid production. This can be interpreted in terms of simultaneous consumption of mother - cell protein and fatty acids. In liver cells, β - oxidation of fatty acids is inhibited by catabolism of αKIC by mechanisms not yet well understood (Williamson et al., 1986). If such an effect occurs in Bacillus, shifting carbon flux away from the leucine pathway would permit oxidation of fatty acids derived from degradation of mother - cell lipids. Thus concurrent, balanced operation of leucine and valine catabolic pathways would allow the cell to scavenge both protein and fatty acids. This ultimate turnover process appears to derive energy almost exclusively from substrate - level phosphorylation; and to be driven to completion by high malic enzyme activity (Sect. 9.6).

Although spore germination and outgrowth were not studied experimentally, the present findings may also have implications for this differentiation process.

Protein breakdown is very important for spore outgrowth, especially energetically: "Approximately 15 - 20 % of the

total protein in spores of B. cereus, B. megaterium and C. fermentans is degraded to free amino acids in the first 20 min of germination. In B. megaterium approximately one half of the free amino acids produced in this process are susequently metabolized, predominantly via oxidative reactions." (Setlow, 1983). It is thus no surprise that i-C13 is by far the predominant fatty acid formed during the first 30 minutes after germination of B. thuringiensis spores; the only other fatty acids formed are i-C16 and i-C14 (Bulla et al., 1975). Similarly Scandella and Kornberg (1969) reported that branched C15 (likely i-C15) fatty acid predominated during the first hour of outgrowth of B. megaterium spores. In other words, leucine pathway activity is again associated with protein breakdown; smaller valine pathway flux likely reflects oxidation of fatty acids derived from early membrane degradation (Foster and Johnstone, 1989). This interpretation is especially relevant to cellular energetics, since there is no TCA cycle activity as such during the first hour after germination (Setlow, 1975). As this author states, "The exact pathway(s) for energy metabolism during germination after the utilization of PGA...remains unclear ...". PGA (3-phosphoglyceric acid) is consumed as an energy and phophorus source in the first minutes of germination, by metabolic pathways which produce neither pyruvate nor lactate, but rather large amounts of acetate (Setlow, 1983). This can also be understood in terms of predominant operation of the leucine pathway.

10. Conclusions and Recommendations

10.1 Conclusions

Given the large number of steps in the procedure for model solution, it is to be expected that the specific flow rates calculated will be subject to considerable uncertainty (see Appendix H). Specifically it is estimated that these values may be in error by up to about 75 per cent. Nevertheless the general consistency and coherence of the results, and the degree to which they agree with the relevant literature, provide considerable reassurance as to their validity and the conclusions derived therefrom.

Thus, based on the findings of the present work, the following conclusions regarding central metabolism in *Bacillus thuringiensis* appear to be warranted:

1) the three branched - chain amino acid (*ie.* valine, leucine and isoleucine) pathways function to some extent as complete amphibolic units throughout the cell cycle; in other words, isobutyryl-, isovaleryl- and 2-methylbutyryl-CoA are simultaneously formed and dehydrogenated;

2) these pathways are functionally integrated with the major pathways of central metabolism, namely glycolysis, and the tricarboxylic acid (TCA) and glyoxylate cycles;

3) these pathways, in conjunction with malic enzyme and certain TCA cycle enzymes, constitute potential cycles

for interconversion and/or terminal oxidation of metabolic intermediates;

4) activation of the valine biosynthetic pathway, which occurs 1.0 to 1.5 hours before t_0, is a key metabolic event associated with initiation of the unbalanced growth process normally leading to sporulation;

5) greatly increased catabolism of isobutyryl-CoA, and to a lesser extent isovaleryl-CoA, at t_0 leads to other metabolic changes characteristic of sporulation, such as induction of malic enzyme and glyoxylate cycle enzymes;

6) during stages III and IV of sporulation, increased leucine pathway flux, at least relative to that of the valine pathway, is associated with an intense process of protein turnover (ie. simultaneous synthesis and degradation), which is essential to spore formation;

7) beginning about stage IV, there is an increase in catabolism of α-ketoisovalerate, at least relative to its use for synthesis of α-ketoisocaproate; thus the catabolic segments of valine and leucine pathways function in tandem, apparently responding to a unitary control mechanism.

10.2 Recommendations for Future Work

The results and conclusions of the present study leave several questions at best partially answered, and pose a

number of new ones. These areas in which more work is felt to be necessary or potentially rewarding are described below.

10.2.1 Verification of Model Results

The following work would reduce the error in the present model; and subject model results to critical tests for verification and/or modification:

1) develop HPLC methodology for separation and more precise quantitation of the non-volatile, especially 2-keto, acids found in *B. thuringiensis* fermentation broths;

2) perform positive identification of poly-β-hydroxy-valerate; and identify certain minor components present in broth and biomass samples (*cf.* Sect. 4.4.7, 4.4.8);

3) use split - medium and split - inoculum methods to achieve reproducible fermentation results;

4) employ more frequent sampling to minimize errors due to interpolation between data points;

5) measure the specificity, if any, towards the three branched - chain acyl-CoA esters of the initial step of fatty acid synthesis in bacilli, *ie.* the reaction catalyzed by acyl-CoA:acyl carrier protein transacylase (Sect. 5.5);

6) measure the kinetic behaviour of CoA - ester intermediates of the catabolic segments of the three BCAA

pathways, especially to corroborate their activation at t_0; this would also probably shed light on metabolic control of these pathways, and their control of other enzyme reactions.

10.2.2. Fermentation Optimization and Control

The following suggestions might enhance our ability to rationally engineer this fermentation through control of environmental conditions:

1) an "acid release ratio", defined as the specific rate of release of short - chain fatty acid divided by the specific rate of incorporation of the corresponding CoA ester into cellular fatty acids, can be calculated for each of acetate, isobutyrate, isovalerate and 2-methyl-butyrate; this ratio appears to vary inversely with the overall rate of consumption (cf. catabolism) of these esters; in combination with the "transamination ratio" described below, this may allow preemptive control of variables such as nutrient addition rate;

2) a "transamination ratio", defined as the specific rate of release of 2-keto (cf. possibly 2-hydroxy) acid, divided by the specific rate of consumption of the corresponding amino acid minus the specific rate of 2-keto acid release, appears to represent a metabolic

control parameter of significant theoretical and possibly practical interest;

3) the observation that poly-β-hydroxybutyrate is formed late in the B. thuringiensis fermentation, in apparent contrast to B. cereus, may allow sufficient insight into the energetics and stoichiometry of δ-endotoxin formation to increase same in practice.

10.2.3 Extension to Other Bacilli

The methodology developed herein appears to be applicable to any member of the genus Bacillus. Furthermore the present results and conclusions, to the extent that they are valid, are expected to be of general relevance to such species. Some specific avenues of investigation which appear to be of interest are as follows:

1) it is very interesting that the magnitude of branched - chain 2-keto acid accumulation under anaerobic conditions was always in the order isoleucine pathway > valine pathway > leucine pathway, since this is the same order as the number of NADH reducing equivalents produced; several questions arise from this observation, amongst others: does this BCKA release order hold for all bacilli? Do strictly aerobic bacilli therefore rely more on the isoleucine pathway? Is there a correlation between

the expression/control of α-ketoglutarate dehydrogenase, and valine versus isoleucine pathway activity?

2) does the specificity of the fatty acid synthetase complex vary within this genus, as concluded by Kaneda (1977)?

10.2.4 Sporulation in Bacilli

The following questions regarding the mechanisms of phenomena associated with sporulation of bacilli appear worthy of study:

1) results of the present study imply a direct relationship between glycolytic flux and valine pathway catabolic activity, once the latter has been induced; if this is in fact true, by what mechanism does this occur?

2) there appears to be a relationship between expression of the valine catabolic pathway and the sporulation - associated sigma factor (ie. σ^H; cf. fumarase; see Sect. 9.7); what is the genetic and/or metabolic basis, if any, of such a relationship?

3) the results obtained appear to be incompatible with operation of the latter half of the TCA cycle in the reverse direction (cf. Sonenshein, 1989); furthermore it is not clear to what extent the "reductive TCA cycle" operates even in E. coli, the organism in which it was

initially reported (cf. Courtright and Henning, 1970); what, therefore, is its role, if any, in bacilli?

4) what is the mechanism of the relationship between protein turnover and leucine/2-ketoisocaproate catabolism which is observed in certain mammalian cells, and apparently also in B. thuringiensis (see Sect. 9.7)?

10.2.5 Relationship to Mammalian Cellular Metabolism

A number of apparent similarities between metabolism in certain mammalian cells and B. thuringiensis (or bacilli) have been noted in the text (cf. Sect. 6.4, 9.7), and in the literature (cf. Weitzman, 1981). Two general questions arise from these observations, namely:

1) to what extent are metabolic regulatory mechanisms involving the branched - chain amino acids and/or their metabolites identical in the two cell types?

2) what are the implications for metabolic evolution of these similarities?

APPENDIX A

Results of Biomass Amino Acid Analyses

BIOMASS SAMPLE	mmoles / g BDM							
	ASP+ASN	THR	SER	GLU+GLN	GLY	ALA	VAL	MET
Vegetative Cells	0.1727 0.1963	0.0984 0.1150	0.0875 0.0976	0.2942 0.3268	0.1565 0.1725	0.2370 0.2570	0.1091 0.1319	0.0749 0.0771
Early Sporulation	0.2397 0.2255	0.1311 0.1169	0.1230 0.1094	0.3974 0.3774	0.1690 0.1657	0.2751 0.2650	0.1307 0.1554	0.0815 0.0775
Spores and Crystals	0.1823 0.1900	0.0842 0.1099	0.1148 0.1093	0.2127 0.2266	0.1481 0.1489	0.1649 0.1667	0.0566 0.1215	0.0336 0.0340

Table A.1: Amino acid composition of biomass at three points in growth cycle: aspartate to methionine.

BIOMASS SAMPLE	mmoles / g BDM						
	ILE	LEU	TYR	PHE	HIS	LYS	ARG
Vegetative Cells	0.0786 0.1013	0.2557 0.2750	0.1026 0.1108	0.0739 0.0715	0.0336 0.0377	0.1541 0.1708	0.0751 0.0842
Early Sporulation	0.1004 0.1233	0.2834 0.2470	0.1060 0.0798	0.0848 0.0736	0.0352 0.0387	0.1644 0.1718	0.0846 0.0846
Spores and Crystals	0.0399 0.0908	0.1455 0.1625	0.0669 0.0586	0.0728 0.0666	0.0318 0.0319	0.0818 0.0872	0.0606 0.0691

Table A.2: Amino acid composition of biomass at three points in growth cycle: isoleucine to arginine.

APPENDIX B

Summary of Data re Branched - chain Amino Acid Pathway Flux Calculations

Flux, mmol/g VDM/hr	GR10X1	GR10X3	GR10X5	GR11X1	GR11X3	GR12X1	GR12X3
ISOLEUCINE	-0.1697	-0.0051	-0.0154	-0.0555	0.0014	-0.0398	0.0054
2-keto-3-methylvalerate	0.2109	0.1942	-0.0067	0.0838	0.1696	0.2468	0.1513
2-methylbutyrate	0.0162	-0.0034	-0.0023	-0.0037	-0.0033	0.0130	0.0303
Net pathway release	0.0574	0.1857	-0.0244	0.0247	0.1677	0.2200	0.1870
LEUCINE	0.0165	0.0074	-0.0124	0.0121	-0.0021	-0.1577	0.0341
2-ketoisocaproate	-0.0420	0.0006	0.0014	-0.0112	-0.0006	-0.0032	-0.0435
isovalerate	0.0035	0.0221	0.0007	-0.0110	-0.0044	0.0310	0.0448
Net pathway release	-0.0221	0.0300	-0.0103	-0.0100	-0.0072	-0.1299	0.0354
VALINE	-0.0784	0.0345	-0.0030	0.0051	0.0273	-0.0774	0.0253
2-KIV + 2-OHIV	-0.0911	0.0166	0.0074	-0.0377	0.0274	0.1054	-0.0195
isobutyrate	0.0127	0.0359	-0.0250	-0.0524	0.0132	0.0602	0.1064
Net pathway release	-0.1567	0.0870	-0.0206	-0.0849	0.0679	0.0882	0.1122

Table B.1: Balances on branched - chain amino acid pathways for three fermentations.

SAMPLE	Coenzyme A Flux to Fatty Acid Synthesis, mmol/g VDM/hr			
	Acetyl-CoA	Isobutyryl-CoA	Isovaleryl-CoA	2-Methylbutyryl-CoA
Run 10				
4.1 hr	0.33530	0.02569	0.01990	0.00730
6.0 hr	0.20690	0.01954	0.00812	0.00280
11.0 hr	0.02534	0.00133	0.00231	-0.00087
Run 11				
4.5 hr	0.26930	0.02209	0.01049	0.00715
9.5 hr	0.02491	0.00100	0.00199	0.00081
Run 12				
4.5 hr	0.29984	0.02378	0.01171	0.01067
6.5 hr	0.22173	0.02296	0.00741	0.00211

Table B.2: Acyl-CoA fluxes to fatty acid biosynthesis used in model solution calculations. Data is plotted in Fig. 9.2 to 9.4.

APPENDIX C

Metabolic Energy Balance Calculations

C.1 Fermentation Characteristics and Nitrogen Balance

The fermentation analyzed below used a defined glucose/ Casamino Acids medium with aeration at 1.4 VVM. The medium contained 6.40 g/l of Casamino Acids as nitrogen source; and was otherwise identical to the fermentation media described in Sect. 4.1. The specific sample examined (GR704) was from late vegetative phase (5.75 hr; 2.165 g BDM/l; 4.27 % W/W [PHB + PHV]).

As a preliminary check, a liquid - and solid - phase nitrogen (N) audit was performed to test for balance, as follows:

1) total N present based on Casamino Acids (CAA's) added:

- CAA's added to medium: 9.73 g in 1520 ml;
- 10 ml of uninoculated medium removed, leaves 9.67 g of CAA's in 1510 ml;
- CAA's added to inoculum: 0.48 g in 80 ml;
- thus after inoculation have 10.15 g of CAA's in 1590 ml;
- 55 ml of broth removed prior to 5.75 hr (assumed homogenous), leaves [(1590 - 55)/1590]*10.15 ≈ 9.80 g of CAA's;
- based on 10 % total N in Casamino Acids (Difco, 1977), total N present ≈ 0.980 g, or [(980 mg)/(14.0067 mg/ mmol)] ≈ 70 mmol N.

2) nitrogen in liquid - phase ammonia:

- (1.409 mmol ammonia/l)*(1.000 mmol N/mmol ammonia) * (1.535 l) ≈ 2.16 mmol N;

3) total N in liquid - phase amino acids (AA_i, i = 1, 16):

- (Σ[(mmol AA_i/l)*(mmol N/mmol AA_i)])*(1.535 l) ≈ 16.64 mmol N;

4) total N in biomass amino acids:

- measured AA's: (Σ[(mmol AA_i/g VDM)*(mmol N/mmol AA_i)]) ≈ 5.380 mmol N/g VDM;

- AA's not measured (ie. CYS, PRO, TRP; Morowitz, 1968): [0.101 + 0.252 + 2*(0.050)] mmol N/g VDM = 0.453 mmol N/g VDM;

- total AA's: [(5.380 + 0.453) mmol N/g VDM]*(2.073 g VDM/l)*(1.535 l) ≈ 18.56 mmol N;

5) total N in non - amino acid biomass (ie. thymine, adenine, guanine, cytosine, uracil; Morowitz, 1968):

[2*(0.024) + 5*(0.140) + 5*(0.140) + 3*(0.140) + 2*(0.115)] mmol N/g VDM = 2.098 mmol N/g VDM;

(2.098 mmol N/g VDM)*(2.073 g VDM/l)*(1.535 l) ≈ 6.68 mmol N;

6) total N apparently present in fermenter:

(2.16 + 16.64 + 18.56 + 6.68) mmol N ≈ 44.0 mmol N;

7) fraction of added N accounted for:

(44.0 mmol N)/(70.0 mmol N) ≈ 0.629.

Thus about 63 per cent of the nitrogen apparently added has been accounted for. The majority of the remainder is presumed to be present in non - measured components of the liquid phase, namely certain amino acids and soluble protein.

C.2 Calculation of α-Keto-3-methylvalerate Dehydrogenation Rate

The rate of α-keto-3-methylvalerate (αKMV) dehydrogenation was estimated since it was the only α-keto acid which accumulated during anaerobic incubation of GR704 (Sect. 5.4). Details of the calculation are as follows:

1) specific rate of isoleucine uptake:

   [(0.317 mmol/l) - (0.259 mmol/l)]/[(0.6667 hr)*(2.073 g VDM/l)] ≈ 0.04197 mmol/g VDM/hr;

2) specific rate of αKMV release:

   [(0.473 mmol/l) - (0.411 mmol/l)]/[(0.6667 hr)*(2.073 g VDM/l)] ≈ 0.04486 mmol/g VDM/hr;

3) specific rate of 2-methylbutyrate release:

   [(0.3143 mmol/l) - (0.3133 mmol/l)]/[(0.6667 hr)*(2.073 g VDM/l)] ≈ 0.0007 mmol/g VDM/hr;

4) net rate of αKMV dehydrogenation:

   (-0.04197 + 0.04486 + 0.0007) mmol/g VDM/hr ≈ 0.0036 mmol/g VDM/hr.

C.3 Molar Flux Balance for Base Case

Specific rates of dehydrogenation of α-ketoisovalerate (αKIV) and α-ketoisocaproate (αKIC) were calculated as follows (Sect. 5.5):

1) αKIV:

[(0.0036 + 0.0195) mmol/g VDM/hr]*[(0.011258 mmol/g VDM/hr)/(0.005727 mmol/g VDM/hr)]

≈ 0.0454 mmol/g VDM/hr;

2) αKIC:

[(0.0036 + 0.0195) mmol/g VDM/hr]*[(0.05816 mmol/g VDM/hr)/(0.005727 mmol/g VDM/hr)]

≈ 0.0235 mmol/g VDM/ hr;

All measured fluxes were entered into the LOTUS™ metabolic flowsheet (Sect. 5.1) along with the three BCKA dehydrogenase fluxes. Solution of the set of molar balances "downstream" from pyruvate led to the following results:

1) no net formation of acetoin/butanediol, but breakdown of acetoin to acetate;

2) no glyoxylate cycle flux;

3) anaplerotic operation of pyruvate (or phospho-enolpyruvate) carboxylase;

4) an apparent pyruvate deficit of about 0.9 mmol/g VDM/hr.

To balance pyruvate use and availability, all flows to biosynthesis not based on measured values were progressively reduced (Sect. 6.2). Pyruvate balance was achieved at 0.7129 times the unadjusted biosynthetic rate. The set of metabolic flows thus obtained is summarized in Fig. 5.3.

C.4 Calculation of Metabolic Energy Requirements

The specific growth rate (μ) was approximated as that observed during the preceding 2.15 hours, as follows:

$\mu \approx [\ln(2.073 \text{ g VDM/l}) - \ln(0.871 \text{ g VDM/l})]/[(5.75 - 3.60) \text{ hr}]$

$\approx 0.4033 \text{ hr}^{-1}$.

Specific requirements of adenosine triphosphate (ATP) equivalents for growth (34.94 mmol ATP/g VDM) and maintenance (1.5 mmol ATP/g VDM/hr) were taken from Stouthamer (1973, 1979) respectively. Although the effective value of the former *in vivo* may be much higher, this phenomenon is open to several interpretations (*ibid.*); thus the "theoretical" value of 34.94 mmol ATP/g VDM was used. The requirement for maintenance energy is also not known with certainty (*ibid.*), but is in any case small compared to the energy needed for growth.

Total specific rate of ATP use was then found:

$(34.94 \text{ mmol ATP/g VDM}) * (0.4033 \text{ hr}^{-1}) + 1.5 \text{ mmol ATP/g VDM/hr}$

$\approx 15.6 \text{ mmol ATP/g VDM/hr}$.

C.5 ATP Production Rate versus P/O Ratio

For each internal, and non - biomass terminal, model flux the stoichiometry of ATP use and/or production by substrate - level phosphorylation, as for reduced cofactors (NADH, $FADH_2$), were taken from Lehninger (1976) and Gottschalk (1979). Transport energy was taken as one mol ATP/ mol AA (Stouthamer, 1973) for the small catabolic uptake of amino acids. Net pathway ATP formation rate was calculated (ibid.,p. 26; Mandelstam and McQuillen, 1973,p. 538) as,

$((P/O)*[H_N + (2/3)*H_F] + SATP)*F_p$, where:

P/O ≡ P/2H ≡ ATP formed per pair of hydrogen atoms oxidized, mmol ATP/mmol reduced cofactor;

H_N ≡ NADH formed, mmol/mmol substrate flux;

H_F ≡ $FADH_2$ formed, mmol/mmol substrate flux;

SATP ≡ ATP formed by substrate - level phosphorylation, mmol ATP/mmol substrate flux;

F_p ≡ pathway flux, mmol/g VDM/hr.

Using an initial estimate for P/O, energy production was summed over all pathways to give apparent total specific ATP production rate. Finally P/O ratio was varied until ATP production and consumption balanced. For the present case energy balance was achieved at P/O ≈ 1.99. Several other cases were similarly examined; complete results are given in Table 5.6.

APPENDIX D

Run 10 Data

TIME, hr	BDM, g/litre	VDM, g/litre	mmoles / litre		micromoles / litre					
			PHB	PHV	i-C12	n-C12	i-C13	a-C13	i-C14	n-C14
3.00	1.49	1.49	0.029	0.000	1.03	0.524	5.92	3.18	5.59	4.48
	[0.01]		[0.000]	[0.000]	[0.07]	[0.223]	[0.13]	[0.17]	[0.06]	[0.08]
4.10	2.63	2.55	0.735	0.159	2.56	1.13	14.1	7.09	10.7	8.29
	[0.03]		[0.011]	[0.005]	[0.11]	[0.07]	[0.3]	[0.29]	[0.7]	[0.50]
6.00	5.69	5.26	4.24	0.63	5.10	1.78	32.7	11.0	21.0	13.6
	[0.13]		[0.36]	[0.050]	[0.17]	[0.03]	[0.0]	[0.7]	[0.5]	[0.2]
8.00	6.77	6.33	4.20	0.738	6.29	1.47	41.4	14.9	31.9	21.7
	[0.01]		[0.23]	[0.008]	[0.20]	[0.01]	[0.2]	[0.4]	[0.1]	[1.3]
11.00	6.20	5.94	2.56	0.438	5.71	1.25	47.0	16.2	36.3	26.2
	[0.16]		[0.43]	[0.008]	[0.16]	[0.07]	[0.7]	[0.8]	[0.6]	[1.6]
17.25	4.56	4.25	3.23	0.351	3.11	0.889	34.1	9.01	44.4	28.0
	[0.08]		[0.81]	[0.124]	[0.41]	[0.135]	[5.2]	[1.68]	[6.3]	[5.1]

Table D.1: Fatty acid composition of biomass, Run 10: i-C12 to n-C14.

TIME, hr	micromoles / litre								
	i-C15	a-C15	n-C15	i-C16	n-C16	i-C16=	n-C16=	i-C17	a-C17
3.00	21.2	11.9	0.000	10.4	5.24	9.27	11.9	0.000	11.1
	[0.9]	[0.1]	[0.000]	[3.4]	[0.70]	[1.24]	[2.0]	[0.000]	[2.1]
4.10	48.8	25.7	0.534	35.8	3.71	17.5	26.5	13.2	13.3
	[4.5]	[0.2]	[0.000]	[0.4]	[0.91]	[4.3]	[4.7]	[2.3]	[1.8]
6.00	108	40.5	1.58	209	13.40	41.9	63.8	35.5	25.4
	[1]	[1.5]	[0.29]	[8]	[3.7]	[11.9]	[8.9]	[2.0]	[0.6]
8.00	138	55.6	8.38	249	8.43	32.4	69.7	30.5	27.7
	[1]	[3.5]	[4.03]	[7]	[0.78]	[3.0]	[5.7]	[3.1]	[4.4]
11.00	161	57.2	4.35	230	14.1	32.0	79.4	39.3	18.5
	[1]	[0.6]	[0.18]	[19]	[4.9]	[6.6]	[6.1]	[2.8]	[0.3]
17.25	161	50.2	5.81	211	14.1	38.1	53.5	33.7	21.1
	[20]	[7.5]	[3.61]	[40]	[8.5]	[13.6]	[12.3]	[5.2]	[3.2]

Table D.2: Fatty acid composition of biomass, Run 10: i-C15 to a-C17. Selected data is plotted in Fig. 6.10.

TIME, hr	mmoles / litre						
	AMMONIA	GLUCOSE	ACETATE	ACETOIN	ISOBUT-YRATE	2-METHYL-BUTYRATE	ISOVAL-ERATE
0.00	..518	64.2	1.08	0.0772	0.0141	0.000	0.000
	[0.006]	[0.8]	[0.02]	[0.0032]			
3.00	1.46	58.2	13.8	0.103	0.0776	0.0868	0.0585
	[0.02]	[1.5]	[1.0]	[0.021]	[0.0121]	[0.0096]	[0.0085]
4.10	1.56	45.6	20.2	0.976	0.354	0.201	0.247
	[0.09]	[1.4]	[1.6]	[0.138]	[0.159]	[0.050]	[0.065]
6.00	1.59	25.1	6.16	0.858	0.339	0.140	0.196
	[0.04]	[0.0]	[0.32]	[0.073]	[0.034]	[0.039]	[0.029]
8.00	0.0358	13.9	1.87	1.93	0.278	0.0695	0.0622
	[0.0007]	-[0.7]	[0.15]	[0.74]	[0.026]	[0.0138]	[0.0020]
11.00	0.340	9.33	2.33	0.0749	0.327	0.0422	0.101
	[0.009]	[0.0]	[0.99]	[0.0199]	[0.029]		[0.028]
17.25	0.340	6.49	5.98	0.190	0.310	0.0309	0.180
	[0.014]	[0.22]	[0.64]	[0.045]	[0.053]	[0.0182]	[0.037]

Table D.3: Concentration of ammonia, glucose and volatile organic products, Run 10. Data is plotted in Fig. 6.1, 6.11, 6.13, 6.14, 9.1 and 9.5.

TIME, hr	mmoles / litre							
	ASP+ASN	THR	SER	GLU+GLN	GLY	ALA	VAL	MET
0.00	1.94	1.04	1.44	3.79	1.21	1.64	1.38	0.362
3.00	1.05	0.733	0.796	2.71	0.862	1.08	1.09	0.298
4.10	0.796 [0.030]	0.380 [0.001]	0.647 [0.006]	2.30 [0.08]	0.580 [0.009]	0.797 [0.049]	0.794 [0.005]	0.214 [0.045]
6.00	0.571	0.232	0.432	1.06	0.391	0.392	0.201	0.159
8.00	0.516	0.200	0.433	0.974	0.393	0.341	0.167	0.0371
11.00	0.496	0.206	0.375	0.920	0.453	0.324	0.165	0.173
17.25	0.535	0.194	0.350	1.06	0.536	0.499	0.183	0.247

Table D.4: Concentration of broth amino acids (after hydrolysis), Run 10: aspartate to methionine. Data is plotted in Fig. 6.4 to 6.7.

TIME, hr	mmoles / litre						
	ILE	LEU	TYR	PHE	HIS	LYS	ARG
0.00	0.935	1.91	0.717	0.731	0.363	1.46	0.742
3.00	0.766	1.44	0.537	0.578	0.375	1.27	0.490
4.10	0.582 [0.038]	0.985 [0.011]	0.502 [0.017]	0.497 [0.031]	0.289 [0.025]	1.15 [0.32]	0.331 [0.019]
6.00	0.244	0.356	0.361	0.343	0.108	0.705	0.109
8.00	0.113	0.314	0.0465	0.0566	0.0253	0.279	0.0872
11.00	0.161	0.432	0.0449	0.0506	0.0779	0.314	0.0795
17.25	0.106	0.593	0.183	0.0538	0.0438	0.394	0.0829

Table D.5: Concentration of broth amino acids (after hydrolysis), Run 10: isoleucine to arginine. Data is plotted in Fig. 6.5 to 6.8.

TIME, hr	mmoles / litre						
	2,3-BUTANE-DIOL	LACTATE	PYRUVATE	aKIV + aOHIV	aKMV	aKIC	SUCCINATE
3.00	0.0237	2.20	2.29	0.0666	0.130	0.0298	0.123
	[0.0054]	[0.17]	[0.62]	[0.0307]	[0.005]	[0.0000]	[0.044]
4.10	1.07	6.23	3.16	0.259	0.478	0.112	0.216
	[[0.50]	[1.22]	[0.71]	[0.059]	[0.046]	[0.032]	[0.125]
6.00	2.02	5.67	0.0621	0.265	0.515	0.132	0.286
	[0.96]	[1.06]		[0.021]	[0.021]	[0.087]	[0.101]
8.00	0.617	0.582	0.148	0.178	0.0729	0.0412	0.269
	[0.053]	[0.184]	[0.059]	[0.018]	[0.0322]	[0.0295]	[0.103]
11.00	0.0505	0.762	0.156	0.0690	0.0688	0.0039	1.54
	[0.0270]	[0.136]	[0.091]	[0.0123]	[0.0447]		[0.32]
17.25	0.000	0.766	0.599	0.125	0.0568	0.000	1.87
	[0.000]	[0.217]	[0.184]	[0.021]	[0.0446]	[0.000]	[0.20]

Table D.6: Concentration of non - volatile organic products, Run 10. Data is plotted in Fig. 6.11, 6.12, 6.13 and 6.15.

APPENDIX E

Run 11 Data

TIME, hr	BDM, g/litre	VDM, g/litre	mmoles / litre		micromoles / litre					
			PHB	PHV	i-C12	n-C12	i-C13	a-C13	i-C14	n-C14
3.00	1.58 [0.01]	1.56	0.098 [0.007]	0.085 [0.009]	2.84 [0.01]	0.937 [0.362]	6.97 [0.17]	6.35 [0.11]	6.96 [0.24]	4.43 [0.20]
4.50	3.41 [0.02]	3.22	1.83 [0.27]	0.305 [0.014]	3.83 [0.12]	1.43 [0.06]	16.4 [0.2]	13.0 [0.1]	12.8 [0.0]	8.44 [0.11]
6.50	5.78 [0.00]	5.50	2.56 [0.45]	0.626 [0.031]	5.04 [0.38]	1.56 [0.16]	27.7 [2.8]	13.1 [0.7]	22.0 [1.9]	13.1 [1.1]
9.50	6.05 [0.01]	5.69	3.41 [0.52]	0.681 [0.073]	7.23 [0.40]	1.38 [0.10]	37.8 [2.3]	15.1 [0.6]	36.3 [1.6]	16.7 [0.8]
14.00	5.48 [0.02]	5.16	3.09 [0.31]	0.555 [0.082]	4.99 [0.36]	1.41 [0.31]	28.8 [0.9]	10.2 [0.8]	38.5 [0.6]	14.5 [0.7]

Table E.1: Fatty acid composition of biomass, Run 11: i-C12 to n-C14.

TIME, hr	micromoles / litre								
	i-C15	a-C15	n-C15	i-C16	n-C16	i-C16=	n-C16=	i-C17	a-C17
3.00	19.8	18.2	0.000	12.7	1.17	10.6	16.4	5.62	8.67
	[0.1]	[0.3]	[0.000]	[0.1]	[0.12]	[0.1]	[0.3]	[0.06]	[0.48]
4.50	48.9	43.0	0.531	91.8	5.19	21.7	36.6	19.3	21.5
	[0.6]	[0.0]	[0.001]	[4.1]	[0.28]	[1.4]	[3.4]	[3.9]	[2.0]
6.50	80.5	46.4	1.65	187	9.22	35.3	58.1	20.8	27.9
	[7.4]	[3.3]	[0.20]	[1]	[1.41]	[3.6]	[4.7]	[2.4]	[2.0]
9.50	114	56.5	4.80	240	16.1	29.3	72.8	25.7	22.2
	[5]	[3.6]	[0.47]	[1]	[0.1]	[3.2]	[6.2]	[1.9]	[5.1]
14.00	102	48.2	1.62	216	11.5	21.6	54.6	22.0	17.8
	[5]	[2.8]	[0.09]	[4]	[0.2]	[0.8]	[2.7]	[0.4]	[1.3]

Table E.2: Fatty acid composition of biomass, Run 11: i-C15 to a-C17. Selected data is plotted in Fig. 7.5.

TIME, hr	mmoles / litre						
	AMMONIA	GLUCOSE	ACETATE	ACETOIN	ISOBUT-YRATE	2-METHYL-BUTYRATE	ISOVAL-ERATE
0.00	0.386	66.8	1.67	0.0781	0.000	0.000	0.000
	[0.006]	[0.1]	[0.05]	[0.0428]	[0.000]	[0.000]	[0.000]
3.00	1.48	55.0	15.6	0.213	0.123	0.0979	0.0513
	[0.04]	[1.5]	[0.5]	[0.072]	[0.022]	[0.0393]	[0.191]
4.50	1.57	41.4	16.5	1.09	0.647	0.237	0.279
	[0.02]	[0.3]	[2.0]	[0.14]	[0.331]	[0.048]	[0.059]
6.50	1.13	20.6	4.23	0.867	0.322	0.000	0.0271
	[0.01]	[1.1]	[0.58]	[0.075]	[0.103]	[0.000]	[0.0213]
9.50	0.0963	12.2	4.23	0.285	0.429	0.0224	0.0458
	[0.0014]	-[1.0]	[0.22]	[0.004]	[0.138]	[0.0178]	[0.0186]
14.00	0.0257	8.60	2.38	0.409	0.714	0.00401	0.220
	[0.0014]	[0.42]	[0.10]	[0.035]	[0.147]		[0.037]

Table E.3: Concentration of ammonia, glucose and volatile organic products, Run 11. Data is plotted in Fig. 7.1, 7.6, 7.8, 7.9, 9.1 and 9.5.

TIME, hr	mmoles / litre							
	ASP+ASN	THR	SER	GLU+GLN	GLY	ALA	VAL	MET
0.00	1.51	0.836	1.17	3.25	0.958	1.41	1.20	0.302
3.00	0.409	0.613	0.351	2.48	0.731	1.03	1.08	0.256
4.50	0.243	0.160	0.272	1.21	0.266	0 613	0.645	0.171
6.50	0.233	0.158	0.158	0.390	0.213	0.233	0.115	0.137
9.50	0.210	0.154	0.162	0.294	0.219	0.179	0.0796	0.117
14.00	0.194	0.124	0.110	0.293	0.249	0.221	0.0831	0.162

Table E.4: Concentration of broth amino acids (after hydrolysis), Run 11: aspartate to methionine.

TIME, hr	mmoles / litre						
	ILE	LEU	TYR	PHE	HIS	LYS	ARG
0.00	0.799	1.66	0.301	0.561	0.416	1.50	0.658
3.00	0.704	1.23	0.245	0.463	0.420	1.39	0.464
4.50	0.401	0.681	0.119	0.357	0.323	1.03	0.268
6.50	0.0709	0.324	0.0224	0.0727	0.199	0.675	0.0689
9.50	0.0508	0.372	0.0310	0.0524	0.0323	0.103	0.0471
14.00	0.474	0.103	0.0270	0.0257	0.0548	0.212	0.0477

Table B.5: Concentration of broth amino acids (after hydrolysis), Run 11: isoleucine to arginine.

TIME, hr	mmoles / litre						
	2,3-BUTANE-DIOL	LACTATE	PYRUVATE	aKIV + aOHIV	aKMV	aKIC	SUCCINATE
3.00	0.0753	4.87	2.74	0.138	0.234	0.0429	0.199
	[0.0111]	[0.76]	[1.39]	[0.022]	[0.048]	[0.0124]	[0.038]
4.50	0.823	6.63	4.19	0.179	0.366	0.0781	0.253
	[0.531]	[0.90]	[0.49]	[0.017]	[0.087]	[0.0117]	[0.083]
6.50	0.401	2.13	0.238	0.114	0.105	0.0364	0.248
	[0.056]	[0.15]	[0.075]	[0.005]	[0.030]	[0.0045]	[0.044]
9.50	0.0329	1.57	0.0641	0.140	0.109	0.00874	0.666
	[0.0073]	[0.53]	[0.0352]	[0.051]	[0.046]	0.00280	[0.009]
14.00	0.0844	0.703	0.0608	0.120	0.0396	0.00560	1.72
	[0.0026]	[0.024]	[0.0081]	[0.017]	[0.0084]		[0.32]

Table E.6: Concentration of non - volatile organic products, Run 11. Data is plotted in 7.6, 7.7, 7.8 and 7.10.

APPENDIX F

Run 12 Data

TIME, hr	BDM, g/litre	VDM, g/litre	mmoles / litre		micromoles / litre					
			PHB	PHV	i-C12	n-C12	i-C13	a-C13	i-C14	n-C14
3.00	0.95 [0.02]	0.95	0.007 [0.001]	0.037 [0.005]	1.66 [0.15]	0.790 [0.187]	3.02 [0.16]	2.28 [0.04]	3.84 [0.05]	2.04 [0.02]
4.50	2.09 [0.03]	2.04	0.407 [0.036]	0.142 [0.013]	3.00 [0.02]	1.12 [0.04]	9.13 [0.07]	8.38 [0.19]	9.22 [0.15]	5.52 [0.02]
6.50	4.40 [0.06]	4.10	2.97 [0.62]	0.483 [0.029]	5.03 [0.67]	1.84 [0.23]	21.3 [2.1]	12.3 [0.8]	16.8 [1.4]	9.59 [0.26]
9.50	6.77 [0.01]	6.48	2.68 [0.08]	0.588 [0.001]	13.1 [0.3]	1.82 [0.05]	48.6 [0.6]	16.7 [0.4]	29.1 [0.4]	17.1 [0.2]
14.00	5.47 [0.05]	5.12	3.39 [0.07]	0.605 [0.019]	8.39 [0.33]	1.21 [0.02]	36.4 [0.9]	11.1 [1.0]	28.2 [1.0]	10.6 [0.5]

Table F.1: Fatty acid composition of biomass, Run 12: i-C12 to n-C14.

TIME, hr	micromoles / litre								
	i-C15	a-C15	n-C15	i-C16	n-C16	i-C16=	n-C16=	i-C17	a-C17
3.00	9.25	8.24	0.000	4.97	0.000	5.81	12.3	6.52	3.73
	[0.64]	[0.28]	[0.000]	[0.18]	[0.000]	[0.42]	[2.0]	[3.37]	[0.82]
4.50	29.9	27.[illegible]	0.000	25.5	2.88	14.4	18.7	6.50	11.3
	[0.3]	[0.8]	[0.000]	[0.5]	[0.00]	[0.0]	[1.1]	[1.28]	[2.7]
6.50	65.3	44.4	1.12	162	7.46	29.5	42.7	16.3	19.8
	[4.7]	[4.0]	[0.11]	[6]	[0.71]	[1.4]	[3.8]	[3.0]	[3.6]
9.50	92.4	49.7	3.76	207	8.99	91.7	74.0	16.0	21.6
	[1.2]	[1.4]	[0.05]	[6]	[0.10]	[1.1]	[1.5]	[0.7]	[0.8]
14.00	76	37.5	1.56	176	7.53	36.1	54.4	11.6	10.9
	[3.1]	[1.2]	[0.00]	[6]	[0.97]	[4.6]	[5.9]	[2.2]	[2.3]

Table F.2: Fatty acid composition of biomass, Run 12: i-C15 to a-C17. Selected data is plotted in Fig. 8.5.

TIME, hr	mmoles / litre						
	AMMONIA	GLUCOSE	ACETATE	ACETOIN	ISOBUT-YRATE	2-METHYL-BUTYRATE	ISOVAL-ERATE
0.00	0.316	65.6	1.47	0.0326	0.0712	0.000	0.000
	[0.003]	[0.8]	[0.33]	[0.0069]	[0.0096]	[0.000]	[0.000]
3.00	1.22	60.7	9.76	0.0612	0.196	0.0294	0.000
	[0.11]	[0.4]	[0.28]	[0.0270]	[0.034]	[0.0124]	[0.000]
4.50	1.74	48.3	20.0	0.626	0.393	0.249	0.173
	[0.09]	[1.1]	[2.3]	[0.112]	[0.003]	[0.003]	[0.006]
6.50	3.26	29.9	9.98	0.668	0.557	0.0916	0.259
	[0.09]	[1.5]	[0.70]	[0.153]	[0.089]	[0.0066]	[0.040]
9.50	0.0605	13.8	4.31	0.233	0.326	0.0229	0.0277
	[0.0014]	-[0.3]	[0.62]	[0.018]	[0.066]	[0.0324]	[0.0092]
14.00	0.0217	10.9	1.50	0.0491	0.592	0.0180	0.163
	[0.0002]	[0.3]	[0.00]	[0.0069]	[0.071]	[0.0023]	[0.005]

Table F.3: Concentration of ammonia, glucose and volatile organic products, Run 12. Data is plotted in Fig. 8.1, 8.6, 8.8, 8.9, 9.1 and 9.5.

TIME, hr	mmoles / litre							
	ASP+ASN	THR	SER	GLU+GLN	GLY	ALA	VAL	MET
0.00	1.50	0.849	1.10	3.10	0.933	1.29	1.36	0.262
3.00	0.745	0.679	0.370	2.45	0.713	1.01	1.00	0.285
4.50	0.359	0.411	0.372	2.18	0.635	0.938	0.948	0.198
6.50	0.215	0.177	0.218	0.436	0.198	0.300	0.187	0.181
9.50	0.231	0.175	0.160	0.310	0.267	0.212	0.124	0.133
14.00	0.195	0.132	0.105	0.290	0.279	0.180	0.111	0.118

Table F.4: Concentration of broth amino acids (after hydrolysis), Run 12: aspartate to methionine.

TIME, hr	mmoles / litre						
	ILE	LEU	TYR	PHE	HIS	LYS	ARG
0.00	0.836	1.49	0.246	0.494	0.263	1.50	0.562
3.00	0.656	1.13	0.202	0.390	0.324	1.14	0.443
4.50	0.518	1.17	0.193	0.422	0.210	1.38	0.413
6.50	0.0983	0.384	0.0438	0.218	0.206	0.905	0.0736
9.50	0.0925	0.211	0.0658	0.0356	0.0610	0.235	0.0545
14.00	0.0792	0.162	0.0520	0.0316	0.0420	0.198	0.0426

Table F.5: Concentration of broth amino acids (after hydrolysis), Run 12: isoleucine to arginine.

TIME, hr	mmoles / litre						
	2,3-BUTANE-DIOL	LACTATE	PYRUVATE	aKIV + aOHIV	aKMV	aKIC	SUCCINATE
3.00	0.0362	2.31	0.697	0.0459	0.122	0.0142	0.136
	[0.0024]	[0.20]	[0.401]	[0.0039]	[0.012]	[0.0095]	[0.024]
4.50	0.286	4.92	2.64	0.0807	0.430	0.0659	0.218
	[0.086]	[0.21]	[1.21]	[0.0104]	[0.013]	[0.0063]	[0.009]
6.50	0.784	6.62	0.624	0.258	0.376	0.208	0.256
	[0.165]	[1.30]	[0.240]	[0.0656]	[0.017]	[0.102]	[0.085]
9.50	0.0728	0.922	0.0905	0.171	0.0803	0.0319	0.245
	[0.0102]	[0.136]	[0.0432]	[0.020]	[0.0350]	[0.0183]	[0.029]
14.00	0.0158	0.759	0.0380	0.147	0.0681	0.000	0.914
	[0.0012]	[0.132]	[0.0114]	[0.004]	[0.0202]	[0.000]	[0.097]

Table F.6: Concentration of non - volatile organic products, Run 12. Data is plotted in 8.6, 8.7, 8.8 and 8.10.

APPENDIX G

Model Calculation Procedure Summary

G.1 Specific Rates

Specific rate of production (mmol/g VDM/hr) of each measured component was calculated according to the method, and using the notation, given in Sect. 5.2. As an example of these calculations, specific production rate of ammonia between 3.00 and 4.10 hours of Run 10 was determined as follows:

1) temporal mid - point, t_k, is (3.00 + 4.10)/2 = 3.55 hr;

2) broth ammonia concentrations at 3.00 hr and 4.10 hr were 1.462 and 1.556 mmol/litre respectively;

3) thus, using equation (5.4),

$$R_{VNH3}(3.55) \approx (1.556 - 1.462)/(4.10 - 3.00)$$
$$\approx 0.08545 \text{ mmol/litre/hr};$$

4) viable biomass (VDM) concentrations at 3.00 hr and 4.10 hr were respectively 1.488 and 2.546 g/litre;

5) log mean viable biomass concentration at t_k was found from equation (5.5) as follows:

$$X'(3.55) \approx \exp\{[\ln(2.546) + \ln(1.488)]/2\} \text{ g VDM/litre}$$
$$\approx 1.946 \text{ g VDM/litre};$$

6) specific consumption rate at t_k was calculated using equation (5.6),

$$R_{MNH3}(3.55) \approx (0.08545)/(1.946) \text{ mmol/g VDM/hr}$$
$$\approx 0.0439 \text{ mmol/g VDM/hr}.$$

Values so calculated were used as input to cubic spline interpolation as described in Sect. 5.2.

G.2 Fluxes to/from Biomass

Net specific flow rates of precursors to biomass, and intermediates produced by biomass degradation, were calculated according to Sect. 5.3; in summary:

1) flux of acetyl-CoA and each branched - chain acyl-CoA to fatty acid synthesis was calculated; these results are shown in Table B.2;

2) flux of each precursor (viz. glucose, aspartate and serine) to non-amino acid biosynthesis (R_{PNj}) was found;

3) flux of individual amino acids to biomass formation (R_{TAj}) was calculated;

4) net rate of biosynthesis/degradation of each amino acid (R_{AAj}) was found by difference;

Values so calculated were used as input to cubic spline interpolation as described in Sect. 5.2.

G.3 BCKA Dehydrogenase Fluxes

Specific rate of dehydrogenation of each branched - chain 2-keto acid, except for the 11 hr sample of Run 10 (see Sect. 6.4.1), was found as follows:

1) flux of 2-keto-3-methylvalerate through BCKA dehydrogenase [ie. FT(I), mmol/g VDM/hr] was calculated as described in Sect. 5.4; inputs to these calculations, and their results, are given in Table B.1;

2) corresponding rates for the valine and leucine pathways [ie. FT(V) and FT(I` respectively] were calculated according to Equation (5.15a,b) of Sect. 5.5; the resulting values are given in Table 5.6.

G.4 Solution of Remaining Molar Balances

The process of final model solution by balancing molar flow rates around all components was performed as described in Sect. 5.1.

APPENDIX H

Summary of Model Error Terms

A formal quantitative error analysis will not be undertaken because of the large number of terms for which only a "best - guess" estimate of the error can be made. The summary of error terms which follows reports results for 4.1 hr and 6.0 hr samples of Run 10 where it is possible to calculate data errors.

Individual error terms and their per cent standard deviations, when calculable, are as follows:

1) sampling time; sample volume: not available;
2) analysis (average): calibration: 3.4%; sample: 12.8%;
3) temporal mid - point specific rate: not available;
4) temporal mid - point biomass concentration: not available;
5) conversion of BDM to VDM basis (average): 5.1%;
6) cubic spline fit and interpolation: not available;
7) detailed biomass composition: not available;
8) simplifications of biosynthetic flows: not available;
9) broth amino acids concentrations: not available;
10) structural simplifications in model of central metabolism: not available;
11) absolute flux of 2-keto-3-methylvalerate through BCKA dehydrogenase: not available;
12) acyl-CoA fluxes to biosynthesis of fatty acids (average): 8.6%.

APPENDIX I

Glossary of Nomenclature and Synonyms

I.1 Chemical Substances

Common Name	Synonym(s)
acetoin	3-hydroxy-2-butanone
a-C15	12-methyltetradecanoic acid
α-hydroxyisovalerate	2-hydroxy-3-methylbutanoic acid; 2-hydroxyisovalerate
α-ketobutyrate	2-oxobutanoic acid; 2-oxobutyrate
α-ketoisocaproate	2-oxo-4-methylpentanoic acid; 2-ketoisocaproate; 2-oxoisocaproate
α-ketoisovalerate	2-oxo-3-methylbutanoic acid; 2-ketoisovalerate; 2-oxoisovalerate
α-keto-β-methylvalerate	2-oxo-3-methylpentanoic acid; 2-keto-3-methylvalerate; 2-oxo-3-methylvalerate
β-hydroxybutyrate	3-hydroxybutanoic acid
β-hydroxyvalerate	3-hydroxypentanoic acid
i-C14	12-methyltridecanoic acid
i-C15	13-methyltetradecanoic acid
i-C16	cis-Δ^{10}-14-methylpentadecenoic acid
isobutyrate	2-methylpropanoic acid
isovalerate	3-methylbutanoic acid
2-methyl- ıtyrate	2-methylbutanoic acid
PHB	poly-β-hydroxybutyrate
PHV	poly-β-hydroxyvalerate

I.2 Enzymes

Reference: Enzyme nomenclature: Recommendations (1978) of the nomenclature committee of the International Union of Biochemistry. New York: Academic Press, Inc.; 1979.

Common Name	IUB Number	Synonym(s)
acetoacetyl-CoA reductase	EC1.1.1.36	D-3-hydroxyacyl-CoA : $NADP^+$ oxido-reductase
acetoacetyl-CoA thiolase	EC2.3.1.9	acetyl-CoA acetyltransferase
acetoacetyl-CoA : succinyl-CoA transferase	EC2.8.3.5	3-ketoacid CoA-transferase
acetohydroxy acid reducto-isomerase	EC1.1.1.86	ketol-acid reductoisomerase
acetohydroxy acid synthetase	EC4.1.3.18	acetolactate synthase; AHAS I-III
aconitase	EC4.2.1.3	aconitate hydratase
acyl-CoA:acyl carrier protein transacylase	EC2.3.1.38	[acyl-carrier-protein] acetyl-transferase
acyl-CoA hydrolase	EC3.1.2.1 (?)	acetyl-CoA hydrolase (?)
α-isopropylmalate synthetase	EC4.1.3.12	2-isopropylmalate synthase
α-ketoglutarate dehydrogenase	EC1.2.4.2	2-oxoglutarate dehydrogenase
β-isopropylmalate isomerase	EC4.2.1.33	3-isopropylmalate dehydratase
β-isopropylmalate dehydrogenase	EC1.1.1.85	3-isopropylmalate dehydrogenase
branched - chain acyl-CoA dehydrogenase	EC1.3.99.3 (cf. EC1.3.99.10	--- isovaleryl-CoA dehydrogenase)

Common Name	IUB Number	Synonym(s)
branched - chain keto acid dehydrogenase	EC1.2.4.4	2-oxoisovalerate dehydrogenase (lipoamide)
branched - chain fatty acid synthetase	(enzyme complex)	(cf. Schweizer, 1989)
citrate synthase	EC4.1.3.7	citrate (si)-synthase
dihydrolipoamide dehydrogenase	EC1.6.4.3	dihydrolipoamide reductase (NAD^+)
dihydroxy acid dehydratase	EC4.2.1.9	2,3-dihydroxyacid hydro-lyase
DNA - dependent RNA polymerase	EC2.7.7.6	RNA nucleotidyl-transferase
enoyl-CoA hydratase	EC4.2.1.17	methylacrylyl-CoA hydratase; crotonase
fumarase	EC4.2.1.2	fumarate hydratase
3-hydroxyisobutyrate dehydrogenase	EC1.1.1.31	3-hydroxyisobutyrate :NAD^+ oxidoreductase
3-hydroxyisobutyryl-CoA hydrolase	EC3.1.2.4	---
hydroxymethyl-glutaryl-CoA lyase	EC4.1.3.4	3-hydroxy-3-methyl-glutaryl-CoA aceto-acetate-lyase
isocitrate lyase	EC4.1.3.1	isocitratase
isocitrate dehydrogenase (NAD^+)	EC1.1.1.41	threo-D_s-isocitrate NAD^+ oxidoreductase (decarboxylating)
isocitrate dehydrogenase ($NADP^+$)	EC1.1.1.42	threo-D_s-isocitrate $NADP^+$ oxidoreductase (decarboxylating)
malate synthase	EC4.1.3.2	L-malate glyoxylate-lyase (CoA-acetylating)
malate dehydrogenase	EC1.1.1.37	L-malate : NAD^+ oxidoreductase

Common Name	IUB Number	Synonym(s)
malic enzyme (NAD^+)	EC1.1.1.38	L-malate : NAD^+ oxidoreductase (oxalacetate - decarboxylating)
malic enzyme ($NADP^+$)	EC1.1.1.40	L-malate : $NADP^+$ oxidoreductase (decarboxylating)
medium - chain acyl-CoA synthetase	EC6.2.1.2	butyryl-CoA synthetase
methylcrotonyl-CoA carboxylase	EC6.4.1.4	3-methylcrotonyl-CoA:carbon-dioxide ligase (ADP-forming)
methylglutaconyl-CoA hydratase	EC4.2.1.18	3-hydroxy-3-methyl-glutaryl-CoA hydro-lyase
methylmalonate semi-aldehyde dehydrogenase	EC1.2.1.27	methylmalonate-semi-aldehyde:NAD^+ oxido-reductase (CoA-propionylating)
methylmalonyl-CoA racemase	EC5.1.99.1	---
methylmalonyl-CoA mutase	EC5.4.99.2	S-methylmalonyl-CoA mutase
phospho-enolpyruvate carboxykinase (ATP)	EC4.1.1.49	ATP:oxaloacetate carboxy-lyase (transphosphor-ylating)
propionyl-CoA carboxylase	EC4.1.1.41	(R)-methylmalonyl-CoA carboxy-lyase
pyruvate carboxylase	EC6.4.1.1	pyruvate:carbon-dioxide ligase (ADP-forming)
pyruvate dehydrogenase	EC1.2.4.1	(generally used for enzyme complex; cf. Lehninger, 1976, p.450 et. seq.)
serine protease	EC3.4.21.14 (?)	subtilisin (?)

Common Name	IUB Number	Synonym(s)
succinate thiokinase (GDP)	EC6.2.1.4	succinyl-CoA synthetase (GDP-forming)
succinate thiokinase (ADP)	EC6.2.1.5	succinyl-CoA synthetase (ADP-forming)
succinate dehydrogenase	EC1.3.99.1	succinate: (acceptor) oxidoreductase
threonine deaminase	EC4.2.1.16	threonine dehydratase
transaminase A	EC2.6.1.1	aspartate aminotransferase
transaminase B	EC2.6.1.42	branched - chain amino acid aminotransferase
transaminase C	EC2.6.1.66	---
transaminase D	EC2.6.1.57	aromatic-amino-acid aminotransferase

I.3 Symbols

Symbol	Definition
AHAS	acetohydroxy acid synthetase
BCAA	branched - chain amino acid
BCKA	branched - chain 2-keto acid
BDM	biomass dry matter, g
C'_{Mj}	cellular concentration of amino acid j, mmol/g VDM
C_j	component j concentration, mmol/l
C_{Mj}	molar concentration in biomass of component j, mmol/g BDM

Symbol	Definition
CW_j	weight concentation in biomass of component j, g/g BDM
FA	fatty acid
FA(x)	acyl-CoA flux to fatty acid synthesis for branched - chain pathway x, mmol/g VDM/h
F_p	pathway flux, mmol/g VDM/h
FT(x)	acyl-CoA flux from BCKA dehydrogenase for pathway x, mmol/g VDM/h
H_F	$FADH_2$ formed, mmol/mmol substrate flux
H_N	NADH formed, mol/mol substrate flux
k_x	fatty acid synthetase activity constant for acyl-CoA primer of pathway x
μ_A	apparent specific growth rate, h^{-1}
MW_j	molecular weight of component j, g/mol
P/O	ATP formed per pair of hydrogen atoms oxidized, mol ATP/mol reduced cofactor
R_{AAj}	specific rate of biosynthesis/catabolism of amino acid j, mmol/g VDM/h
R_{FA}	rate of fatty acids production, mmol/g VDM/h
R_j	molar response factor for component j
R_{Nj}	specific molar consumption/production rate of component j, mmol/g VDM/h
R_{PNasp}	specific rate of aspartate use for non - amino acid biosynthesis, mmol/g VDM/h
R_{PNj}	flux of precursor conponent j to non - amino acid biosynthesis, mmol/g VDM/h
R_{PNglc}	specific rate of glucose use for non - amino acid biosynthesis, mmol/g VDM/h
R_{PNser}	specific rate of serine use for non - amino acid biosynthesis, mmol/g VDM/h

Symbol	Definition
R_{TAj}	total cellular requirement for amino acid j, mmol/g VDM/h
R_{Vj}	volumetric molar consumption/production rate of component j, mmol/l/h
SATP	ATP formed by substrate - level phosphorylation, mol ATP/mol substrate flux
SA(x)	specific rate of acyl-CoA formation from the corresponding short - chain acid for pathway x, mmol/g VDM/h
t_i	time of sample i, h
t_k	temporal midpoint between consecutive samples, h
VDM	biomass dry matter exclusive of PHB and PHV, g
x	isoleucine (I), leucine (L) or valine (V)
X	biomass concentration, g BDM/l
X'	reduced biomass concentration, g VDM/l

BIBLIOGRAPHY

Ambler, R.P. Standards and accuracy in amino acid analysis. In: Rattenbury, J.M., ed. Amino acid analysis. Chichester, England: Ellis Horwood Ltd.; 1981;p. 119-137.

Anderson, T.B. Effects of carbon:nitrogen ratio and oxygen on the growth kinetics of Bacillus thuringiensis and yield of bioinsecticidal crystal protein. London, Ontario, Canada: University of Western Ontario; 1990. M.E.Sc. Dissertation.

Andreoli, A.J.; Saranto, J.; Baecker, P.A.; Suehiro, S.; Escamilla, E.; Steiner, A. Biochemical properties of forespores isolated from Bacillus cereus. In: Gerhardt, P.; Costilow, R.N.; Sadoff, H.L., eds. Spores VI. Washington: American Society for Microbiology; 1975:p. 418-424.

Andrews, R.E., Jr.; Bechtel, D.B.; Campbell, B.S.; Davidson, L.I.; Bulla, L.A., Jr. Solubility of parasporal crystals of Bacillus thuringiensis and presence of toxin protein during sporulation, germination, and outgrowth. In: Levinson, H.S.; Sonenshein, A.L.; Tipper, D.J., eds. Sporulation and germination. Washington: American Society for Microbiology; 1981;p. 174-177.

Aronson, A.I.; Fitz-James, P. Structure and morphogenesis of the bacterial spore coat. Bacteriol. Rev. 40:360-402; 1976.

Aronson, J.N.; Borris, D.P.; Doerner, J.F.; Akers, E. Gamma-aminobutyric acid pathway and modified tricarboxylic acid cycle activity during growth and sporulation of Bacillus thuringiensis. Appl. Microbiol. 30:489-492; 1975a.

Aronson, J.N.; Doerner, J.F.; Akers, A.W.; Borris, D.P.; Mani, M. Gamma-aminobutyric acid pathway of glutamate metabolism by Bacillus thuringiensis. In: Gerhardt, P.; Costilow, R.N.; Sadoff, H.L., eds. Spores VI. Washington: American Society for Microbiology; 1975b;p. 404-410.

Barman, T.E. Enzyme handbook. New York: Springer-Verlag New York Inc.; 1969. 2 vol.

Bender, D.A. Amino acid metabolism. 2nd ed. Chichester, England: John Wiley and Sons Ltd.; 1985.

Benjamin, J.R.; Cornell, C.A. Probability, statistics, and decision for civil engineers. New York: McGraw - Hill, Inc.; 1970.

Bergey's manual of determinative bacteriology. 8th ed. Buchanan, R.E.; Gibbons, N.E., eds. Baltimore: Williams and Wilkins Co.; 1974.

Blackburn, S. Sample preparation and hydrolytic methods. In: Blackburn, S., ed. Amino acid determination: Methods and techniques. 2nd ed., revised and expanded. New York: Marcel Dekker, Inc.; 1978;p. 7-37.

Boudreaux, D.P.; Freese, E. Sporulation in Bacillus subtilis is independent of membrane fatty acid composition. J. Bacteriol. 148:480-486; 1981.

Boudreaux, D.P.; Eisenstadt, E.; Iijima, T.; Freese, E. Biochemical and genetic characterization of an auxotroph of Bacillus subtilis altered in the acyl-CoA:acyl-carrier-protein transacylase. Eur. J. Biochem. 115:175-181; 1981.

Braunegg, G.; Sonnleitner, B.; Lafferty, R.M. A rapid gas chromatographic method for the determination of poly-β-hydroxybutyric acid in microbial biomass. Eur. J. Appl. Microbiol. Biotechnol. 6:29-37; 1978.

Braunstein, A.E. Amino group transfer. In: Boyer, P.D., ed. The Enzymes. Vol. IX, Pt. B. 2nd ed. New York: Academic Press, Inc.; 1973.

Brock, T.D. Chloramphenicol. Bacteriol. Rev. 25:32-48; 1961.

Bulla, L.A., Jr.; Bechtel, D.B.; Kramer, K.J.; Shethna, Y.I.; Aronson, A.I.; Fitz-James, P.C. Ultrastructure, physiology, and biochemistry of Bacillus thuringiensis. CRC Crit. Rev. Microbiol. 8:147-204; 1980-81.

Bulla, L.A., Jr.; Bennett, G.A.; Shotwell, .L. Physiology of sporeforming bacteria associated with insects: II. Lipids of vegetative cells. J. Bacteriol. 104:1246-1253; 1970.

Bulla, L.A., Jr.; Nickerson, K.W.; Mounts, T.L.; Iandolo, J.J. Biosynthesis of fatty acids during germination and outgrowth of Bacillus thuringiensis spores. In: Gerhardt, P.; Costilow, R.N.; Sadoff, H.L., eds. Spores VI. Washington, D.C.: American Society for Microbiology; 1975:p. 520-525.

Bulla, L.A., Jr.; St. Julian, G.; Rhodes, R.A.; Hesseltine, C.W. Physiology of sporeforming bacteria associated with insects. I. Glucose catabolism in vegetative cells. Can. J. Microbiol. 16:243-248; 1970.

Bulla, L.A., Jr.; St. Julian, G.; Rhodes, R.A. Physiology of sporeforming bacteria associated with insects. III. Radiorespirometry of pyruvate, acetate, succinate, and glutamate oxidation. Can. J. Microbiol. 17:1073-1079; 1971.

Bulla, L.A., Jr.; St. Julian, G. Lipid metabolism during bacterial growth and sporulation: Phospholipid pattern in Bacillus thuringiensis and Bacillus popilliae. In: Halvorson, H.O.; Hanson, R.; Campbell, L.L., eds. Spores V. Washington: American Society for Microbiology; 1972;p. 191-196.

Burges, H.D., ed. Microbial control of pests and plant diseases 1970-1980. London: Academic Press (London) Ltd.; 1981.

Butterworth, P.H.W.; Bloch, K. Comparative aspects of fatty acid synthesis in Bacillus subtilis and Escherichia coli. Eur. J. Biochem. 12:496-501; 1970.

Carroll, J.; Li, J.; Ellar, D.J. Proteolytic processing of a coleopteran-specific δ-endotoxin produced by Bacillus thuringiensis var. tenebrionis. Biochem. J. 261:99-105; 1989.

Chalmers, R.A.; Lawson, A.M. Organic acids in man: Analytical chemistry, biochemistry and diagnosis of the organic acidurias. London:Chapman and Hall Ltd.; 1982.

Chalmers, R.A.; Lawson, A.M.; Borud, O. Gas chromatographic and mass spectrometric studies on urinary organic acids in a patient with congenital lactic acidosis due to pyruvate decarboxylase deficiency. Clin. Chim. Acta 77:117-124; 1977.

Cheng, Y.-S.E.; Aronson, A.I. Alterations of spore coat processing and protein turnover in a Bacillus cereus mutant with a defeccive postexponential intracellular protease. Proc. Natl. Acad. Sci. USA 74:1254-1258; 1977.

Conner, R.M.; Hansen, P.A. Effects of valine, leucine, and isoleucine on the growth of Bacillus thuringiensis and related bacteria. J. Invert. Pathol. 9:12-18; 1967.

Corkey, B.E.; Martin-Requero, A.; Walajtys-Rode, E.; Williams, R.J.; Williamson, J.R. Regulation of the branched chain α-ketoacid pathway in liver. J. Biol. Chem. 257:9668-9676; 1982.

Courtright, J.B.; Henning, U. Malate dehydrogenase mutants in Escherichia coli K-12. J. Bacteriol. 102:722-728; 1970.

Daniel, J.; Dondon, L.; Danchin, A. 2-Ketobutyrate: a putative alarmone of Escherichia coli. Mol. Gen. Genet. 190: 452-458; 1983.

Dawes, E.A.; Senior, P.J. The role and regulation of energy reserve polymers in micro-organisms. Adv. Microb. Physiol. 10:135-266; 1973.

De Felice, M.; Levinthal, M.; Iaccarino, M.; Guardola, J. Growth inhibition as a consequence of antagonism between related amino acids: Effect of valine in Escherichia coli K-12. Microbiol. Rev. 43:42-58; 1979.

Diesterhaft, M.D.; Freese, E. Role of pyruvate carboxylase, phosphoenolpyruvate carboxykinase, and malic enzyme during growth and sporulation of Bacillus subtilis. J. Biol. Chem. 24 :6062-6070; 1973.

Difco manual of dehydrated culture media and reagents for microbiological and clinical laboratory procedures. 9th ed. Detroit, Michigan: Difco Laboratories Inc.; 1977.

Ellar, D.J.; Eaton, M.W.; Hogarth, C.; Wilkinson, B.J.; Deans, J.; LaNauze, J. Comparative biochemistry and function of forespore and mother-cell compartments during sporulation of Bacillus megaterium cells. In: Gerhardt, P.; Costilow, R.N.; Sadoff, H.L., eds. Spores VI. Washington: American Society for Microbiology; 1975:p. 425-433.

Findlay, R.H.; White, D.C. Polymeric beta-hydroxyalkanoates from environmental samples and Bacillus megaterium. Appl. Environ. Microbiol. 45:71-78; 1983.

Fitz-James, P.; Young, E. Morphology of sporulation. In: Gould, G.W.; Hurst, A., eds. The bacterial spore. London: Academic Press Inc. (London) Ltd.; 1969:p. 39-72.

Foster, S.J.; Johnstone, K. The trigger mechanism of bacterial spore germination. In: Smith, I.; Slepecky, R.A.; Setlow, P., eds. Regulation of procaryotic development. Washington: American Society for Microbiology; 1989:p. 89-108.

Freese, E.; Fujita, Y. Control of enzyme synthesis during growth and sporulation. In: Schlessinger, D., ed. Microbiology - 1976. Washington: American Society for Microbiology; 1976.

Freese, E.; Heinze, J. Metabolic and genetic control of bacterial sporulation. In: Hurst,A.; Gould, G.W., eds. The bacterial spore. Vol. 2. London: Academic Press Inc. (London) Ltd.; 1983:p. 101-172.

Frenkel, R. Regulation and physiological functions of malic enzymes. Curr. Topics Cell. Reg. 9:157-181; 1975.

Goldberg, A.L.; Tischler, M.E. Regulatory effects of leucine on carbohydrate and protein metabolism. In: Walser, M.; Williamson, J.R., eds. Metabolism and clinical implications of branched chain amino and ketoacids. Amsterdam: Elsevier North Holland, Inc.; 1981:p. 205-216.

Gollakota, K.G.; Halvorson, H.O. Biochemical changes occurring during sporulation of Bacillus cereus: Inhibition of sporulation by α-picolinic acid. J. Bacteriol. 79:1-8; 1960.

Goodman, H.M.; Frick, G.P. The metabolism of branched-chain amino acids in adipose tissue. In: Odessey, R., ed. Problems and potential of branched-chain amino acids in physiology and medicine. Amsterdam: Elsevier Biomedical Press BV; 1986:p. 173-198.

Gordon, R.E.; Haynes, W.C.; Pang, C.H.-N. The genus Bacillus. Agriculture Handbook No. 427. Washington: U.S. Dept. of Agriculture, Agricultural Research Service; 1973.

Gottschalk, G. Bacterial metabolism. 2nd, corrected printing. New York: Springer-Verlag New York Inc.; 1979.

Graupe, D. Identification of systems. New York: Van Nostrand Reinhold Co.; 1972.

Halvorson, H.O. Rapid and simultaneous sporulation. J. Appl. Bacteriol. 20:305-314; 1957.

Handbook of chromatography. Vol. II. Zweig, G.; Sherma, J., eds. Cleveland:CRC Press, Inc.; 1972.

Hansen, R.G.; Henning, U. Regulation of pyruvate dehydrogenase activity in Escherichia coli K12. Biochim. Biophys. Acta 122:355-358; 1966.

Hanson, R.S.; Blicharska, J.; Szulmajster, J. Relationship between the tricarboxylic acid cycle enzymes and sporulation of B. subtilis. Biochem. Biophys. Res. Commun. 17:1-7; 1964.

Hanson, R.S.; Srinivasan, V.R.; Halvorson, H.O. Biochemistry of sporulation: I. Metabolism of acetate by vegetative and sporulating cells. J. Bacteriol. 85:451-460; 1963.

Harrison, D.F. The regulation of respiration rate in growing bacteria. Adv. Microb. Physiol. 14:243-313; 1976.

Haynes, W.C.; Wickerham, L.J.; Hesseltine, C.W. Maintenance of cultures of industrially important microorganisms. Appl. Microbiol. 3:361-368; 1955.

Holmberg, A.; Sievänen, R.; Carlberg, G. Fermentation of B. thuringiensis for exotoxin production: process analysis study. Biotechnol. Bioeng. 22:1707-1724; 1980.

Holms, W.H. The central metabolic pathways of Escherichia coli: Relationship between flux and control at a branch point, efficiency of conversion to biomass, and excretion of acetate. Curr. Topics Cell. Reg. 28:69-105; 1986.

Huseby, N.-E.; Störmer, F.C. The pH 6 acetolactate-forming enzyme from Aerobacter aerogenes: the effect of 2-oxobutyrate upon the enzyme activity. Eur. J. Biochem. 20:215-217; 1971.

Iaccarino, M.; Guardola, J.; De Felice, M.; Favre, R. Regulation of isoleucine and valine biosynthesis, Curr. Topics Cell. Reg. 14:29-73; 1978.

Ikeda, Y.; Dabrowski, C.; Tanaka, K. Separation and properties of five distinct acyl-CoA dehydrogenases from rat liver mitochondria. J. Biol. Chem. 258:1066-1076; 1983.

Ishihara, H.; Nagano, H.; Nishihara, T.; Kondo, M. Studies on lipids of spore-forming bacteria: II. Changes in fatty acid composition of Bacillus subtilis cells during growth and sporulation. Nippon Saikingaku Zasshi 32:703-707; 1977.

Jakobs, C.; Solem, E.; Ek, J.; Halvorsen, K.; Jellum, E. Investigation of the metabolic pattern in maple syrup urine disease by means of glass capillary gas chromatography and mass spectrometry. J. Chromatogr. 143:31-38; 1977.

Johansen, L.; Bryn, K.; Störmer, F.C. Physiological and biochemical role of the butanediol pathway in Aerobacter (Enterobacter) aerogenes. J. Bacteriol. 123:1124-1130; 1975.

Jones, C.W. Aerobic respiratory systems in bacteria. In: Haddock, B.A.; Hamilton, W.A., eds. Microbial energetics. Cambridge: Cambridge University Press; 1977:p. 25-59. (27th Symp. Soc. Gen. Microbiol.).

Jones, C.W. Energy metabolism in aerobes. In: Quayle, J.R., ed. Microbial biochemistry. Baltimore, MD: University Park Press; 1979:p. 49-84. (Kornberg, H.L.; Phillips, D.C., eds. International review of biochemistry; vol. 21).

Juni, E.; Heym, G.A. A cyclic pathway for the bacterial dissimilation of 2,3-butanediol, acetylmethylcarbinol, and diacetyl: I. General aspects of the 2,3-butanediol cycle. J. Bacteriol. 71:425-432; 1956.

Kaneda, T. Biosynthesis of branched-chain fatty acids: IV. Factors affecting relative abundance of fatty acids produced by Bacillus subtilis. Can. J. Microbiol. 12:501-514; 1966.

Kaneda, T. Fatty acids in the genus Bacillus: I. Iso- and anteiso-fatty acids as characteristic constituents of lipids in 10 species. J. Bacteriol. 93:894-903; 1967.

Kaneda, T. Fatty acids in the genus Bacillus: II. Similarity in the fatty acid compositions of Bacillus thuringiensis, Bacillus anthracis, and Bacillus cereus. J. Bacteriol. 95:2210-2216; 1968.

Kaneda, T. Factors affecting the relative ratio of fatty acids in Bacillus cereus. Can. J. Microbiol. 17:269-275; 1971.

Kaneda, T. Biosynthesis of branched long-chain fatty acids from the related short-chain α-keto acid substrates by a cell-free system of Bacillus subtilis. Can. J. Microbiol. 19:87-96; 1973.

Kaneda, T. Fatty acids of the genus Bacillus: an example of branched - chain preference. Bacteriol. Rev. 41:391-418; 1977.

Kaneda, T.; Smith, E.J. Relationship of primer specificity of fatty acid de novo synthetase to fatty acid composition in 10 species of bacteria and yeasts. Can. J. Microbiol. 26:893-898; 1980.

Kaneda, T.; Smith, E.J.; Naik, D.N. Fatty acid composition and primer specificity of de novo fatty acid synthetase in Bacillus globispores, Bacillus insolitus, and Bacillus psychrophilus. Can. J. Microbiol. 29:1634-1641; 1983.

Kates, M. Techniques of lipidology: Isolation, analysis and identification of lipids. 2nd revised ed. Amsterdam:Elsevier Science Publishers B.V.; 1986.(Burdon, R.H.; van Knippenberg, P.H. Laboratory techniques in biochemistry and molecular biology; vol. 3, part 2).

Keynan, A,; Sandler, N. Spore research in historical perspective. In: Hurst, A.; Gould, G.W., eds. The bacterial spore. Vol. 2. London: Academic Press Inc. (London) Ltd.; 1983:p. 1-48.

Kobayashi, K.; Doi, S.; Negoro, S.; Urabe, I.; Okada, H. Structure and properties of malic enzyme from Bacillus stearothermopholus. J. Biol. Chem. 264:3200-3205; 1989.

Kominek, L.A.; Halvorson, H.O. Metabolism of poly-β-hydroxybutyrate and acetoin in Bacillus cereus. J. Bacteriol. 90:1251-1259; 1965.

Kurstak, E., ed. Microbial and viral pesticides. New York: Marcel Dekker, Inc.; 1982.

Lang, D.R.; Lundgren, D.G. Lipid composition of Bacillus cereus during growth and sporulation. J. Bacteriol. 101:483-489; 1970.

Laskin, A.I.; Lechevalier, H.A., eds. Handbook of microbiology. Vol. 2. 2nd ed. Cleveland: CRC Press, Inc.; 1977.

Lehninger, A.L. Biochemistry: the molecular basis of cell structure and function. 2nd ed. New York: Worth Publishers, Inc.; 1976.

Lereclus, D.; Bourgouin, C.; Lecadet, M.M.; Klier, A.; Rapoport, G. Role, structure, and molecular organization of the genes coding for the parasporal δ-endotoxins of Bacillus thuringiensis. In: Smith, I.; Slepecky, R.A.; Setlow, P., eds. Regulation of procaryotic development. Washington: American Society for Microbiology; 1989:p. 255-276.

Li, J.B.; Odessey, R. Regulation of protein turnover in heart and skeletal muscle by branched-chain amino acids and the keto acids. In: Odessey, R., ed. Problems and potential of branched-chain amino acids in physiology and medicine. Amsterdam: Elsevier Biomedical Press BV; 1986:p. 83-106.

Loken, J.P.; Stormer, F.C. Acetolactate decarboxylase from Aerobacter aerogenes: purification and properties. Eur. J. Biochem. 14:133-137; 1970.

Lowe, P.N.; Hodgson, J.A.; Perham, R.N. Dual role of a single multienzyme complex in the oxidative decarboxylation of pyruvate and branched - chain 2-oxo acids in Bacillus subtilis. Biochem. J. 215:133-148; 1983.

Macrae, R.M.; Wilkinson, J.F. Poly-β-hydroxybutyrate metabolism in washed suspensions of Bacillus cereus and Bacillus megaterium. J. Gen. Microbiol. 19:210-222; 1958.

Mandelstam, J. The free amino acids in growing and non-growing populations of Escherichia coli. Biochem. J. 69:103-110; 1958.

Mandelstam, J.; McQuillen, K., eds. Biochemistry of bacterial growth. 2nd ed. New York: John Wiley & Sons; 1973.

Marshall, V.P.; Sokatch, J.R. Regulation of valine catabolism in Pseudomonas putida. J. Bacteriol. 110:1073-1081; 1972.

Martin-Requero, A.; Corkey, B.E.; Cerdan, S.; Walajtys-Rode, E.; Parrilla, R.L.; Williamson, J.R. Interactions between α-ketoisovalerate metabolism and the pathways of gluconeogenesis and urea synthesis in isolated hepatocytes. J. Biol. Chem. 258:3673-3681; 1983.

Massey, L.K.; Sokatch, J.R.; Conrad, R.S. Branched - chain amino acid catabolism in bacteria. Bacteriol. Rev. 40:42-54; 1976.

Megraw, R.E.; Beers, R.J. Glyoxylate metabolism in growth and sporulation of Bacillus cereus. J. Bacteriol. 87:1087-1093; 1964.

Meister, A. Biochemistry of the amino acids. 2nd ed. New York: Academic Press, Inc.; 1965. 2 vol.

Miller, G.L. Use of dinitrosalicylic acid reagent for determination of reducing sugar. Analytical Chem. 31:426-428; 1959.

Miller, G.L.; Blum, R.; Glennon, W.E.; Burton, A.L. Measurement of carboxymethylcellulase activity. Analytical Biochem. 1:127-132; 1960.

Moat, A.G.; Foster, J.W. Microbial physiology. 2nd ed. New York: Wiley-Interscience; 1988.

Monro, R.E. Protein turnover and the formation of protein inclusions during sporulation of Bacillus thuringiensis. Biochem. J. 81:225-232; 1961.

Morowitz, H.J. Energy flow in biology - biological organization as a problem in thermal physics. New York: Academic Press, Inc.; 1968;p. 84.

Murai, T.; Tokushige, M.; Nagai, J.; Katsuki, H. Physiological functions of NAD- and NADP-linked malic enzymes in Escherichia coli. Biochem. Biophys. Res. Commun. 43:875-881; 1971.

Murai, T.; Tokushige, M.; Nagai, J.; Katsuki, H. Studies on regulatory functions of malic enzymes: I. Metabolic functions of NAD- and NADP-linked malic enzymes in Escherichia coli. J. Biochem. (Tokyo) 71:1015-1028; 1972.

Murrell, W.G. The biochemistry of the bacterial endospore. Adv. Microb. Physiol. 1:133-251; 1967.

Murrell, W.G. Chemical composition of spores and spore structures. In: Gould, G.W.; Hurst, A., eds. The bacterial spore. London: Academic Press Inc. (London) Ltd.; 1969:p. 215-273.

Naik, D.N.; Kaneda, T. Biosynthesis of branched long-chain fatty acids by species of Bacillus: relative activity of three α-keto acid substrates and factors affecting chain length. Can. J. Microbiol. 20:1701-1708; 1974.

Nakata, H.M. Effect of pH on intermediates produced during growth and sporulation of Bacillus cereus. J. Bacteriol. 86:577-581; 1963.

Nakata, H.M. Role of acetate in sporogenesis of Bacillus cereus. J. Bacteriol. 91:784-788; 1966.

Nakata, H.M.; Halvorson, H.O. Biochemical changes occurring during growth and sporulation of Bacillus cereus. J. Bacteriol. 80:801-810; 1960.

Nakazawa, A. Threonine deaminase - degradative (Clostridium tetanomorphum). In: Colowick, S.P.; Kaplan, N.O., eds. Methods in enzymology. Vol. XVIIB. New York: Academic Press, Inc.; 1971:p. 571-575.

Nickerson, K.W.; Bulla, L.A., Jr. Lipid metabolism during bacterial growth, sporulation, and germination: an obligate nutritional requirement in Bacillus thuringiensis for compounds that stimulate fatty acid synthesis. J. Bacteriol. 123:598-603; 1975.

Nickerson, K.W ; Bulla, L.A., Jr.; Mounts, T.L. Lipid metabolism during bacterial growth, sporulation, and germination: differential synthesis of individual branched - and normal - chain fatty acids during spore germination and outgrowth of Bacillus thuringiensis. J. Bacteriol. 124:1256-1262; 1975.

Nickerson, K.W.; De Pinto, J.; Bulla, L.A., Jr. Sporulation of Bacillus thuringiensis without concurrent derepression of the tricarboxylic acid cycle. J. Bacteriol. 117:321-323; 1974.

Nickerson, K.W.; St. Julian, G.; Bulla, L.A., Jr. Physiology of sporeforming bacteria associated with insects: Radiorespirometric survey of carbohydrate metabolism in the 12 serotypes of Bacillus thuringiensis. Appl. Microbiol. 28: 129-132; 1974.

Nickerson, K.W.; Zarnick, W.J.; Kramer, V.C. Poly-β-hydroxybutyrate parasporal bodies in Bacillus thuringiensis. FEMS Microbiol. Lett. 12:327-331; 1981.

Odessey, R. Metabolic regulation of branched-chain amino acid catabolism. In: Odessey, R., ed. Problems and potential of branched-chain amino acids in physiology and medicine. Amsterdam: Elsevier Biomedical Press BV; 1986:p. 49-80.

Odessey, R., ed. Problems and potential of branched-chain amino acids in physiology and medicine. Amsterdam: Elsevier Biomedical Press BV; 1986.

Ohné, M. Regulation of the dicarboxylic acid part of the citric acid cycle in Bacillus subtilis. J. Bacteriol. 122: 224-234; 1975.

Ohné, M.; Rutberg, B. Repression of sporulation in Bacillus subtilis by L-malate. J. Bacteriol. 125:453-460; 1976.

Piggot, P.J. Revised genetic map of Bacillus subtilis 168. In: Smith, I.; Slepecky, R.A.; Setlow, P., eds. Regulation of procaryotic development. Washington: American Society for Microbiology; 1989:p. 1-41.

Press, W.H.; Flannery, B.P.; Teukolsky, S.A.; Vetterling, W.T. Numerical recipes: The art of scientific computing. New York: Cambridge University Press; 1986.

Randle, P.J.; Lau, K.S.; Parker, P.J. Regulation of branched-chain 2-oxoacid dehydrogenase complex. In: Walser, M.; Williamson, J.R., eds. Metabolism and clinical implications of branched chain amino and ketoacids. Amsterdam: Elsevier North Holland, Inc.; 1981:p. 13-22.

Roberts, C.M.; Sokatch, J.R. Branched chain amino acids as activators of branched chain ketoacid dehydrogenase. Biochem. Biophys. Res. Commun. 82:828-833; 1978.

Rodwell, V.W. Biosynthesis of amino acids and related compounds. In: Greenberg, D.M., ed. Metabolic pathways. Vol. III. 3rd ed. New York: Academic Press, Inc.; 1969;p. 317-373.

Roels, J.A. Energetics and kinetics in biotechnology. Amsterdam: Elsevier Biomedical Press BV; 1983:115.

Rowe, G.E.; Margaritis, A. Bioprocess developments in the production of bioinsecticides by Bacillus thuringiensis. CRC Crit. Rev. Biotechnol. 6:87-127; 1987.

Sakharova, Z.V.; Ignatenko, Yu.N.; Shchul'ts, F.; Khovrychev, M.P.; Rabotnova, I.L. Kinetics of the growth and development of Bacillus thuringiensis during batch culturing. Microbiol. (USSR) 54:483-488; 1985. Translation of Mikrobiologiya 54(4):604-609; 1985.

Sanwal, B.D. Allosteric controls of amphibolic pathways in bacteria. Bacteriol. Rev. 34:20-39; 1970.

Sanwal, B.D. Regulatory characteristics of the diphosphopyridine nucleotide-specific malic enzyme of Escherichia coli. J. Biol. Chem. 245:1212-1216; 1970.

Sanwal, B.D.; Smando, R. Malic enzyme of Escherichia coli: Diversity of the effectors controlling enzyme activity. J. Biol. Chem. 244:1817-1823; 1969.

Scandella, C.J.; Kornberg, A. Biochemical studies of bacterial sporulation and germination: XV. Fatty acids in growth, sporulation, and germination of Bacillus megaterium. J. Bacteriol. 98:82-86; 1969.

Schaeffer, P.; Millet, J.; Aubert, J.-P. Catabolite repression of bacterial sporulation. Proc. Natl. Acad. Sci. USA 54:704-711; 1965.

Schwartz, E.R.; Old, L.O.; Reed, L.J. Regulatory properties of pyruvate dehydrogenase from Escherichia coli. Biochem. Biophys. Res. Commun. 31:495-500; 1968.

Schweizer, E. Biosynthesis of fatty acids and related compounds. In: Ratledge, C.; Wilkinson, S.G., eds. Microbial lipids. Vol. 2. London: Academic Press Ltd.; 1989:p. 3-50.

Setlow, P. Energy and small-molecule metabolism during germination of Bacillus spores. In: Gerhardt, P.; Costilow, R.N.; Sadoff, H.L., eds. Spores VI. Washington: American Society for Microbiology; 1975:p. 443-450.

Setlow, P. Germination and outgrowth. In: Hurst,A.; Gould, G.W., eds. The bacterial spore. Vol. 2. London: Academic Press Inc. (London) Ltd.; 1983:p. 211-254.

Shizuta, Y.; Tokushige, M. Threonine deaminase (degradative) (Escherichia coli). In: Colowick, S.P.; Kaplan, N.O., eds. Methods in enzymology. Vol. XVIIB. Academic Press, Inc.; 1971;p. 575-580.

Singer, S.; Rogoff, M.H. Inhibition of growth of Bacillus thuringiensis by amino acids in defined media. J. Invert. Pathol. 12:98-104; 1968.

Singh, R.M.M. Role of tricarboxylic acid cycle in bacterial sporulation. Biochem. Biophys. Res. Commun. 39:651-654; 1970.

Sokatch, J.R. Metabolism of branched-chain amino acids in bacteria. In: Odessey, R., ed. Problems and potential of branched-chain amino acids in physiology and medicine. Amsterdam: Elsevier Biomedical Press BV; 1986:p. 31-47.

Sonenshein, A.L. Recent progress in metabolic regulation of sporulation. In: Hoch, J.A.; Setlow, P., eds. Molecular biology of microbial differentiation. Washington: American Society for Microbiology; 1985:p. 185-193.

Sonenshein, A.L. Metabolic regulation of sporulation and other stationary-phase phenomena. In: Smith, I.; Slepecky, R.A.; Setlow, P., eds. Regulation of procaryotic development. Washington: American Society for Microbiology; 1989:p. 109-130.

Stormer, F.C. Evidence for regulation of Aerobacter aerogenes pH 6 acetolactate-forming enzyme by acetate ion. Biochem. Biophys. Res. Commun. 74:898-902; 1977.

Stormer, F.C. The pH 6 acetolactate-forming enzyme from Aerobacter aerogenes. J. Biol. Chem. 243:3735-3739; 1968.

Stouthamer, A.H. A theoretical study on the amount of ATP required for synthesis of microbial cell material. Antonie van Leeuw. 39:545-565; 1975.

Stouthamer, A.H. The search for correlation between theoretical and experimental growth yields. In: Quayle, J.R., ed. Microbial biochemistry. Baltimore, MD: University Park Press; 1979:p. 1-47. (Kornberg, H.L.; Phillips, D.C., eds. International review of biochemistry; vol. 21).

Szulmajster, J.; Keryer, E. Isolation and properties of thermosensitive mutants of Bacillus subtilis deficient in intracellular protease activity. In: Gerhardt, P.; Costilow, R.N.; Sadoff, H.L., eds. Spores VI. Washington: American Society for Microbiology; 1975:p. 271-278.

Umbarger, H.E. Amino acid biosynthesis and its regulation. Ann. Rev. Biochem. 47:533-606; 1978.

Vinter, V. Physiology and biochemistry of sporulation. In: Gould, G.W.; Hurst, A., eds. The bacterial spore. London: Academic Press Inc. (London) Ltd.; 1969:p. 73-123.

Weatherburn, M.W. Phenol-hypochlorite reaction for determination of ammonia. Analytical Chem. 39:971-974; 1967.

Weber, M.W.; Broadbent, D.A. Electron transport in membranes from spores and from vegetative and mother cells of Bacillus subtilis. In: Gerhardt, P.; Costilow, R.N.; Sadoff, H.L., eds. Spores VI. Washington: American Society for Microbiology; 1975:p. 411-417.

Weitzman, P.D.J. Unity and diversity in some bacterial citric acid-cycle enzymes. Adv. Microb. Physiol. 22:185-244; 1981.

Willecke, K.; Pardee, A.B. Fatty acid-requiring mutant of Bacillus subtilis defective in branched chain α-keto acid dehydrogenase. J. Biol. Chem. 246:5264-5272; 1971.

Williamson, J.R.; Corkey, B.E.; Martin-Requero, A.; Walajtys-Rode, E.; Coll, K.E. Metabolic repercussions of branched-chain keto acid metabolism in liver. In: Odessey, R., ed. Problems and potential of branched-chain amino acids in physiology and medicine. Amsterdam: Elsevier Biomedical Press BV; 1986:p. 135-172.

Young, I.E.; Fitz-James, P.C. Chemical and morphological studies of bacterial spore formation: II. Spore and parasporal protein formation in Bacillus cereus var. alesti. J. Biophys. Biochem. Cytol. 6:483-498; 1959.

Yousten, A.A.; Hanson, R.S. Sporulation of tricarboxylic acid cycle mutants of Bacillus subtilis. J. Bacteriol. 109: 886-894; 1972.

Yousten, A.A.; Rogoff, M.H. Metabolism of Bacillus thuringiensis in relation to spore and crystal formation. J. Bacteriol. 100:1229-1236; 1969.

Zahner, V.; Momen, H.; Salles, C.A.; Rabinovitch, L. A comparative study of enzyme variation in Bacillus cereus and Bacillus thuringiensis. J. Appl. Bacteriol. 67:275-282; 1989.